

DAC-60963

CR 61566

GPO PRICE \$ _____

CSFTI PRICE(S) \$ _____

Hard copy (HC) 3.00

Microfiche (MF) _____

ff 653 July 65

FACILITY FORM 802

N68-20358

(ACCESSION NUMBER)

(THRU)

253

(PAGES)

1

(CODE)

CR-61566

(NASA CR OR TMX OR AD NUMBER)

30

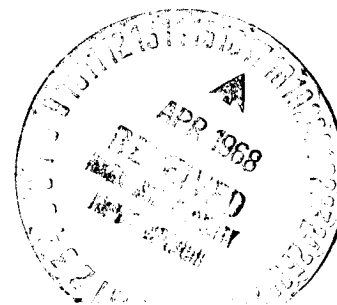
(CATEGORY)

CREW MOTION AND THE DYNAMIC ENVIRONMENT OF SPACEBORNE EXPERIMENTS

DOUGLAS



MISSILE & SPACE SYSTEMS DIVISION



JANUARY 1968

CREW MOTION AND THE DYNAMIC ENVIRONMENT OF SPACEBORNE EXPERIMENTS

DAC-60963

JANUARY 1968

PREPARED BY
W.A. BEAUDRY
W.S. CLARK
R.H. GRIMES
M.A. IANNCE
W.C. MIDDLETON
J.E. NASSIR

John C. Walker

APPROVED BY
J.C. WALKER
ACTING CHIEF ENGINEER
ADVANCE FLIGHT MECHANICS

PREPARED FOR THE NATIONAL AERONAUTICS
AND SPACE ADMINISTRATION UNDER
CONTRACT NUMBER NAS8-21129



MISSILE & SPACE SYSTEMS DIVISION

5
PRECEDING PAGE, BLANK NOT FILMED.

CONTENTS

Section 1	SUMMARY AND INTRODUCTION	1-1
Section 2	CREW MOTION	2-1
	2.1 Operational and Experimental Requirements	2-1
	2.2 Exercise and Locomotion	2-2
	2.3 Motion Constraints	2-3
	2.4 Reflex Actions	2-6
Section 3	VEHICLE DYNAMICS	3-1
	3.1 Configurations and Coordinate Systems	3-1
	3.2 Rigid-Body Equations of Motion	3-5
	3.3 Flexible-Body Equations of Motion	3-12
	3.4 Crew-Motion Input Data	3-15
	3.5 Data Reduction	3-21
	3.6 Results	3-23
Section 4	CREW-MOTION ISOLATION DEVICES	4-1
	4.1 Mass Balance	4-1
	4.2 Shock Mounting	4-8
	4.3 Tuned Spring Mass Isolators	4-13
	4.4 Pivoted Tuned Isolator	4-24
Section 5	CONCLUSIONS AND RECOMMENDATIONS	5-1
Appendix A	SURVEY OF REQUIRED DYNAMIC ENVIRONMENT	A-1
Appendix B	COMPUTING PROGRAMS	B-1
BIBLIOGRAPHY		

Section 1

SUMMARY AND INTRODUCTION

1.1 SUMMARY

An analytic study of the effect of crew motion on the dynamic environment of orbiting laboratories was conducted by the Missile and Space Systems Division of the Douglas Aircraft Company for the NASA Marshall Space Flight Center.

A computer program was used to determine the dynamic environment resulting from previously generated experimental data describing crew-motion force and moment histories. It is shown that the resulting acceleration histories exceed the requirements of nearly all the proposed low-acceleration propellant experiments, and the attitude histories exceed the requirements of a substantial but small portion of the pointing experiments.

A number of methods are suggested for improving the design of the laboratories to minimize crew motions. Among these methods are the use of multifunctional displays and controls; the inclusion of food, water, and relief facilities at the crew station; design of the environmental control system to minimize unconscious movements caused by the environment; etc.

Five passive systems were investigated for minimizing the force transmitted to the vehicle. Two of the systems show sufficient promise to recommend further study. The analyses included indicate that these two devices could reduce the attitude error to within the requirements of all pointing experiments surveyed and substantially increase the number of propellant experiments possible (although a majority of the propellant experiments surveyed would still be unfeasible). Further refinement of the analyses of these isolators coupled with passive isolation systems for the experiments could conceivably lower the acceleration errors on the larger configurations to within all but the most stringent experiment requirements.

1.2 INTRODUCTION

The purpose of the manned orbiting laboratories being designed is to provide a work area in which experiments requiring some aspect of the exotic environment associated with an orbiting vehicle may be conducted. To be carried out adequately, these experiments require a certain amount of stability of the working platform. That is, each experiment requires certain tolerances on the dynamic environment of the experimental package to ensure reliable data. Many optical experiments require stringent pointing and pointing stability, whereas propellant experiments require low tolerances on experiment acceleration. Appendix A contains the results of a survey to find the dynamic environment tolerances required by orbiting laboratory experiments. The Apollo Telescope Mount and Project Thermo experiments were included in the survey. The results of this survey are illustrated in Figures 1-1 and 1-2, which show distributions of pointing accuracy and acceleration accuracy versus the time duration required, with the number of experiments parameterized.

Recent studies (References 1 and 2) have suggested that the motion of the crew members presents the most significant potential for detrimentally affecting the dynamic environment of these experiments. This results because the fundamental frequencies associated with crew motion are substantially greater than the control system bandwidths of the large manned laboratories, and hence are essentially uncontrolled.

Experimental data has been obtained by Fuhrmeister and Fowler (Reference 1) and Tewell and Murrish (Reference 2) specifically for estimating this crew motion effect. In addition, a study conducted by Hixson and Beischer (Reference 3) furnishes applicable data. These studies present three of the four techniques for simulating a zero-g environment.

This report presents the results of a 6-month study to determine (1) if crew-motion generated dynamics exceed experimental tolerances, and (2) if so, what methods can be used to minimize this situation.

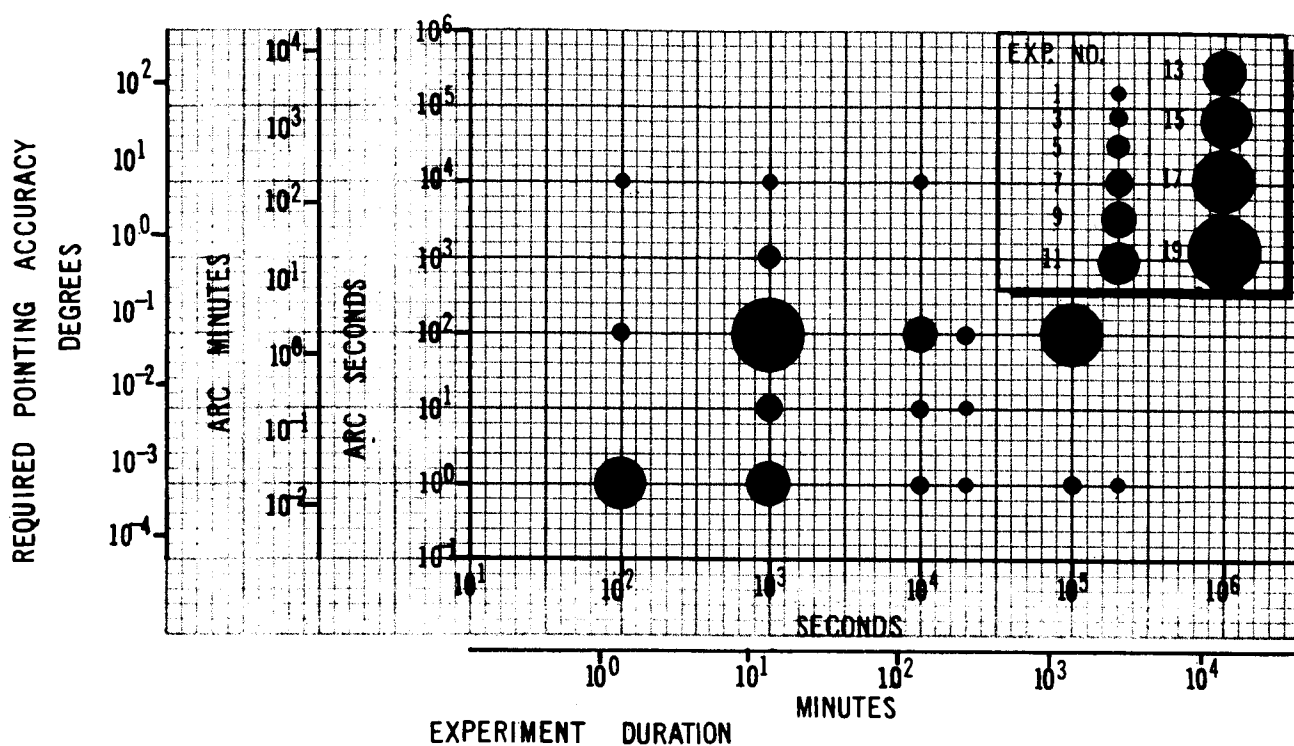


Figure 1-1. Pointing Accuracy vs Time Required

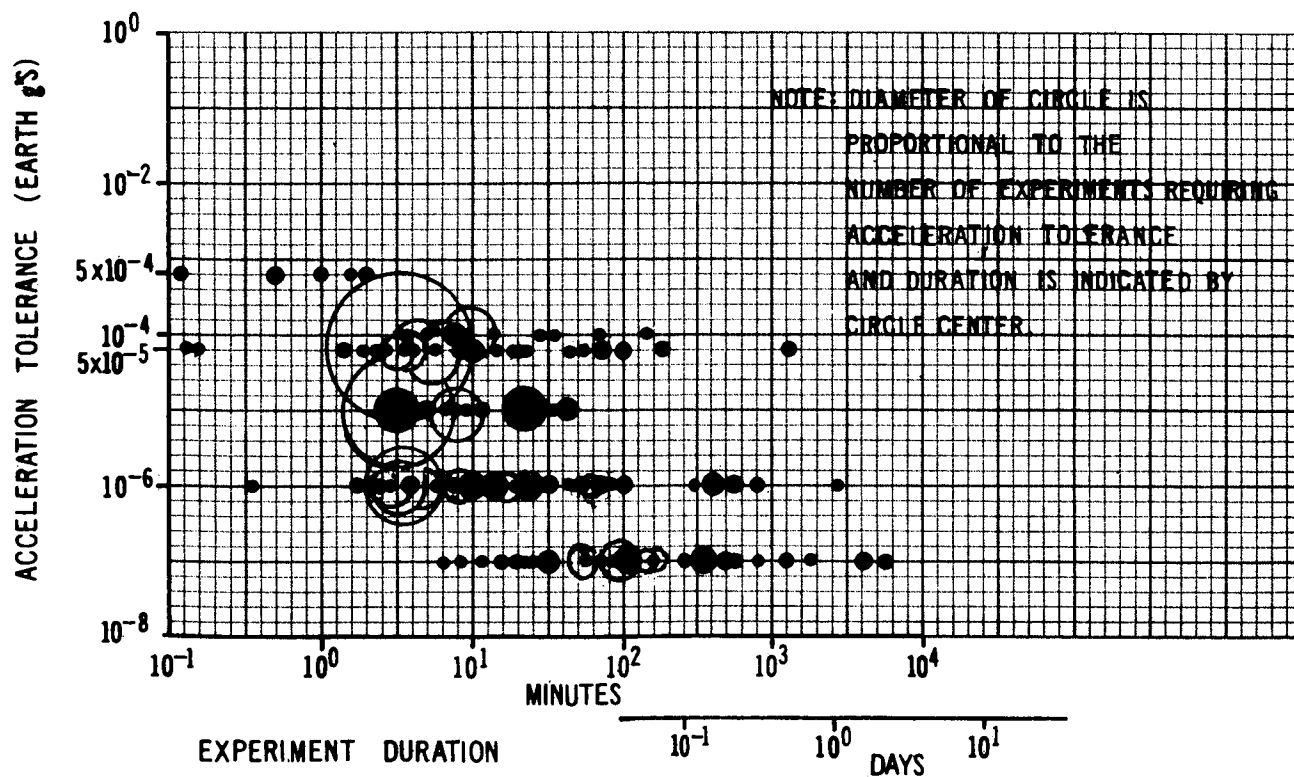


Figure 1-2. Acceleration Tolerance vs Time Required

The study approach consisted of four steps, as follows:

1. The required experiment dynamic environment tolerances were compiled.
2. A computer program was used to determine the actual dynamic environment for several vehicle configurations. The data in References 1 and 2 were used to represent crew motion.
3. Various methods of crew restraint were considered, including instructional, medical, and mechanical.
4. A number of isolation devices were considered, including mass balance, shock mounting, and several spring damper configurations.

Section 2

CREW MOTION

Some crew motions are predictable because of operations or experimental requirements; i.e., the need to exercise, relocation of crew members, or the need to satisfy various body functions. In addition, certain reflex actions, such as scratching, coughing, and sneezing, may occur at random times. Crew motion from all these sources can be controlled to some extent if attention is paid to the problem during the design of the vehicle and work-rest cycle.

2.1 OPERATIONAL AND EXPERIMENTAL REQUIREMENTS

Operational requirements consist of those monitoring and control tasks necessitated by various vehicle functions. Experimental requirements consist of monitoring and controlling experimental apparatuses and participation in those experiments in which the astronauts are the subjects.

Most of the astronaut's time in both the command module and experiment station will be devoted to monitoring. Many experiments have been conducted in recent years to evaluate the monitoring performance, or vigilance, during extended periods of time under various conditions. However, vigilance has apparently not been measured when the human operator was required to remain essentially immobile. During ground-based studies, a certain amount of motion is required just to relieve the pressure points where body contact is made with the chair. Motion for this reason will not be required in space.

Appreciable decrements in vigilance over relatively brief periods of 30 to 40 min have been obtained in a number of studies of simple monitoring, involving no evaluation or judgment on the part of the operator. However, essentially no decrements in vigilance have been found over periods of several hours with tasks comparable to those the astronauts will be performing, which involve monitoring various stimulus sources with a continual requirement

for evaluative decisions. One of the more demanding studies of vigilance (Reference 4) required subjects to perform a complex monitoring task, comparable to astronaut duties, over a period of 18 hours, consisting of six 3-hour sessions interrupted by 9-min breaks. The subjects were not instructed to remain immobile; however, they were required to keep their arms on armrests. Both detection latency (time between signal and deactivation of armrest button) and movement latency (time between deactivation of armrest button and activation of the proper switch) were measured. During the first 12 hours, 90% or more of the signals were detected. At the end of 18 hours, approximately 80% of the signals were detected. Decrements in detection and movement latencies were less than 1/2 sec. This study and other studies have found monitoring decrement to be larger for peripheral display elements. For this reason, multipurpose displays and controls should be employed as much as possible in the monitoring and control of the various experiments. When the same displays and controls are used for a number of different experiments, they can be centrally located to reduce scan and reach movements. Multipurpose TV monitors are now included in Project Thermo to present views from a number of different cameras at different times.

2.2 EXERCISE AND LOCOMOTION

Prolonged periods of crew immobility in a weightless environment may bring about many physiological adaptations. Potential circulating adaptations have been given considerable recent attention. An efficient system of reflex circulatory mechanisms has evolved in man, which compensates for the hydrostatic pressure due to gravity. The loss of cardiovascular adaptability, because of disuse of these compensatory reflexes, is well known from clinical observations after prolonged bed rest and from experimental studies involving bed rest or liquid immersion. Following the exposure of human subjects to these conditions, tilt-table tests reveal a deterioration in the capacity of the circulatory system to adjust to an erect posture. Functional tests also reveal a reduced capacity to withstand increased temperature, physical exertion, or acceleration. In a weightless environment, there will be no hydrostatic pressure effects, and therefore, no demand upon the reflex compensatory mechanisms. Thus, it has been predicted that weightlessness will bring about a decrease in the capacity for cardiovascular support similar to that

observed after bed rest or liquid immersion. This prediction is supported by evidence already obtained from manned space flights. Postorbital examinations have demonstrated symptoms of circulatory deconditioning after flights as short as six orbits.

There is evidence that cardiovascular deconditioning is also produced by confinement. Subjects seated in ground-based simulators for prolonged periods have shown evidence of deconditioning. (The subjects were exposed to hydrostatic pressure in the circulatory system but to limited motion.) Therefore, the effects of deconditioning may be more pronounced when the weightlessness of space is combined with prolonged periods of almost complete immobility.

A number of methods have been suggested to alleviate cardiovascular and other types of deconditioning that might occur. Exercise has often been proposed as a remedial method with widespread physiological effects. Forces generated by isotonic exercise routines could severely disturb Thermo experiments. These routines could be omitted during the initial seven days of a mission without compromising crew health or re-entry performance.

Crew duties within the mission vehicles will require locomotion between work locations. The programmed frequency of locomotion will be a function of the work-rest cycle. Preliminary studies (References 1 and 2) have shown that locomotion as well as exercise could interfere with the force environment of a majority of the experiments. Therefore, work-rest cycles and experiment schedules must be carefully coordinated to ensure that critical experiments are not disturbed. However, weightlessness and immobility may combine to reduce vigilance (Section 2.1) during the experiments.

2.3 MOTION CONSTRAINTS

During manned versions of the Apollo Telescope Mount (ATM) and project Thermo missions, three astronauts will be on board with different schedules for their primary activities of consuming and eliminating food and liquid, sleeping, resting, and working. Various schedules have been considered to arrive at an estimate of periods during which all three astronauts can be virtually immobile. Figure 2-1 shows three 6-hour periods of reduced crew motion that could be made available each day for experimentation during a

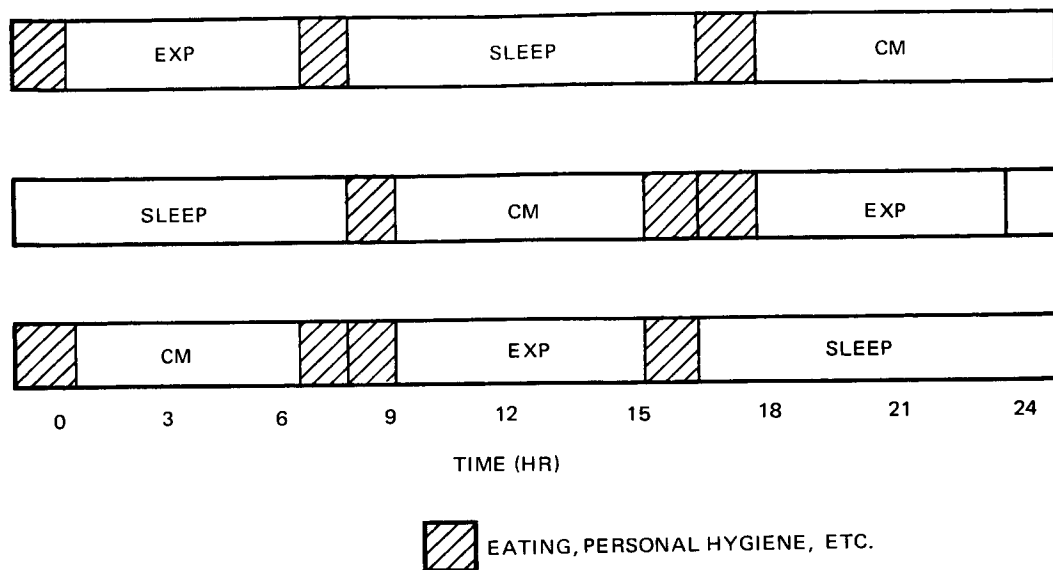


Figure 2-1. Example Work Rest Cycle

relatively short mission, such as the seven days required for Project Thermo. Each man would perform during two of the 6-hour periods and sleep through the other. Because most of the Thermo experiments are shorter than six hours, a schedule this demanding will not be necessary. However, it is possible that the astronauts could maintain such a schedule for seven days given proper design for comfort and performance and adequate training.

There are three basic methods of constraining the movement of the crew members: training, medical, and mechanical. All three methods treat the astronauts directly, essentially acting on the source of the disturbances from crew motion.

Crew members could be trained to remain as motionless as possible during crew station activities and to perform routine control operations in a slow-motion manner when critical experiments are in operation. Because impulse is directly related to velocity, the slow motion would minimize the maximum disturbance impulse, and by lowering the fundamental frequency of the

crew-motion disturbance, it could bring it within the bandpass of the vehicle control system, thus allowing closed-loop compensation. An effective method would have to be developed for indicating to the crew members the level of activity constraint required for the experiments under operation. Feasible results from this approach should be determined in a ground-based simulation study.

Progressive relaxation techniques are particularly promising (References 5 and 6). These techniques have proved effective in reducing muscular activity over prolonged periods; there is evidence that they can be employed in such a manner as to maintain alertness. Additional research on the effectiveness of this approach appears warranted.

Drugs can be used to reduce unwanted motion. As an example, antihistamine drugs reduce the probability of coughing or sneezing; they also reduce skin irritation, thus minimizing the need to scratch. A tranquilizer could be used, provided one can be found that promotes relaxation without altering vigilance. Because of undesirable side effects, the use of drugs is not generally recommended.

Limb restraints can be reduced to a minimum in a shirt-sleeve environment or with a pressure suit which permits the ability to maintain any required limb position without effort from the astronaut. Under these conditions, the break-out force from any restraining device should be no more than that necessary to maintain the limb in the required position without conscious control (i.e., just sufficient to eliminate drift of the limbs). Physical restraint of the limbs beyond this is not recommended for the astronauts in either the command module or the experiment station for safety reasons. However, complete but defeatable physical restraint of the sleeping astronaut can be considered. It has long been known that restraint of muscular movements is conducive to relaxation and sleep. Mental institutions today frequently place an agitated patient in a cold pack. This consists of wrapping the patient in cold wet sheets in such a manner that virtually no muscular movement is possible. The patient is usually asleep within a few minutes after the wrapping process. Evidence indicates that the effective agent is primarily the restraint rather than the cold temperature.

Certain provisions can be made to increase astronaut tolerance of the prolonged immobility required in this schedule. These include: a low residue diet to decrease the frequency of defecation, a relief tube for urination, and provisions for the intake of liquid nourishment or water within each crew station without requiring gross body movements.

2.4 REFLEX ACTIONS

The design for comfort must receive high priority when crew motion must be restrained. Data are not available to show the amount of crew motion that can be expected as a function of environmental conditions. However, an optimum range can be identified for most parameters which will insure comfort and physiological well-being in Earth-type environments. Generally, crew motion will increase as conditions depart from the optimum. The various environmental parameters interact in such a manner that the optimum for any one is determined by the others. For example, optimum temperature is determined by the gaseous composition of the atmosphere, the air velocity, the thermal properties of the surrounding area, the force environment, the amount of energy expended by the crew, and the characteristics of their garments.

Although man can withstand prolonged exposure to a wide range of temperatures, the comfort range to promote minimum crew motion is no more than 10°. At the lower end of this range a slight tremor may occur, along with reduced capability for fine control and the need for occasional gross movements to increase the production of body heat. At the upper end of this range, the basal metabolic rate will increase, tending to produce a higher activity level, and slight perspiration will occur, which may increase the need to scratch.

Humidity must also be maintained within a close tolerance. Pilots often complain that the bottled oxygen they breath at high altitude does not contain sufficient water vapor. This causes irritation of the throat and nasal passages, and it occasionally causes violent coughing. Skin irritation and the need to scratch can be produced with either excessive dryness or moisture.

In designing for crew immobility, additional weight may be justified for the atmospheric control system. Trace contaminants will cause irritation, and a relatively small increase in CO_2 will result in an increase in respiration volume, respiration rate, and pulse rate.

Section 3

VEHICLE DYNAMICS

A digital computer program (CREWMO) was prepared to mechanize the equations of motion of an orbiting space vehicle. Only crew-motion disturbances are assumed to act on the vehicle, and the vehicle is assumed to be uncontrolled. The equations of motion contain both rigid-body and first-bending mode effects. The computer program accepts as input crew-motion disturbances (either time histories or Fourier series) and calculates the angular error, angular rate, and total acceleration at selected experiment stations in the vehicle. A listing of the computer program in Fortran IV language and a list of the input-output variables is contained in Appendix B.

A second program, also listed in Appendix B, takes force-time histories in a discrete format or in forms of Fourier Series coefficients and yields a set of Fourier Series coefficients which represent a force-time history corrected for certain dynamic realities. A set of six functionals are employed to reduce the large amount of computer-generated time histories, to a set of real numbers which, hopefully, will provide useful measures of the dynamic environment. Peak angular excursions for the larger space laboratories are shown to be on the order of 1 to 2 arc sec, whereas the peak rates are from 2 to 3 arc sec/sec. Peak accelerations are shown to range from 3×10^{-5} to 46×10^{-5} g for the larger vehicles.

3.1 CONFIGURATIONS AND COORDINATE SYSTEMS

The CREWMO program was applied to three prospective space laboratory configurations. These configurations are shown in Figures 3-1 to 3-3, with all pertinent rigid-body parameters. Configurations 1 and 2 represent the condition of the Apollo/S-IVB workshop cluster laboratory, at the end of the first and second experiment activity phase respectively. These configurations were chosen because all consumables will be expended in these phases of the mission. Thus, the mass and inertia of the vehicle will be minimum, and

VEHICLE PARAMETERS	
WEIGHT = 78,932 LB	
MOI	AXIS I - 3.1636
(FT-LB-SEC ²)	AXIS II - 20.1863
	AXIS III - 18.3998
CENTER OF GRAVITY	X _R - 1,689 IN.
STATION	Y _R - 46.4 IN.
	Z _R - -37.7 IN.

ORIENTATION OF PRINCIPAL AXES				
TO FROM	AXIS AXIS	X _R	Y _R	Z _R
I		11.7°	99.2°	97.1°
II		87.1°	38.2°	128.0°
III		78.7°	53.4°	38.9°

OUTPUT STATIONS (IN.)			
NUMBER	X _c	Y _c	Z _c
①	1,280	0	0
②	1,380	0	0
③	1,480	0	0
④	1,580	0	0
⑤	1,689	0	0
⑥	1,860	0	0
⑦	2,035	0	0
⑧	1,985	-15.0	-125
⑨	1,985	0	0
⑩	1,985	275	0

CREW STATIONS (IN.)			
NUMBER	X _c	Y _c	Z _c
①	1,985	125	18
②	1,480	-75	0
③	1,380	-50	-50

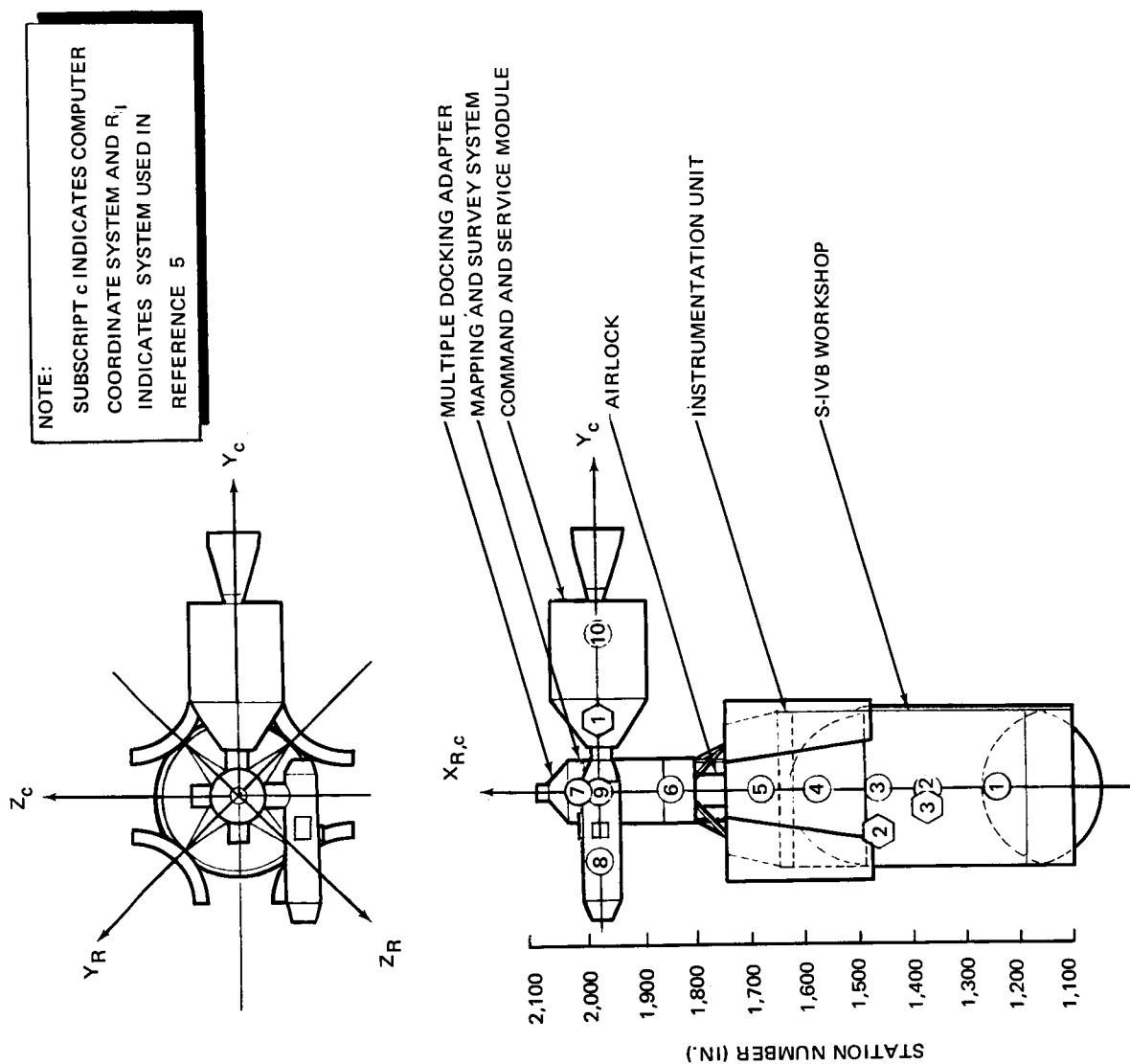


Figure 3-1. Vehicle Configuration 1

VEHICLE PARAMETERS	
WEIGHT = 105,490 LB	
MOI	$\left\{ \begin{array}{l} \text{AXIS I} - 4.555 \times 10^5 \\ \text{AXIS II} - 34.750 \times 10^5 \\ \text{AXIS III} - 32.350 \times 10^5 \end{array} \right.$
(FT-LB-SEC)	
CENTER OF GRAVITY STATION	$\left\{ \begin{array}{l} X_R - 1,829 \text{ IN.} \\ Y_R - 38.5 \text{ IN.} \\ Z_R - -28.9 \text{ IN.} \end{array} \right.$

ORIENTATION OF PRINCIPAL AXES				
FROM AXIS	TO AXIS	X_{R1}	Y_{R1}	Z_{R1}
I		3.31°	87.3°	91.9°
II		89.1°	141.0°	129.0°
III		86.8°	128.9	39.1°

OUTPUT STATIONS (IN.)				
NUMBER	X_c	Y_c	Z_c	
①	2,007	73.5	0	
②	1,303	0	0	
③	1,598	0	0	
④	2,007	352.3	0	
⑤	1,764	0	0	
⑥	1,902	0	0	
⑦	2,007	0	0	
⑧	2,075	0	-125	
⑨	2,300	0	0	
⑩	2,007	57.5	0	

INPUT STATIONS (IN.)				
NUMBER	X_c	Y_c	Z_c	
①	2,050	110	-24	
②	1,303	48	0	
③	1,598	47.65	0	
④	2,140	-12.0	0	
⑤	2,300	-18.0	0	

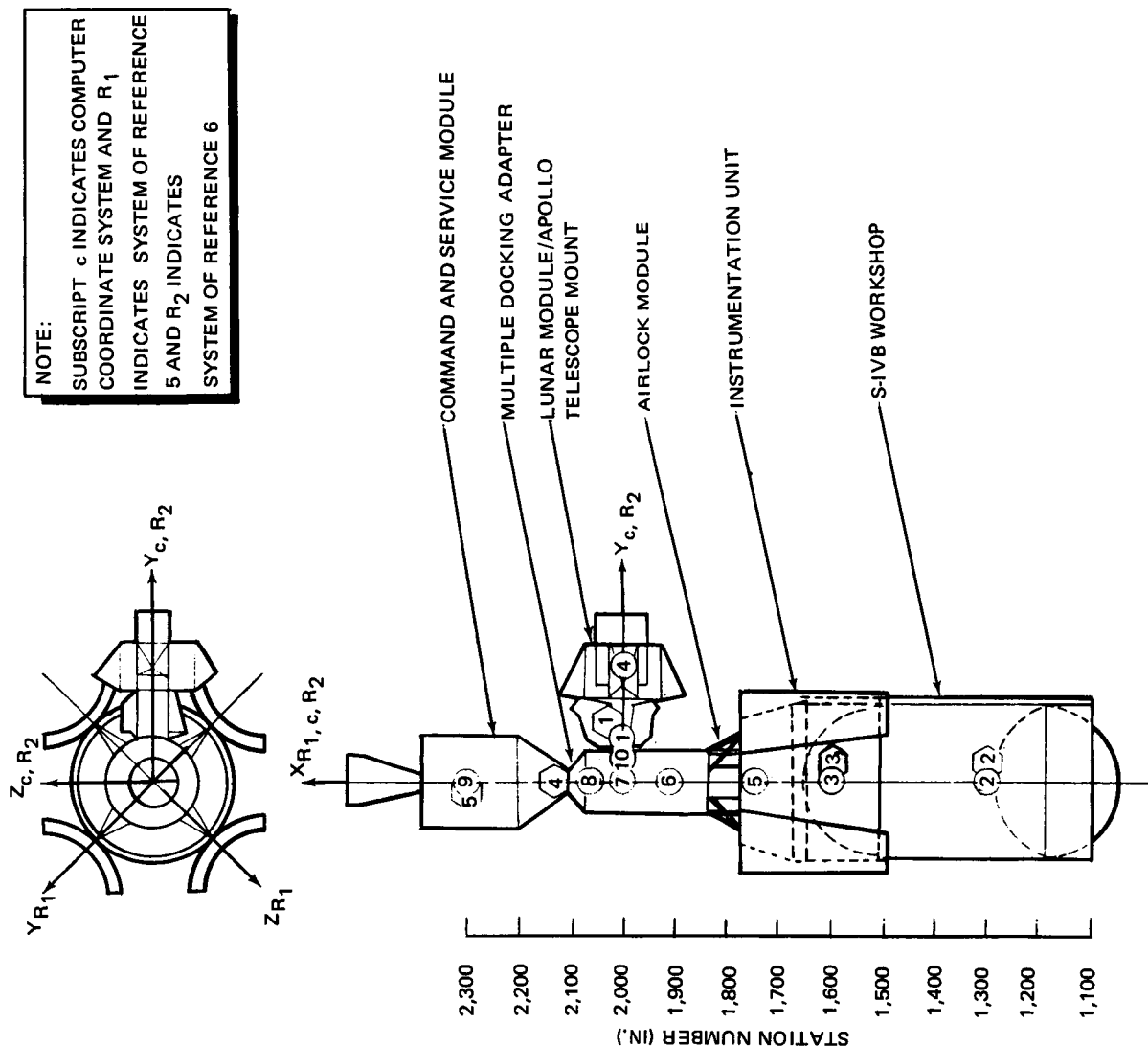


Figure 3-2. Vehicle Configuration 2

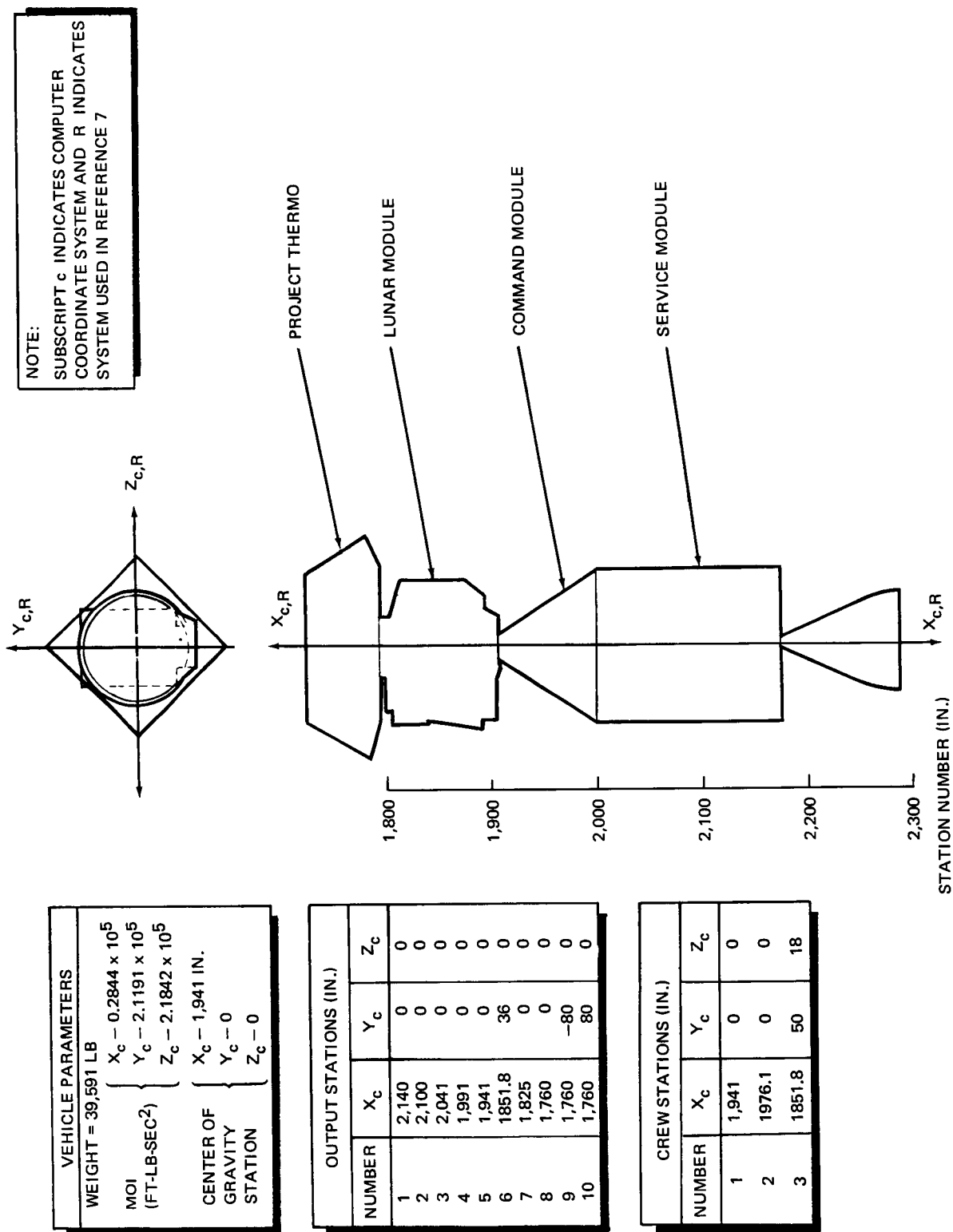


Figure 3-3. Vehicle Configuration 3

hence, the sensitivity of the dynamics to crew motion will be maximum. The rigid-body parameters for these configurations were taken from Reference 7. Configuration 2 was used to analyze the effect of first-mode bending. The bending parameters were extracted from Reference 8; they are presented in tabular form in Tables 3.1 and 3.2 and in graphical form in Figures 3-4 and 3-5. The configurations of References 7 and 8 differ slightly: the weight in Reference 8 is about 5% larger and the length about 2% longer. These differences are small enough to be neglected for the purposes of this study. Configuration 3 represents the most probable manned version of Project Thermo. This smaller vehicle is necessary since the constant acceleration levels required by the experiments would otherwise require exceptionally large thrusters. Rigid-body parameters for this configuration are from Reference 9.

3.2 RIGID-BODY EQUATIONS OF MOTION

The rigid-body equations of motion are written under the assumption that the laboratory has an uncontrolled, undisturbed (except for crew motion), inertial orientation and is in a perfectly circular orbit about the Earth.

The equation for the acceleration \vec{A} at an experiment station due to a force \vec{F}_c applied at a crew station is

$$\vec{A} = \vec{A}_T + \vec{\omega} \times \vec{R} + \vec{\omega} \times (\vec{\omega} \times \vec{R}) + 2\vec{\omega} \times \dot{\vec{R}} + \ddot{\vec{R}} \quad (3-1)$$

where

$$\vec{A}_T = \frac{1}{M} \vec{F}_c \quad (3-2)$$

$$\vec{H}_B = I\vec{\omega}, \quad (3-3)$$

$$\dot{\vec{\omega}} = I^{-1} [\vec{p} \times \vec{F}_c + \vec{M}_c - \vec{\omega} \times \vec{H}_B]. \quad (3-4)$$

The vectors in these equations are defined in Figure 3-6, and I is the inertia matrix in spacecraft geometric axis.

Table 3-1
MODAL DISPLACEMENTS FOR THE AAP-3/AAP-4 CLUSTER IN IN.-LB/SEC UNITS

Mode 1

Frequency = 1.9955420E 00 cps		Generalized Mass = 8.1771069E 01 lb-sec ² /in.			
Mode	X	Y	Z	(THETA)X	(THETA)Y (THETA)Z
1	-2.3400894E-01	-2.6569460E-01	0.0000000E-39	0.0000000E-39	0.0000000E-39 5.7653624E-04
2	-2.3342350E-01	-9.3715825E-02	0.0000000E-39	0.0000000E-39	0.0000000E-39 5.6156914E-04
3	-2.3284515E-01	-4.2772285E-02	0.0000000E-39	0.0000000E-39	0.0000000E-39 5.4134159E-04
4	-2.3201660E-01	2.2043578E-03	0.0000000E-39	0.0000000E-39	0.0000000E-39 5.0528759E-04
5	-2.2996602E-01	6.3181276E-02	0.0000000E-39	0.0000000E-39	0.0000000E-39 2.7259198E-04
6	-2.2843573E-01	8.7690494E-02	0.0000000E-39	0.0000000E-39	0.0000000E-39 9.6051403E-05
7	-2.2328311E-01	8.7716861E-02	0.0000000E-39	0.0000000E-39	0.0000000E-39 9.5551314E-05
8	-2.2905003E-01	9.6982815E-02	0.0000000E-39	0.0000000E-39	0.0000000E-39 1.2224630E-04
9	-2.2862980E-01	8.7788268E-02	0.0000000E-39	0.0000000E-39	0.0000000E-39 7.2097103E-05
10	-2.2364564E-01	8.7730489E-02	0.0000000E-39	0.0000000E-39	0.0000000E-39 8.6127986E-05
11	-2.2909242E-01	9.7497941E-02	0.0000000E-39	0.0000000E-39	0.0000000E-39 2.5090412E-04
12	-1.7114670E-01	8.7909530E-02	0.0000000E-39	0.0000000E-39	0.0000000E-39 -6.4451805E-03
13	-2.2038132E-01	8.7743891E-02	0.0000000E-39	0.0000000E-39	0.0000000E-39 8.6059676E-05
14	-2.2971173E-01	1.1575563E-01	0.0000000E-39	0.0000000E-39	0.0000000E-39 2.5731666E-04
15	1.0000000E-00	8.8157333E-02	0.0000000E-39	0.0000000E-39	0.0000000E-39 -6.4787021E-03
16	-2.3139394E-01	1.6730792E-01	0.0000000E-39	0.0000000E-39	0.0000000E-39 2.9307316E-04

Table 3-2

MODAL DISPLACEMENTS FOR THE AAP-3/AAP-4 CLUSTER IN IN. -LB/SEC UNITS

Mode 2

Frequency = 2.3035546E 00 cps		Generalized Mass = 1.1527604E 02 lb-sec ² /in.			
Mode	X	Y	Z	(THETA)X	(THETA)Y (THETA)Z
1	0.000000E-39	0.000000E-39	-1.2469625E-01	-2.4438795E-03	7.0398325E-05 0.000000E-39
2	0.000000E-39	0.000000E-39	-1.4389127E-01	-2.4218471E-03	7.7155317E-04 0.000000E-39
3	0.000000E-39	0.000000E-39	-1.4878639E-01	-2.4010268E-03	8.8299879E-05 0.000000E-39
4	0.000000E-39	0.000000E-39	-1.5322243E-01	-2.3671564E-03	1.1030482E-04 0.000000E-39
5	0.000000E-39	0.000000E-39	-1.7040796E-01	-2.1901388E-03	2.7635632E-04 0.000000E-39
6	0.000000E-39	0.000000E-39	-2.0075641E-01	-1.9065221E-03	4.2177496E-04 0.000000E-39
7	0.000000E-39	0.000000E-39	-9.1087223E-02	-1.9085673E-03	4.2201561E-04 0.000000E-39
8	0.000000E-39	0.000000E-39	-2.4100363E-01	-1.9420798E-03	5.3587402E-04 0.000000E-39
9	0.000000E-39	0.000000E-39	-3.0345000E-01	-1.8762720E-03	4.2204190E-04 0.000000E-39
10	0.000000E-39	0.000000E-39	-6.0488647E-02	-1.9164137E-03	4.2871034E-04 0.000000E-39
11	0.000000E-39	0.000000E-39	-2.4322971E-01	-1.9788337E-03	1.1009709E-03 0.000000E-39
12	0.000000E-39	0.000000E-39	-2.5492544E-01	6.8785695E-03	4.4019772E-04 0.000000E-39
13	0.000000E-39	0.000000E-39	1.6187715E-02	-1.9165249E-03	4.2874402E-04 0.000000E-39
14	0.000000E-39	0.000000E-39	-3.2289879E-01	-1.9878673E-03	1.1294191E-03 0.000000E-39
15	0.000000E-39	0.000000E-39	1.0000000E-00	6.9238567E-03	4.4072818E-04 0.000000E-39
16	0.000000E-39	0.000000E-39	-5.4951824E-01	-2.0401771E-03	1.2914418E-03 0.000000E-39

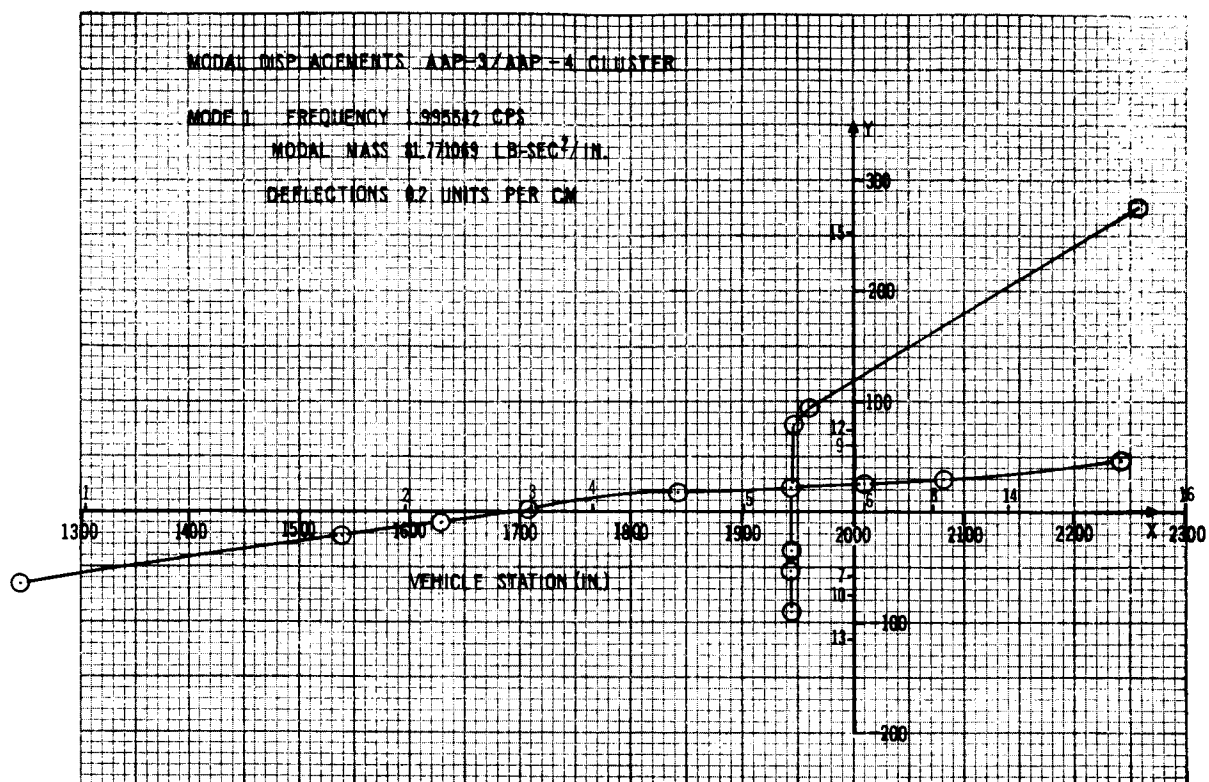


Figure 3-4. Pitch Axis Bending Parameters

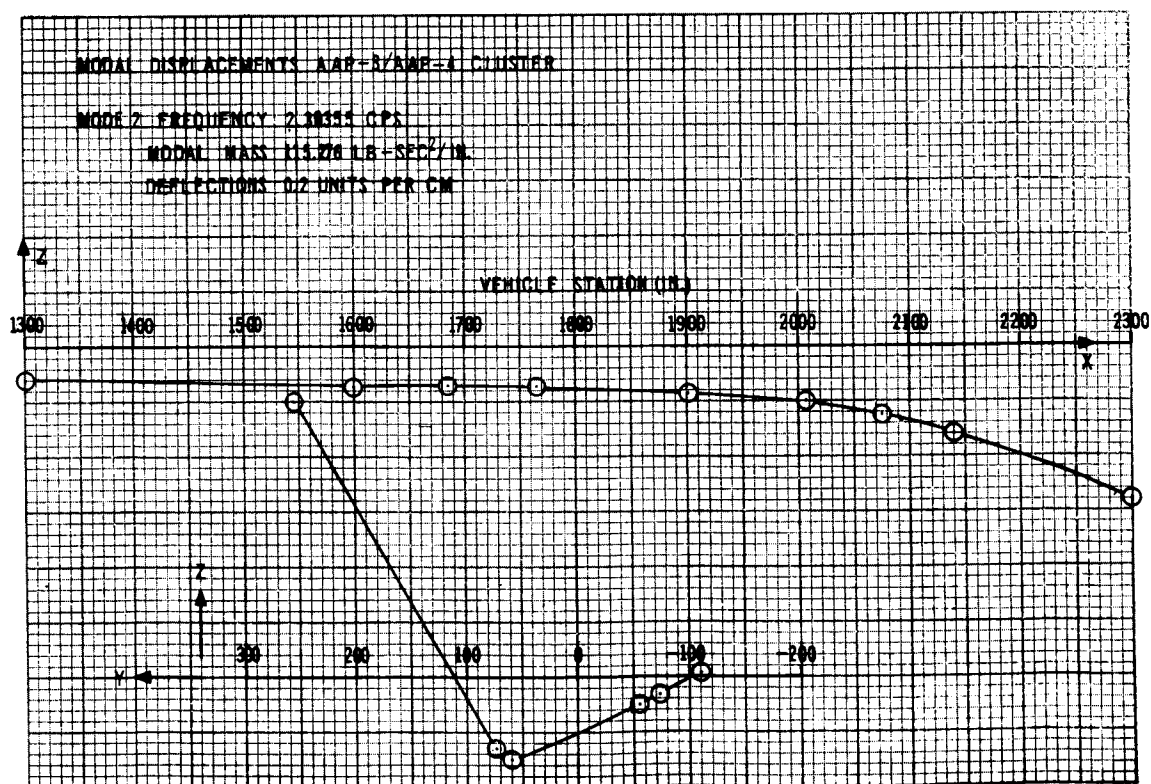


Figure 3-5. Yaw Axis Bending Parameters

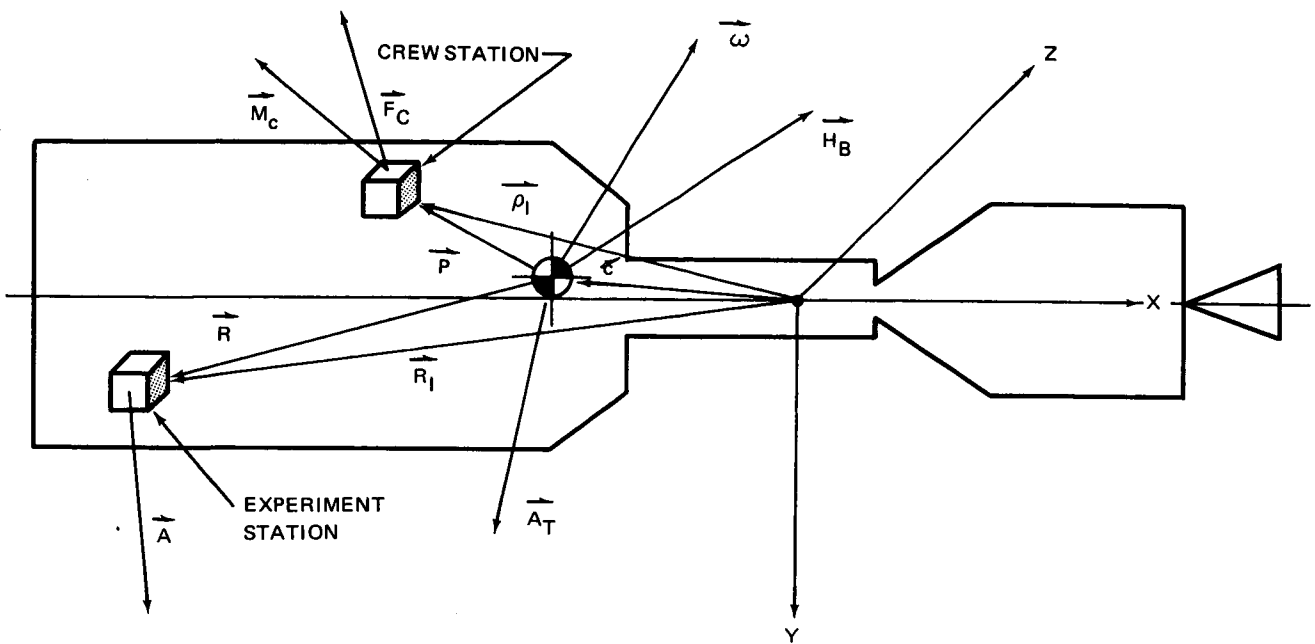


Figure 3-6. Definition of Vectors

Equation 3-1 states that the acceleration of an experiment station, located at \vec{R} from the center of mass, is given by the sum of the acceleration of the center of mass \vec{A}_T , the tangential acceleration $\vec{\omega} \times \vec{R}$, the centripetal acceleration due to rotation $\vec{\omega} \times (\vec{\omega} \times \vec{R})$, the coriolis acceleration $2\vec{\omega} \times \dot{\vec{R}}$ caused by rotation and a velocity of the experiment with respect to the vehicle $\dot{\vec{R}}$, and the acceleration of the experiment with respect to the vehicle $\ddot{\vec{R}}$. For the rigid-body situation the experiment is fixed with respect to the vehicle, and hence $\dot{\vec{R}} = \ddot{\vec{R}} = 0$. Then Equation 3-1 reduces to

$$\vec{A} = \vec{A}_T + \vec{\omega} \times \vec{R} + \vec{\omega} \times (\vec{\omega} \times \vec{R}) . \quad (3-5)$$

Equation 3-2 simply restates Newton's law, and Equation 3-3 is the definition of momentum. Equation 3-4 states Euler's law of rotational motion.

The components of the vectors in Equations 3-1 to 3-5 are in a coordinate system parallel to vehicle geometric axes but with its origin at the center of mass. However, it is convenient to input the experiment location \vec{R}_I , crew station $\vec{\rho}_I$ and center of mass location \vec{C} in vehicle geometric axes directly.

Then

$$\vec{R} = \vec{R}_I - \vec{C} \quad (3-6)$$

and

$$\vec{\rho} = \vec{\rho}_I - \vec{C} \quad (3-7)$$

Since the vehicle inertia I_d is given in principal axes, it must be converted to vehicle geometric axes by

$$I = T I_d T^T \quad (3-8)$$

where

$$T = \begin{bmatrix} \cos \phi_{x,I} & \cos \phi_{x,II} & \cos \phi_{x,III} \\ \cos \phi_{y,I} & \cos \phi_{y,II} & \cos \phi_{y,III} \\ \cos \phi_{z,I} & \cos \phi_{z,II} & \cos \phi_{z,III} \end{bmatrix} \quad (3-9)$$

and $\phi_{\alpha,i}$ is the angle between the α and i axes. The crew-motion forces F and couples K are given in crew-station coordinates and must be converted to vehicle geometric axes

$$\vec{F}_c = T_1 \vec{F}, \quad (3-10)$$

$$\vec{M}_c = T_1 \vec{M}, \quad (3-11)$$

where T_1 is the coordinate transformation from crew station to vehicle geometric axes:

$$T = \begin{bmatrix} \cos \phi_{x, x_c} & \cos \phi_{x, y_c} & \cos \phi_{x, z_c} \\ \cos \phi_{y, x_c} & \cos \phi_{y, y_c} & \cos \phi_{y, z_c} \\ \cos \phi_{z, x_c} & \cos \phi_{z, y_c} & \cos \phi_{z, z_c} \end{bmatrix} . \quad (3-12)$$

The crew-motion forces and couples are given in either time history or Fourier Series form. When they are given as the coefficients of a Fourier Series, the time history is generated from

$$F_i = \frac{1}{2} A_{oi} + \sum_{j=1}^7 A_{ij} \cos j\Omega t + \sum_{j=1}^7 B_{ij} \sin j\Omega t , \quad (3-13)$$

$$M_i = \frac{1}{2} A_{Koi} + \sum_{j=1}^7 A_{Kij} \cos j\Omega t + \sum_{j=1}^7 B_{Kij} \sin j\Omega t , \quad (3-14)$$

where A_{oi} , A_{ij} , B_{ij} , A_{Koi} , A_{Kij} , B_{Kij} are the Fourier coefficients, Ω is the fundamental frequency, and t is time.

The Euler angles β_i , describing the orientation of the vehicle geometric axes with respect to an inertial axes system are used to indicate attitude error since these angles would be measured by an on-board stable platform. Conversely, the vehicle geometric rate $\vec{\omega}$ is used to indicate attitude rate rather than $\dot{\vec{\beta}}$, since the former would be measured by body-mounted rate gyros. The Euler angle rates are derived from $\vec{\omega}$ by a transformation matrix T_2 :

$$\vec{\dot{\beta}} = T_2 \vec{\omega} \quad (3-15)$$

where

$$T_2 = \begin{bmatrix} 0 & \frac{\sin \beta_3}{\cos \beta_2} & \frac{\cos \beta_3}{\cos \beta_2} \\ 0 & \cos \beta_3 & -\sin \beta_3 \\ 1 & \sin \beta_3 \tan \beta_2 & \cos \beta_3 \tan \beta_2 \end{bmatrix} \quad (3-16)$$

and

$$\vec{\beta} = \int_0^t \dot{\vec{\beta}} dt . \quad (3-17)$$

Since the Euler angles and body rates are found to be very small, Equation 3-15 could be approximated as

$$\dot{\vec{\beta}} = \begin{bmatrix} 0 & 0 & 1 \\ 0 & 1 & 0 \\ 1 & 0 & 0 \end{bmatrix} \vec{\omega} . \quad (3-18)$$

However, this simplification was not made in the computer program.

3.3 FLEXIBLE-BODY EQUATIONS OF MOTION

The effect of body bending is to cause the experiment to move with respect to the rigid-body coordinate system. This means that the $\vec{\dot{R}}$ and $\vec{\ddot{R}}$ terms of Equation 3-1 are no longer zero. Instead,

$$\vec{\dot{R}} = \sum_{i=1}^2 \vec{\phi}_i(\vec{R}) \dot{\xi}_i(t) , \quad (3-19)$$

$$\vec{\ddot{R}} = \sum_{i=1}^2 \vec{\phi}_i(\vec{R}) \ddot{\xi}_i(t) , \quad (3-20)$$

where $\xi_1(t)$ is a generalized bending coordinate describing the bending dynamics about the z axis, and $\xi_2(t)$ describes the bending dynamics about the y axis. The $\vec{\phi}_1(\vec{R})$ vector consists of the modal deflection constants for bending deflections along the x and y axes, and $\vec{\phi}_2(\vec{R})$ consists of similar constants for bending deflections along the z axis. It follows from Tables 3-1 and 3-2 that the modal deflection vectors can be written as

$$\vec{\phi}_1(\vec{R}) = \begin{bmatrix} \phi_{1,x}(R_x, R_y) \\ \phi_{1,y}(R_x, R_y) \\ 0 \end{bmatrix}, \quad (3-21)$$

$$\vec{\phi}_2(\vec{R}) = \begin{bmatrix} 0 \\ 0 \\ \phi_{2,z}(R_x, R_y) \end{bmatrix}, \quad (3-22)$$

Therefore, Equations 3-19 and 3-20 become

$$\begin{bmatrix} \dot{R}_x \\ \dot{R}_y \\ \dot{R}_z \end{bmatrix} = \begin{bmatrix} \phi_{1,x}(R_x, R_y) \dot{\xi}_1(t) \\ \phi_{1,y}(R_x, R_y) \dot{\xi}_1(t) \\ \phi_{2,z}(R_x, R_y) \dot{\xi}_2(t) \end{bmatrix}, \quad (3-23)$$

$$\begin{bmatrix} \ddot{R}_x \\ \ddot{R}_y \\ \ddot{R}_z \end{bmatrix} = \begin{bmatrix} \phi_{1,x}(R_x, R_y) \ddot{\xi}_1 \\ \phi_{1,y}(R_x, R_y) \ddot{\xi}_1 \\ \phi_{2,z}(R_x, R_y) \ddot{\xi}_2 \end{bmatrix}. \quad (3-24)$$

By definition, the generalized bending coordinates ξ_1 and ξ_2 must satisfy the differential equation

$$\ddot{\xi}_i + 2\zeta_i \dot{\xi}_i + \omega_i^2 \xi_i = Q_i \quad i = 1, 2 \quad (3-25)$$

where ω_i is the i^{th} modal frequency obtained from Figure 3-4 or 3-5, ζ_i is the damping ratio of the i^{th} moment (selected as 0.01 on the basis of past experience), and Q_i is the generalized force exciting the i^{th} mode:

$$Q_i = \frac{1}{m_i} \left[\vec{\phi}_i(\vec{\rho}) \cdot \vec{F}_c + \vec{\theta}_i(\vec{\rho}) \cdot \vec{M}_s(\vec{\rho}) \right] \quad i = 1, 2 \quad (3-26)$$

where $\vec{\theta}_i(\vec{\rho})$ is the modal slope coefficient vector for the i^{th} mode.

These can be written as

$$\vec{\theta}_1(\vec{\rho}) = \begin{bmatrix} 0 \\ 0 \\ \theta_z(\rho_x, \rho_y) \end{bmatrix}, \quad (3-27)$$

$$\vec{\theta}_2(\vec{\rho}) = \begin{bmatrix} \theta_x(\rho_x, \rho_y) \\ \theta_y(\rho_x, \rho_y) \\ 0 \end{bmatrix}. \quad (3-28)$$

And $\vec{M}_s(\vec{\rho})$ is the sectional bending moment at the crew station. It is defined by Equation 3-29 when the crew force is applied to the x axis and by Equation 3-30 when the force is applied to the y axis:

$$\vec{M}_s(\vec{\rho}) = \vec{\rho} \times \vec{F}_c \Big|_{\rho_x = 0} + \vec{K}_c, \quad (3-29)$$

$$\vec{M}_s(\vec{\rho}) = \vec{\rho} \times \vec{F}_c \Big|_{\rho_y = 0} + \vec{K}_c . \quad (3-30)$$

3.4 CREW MOTION INPUT DATA

The crew motions used in the study along with the source of the numerical data are listed in Table 3-3. The list was limited to those activities which would occur at crew stations. Locomotion and exercise activities were not included because preliminary analyses indicated that the acceleration environment resulting from these activities would greatly exceed the experiment tolerances. The experimental error quoted in Reference 2 is less than 6%. Therefore, this data could have been used in its raw form. However, since the use of the raw data leads to certain confusing results (e.g., steady-state drift rates) and since the Fourier Series format lends itself so well to corrective techniques, the data of Reference 6 was modified to make it conform to certain known dynamic realities.

Figure 3-7 shows the mathematical model used in the following analysis. The astronaut is represented by a linear actuator, a mass firmly attached to the vehicle, and a movable mass m . The crew motion is assumed to consist of moving mass m as a function of time, such that the mass m is at rest relative to the vehicle at times $t = 0$ and T . In fact all initial conditions of the system are assumed to be zero. Since the force F_c is internal to the system, the center of gravity of the system does not move in inertial space. Further, since the force F_c always acts normal to the centerline of the vehicle, motions of m and the vehicle center of mass M will always be in the Z_m and Z_M directions respectively. Therefore, the center of mass equation yields

$$mZ_m = MZ_M , \quad (3-31)$$

and since

$$Z_r = Z_m + Z_M , \quad (3-32)$$

$$Z_r = \frac{m+M}{M} Z_m , \quad (3-33)$$

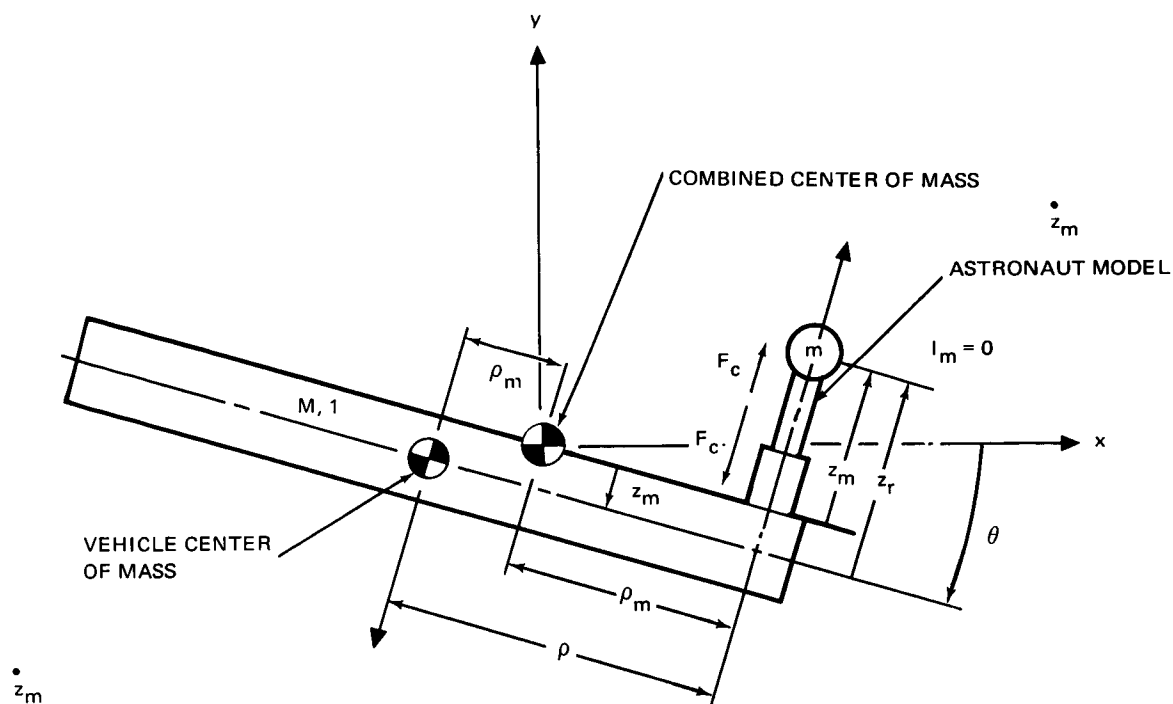


Figure 3-7. Simplified Man/Vehicle Model

differentiating twice with respect to time

$$\dot{Z}_r = \frac{m+M}{M} \dot{Z}_m, \quad (3-34)$$

$$\ddot{Z}_r = \frac{m+M}{M} \ddot{Z}_m. \quad (3-35)$$

However,

$$\ddot{Z}_m = F_c / m. \quad (3-36)$$

Therefore,

$$\ddot{Z}_r = \frac{m+M}{mM} F_c, \quad (3-37)$$

and

$$\dot{Z}_r(t) = \frac{m+M}{mM} \int_0^t F_c(\tau) d\tau, \quad (3-38)$$

$$Z_r(t) = \frac{m+M}{mM} \int_0^t \int_0^\tau F_c(\gamma) d\gamma . \quad (3-39)$$

Finally, since from continuity and

$$\ddot{Z}_r(0) = \ddot{Z}_r(T) = \dot{Z}_r(T) = Z_r(T) = 0 , \quad (3-40)$$

it follows that

$$F_c(0) = F_c(T) = 0 , \quad (3-41)$$

$$\int_0^t F_c(\tau) d\tau = 0 , \quad (3-42)$$

$$\int_0^t \int_0^\tau F_c(\gamma) d\gamma = 0 . \quad (3-43)$$

Representing F_c by a Fourier Series

$$F_c(t) = \frac{A_0}{2} + \sum_{n=1}^m A_n \cos n\Omega t + \sum_{n=1}^m B_n \sin n\Omega t \quad (3-44)$$

where

$$\Omega = \frac{2\pi}{T} , \quad (3-45)$$

then

$$\int_0^T F_c(\tau) = \frac{1}{2} A_0 T + \sum_{n=1}^m \frac{A_n}{n\Omega} \sin n\Omega t \Big|_0^T - \sum_{n=1}^m \frac{B_n}{n\Omega} \cos n\Omega t \Big|_0^T \quad (3-46)$$

$$= \frac{1}{2} A_0 T . \quad (3-47)$$

So Condition 3-42, which requires that the net impulse be zero, implies

$$A_0 = 0 . \quad (3-48)$$

Condition 3-41 becomes

$$F(T) = F(0) = 0 = \sum_{n=1}^m A_n = 0 , \quad (3-49)$$

whereas condition 3-45 yields

$$\int_0^T \int_0^t F_c(\tau) d\tau = \frac{1}{\Omega} \sum_{n=1}^m \frac{B_n}{n} = 0 . \quad (3-50)$$

There are an infinite number of solutions to Equations 3-49 and 3-50. These equations will be satisfied so as to best approximate the experimental force-time curve in the sense of least squares. To this end we will assume that the experimental force-time function $F(t)$ is given, and that we wish to approximate it by a new function

$$F'(t) = \sum_{n=1}^m A'_n \cos n\Omega t + \sum_{n=1}^m B'_n \sin n\Omega t , \quad (3-51)$$

such that

$$E = \frac{\min}{A'_n, B'_n} \int_0^T \left[F(t) - F'(t) \right]^2 dt \quad (3-52)$$

subject to the constraint of Equations 3-49 and 3-50.

To accomplish this, the constraint equations will be adjoined to Equation 3-52 with undetermined multipliers in the usual Lagrange multiplier technique. The function to be minimized becomes

$$E = \int_0^T \left[F(t) - \left(\sum_{n=1}^m A_n' \cos n\Omega t + B_n' \sin n\Omega t \right) \right]^2 dt + \lambda_1 \sum_{n=1}^m A_n' + \lambda_2 \sum_{n=1}^m B_n' . \quad (3-53)$$

The condition for a minimum is

$$\frac{\partial E}{\partial B_J} = \frac{\partial E}{\partial A_J} = 0 \quad J = 1, m . \quad (3-54)$$

Applying these relations to Equation 3-53,

$$\frac{\partial E}{\partial A_J} = 0 = -2 \int_0^T \left[F(t) - \left(\sum_{n=1}^m A_n' \cos n\Omega t + B_n' \sin n\Omega t \right) \right] \cos J\Omega t dt + \lambda_1 , \quad (3-55)$$

$$\frac{\partial E}{\partial B_J} = 0 = -2 \int_0^T \left[F(t) - \left(\sum_{n=1}^m A_n' \cos n\Omega t + B_n' \sin n\Omega t \right) \right] \sin J\Omega t dt + \frac{\lambda_2}{J} . \quad (3-56)$$

Noting that

$$\int_0^T \sin n\Omega t \cos J\Omega t dt = 0 , \quad (3-57)$$

$$\int_0^T \sin n\Omega t \sin J\Omega t dt = 0 \quad \text{if } J \neq n = \frac{T}{2} \quad \text{if } J = n , \quad (3-58)$$

$$\int_0^T \cos n\Omega t \cos J\Omega t dt = 0 \quad \text{if } J \neq n = \frac{T}{2} \quad \text{if } J = n, \quad (3-59)$$

yields

$$A_{J'} = \frac{2}{T} \int_0^T F(t) \cos J\Omega t dt - \frac{\lambda_1}{T}, \quad (3-60)$$

$$B_{J'} = \frac{2}{T} \int_0^T F(t) \sin J\Omega t dt - \frac{\lambda_2}{JT}. \quad (3-70)$$

Now the first terms on the right in Equations 3-60 and 3-70 are the ordinary unconstrained Fourier coefficients of Equation 3-47. Therefore, we can write Equations 3-60 and 3-70.

$$A_{J'} = A_J - \frac{\lambda_1}{T}, \quad (3-71)$$

$$B_{J'} = B_J - \frac{\lambda_2}{JT}. \quad (3-72)$$

Substituting Equations 3-71 and 3-72 in the constraint Equations 3-49 and 3-50, we determine the Lagrange multipliers

$$\lambda_1 = \frac{T}{m} \sum_{J=1}^m A_J, \quad (3-73)$$

$$\lambda_2 = T \sum_{J=1}^m \frac{B_J}{J} \bigg/ \sum_{J=1}^m \frac{1}{J^2}. \quad (3-74)$$

Inserting Equations 3-73 and 3-74 into Equations 3-71 and 3-72, we obtain the expressions for the revised coefficients

$$A_{K'} = A_K - \frac{1}{m} \sum_{J=1}^m A_J , \quad (3-75)$$

$$B_{K'} = B_K - \frac{1}{K} \sum_{J=1}^m \frac{B_J}{J} \bigg/ \sum_{J=1}^m \frac{1}{J^2} . \quad (3-76)$$

Equations 3-75 and 3-76 state that in order to obtain the best fit to the experimental data in a least-squares sense subject to the constraint Equations 3-49 and 3-50, it is merely necessary to correct the ordinary unconstrained Fourier coefficients as indicated.

Figure 3-8 shows a comparison of the force histories resulting from the corrected and uncorrected Fourier coefficients for the case of console operation push-pull minimum. The figure shows fairly close agreement, except at the beginning and end. Reference to the actual force histories (Reference 1) indicates that the corrected coefficients result in closer agreement than the uncorrected (published) coefficients.

3.5 DATA REDUCTION

The basic approach to this study required the generation of an enormous amount of data, specifically, a permutation of the following parameters: 3 vehicle configurations, 6 to 8 types of crew motion, 10 experiment locations, 3 to 5 crew locations, and 2 crew station orientations. These permutations resulted in a large number of runs (somewhere between 1,080 and 2,400). Each run resulted in between 3 and 7 graphs for a total of from 3,240 to 16,800 graphs for the entire run schedule. The actual number of resulting graphs were never counted, but the best guess is that about 6,000 graphs were plotted. The usefulness of such a large amount of raw data is highly doubtful. Therefore, 6 functionals were used to reduce the results of each case to 22 real numbers. The functionals used were the following:



Figure 3-8. Comparison of Force Histories Resulting from Corrected and Uncorrected Fourier Coefficients

1. Maximum acceleration (resultant and three components).
2. Maximum velocity (resultant and three components).
3. Maximum angular velocity (resultant and three components).
4. Maximum angular displacement (resultant and three components).
5. Root-Mean-Square (RMS) of acceleration components.
6. Root-Mean-Square (RMS) of velocity components.

Items 1, 3, and 4 of this list are self-explanatory. Item 2, maximum velocity, was chosen for two reasons: first, some of the acceleration experiments are not only dependent on the maximum acceleration but also on the time duration or frequency content of the acceleration history, which implies a measure of the velocity; and second, the square of the velocity is related to the maximum kinetic energy imparted to the experiment. Item 5, RMS acceleration components, gives a measure of the standard deviation of the acceleration history (the average of the acceleration history is zero because of the conservation of momentum). Finally, Item 6, RMS velocity components, can be interpreted as either the standard deviation of the velocity history (again, the average value is zero) or as a measure of the average value of kinetic energy imparted to the system.

3.6 DISCUSSION OF COMPUTED RESULTS

Fifty-four cases were computed for the three vehicle configurations under consideration. Sketches of the configurations with their dynamic parameters and a list of the output stations and crew stations are shown in Figures 3-1 to 3-3. A code composed of three numbers and the abbreviated name of a crew motion is used to distinguish between the cases. The first number is the vehicle configuration, the second is the number of the crew station location, and the third the number of a crew station orientation. The complete code describing the results of a computer run, for instance, might be 1-4-3 T. Max. This would refer to Spacecraft Configuration 1, Crew Motion Input Station 4, Crew Member Orientation 3, and the type of crew-motion disturbance: console operation torquing maximum.

The angular orientation of the crew station coordinate system relative to the spacecraft coordinate system is given by the 3-x-3 direction cosine matrix which transforms the input forces and moments from the crew station to the

spacecraft reference system. Since the crew-member orientations used were all multiples of 90° , the direction cosine matrixes have only three nonzero elements, and the nonzero elements are ± 1 . A second three-digit code was devised which enables the direction cosine matrix to be reconstructed. The order of the code corresponds to the rows of the matrix and the digits indicate which column of the particular row contains the unit and whether it has a plus or minus sign. For example, Orientation No. 1 has the code 1-32 from which one can reconstruct the direction cosine matrix.

$$\begin{bmatrix} 1 & 0 & 0 \\ 0 & 0 & -1 \\ 0 & 1 & 0 \end{bmatrix}$$

The codes corresponding to the crew station orientation number are listed in Table 3-3.

Table 3-3
CREW MEMBER ORIENTATIONS

Orientation No.	1	2	3	4	5	6	7
Code	1-32	123	312	-12-3	-132	1-2-3	3-1-2
Orientation No.	8	9	10	11			
Code	13-2	2-13	-3-12	-132			

The crew-motion input force and moment curves were corrected to conform to dynamical reality as described in Section 3.4. Figures 3-9 to 3-32 are graphs of the forces and moments versus time for the various crew motions used. The coefficients of the Fourier expansions used to generate the graphs are given in Tables 3-4 to 3-6. The seven columns correspond to the range of the index on the coefficients in increasing order (1 to 7) from left to right, and the three rows correspond to the X, Y, Z components respectively.

Table 3-7 and 3-8 summarize the peak angular excursions and peak angular

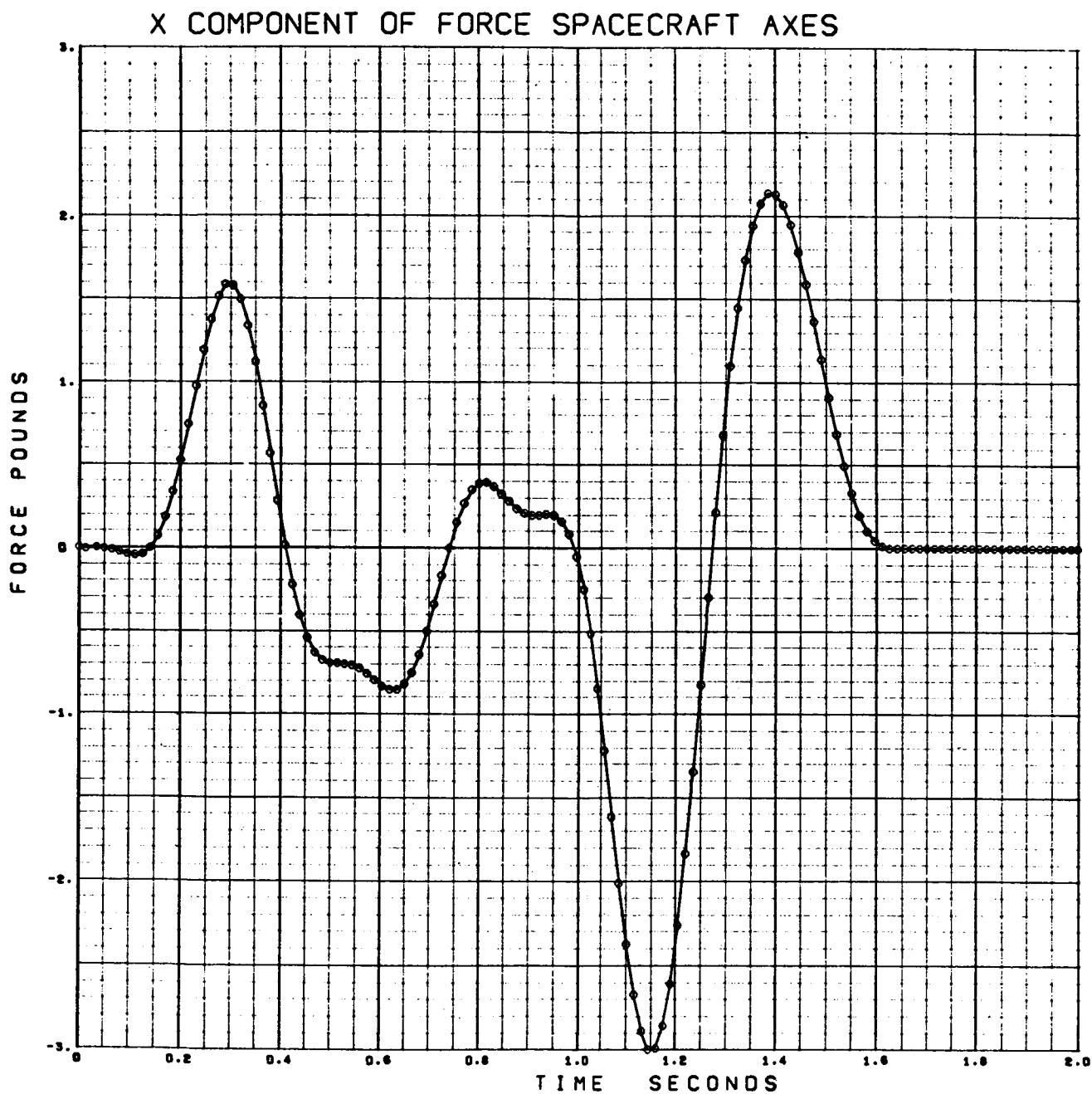


Figure 3-9. Console Operation Push-Pull Maximum (X Component of Force Spacecraft Axes)

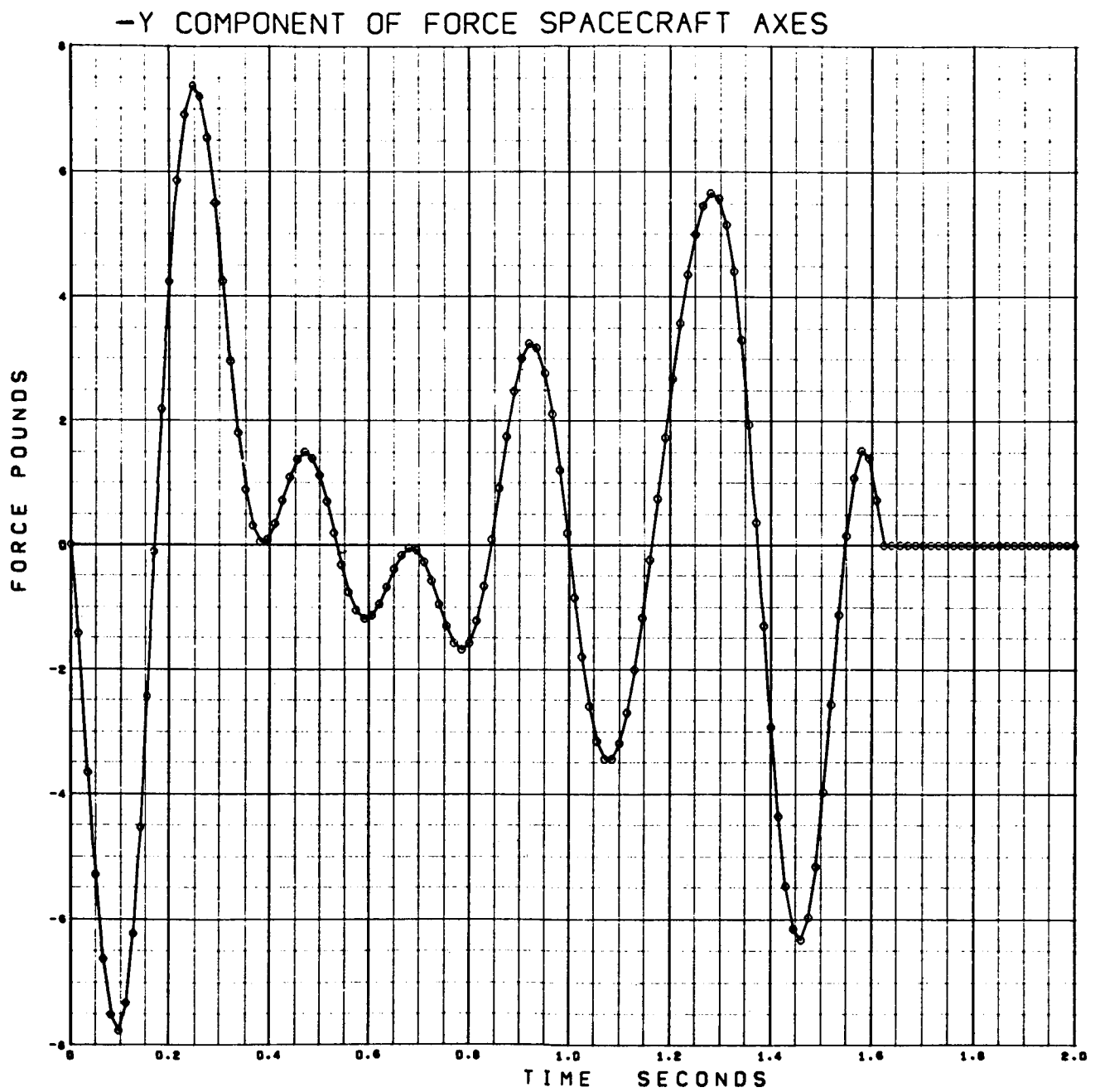


Figure 3-10. Console Operation Push-Pull Maximum (-Y Component of Force Spacecraft Axes)

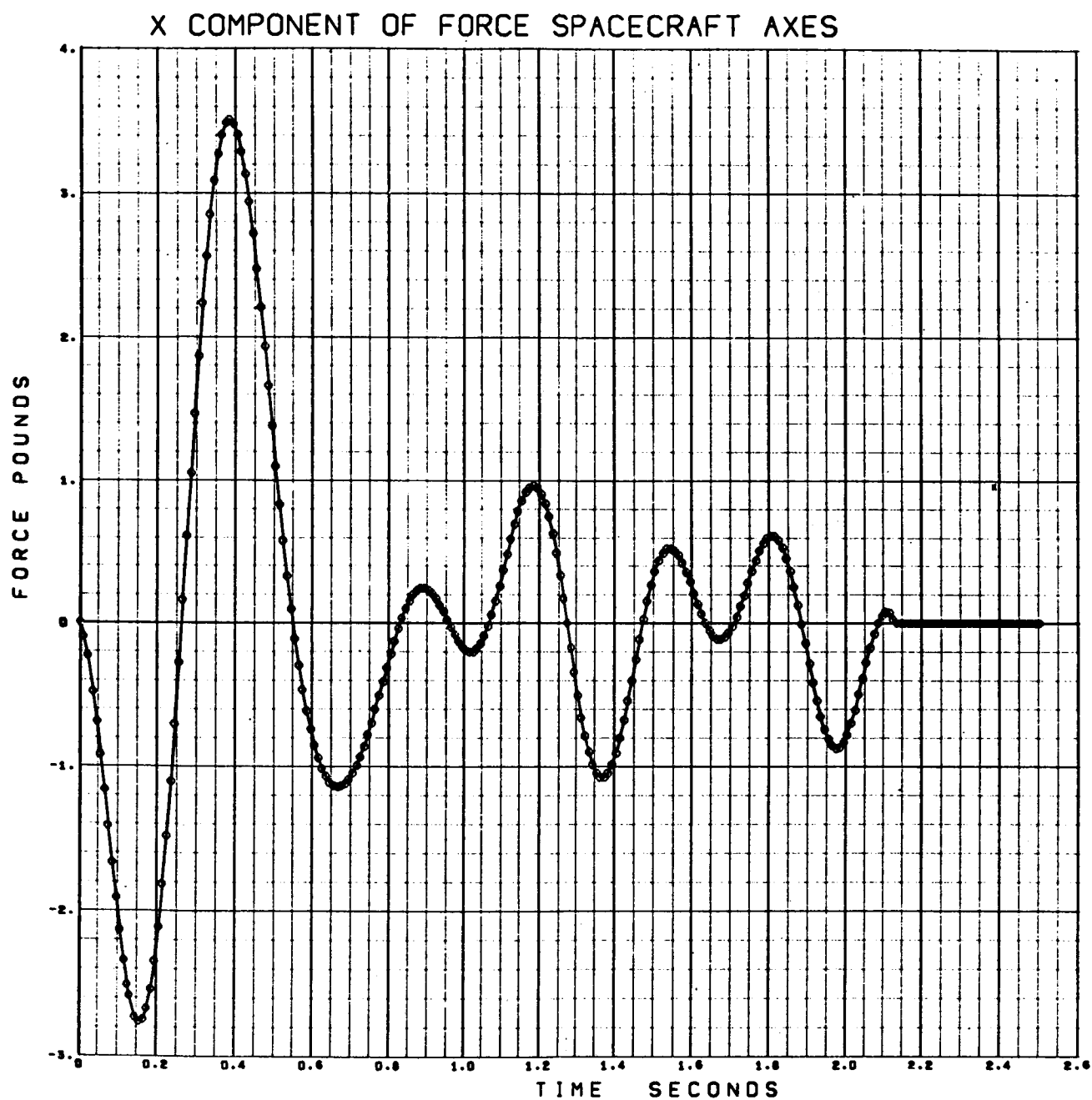


Figure 3-11. Console Operation Push-Pull Nominal (X Component of Force Spacecraft Axes)

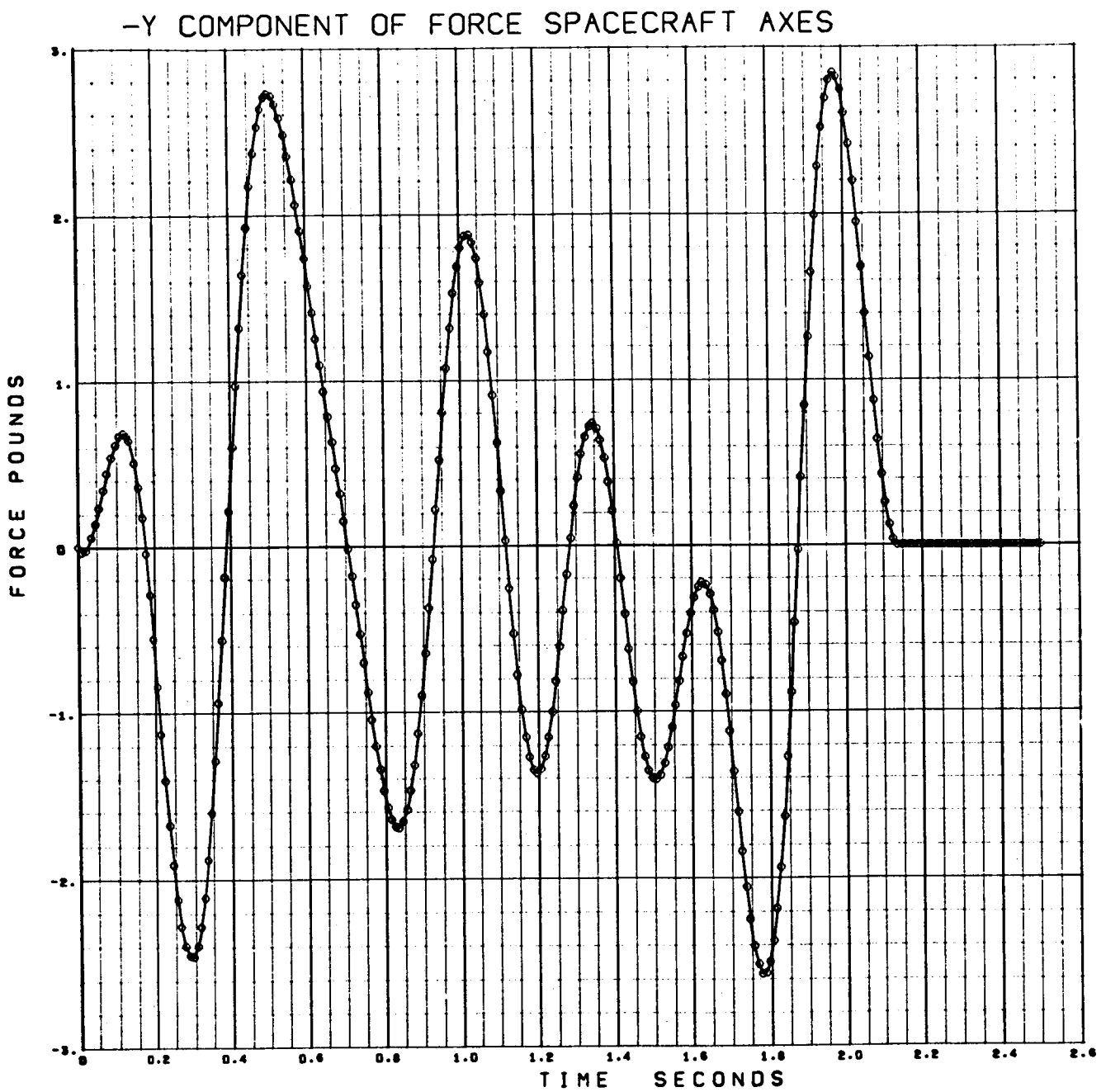


Figure 3-12. Console Operation Push-Pull Nominal (-Y Component of Force Spacecraft Axes)

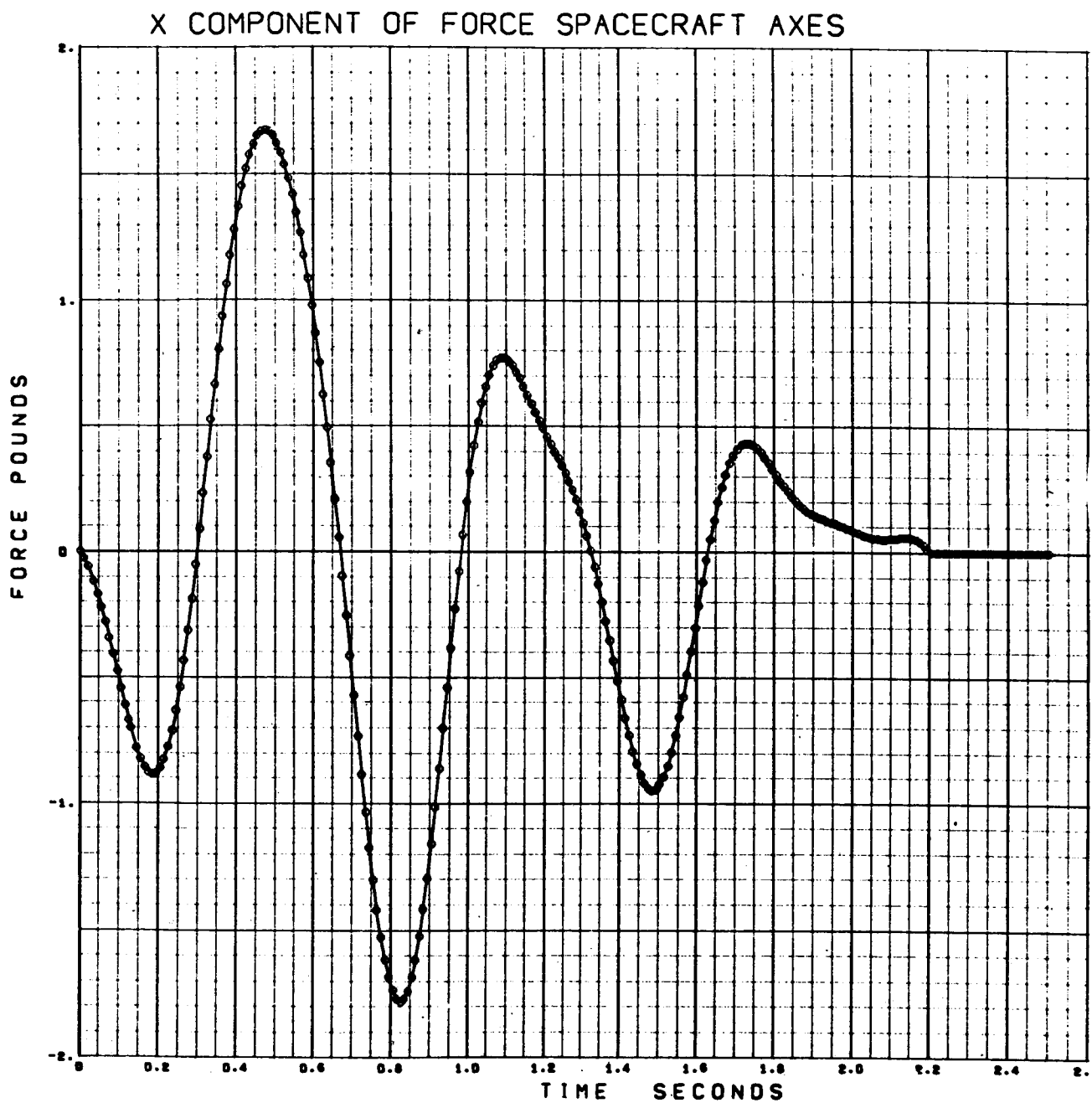


Figure 3-13. Console Operation Push-Pull Minimum (X Component of Force Spacecraft Axes)

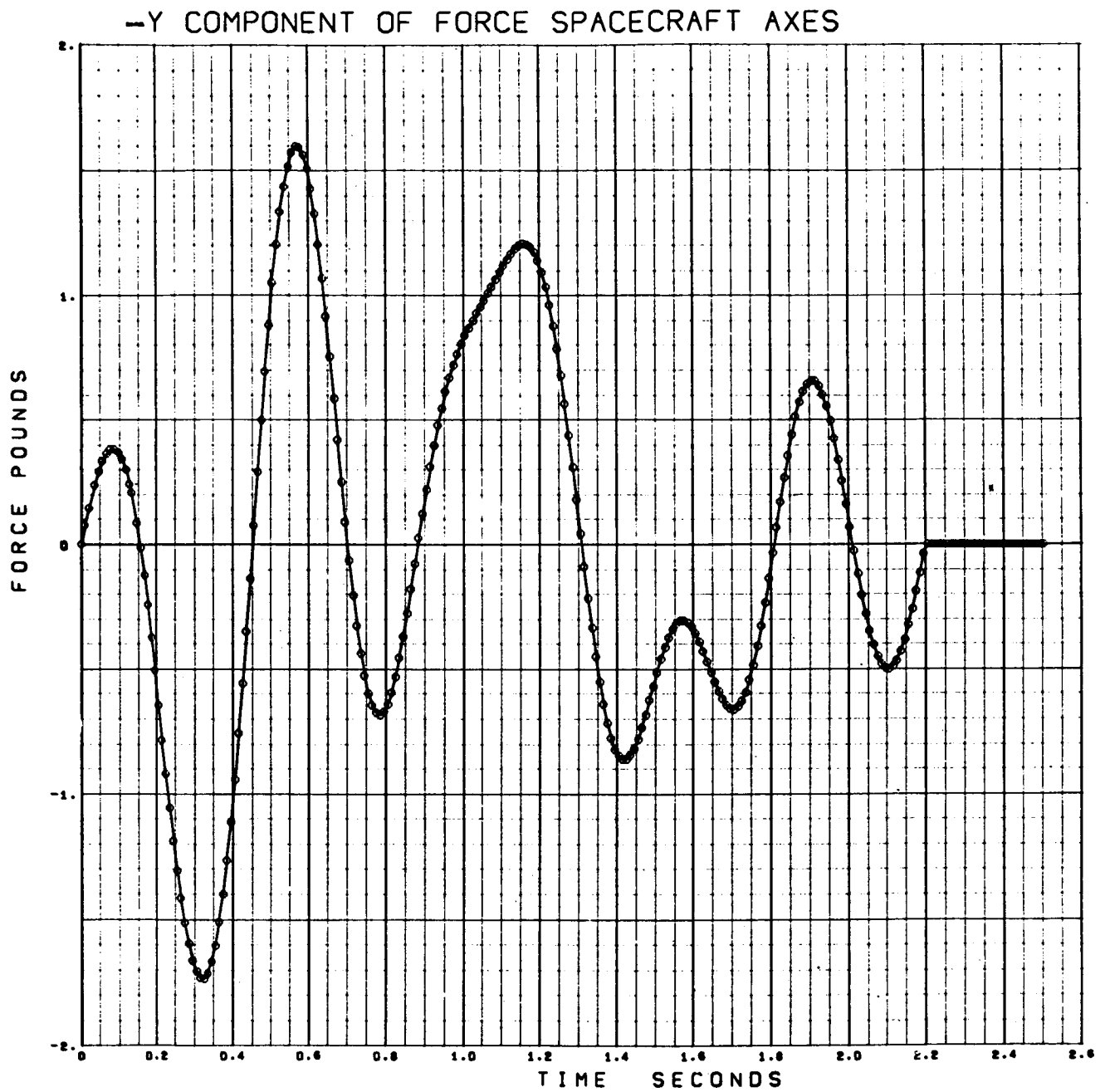


Figure 3-14. Console Operation Push-Pull Minimum (-Y Component of Force Spacecraft Axes)

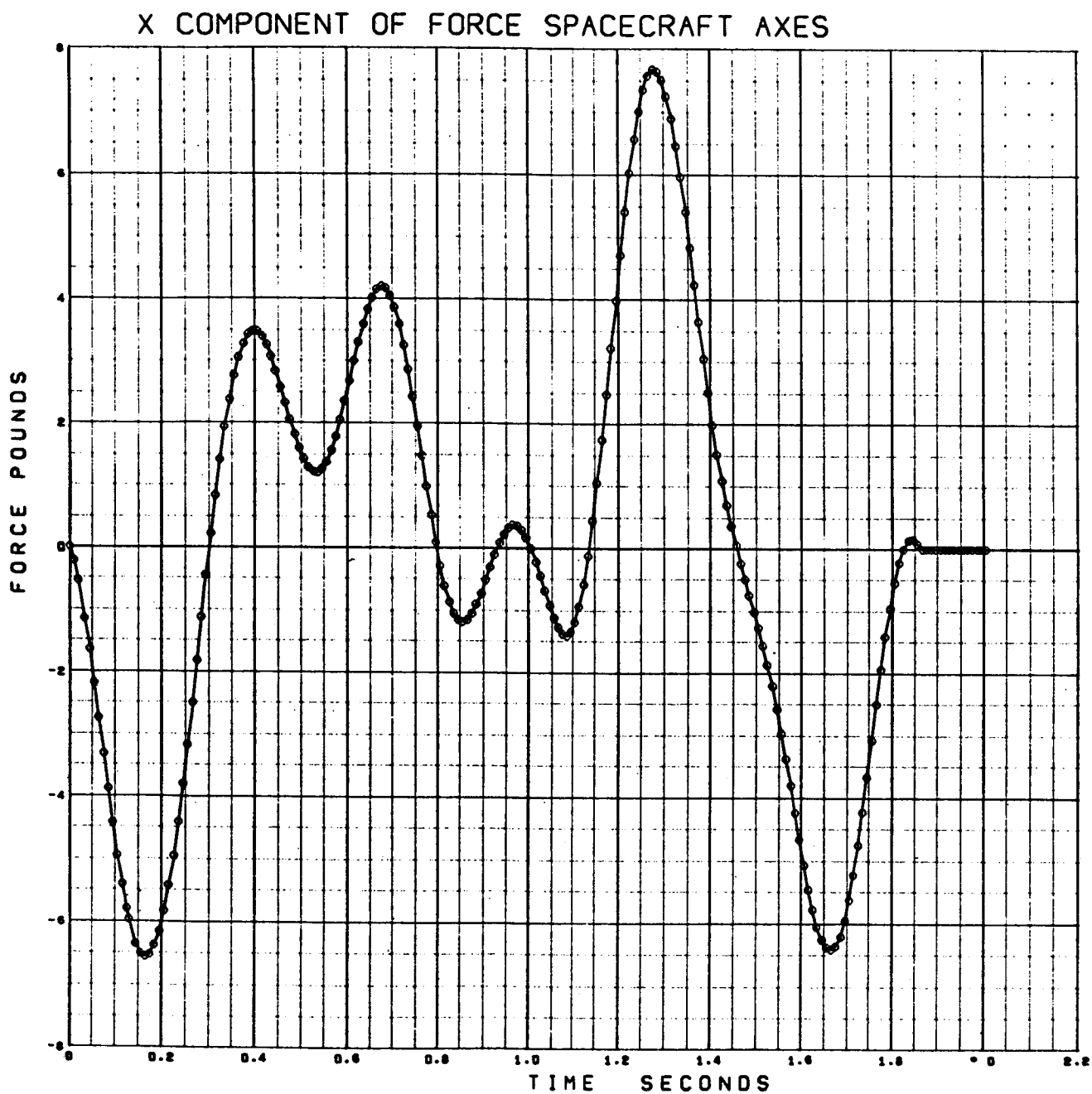


Figure 3-15. Console Operations Torquing Maximum (X Component of Force Spacecraft Axes)

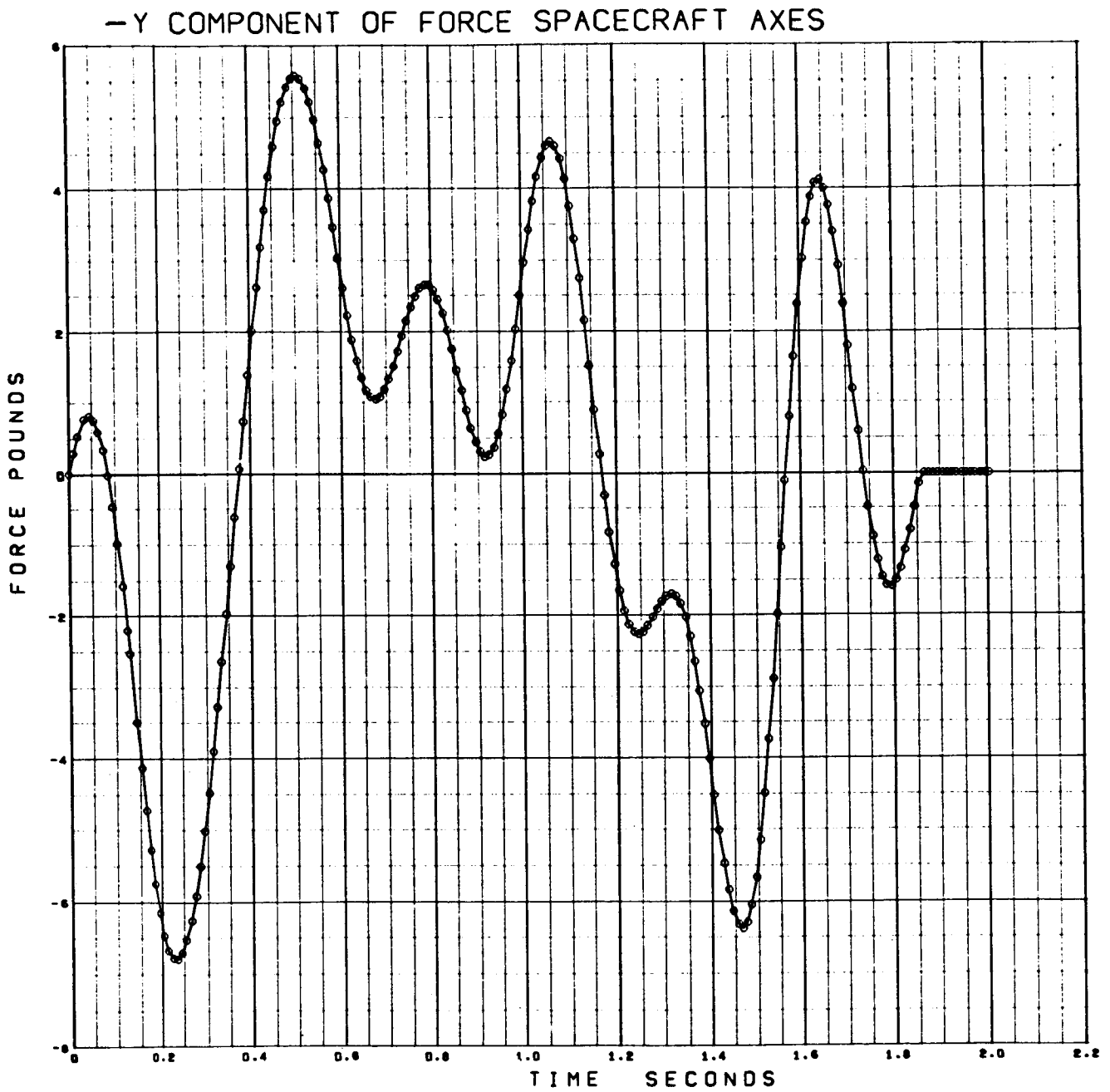


Figure 3-16. Console Operation Torquing Maximum (-Y Component of Force Spacecraft Axes)

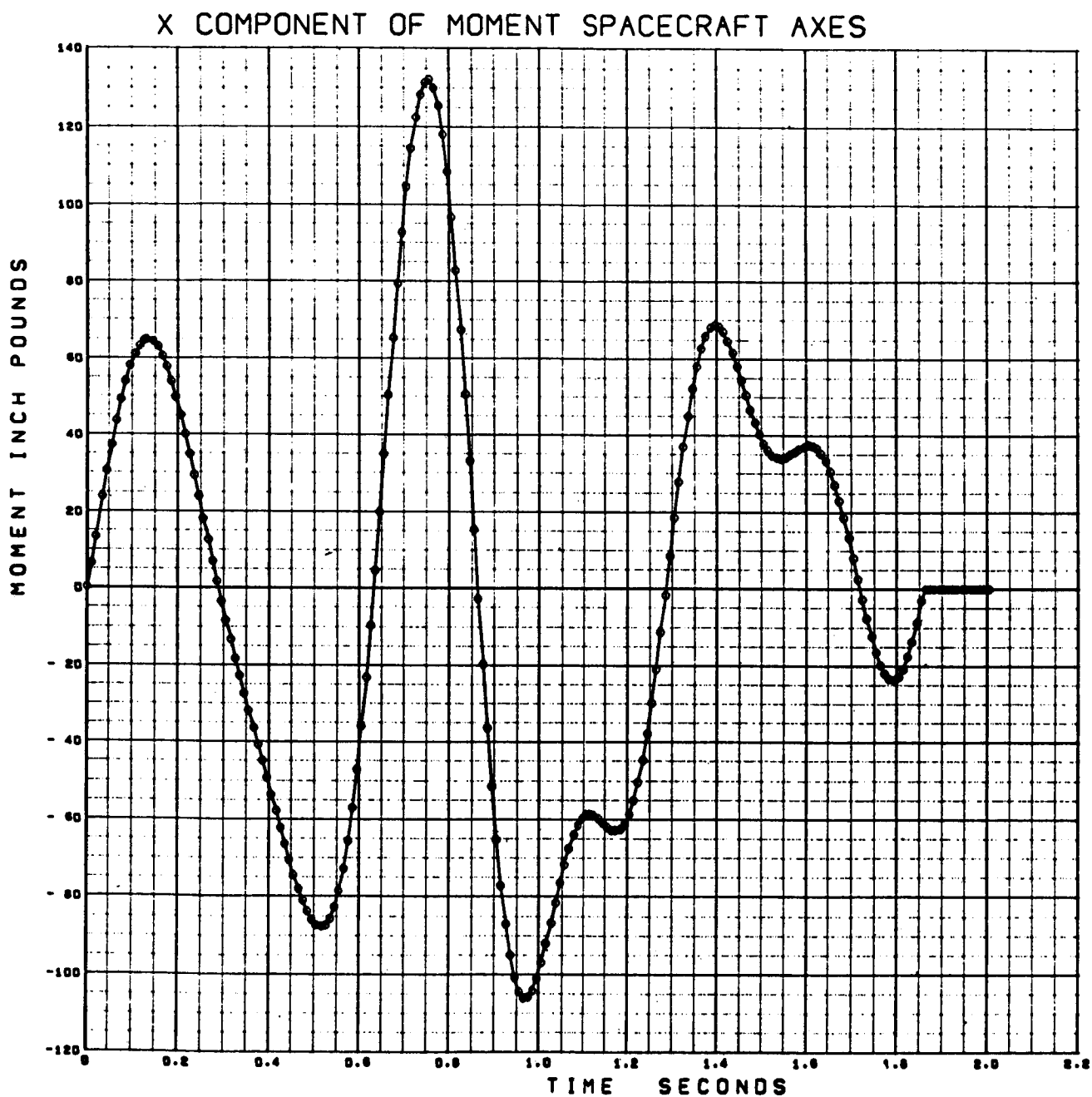


Figure 3-17. Console Operation Torquing Maximum (X Component of Moment Spacecraft Axes)

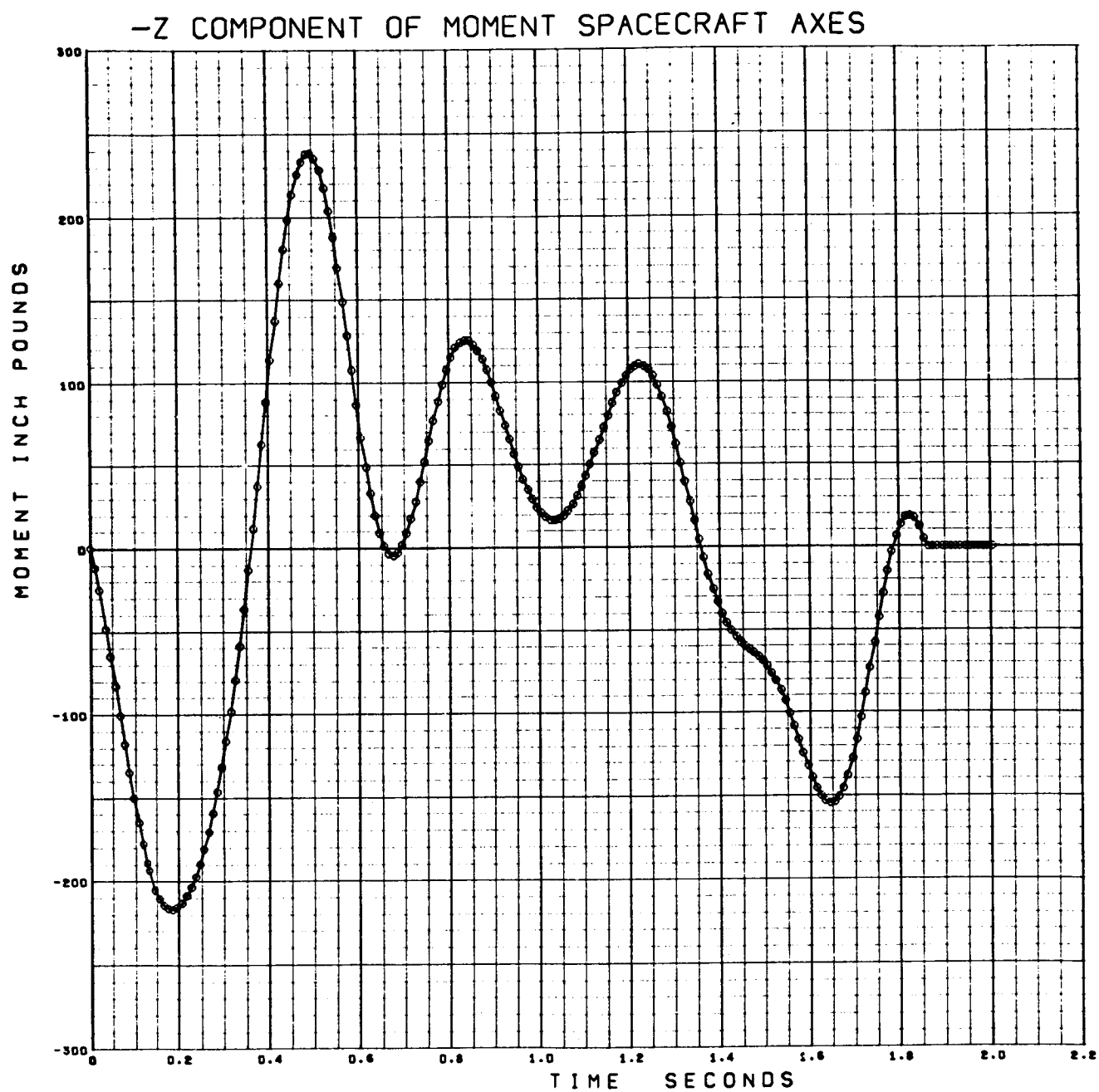


Figure 3-18. Console Operation Torquing Maximum (\bar{r} -Z Component of Moment Spacecraft Axes)

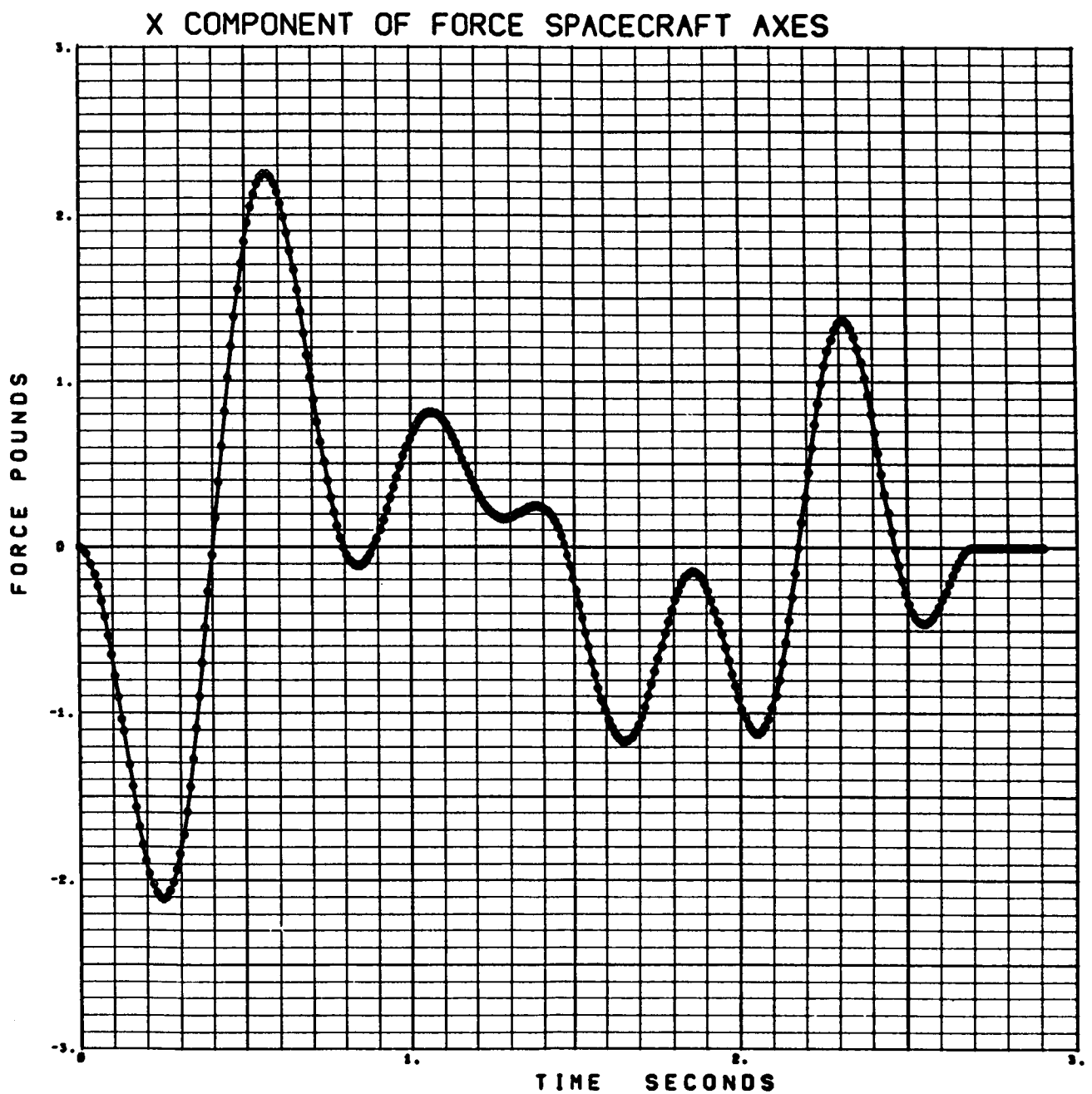


Figure 3-19. Console Operation Torquing Nominal (X Component of Force Spacecraft Axes)

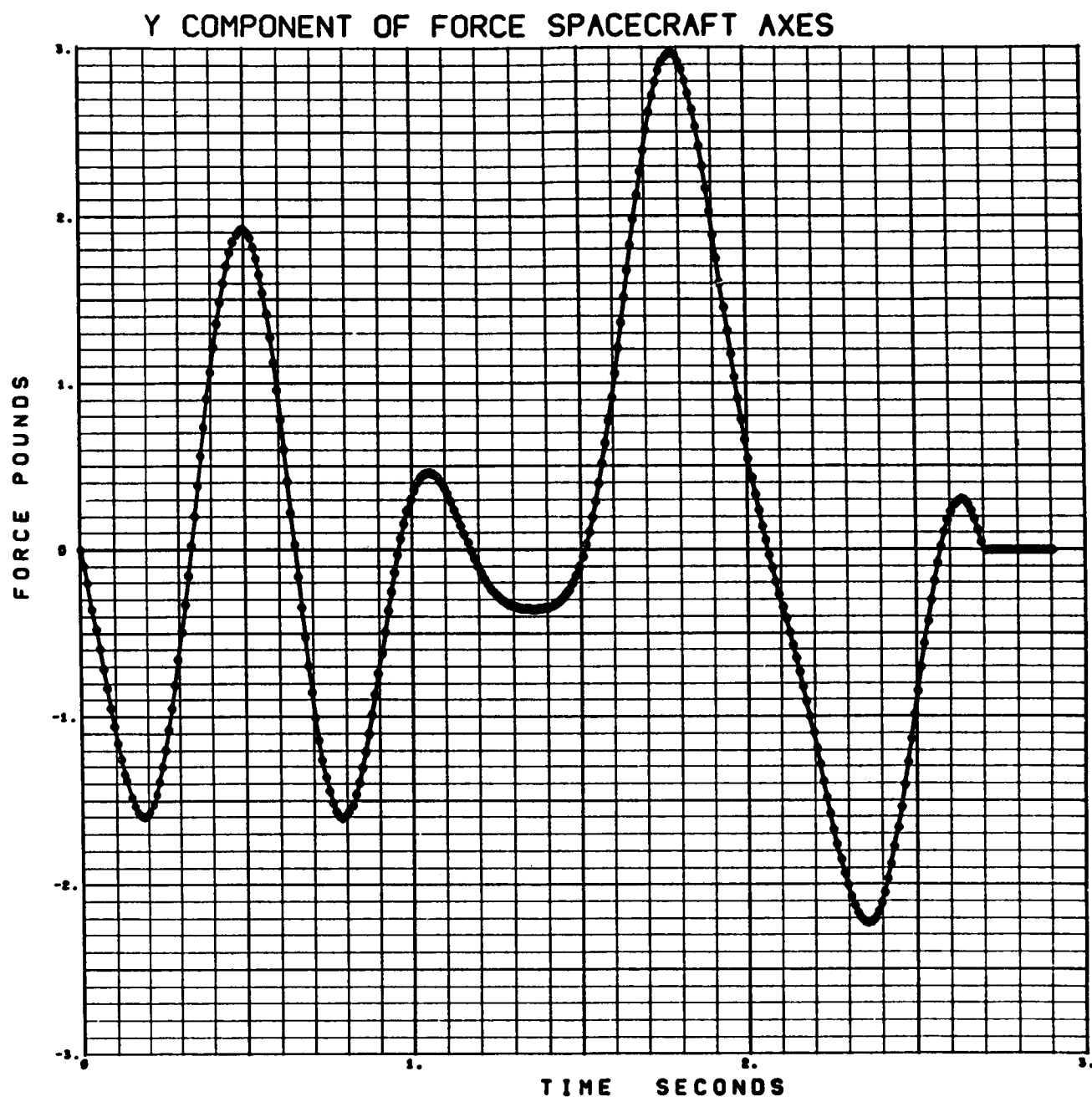


Figure 3-20. Console Operation Torquing Nominal (Y Component of Force Spacecraft Axes)

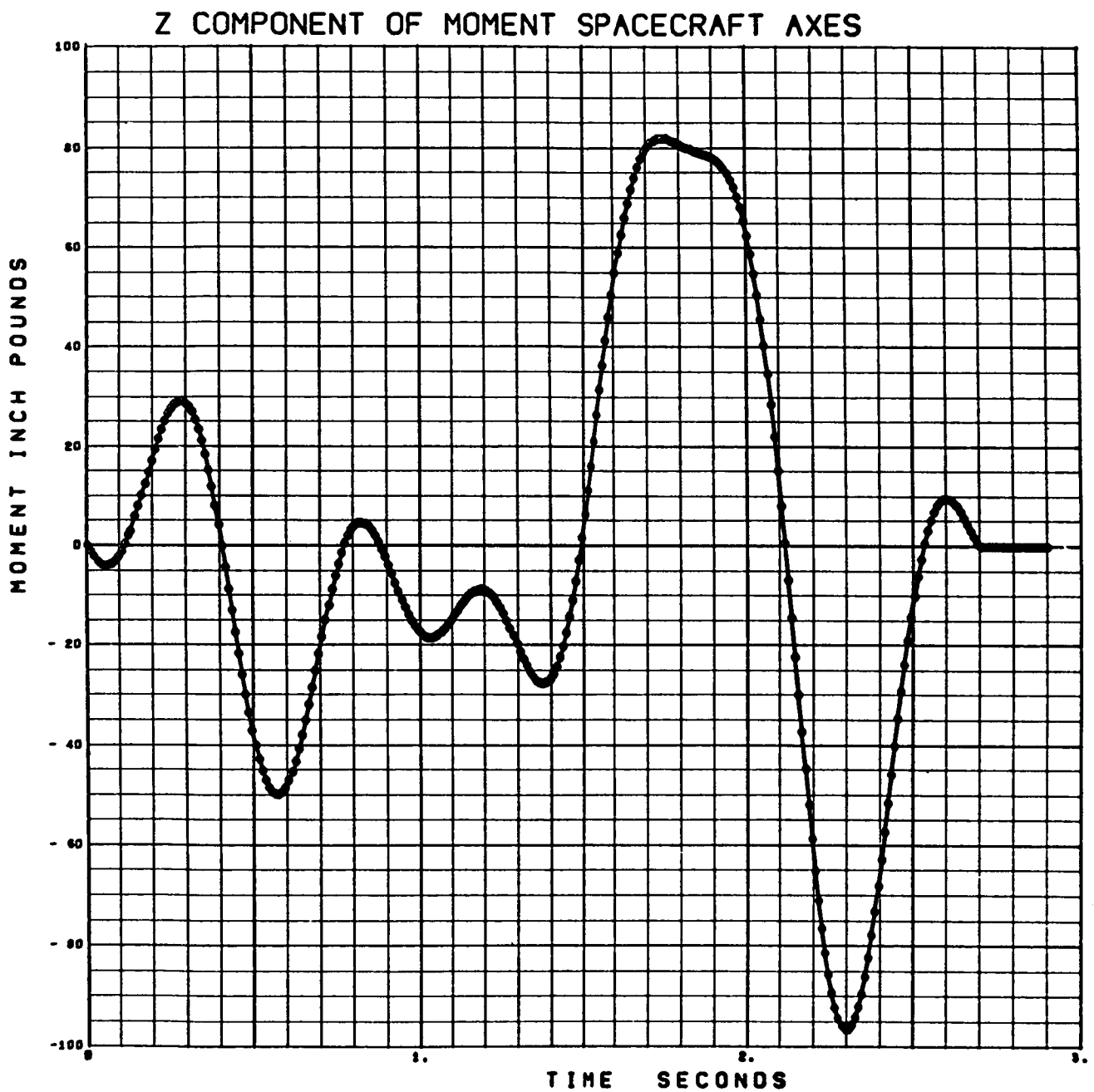


Figure 3-21. Console Operation Torquing Nominal (Z Component of Moment Spacecraft Axes)

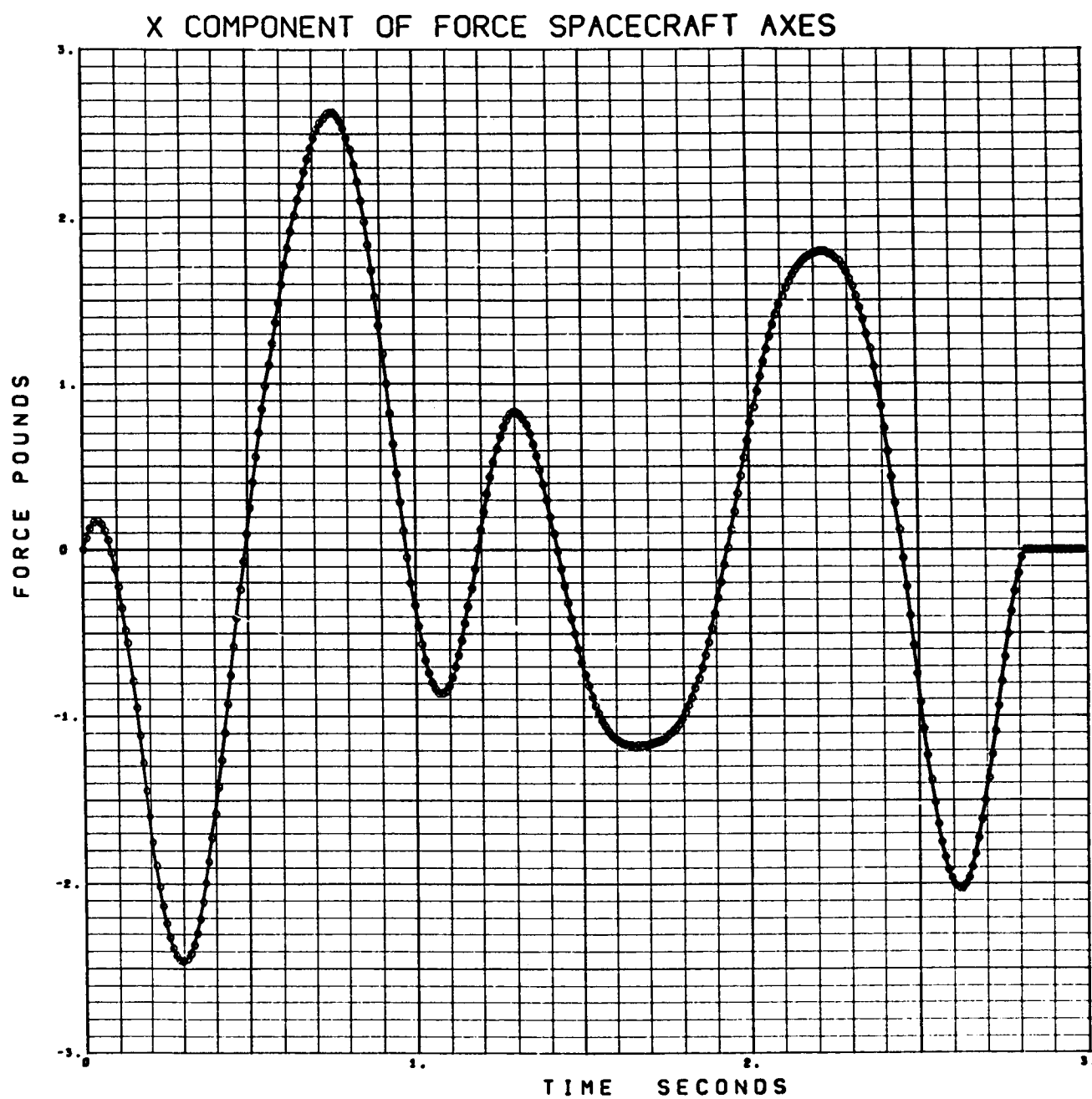


Figure 3-22. Console Operation Torquing Minimum (X Component of Force Spacecraft Axes)

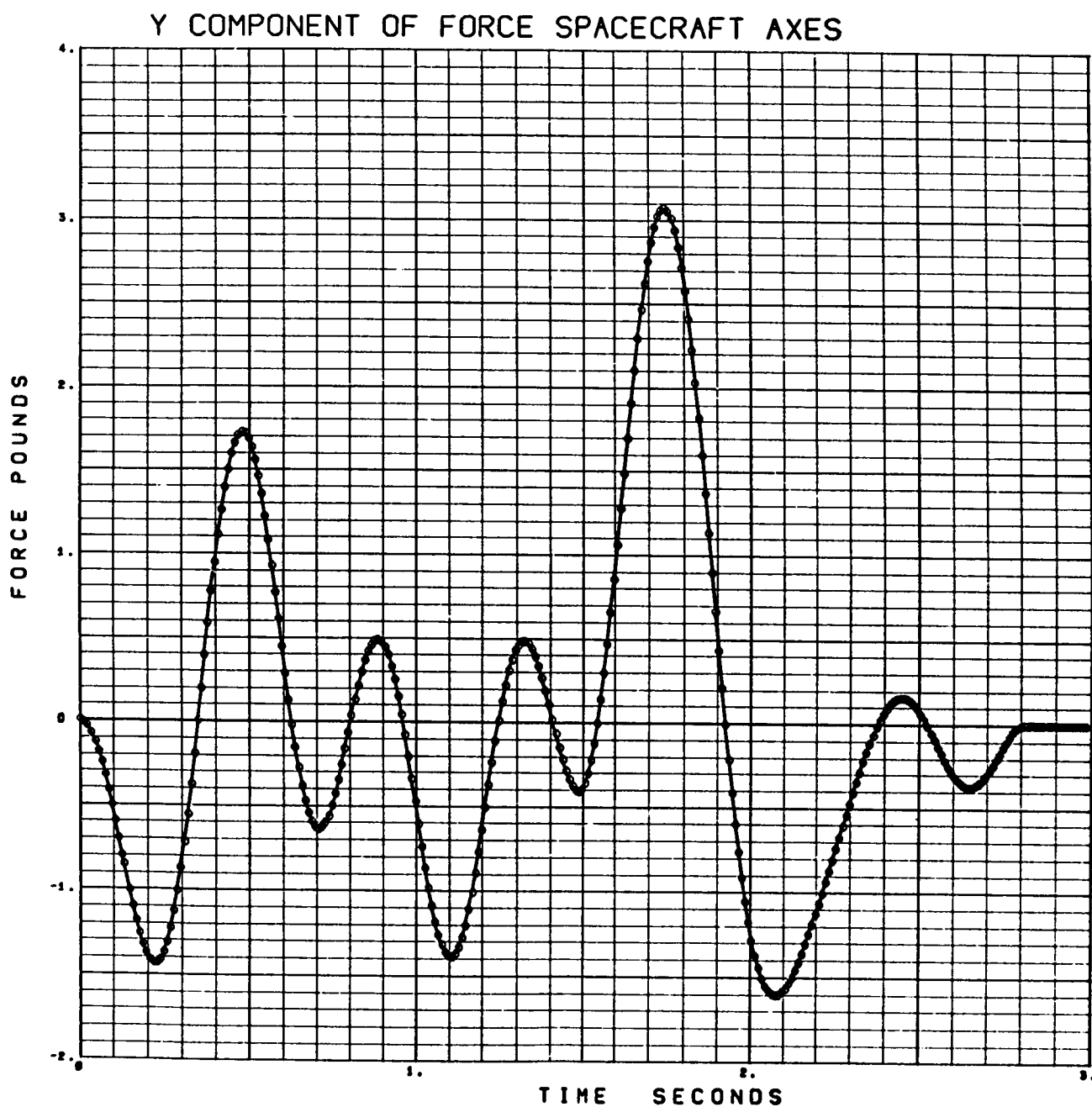


Figure 3-23. Console Operation Torquing Minimum (Y Component of Force Spacecraft Axes)

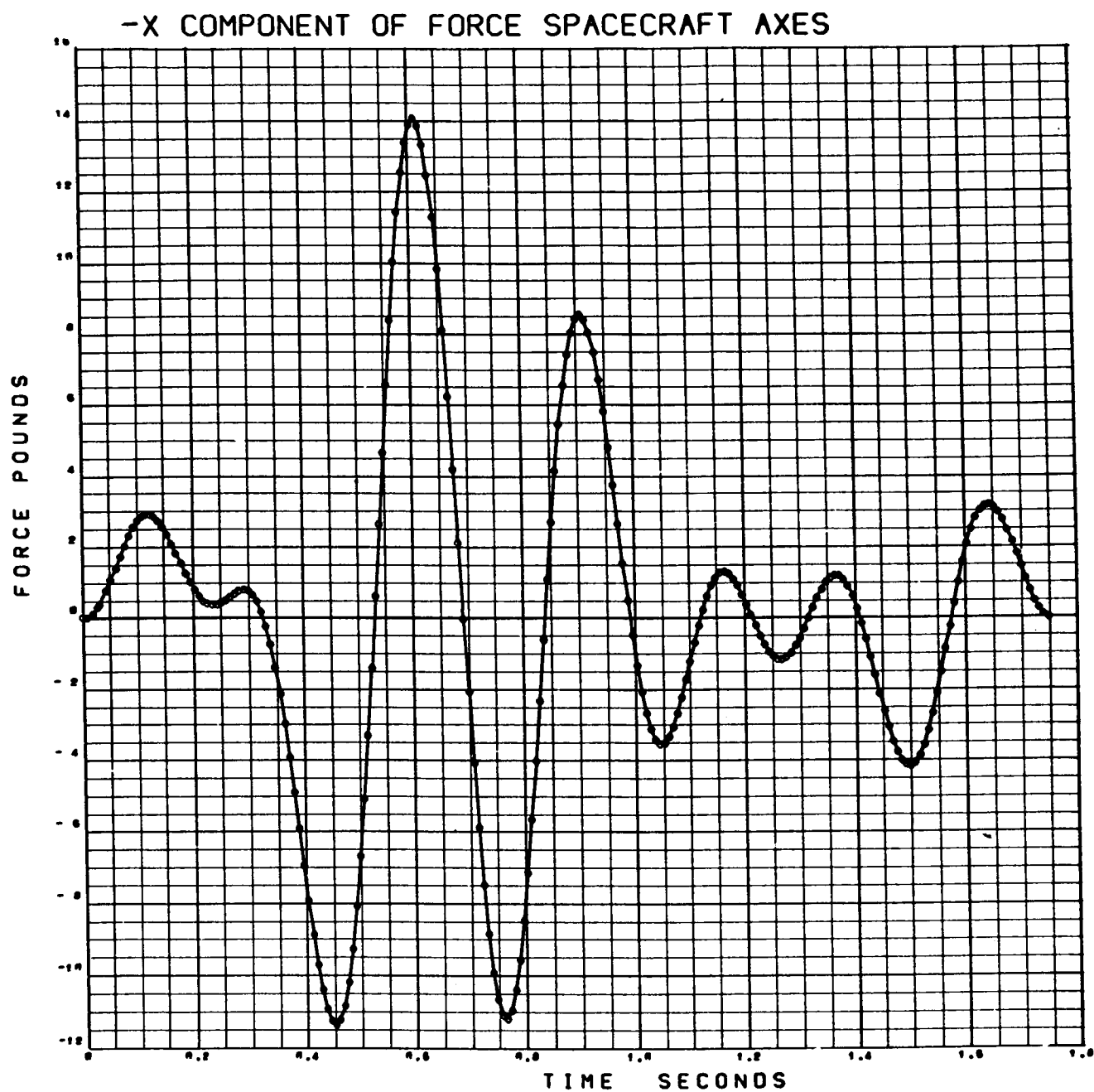


Figure 3-24. Cough (-X Component of Force Spacecraft Axes)

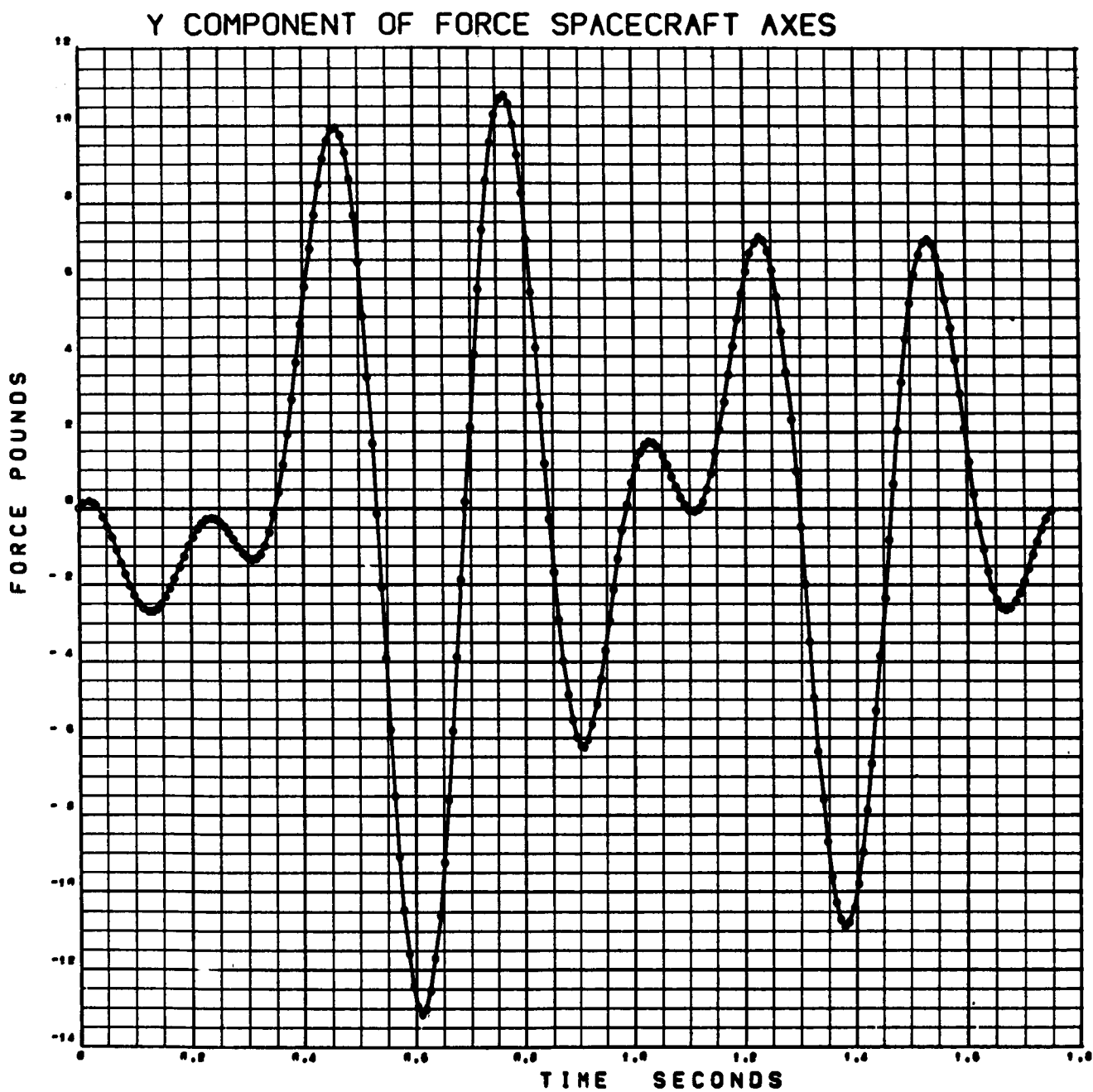


Figure 3-25. Cough (Y Component of Force Spacecraft Axes)

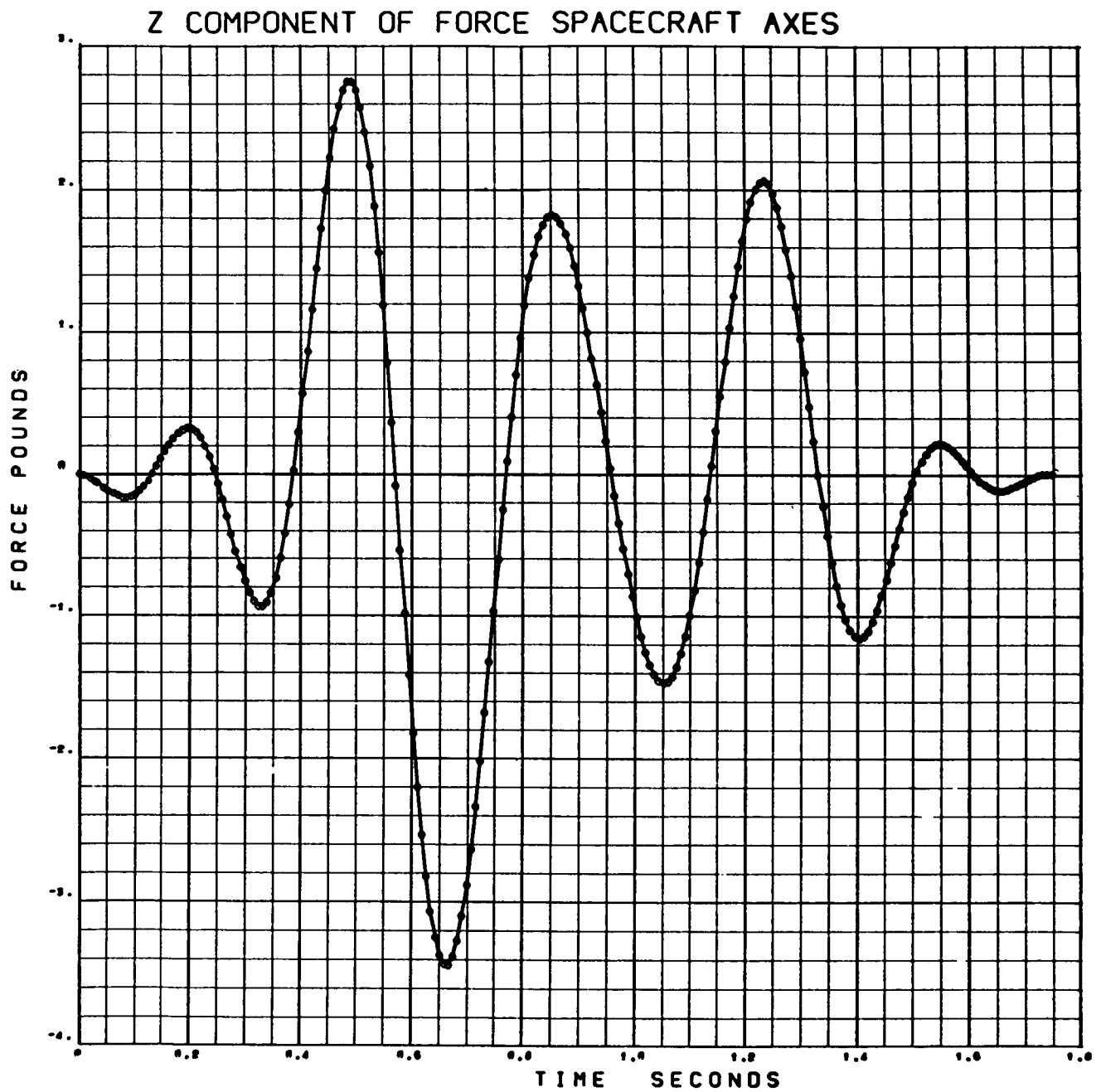


Figure 3-26. Cough (Z Component of Force Spacecraft Axes)

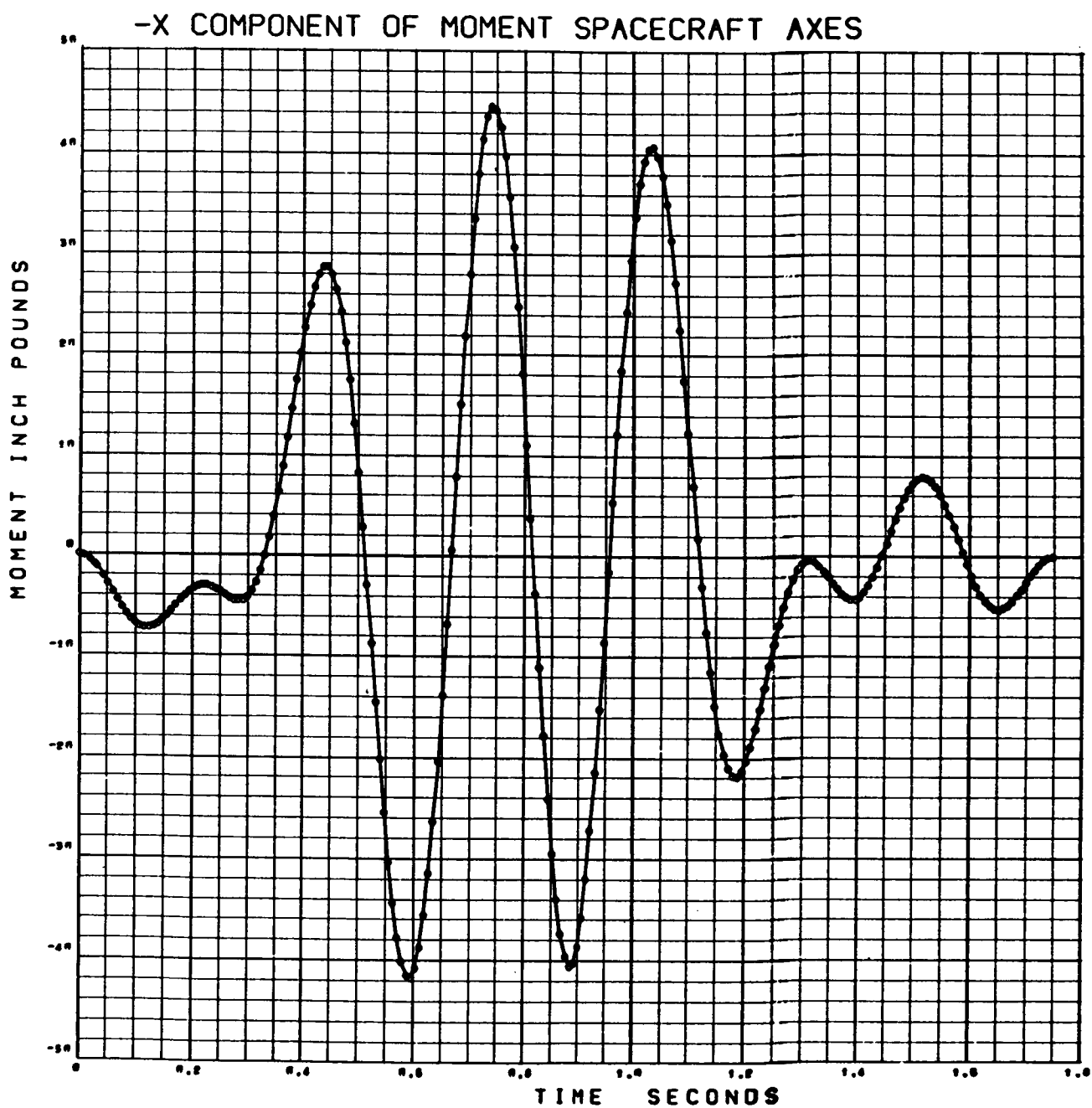


Figure 3-27. Cough (-X Component of Force Spacecraft Axes).

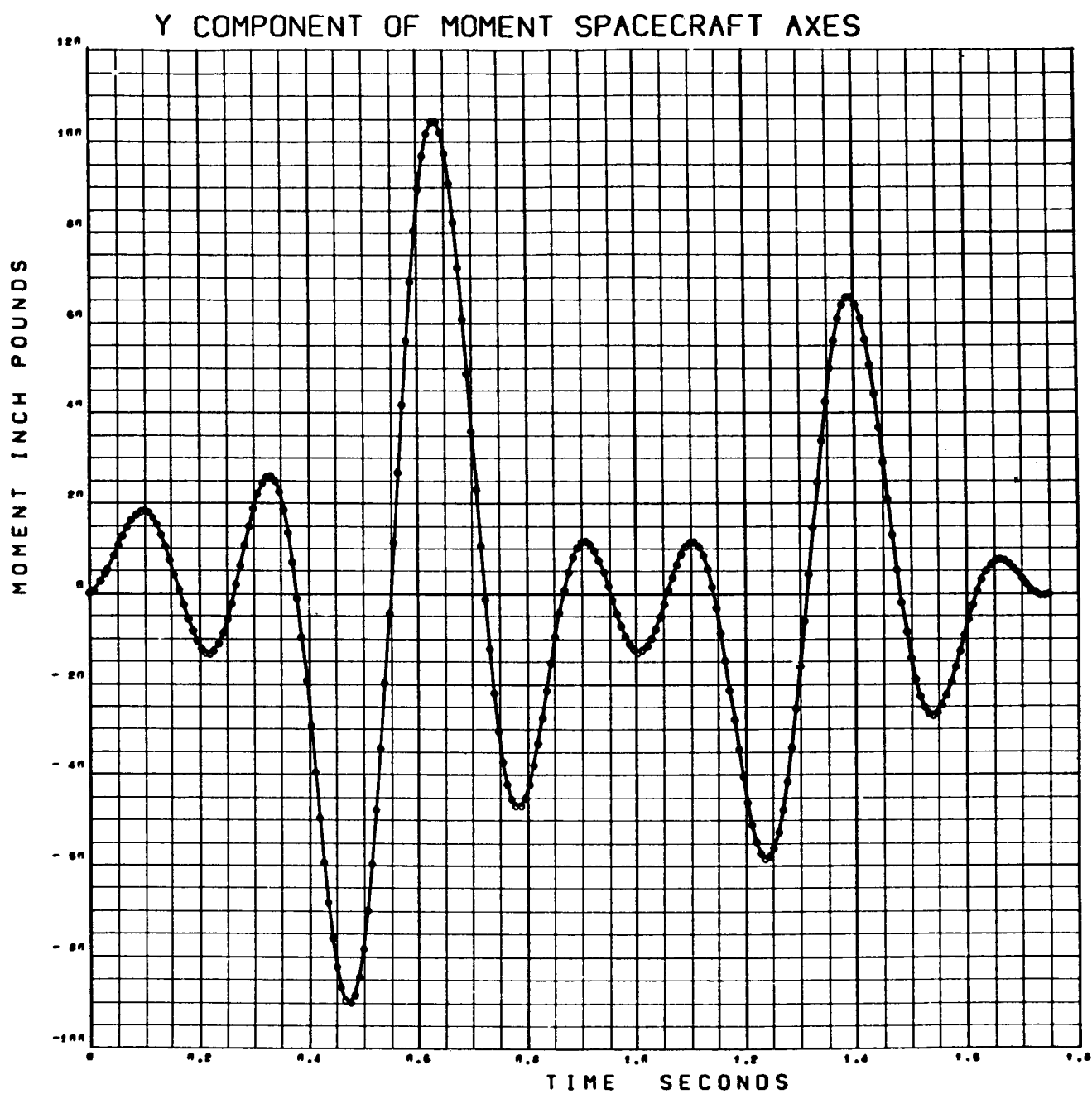


Figure 3-28. Cough (Y Component of Moment Spacecraft Axes)

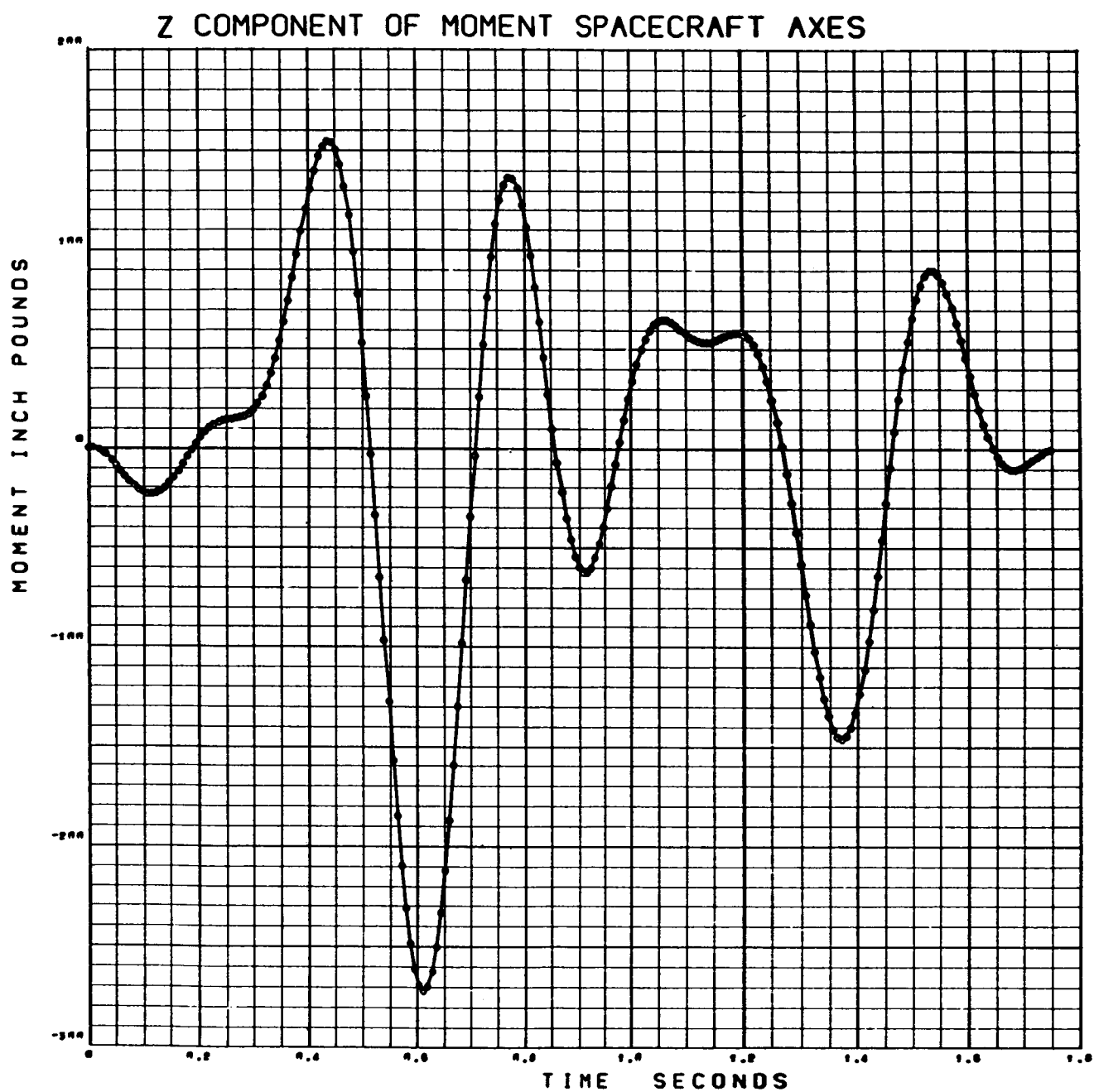


Figure 3-29. Cough (Z Component of Moment Spacecraft Axes)

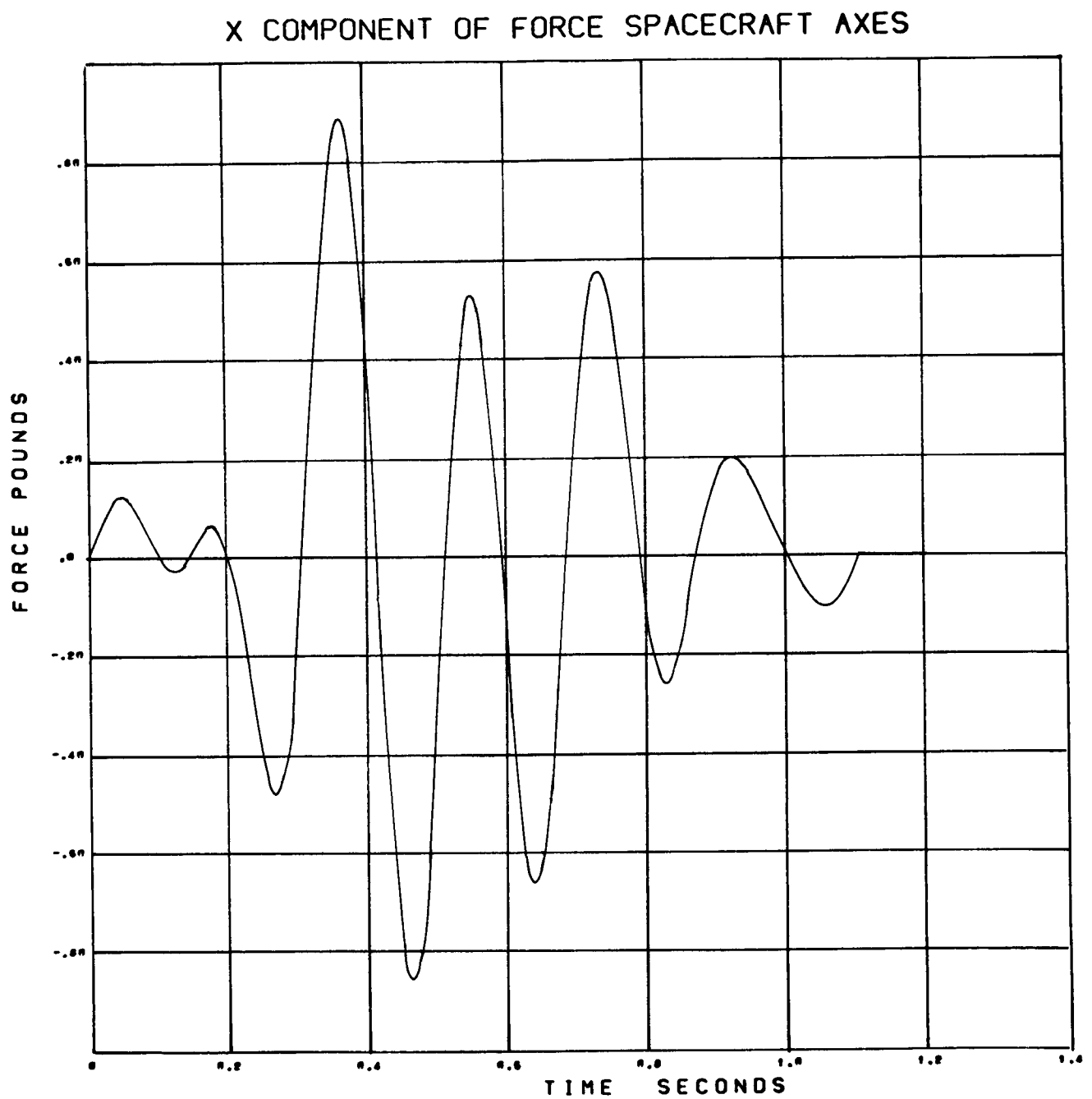


Figure 3-30. Heartbeat (X Component of Force Spacecraft Axes)

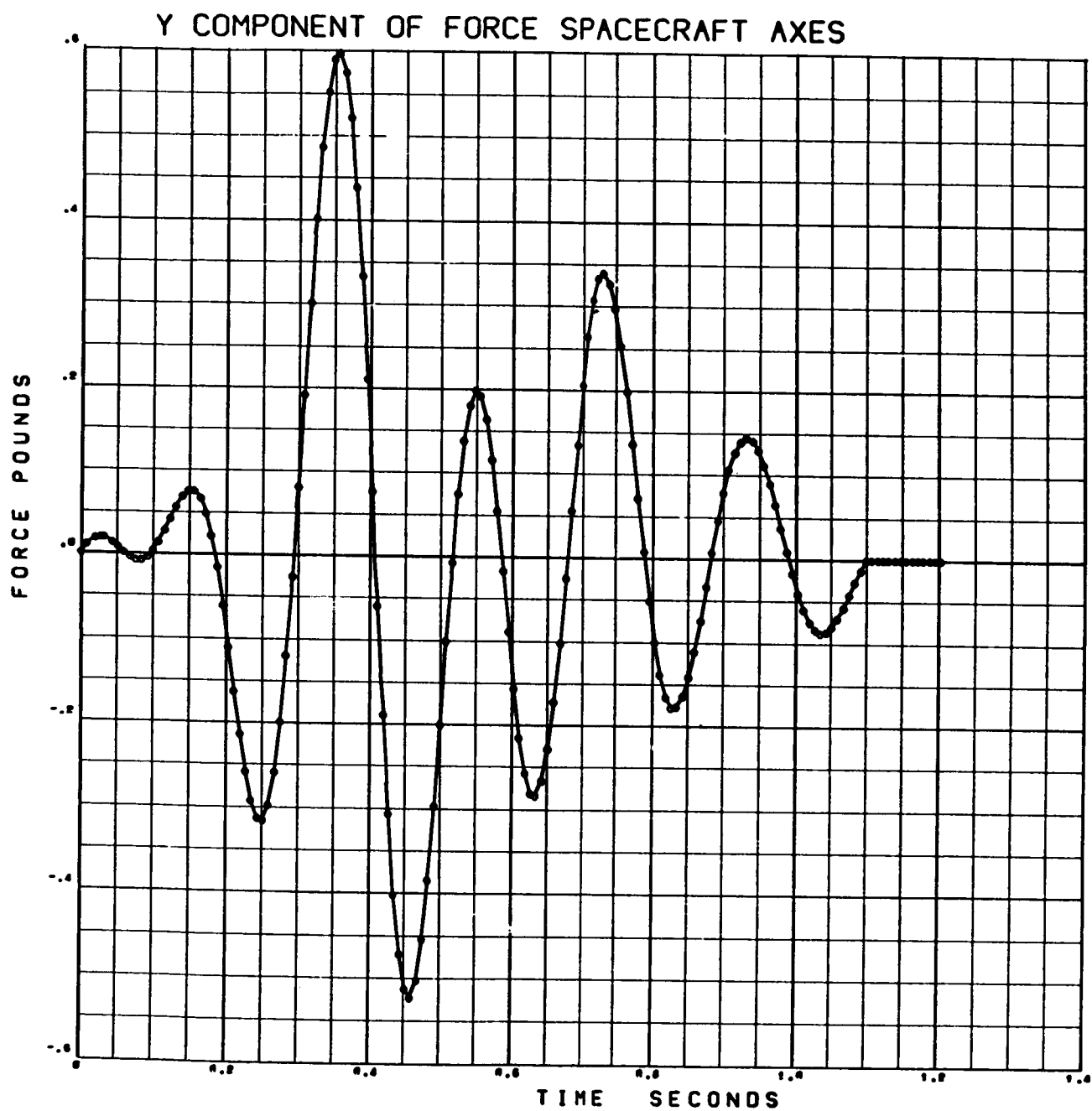


Figure 3-31. Heartbeat (Y Component of Force Spacecraft Axes)

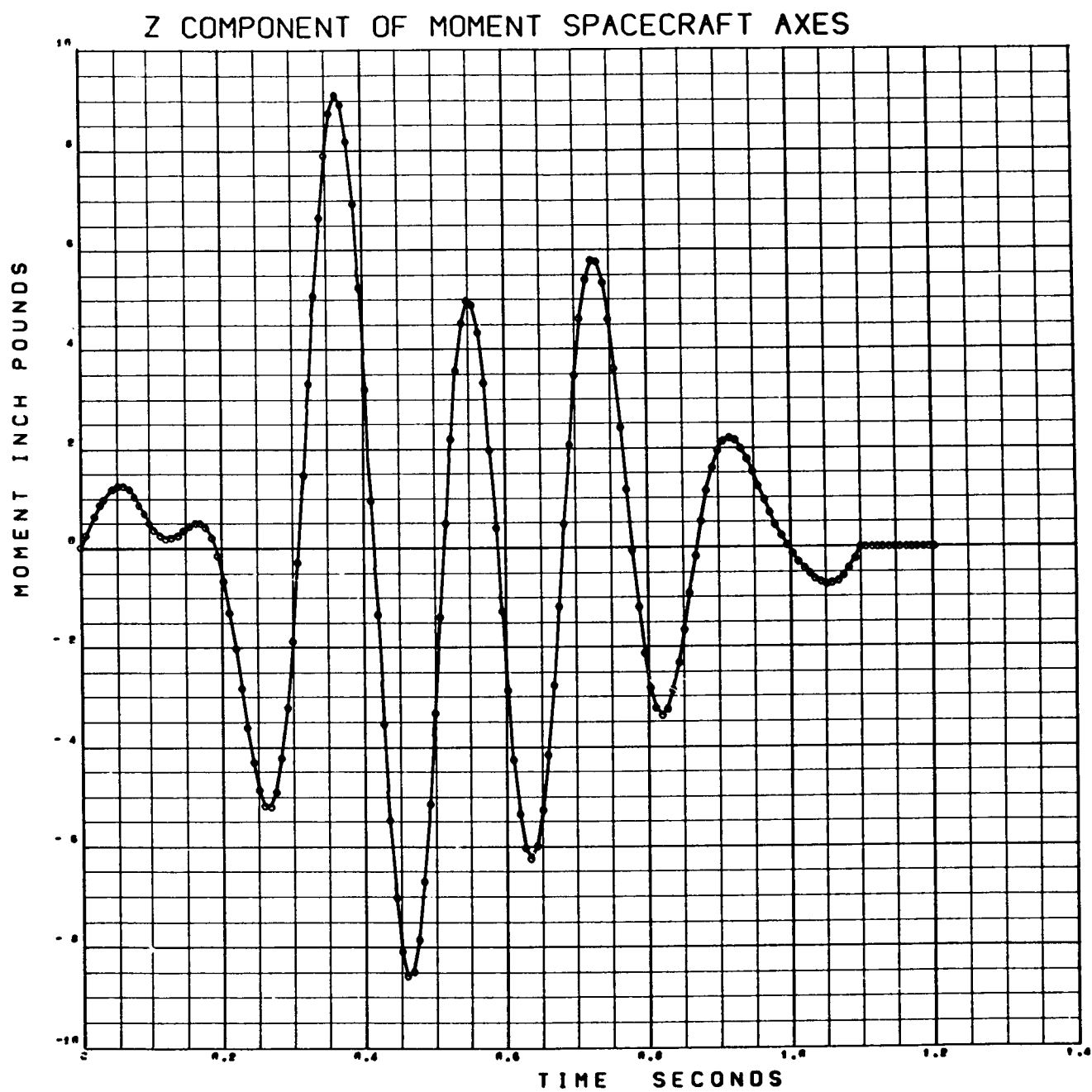


Figure 3-32. Heartbeat (Z Component of Force Spacecraft Axes)

Table 3-5 A

CONSOLE OPERATION TORQUE MAXIMUM

FOURIER FREQ 0.33780500+01 TIME = 0.18600000+01						
FORCE COSINE COEF						
-0.27080759+01	-0.24971479+01	0.20357200+01	0.12044660+01	0.79360780-00	0.12894500+01	-0.11802000+00
0.18586850+01	-0.77851155-00	-0.86406795-00	-0.30707076-00	0.14613651-00	0.93576885-00	-0.99094005-00
-0.00000000	-0.00000000	-0.00000000	-0.00000000	-0.00000000	-0.00000000	-0.00000000
FORCE SINE COEF						
0.42382974-01	0.53117084-00	0.28179936-00	-0.14764881+01	-0.43099160-00	0.81553658-00	-0.57752749-00
-0.10829881+01	0.16008840+01	0.27861923+01	-0.41477862-00	-0.12143304+01	-0.12826933+01	-0.60089217-00
-0.00000000	-0.00000000	-0.00000000	-0.00000000	-0.00000000	-0.00000000	-0.00000000
MOMENT COSINE COEF						
0.22967682+02	0.41396432-00	0.17437911+01	-0.25078482+02	0.15126846+02	-0.20999177+02	0.58329443+01
0.00000000	0.00000000	0.00000000	0.00000000	0.00000000	0.00000000	0.00000000
0.10554102+03	0.33195668+02	-0.47280974+02	-0.65504989+02	-0.12891470+02	-0.25311952+01	-0.10528050+02
MOMENT SINE COEF						
-0.72826090+01	-0.29159071+02	0.64705927+02	-0.89542472+01	0.10570978+01	0.11845655+02	0.24245776+01
-0.00000000	-0.00000000	-0.00000000	-0.00000000	-0.00000000	-0.00000000	-0.00000000
-0.28696036+02	0.13578034+02	0.49343979+02	0.30199445+02	-0.38274383+02	0.22134979+02	0.13124155+02

CONSOLE OPERATION TORQUE NOMINAL

FOURIER FREQ 0.23271000+01 TIME = 0.27000000+01						
FORCE COSINE COEF						
-0.12527284-00	-0.35451974-00	-0.44363254-00	0.11278856+00	0.33712606-00	0.35583226-00	0.11767826+00
-0.64336316-00	-0.38022176-00	0.41740105-00	-0.13591026-00	0.52831194-00	0.33942875-00	-0.12564655-00
-0.00000000	-0.00000000	-0.00000000	-0.00000000	-0.00000000	-0.00000000	-0.00000000
FORCE SINE COEF						
0.42801756-00	-0.55209826-00	-0.46821854-00	-0.45111408-00	0.21717518-00	0.49762518-00	-0.66427331-01
-0.22816201-00	0.10400503+01	0.43893799-01	-0.98000865-00	-0.23880028-00	-0.11027861-01	-0.83259637-01
-0.00000000	-0.00000000	-0.00000000	-0.00000000	-0.00000000	-0.00000000	-0.00000000

CONSOLE OPERATION TORQUE MINIMUM

FOURIER FREQ 0.22360100+01 TIME = 0.28100000+01						
FORCE COSINE COEF						
-0.32862956-00	-0.11670491+01	-0.20310816-00	0.10497530+01	0.21085134-00	0.21622294-00	0.22195950-00
-0.35160040-00	0.58659650-01	-0.23511510-01	-0.54159880-00	0.29948510-00	0.49443820-00	0.64127749-01
-0.00000000	-0.00000000	-0.00000000	-0.00000000	-0.00000000	-0.00000000	-0.00000000
FORCE SINE COEF						
0.12926918-00	-0.60989376-00	-0.30395206-01	0.23791807-00	0.50921071-00	-0.33538453-01	0.21054266-00
-0.34165516-01	0.63106120-00	-0.80815237-00	-0.18781210-00	0.17456074-00	-0.41630614-00	0.48610993-00
-0.00000000	-0.00000000	-0.00000000	-0.00000000	-0.00000000	-0.00000000	-0.00000000

Note: The columns correspond to coefficient index (1 to 7) from left to right; the rows correspond to x, y, z coefficients from top to bottom.

Table 3-4 *7*
CONSOLE OPERATION PUSH-PULL MAXIMUM

FOURIER FREQ 0.38785100+01 TIME = 0.16200000+01									
FORCE COSINE COEF									
0.67174861-00	0.37448520-00	-0.10555470+01	-0.37205600-00	0.29560592-00	0.19467550-00	-0.10891270+00			
0.64454013-00	0.19306831+01	0.19201851+01	-0.54048597-00	-0.18915989+01	-0.70604870-00	-0.13572750+01			
-0.00000000	-0.00000000	-0.00000000	-0.00000000	-0.00000000	-0.00000000	-0.00000000			
FORCE SINE COEF									
0.28198965-00	-0.27928178-00	-0.69875419-00	0.17879912-00	0.17966870-00	-0.44201192-01	0.12111854+00			
-0.38168985-00	-0.63714757-00	-0.60530527-01	-0.32765229-00	0.22971135+01	0.16700809+01	0.45208821-00			
-0.00000000	-0.00000000	-0.00000000	-0.00000000	-0.00000000	-0.00000000	-0.00000000			

CONSOLE OPERATION PUSH-PULL NOMINAL

FOURIER FREQ 0.29498500+01 TIME = 0.21300000+01									
FORCE COSINE COEF									
-0.14359835-00	-0.50321735-00	-0.92128235-00	0.16033115-00	0.63857085-00	0.33428015-00	0.43491595-00			
-0.12647690-00	-0.26848706-00	-0.34276906-00	-0.90604636-00	0.33814404-00	0.47530974-00	0.83032501-00			
-0.00000000	-0.00000000	-0.00000000	-0.00000000	-0.00000000	-0.00000000	-0.00000000			
FORCE SINE COEF									
0.20051130-00	0.21324784-00	-0.37497860-00	-0.66745547-00	-0.44061323-00	0.37168685-00	0.76274457-01			
-0.46775536-00	0.21184158-00	0.99240312-00	0.52221474-00	-0.46078793-00	0.31991326-00	-0.42477019-00			
-0.00000000	-0.00000000	-0.00000000	-0.00000000	-0.00000000	-0.00000000	-0.00000000			

CONSOLE OPERATION PUSH-PULL MINIMUM

FOURIER FREQ 0.28559900+01 TIME = 0.22000000+01									
FORCE COSINE COEF									
0.12818680-00	-0.20210865-00	-0.65079840-00	0.57946865-00	0.11458132+00	0.59963100-02	0.24674000-01			
0.34439738-00	-0.23632782-00	0.16809450-00	-0.53060982-00	0.17364598-00	0.21369030-00	-0.13289060-00			
-0.00000000	-0.00000000	-0.00000000	-0.00000000	-0.00000000	-0.00000000	-0.00000000			
FORCE SINE COEF									
0.11467565+00	0.14988648-00	-0.56385135-00	-0.81148191-01	0.72327430-01	-0.95210934-01	0.14015127-00			
-0.11341032+00	0.33933586-00	0.39902987-00	-0.25204837-00	-0.46926102-00	-0.24553801-00	0.59638094-01			
-0.00000000	-0.00000000	-0.00000000	-0.00000000	-0.00000000	-0.00000000	-0.00000000			

Note: The columns correspond to coefficients index (1 to 7) from left to right; the rows correspond to x, y, z coefficients from top to bottom.

TABLE 3-4 B
FOLDOUT FRAME *21*

Table 3-7
RIGID-BODY PEAK ANGULAR EXCURSION

Vehicle Configuration	Input Station	Crew Motion							
		Console Operation						Heartbeat	Cough
		Push-Pull			Torquing				
		Maximum	Nominal	Minimum	Maximum	Nominal	Minimum		
1	1	0.22/6	0.17/6	0.16/6	0.44/6	0.51/6	0.33/6		
	2					0.84/1 0.73/2	0.55/1 0.48/2	0.004/1	0.27/1
	3					0.59/3 0.34/1	0.28/3 0.24/1		
	4					0.95/5 0.43/4	0.62/5 0.27/4		
	5					1.31/1 1.03/3	0.80/3 0.80/1		
2	1		0.42/7	0.48/7		0.76/7 0.50/8	0.96/7 0.22/8	0.01/7	0.40/7
	2					0.83/2 0.70/9	0.82/9 0.38/2		
	3					1.44/2 0.89/9	1.26/9 0.80/2		
3	1		0.00/11	0.00/11		0.69/11	0.00/2	0.002/11	0.24/11
	2		0.27/10	0.35/10		5.37/10	0.65/10		
	3		2.99/1	3.21/1		9.06/1	5.81/1		

NOTE: The upper entry is the largest peak excursion in arcsec, and the lower entry is the minimum peak excursion observed for any orientation. The number following the slash mark is the crew member orientation number from Table 3-3, for which the corresponding peak value was observed.

Table 3-6 *7*
COUGH

FOURIER FREQ 0.35903900+01 TIME = 0.18000000+01									
FORCE COSINE COEF									
0.76516327-01	-0.14716666+01	-0.14946462+01	0.11679597+01	0.13365398+01	-0.29208211+01	0.33061182+01			
-0.34879414-00	-0.30294503-00	-0.15123076-00	0.41767413-00	-0.13050494+01	-0.24912848+01	0.41816300+01			
0.52426851-01	-0.26226359-00	-0.40526507-01	0.10179601+01	-0.12618987+01	0.94301330-01	0.40000053-00			
FORCE SINE COEF									
0.15946499-00	0.10080934+00	-0.96027109-00	-0.18850627+01	0.42810690+01	-0.16121931+01	-0.42199945-01			
0.21548027-00	0.54402652-00	-0.15594341+01	-0.34899589+01	0.42698296+01	0.30025782-00	0.55906940-02			
-0.70904400-01	0.31886502-00	-0.27874383-00	-0.14332246-00	0.41600960-00	-0.27766767-00	0.23051954-01			
MOMENT COSINE COEF									
0.16908493+01	-0.13686059-00	0.32462589+01	0.27251893+01	-0.13386141+02	0.17077034+02	-0.11216330+02			
0.19147521+01	0.40707161+01	0.51012504-00	-0.16328638+02	0.23962788+02	0.14474338+02	-0.28604081+02			
0.66801868+01	0.85009222+01	-0.25549276+02	0.98419692+01	-0.82528754+01	-0.35180062+02	0.43959138+02			
MOMENT SINE COEF									
-0.81572475-00	-0.83012094-00	0.50366315+01	0.31844652+01	-0.87713964+01	0.31273283+01	-0.78052212-01			
0.16484082-01	-0.10923234+02	0.14364695+02	0.14065928+02	-0.20084381+02	0.66878535+01	0.29857257-00			
-0.18422371+01	0.36475831+02	-0.45513545+02	-0.57418472+02	0.73447127+02	-0.83851153+01	-0.11324941+01			

HEARTBEAT

FOURIER FREQ 0.57119800+01 TIME = 0.11000000+01									
FORCE COSINE COEF									
0.31852881-01	-0.63437041-01	0.11266874+00	-0.46431034-01	-0.24807210-00	0.37126835-00	-0.15784980-00			
0.10203394-01	-0.60476211-01	0.94055591-01	-0.45709430-01	-0.16789360-00	0.20576835-00	-0.35948086-01			
0.00000000	0.00000000	0.00000000	0.00000000	0.00000000	0.00000000	0.00000000			
FORCE SINE COEF									
-0.19534352-01	-0.29521543-01	0.12166239-01	0.10018206+00	-0.19748025-01	0.11470724-01	0.50624093-01			
-0.80339524-02	-0.66578465-02	-0.28314630-01	0.92583655-01	-0.31451491-02	-0.39119640-01	0.33628991-01			
0.00000000	0.00000000	0.00000000	0.00000000	0.00000000	0.00000000	0.00000000			
MOMENT COSINE COEF									
0.00000000	0.00000000	0.00000000	0.00000000	0.00000000	0.00000000	0.00000000			
0.00000000	0.00000000	0.00000000	0.00000000	0.00000000	0.00000000	0.00000000			
0.32223108-00	-0.41549603-00	0.12097935+01	-0.81392702-00	-0.23287476+01	0.37347940+01	-0.17086479+01			
MOMENT SINE COEF									
0.00000000	0.00000000	0.00000000	0.00000000	0.00000000	0.00000000	0.00000000			
0.00000000	0.00000000	0.00000000	0.00000000	0.00000000	0.00000000	0.00000000			
-0.17616589-00	-0.27599383-00	0.22480714-01	0.12421673+01	-0.18245520-00	-0.17929794-00	0.43750980-00			

Note: The columns correspond to coefficient index (1 to 7) from left to right; the rows correspond to x, y, z components from top to bottom.

Table 3-8
RIGID-BODY PEAK ANGULAR VELOCITY

Vehicle Configuration	Input Station	Crew Motion							Heartbeat	Cough
		Console Operation				Torquing		Minimum		
		Push-Pull		Maximum	Nominal					
		Maximum	Nominal			Minimum	Maximum			
1	1	1.32/6	0.70/6	0.46/6	1.56/6	1.08/6	0.57/6			
	2					1.74/1 1.50/2	1.44/1 1.24/2		0.08/1 2.00/1	
	3					1.36/1 0.70/3	0.70/3 0.64/1			
	4					1.97/5 0.90/4	1.60/5 0.81/4			
	5					2.74/1 2.08/3	2.16/3 2.04/1			
2	1		1.91/7	1.32/7		1.92/7 1.12/8	2.52/7 0.75/8		0.16/7 4.26/7	
	2					1.92/9 1.83/2	2.05/9 1.84/2			
	3					3.05/2 2.73/9	3.14/9 2.74/2			
3	1		0.00/11	0.00/11		1.77/11	0.00/2	0.03/11	1.86/11	
	2		1.16/10	0.88/10		13.80/10	1.63/10			
	3		12.63/1	7.98/1		18.81/1	14.74/1			

NOTE: The upper entry is the largest peak resultant angular velocity in arcsec/sec, and the lower entry is the minimum peak for any orientation. The number following the slash mark is the crew member orientation number from Table 3-3, for which the corresponding peak value was observed.

NOTE: The upper entry is the largest peak resultant angular velocity in arcsec/sec, and the lower entry is the minimum peak for any orientation. The number following the slash mark is the crew member orientation number from Table 3-3, for which the corresponding peak value was observed.

velocities obtained for the cases computed. Tables 3-9 to 3-55 are tables of functional values (Section 3.5) for all the cases computed, except Cases 1-1-6 (all crew motions), which were computed before the desirability of data compaction became evident and the computation of the functional values was added to the program. Figures 3-33 through 3-92 are time histories of angular velocity, angular excursion, and resultant acceleration at the output stations for Cases 1-2-1 Heartbeat, 2-1-1 Cough, and 3-1-11 Cough. Cases 1-2-1 Heartbeat are augmented by time histories of the bending-mode amplitudes and the resultant bending acceleration due to elastic forces at each output station.

A few general observations may be made about the computed results. In the case of Configuration 1, for which bending effects are included, the accelerations observed at experiment stations are generally augmented by the elastic motions, particularly at Output Stations 1 and 4 which are located on the relatively flexible Lunar Excursion Module/ATM branch. The augmentation is particularly marked when the crew-motion input station is in the LEM as in Cases 1-1-6 (all crew motions), since crew-motion forces at this location are particularly effective in exciting the bending modes. For instance, for Case 1-1-6T. Max. (the worst of these cases), the maximum resultant acceleration at Output Station 4 was 40×10^{-5} g's, whereas at all other output stations the peak resultant accelerations for this case were approximately 15×10^{-5} g's. Also for this case the maximum rigid-body angular excursion was 0.44 arc sec, whereas the elastic angular deflection at Station 4 (the approximate location of the ATM) was 1.56 arc sec (nearly the same at Output Station 1). At other output stations the elastic angular deflection was only about a twentieth of this value. The mode amplitude curves (Figures 3-49 and 3-50) can be converted to elastic angular deflection curves by multiplying the ordinate scale by the modal slope coefficient from Table 3-1 or 3-2 for the output station of interest. It is perhaps worth noting that the tolerances of interest are very small quantities. A vibration having an amplitude of 2.44×10^{-4} in. and a frequency of 2 cps (the first mode-bending frequency) results in a peak vibrational acceleration of 10^{-4} g's. A relative motion of 10^{-3} in. over a distance of 200 in. (roughly the distance from Output Station 4 to the hinge point) produces an angle of one arc sec.

Table 3-9
FUNCTIONAL VALUES, CASE 1-2-1 TN

SERIAL 772352

PEAK ANG. VEL. ARCSEC PER SEC
RESULT. 1.7412 WX .5698 WY 1.6453 WZ -.0060

PEAK EULER ANG. ARCSEC
TOTAL .8449 B1 .0029 B2 -.7984 B3 -.2765

PEAK ACCELERATION 1E-05 GS

	RESULT.	X COMP.	Y COMP.	Z COMP.
STA. NO. 1	2.0273	-1.9965	.3687	1.2925
STA. NO. 2	8.0250	-2.0127	-1.1126	8.0112
STA. NO. 3	5.0653	-2.0125	-.3921	5.0294
STA. NO. 4	5.3754	5.2408	.3698	2.9928
STA. NO. 5	3.4550	-2.0120	.0271	3.3627
STA. NO. 6	2.4484	-2.0113	.2652	1.9917
STA. NO. 7	2.0875	-2.0107	.3678	.9999
STA. NO. 8	2.0143	-2.0110	.4088	-.5163
STA. NO. 9	3.0100	-2.0118	.7011	-2.5274
STA. NO. 10	2.1933	-2.0122	.3682	1.2927

PEAK VELOCITY 1E-03 IN PER SEC

	RESULT.	X COMP.	Y COMP.	Z COMP.
	1.6263	-1.5952	-.1201	.8934
	6.2751	-1.5820	-.3506	6.2631
	3.9309	-1.5821	-.1276	3.9045
	2.5265	-2.3966	-.1204	1.9551
	2.6509	-1.5824	.0201	2.5822
	1.7341	-1.5828	-.0889	1.4930
	1.5990	-1.5831	-.1198	.6963
	1.5835	-1.5829	-.1319	.2214
	1.9743	-1.5825	-.2207	-1.9414
	1.6080	-1.5842	-.1199	.8624

RMS ACCELERATION 1E-05 GS

	X COMP.	Y COMP.	Z COMP.
STA. NO. 1	.9380	.1827	.4829
STA. NO. 2	.9943	.5514	3.3193
STA. NO. 3	.9938	.1948	2.0601
STA. NO. 4	2.2521	.1832	1.4152
STA. NO. 5	.9923	.0119	1.3549
STA. NO. 6	.9903	.1315	.7759
STA. NO. 7	.9888	.1822	.3742
STA. NO. 8	.9894	.2025	.2751
STA. NO. 9	.9917	.3472	1.2018
STA. NO. 10	.9891	.1824	.4873

RMS VELOCITY 1E-03 IN PER SEC

	X COMP.	Y COMP.	Z COMP.
	.6617	.0568	.3860
	.6640	.1712	2.8083
	.6640	.0612	1.7543
	.9888	.0569	.7539
	.6639	.0093	1.1617
	.6638	.0413	.6694
	.6637	.0566	.2982
	.6638	.0628	.0952
	.6639	.1074	.8030
	.6636	.0567	.3667

Table 3-10
FUNCTIONAL VALUES, CASE 1-2-2 TN

SERIAL 772352

PEAK ANG. VEL. ARCSEC PER SEC
RESULT. 1.5013 WX .0684 WY .0198 WZ-1.4997

PEAK EULER ANG. ARCSEC
TOTAL .7292 B1 .7285 B2 -.0078 B3 -.0319

PEAK ACCELERATION 1E-05 GS

	RESULT.	X COMP.	Y COMP.	Z COMP.
STA. NO. 1	2.4590	-2.1119	1.3882	.0141
STA. NO. 2	8.3081	-2.8900	8.3074	-.0497
STA. NO. 3	5.1505	-2.8862	5.1437	-.0198
STA. NO. 4	9.5288	9.4925	1.3894	.0637
STA. NO. 5	3.7056	-2.8769	3.4238	-.0124
STA. NO. 6	3.3471	-2.8633	2.1596	-.0274
STA. NO. 7	3.1311	-2.8532	1.3871	-.0396
STA. NO. 8	3.0258	-2.8575	1.0040	-.0475
STA. NO. 9	2.8911	-2.8728	-2.0680	-.0741
STA. NO. 10	2.8629	-2.5685	1.3876	.0188

PEAK VELOCITY 1E-03 IN PER SEC

	RESULT.	X COMP.	Y COMP.	Z COMP.
	1.7136	-1.6442	.9776	-.0113
	6.2767	1.7159	6.2600	.0353
	4.0320	1.7146	3.9950	.0160
	3.8851	-3.8595	.9777	.0522
	2.8501	1.7113	2.7314	-.0102
	2.0216	1.7066	1.7157	-.0226
	1.8265	1.7031	.9775	-.0326
	1.7679	1.7046	.5165	-.0391
	1.7124	1.7099	-1.3142	-.0607
	1.6593	-1.5518	.9775	-.0140

RMS ACCELERATION 1E-05 GS

	X COMP.	Y COMP.	Z COMP.
STA. NO. 1	1.0552	.6376	.0071
STA. NO. 2	1.2465	3.2361	.0234
STA. NO. 3	1.2448	2.0534	.0084
STA. NO. 4	4.3258	.6383	.0270
STA. NO. 5	1.2409	1.4320	.0056
STA. NO. 6	1.2352	.9635	.0112
STA. NO. 7	1.2309	.6371	.0165
STA. NO. 8	1.2327	.4717	.0201
STA. NO. 9	1.2391	.8578	.0322
STA. NO. 10	1.1990	.6373	.0086

RMS VELOCITY 1E-03 IN PER SEC

	X COMP.	Y COMP.	Z COMP.
	.6623	.4491	.0058
	.7452	2.6861	.0199
	.7450	1.7397	.0066
	1.6520	.4493	.0229
	.7444	1.2122	.0046
	.7436	.7774	.0100
	.7430	.4490	.0148
	.7432	.2471	.0179
	.7442	.5436	.0286
	.6873	.4491	.0074

Table 3-11
FUNCTIONAL VALUES, CASE 1-3-1 TN

SERIAL 772352

PEAK ANG. VEL. ARCSEC PER SEC
RESULT. .6977 WX .2255 WY .6602 WZ -.0025

PEAK EULER ANG. ARCSEC
TOTAL .3430 B1 .0012 B2 -.3246 B3 -.1100

PEAK ACCELERATION 1E-05 GS

	RESULT.	X COMP.	Y COMP.	Z COMP.
STA. NO. 1	2.5517	-2.0148	.3667	2.2680
STA. NO. 2	4.9984	-2.0329	-1.1072	4.9690
STA. NO. 3	3.8169	-2.0327	-.3903	3.7599
STA. NO. 4	5.4140	5.2224	.3677	3.5999
STA. NO. 5	3.1940	-2.0322	.0138	3.0803
STA. NO. 6	2.7623	-2.0315	.2636	2.5258
STA. NO. 7	2.5237	-2.0309	.3657	2.1215
STA. NO. 8	2.4206	-2.0312	.4066	1.8867
STA. NO. 9	2.3179	-2.0320	.6975	-1.5140
STA. NO. 10	2.6747	-2.0315	.3662	2.2885

PEAK VELOCITY 1E-03 IN PER SEC

RESULT.	X COMP.	Y COMP.	Z COMP.
1.8104	-1.6115	-.1162	1.6592
3.8447	-1.5993	-.3459	3.8245
2.9232	-1.5995	-.1227	2.8772
2.6684	-2.3995	-.1165	2.4997
2.4254	-1.5997	.0082	2.3490
2.0285	-1.6001	-.0846	1.9118
1.7500	-1.6004	-.1159	1.5834
1.6945	-1.6003	-.1283	1.5773
1.6002	-1.5998	-.2179	.7972
1.8107	-1.6008	-.1160	1.6451

RMS ACCELERATION 1E-05 GS

	X COMP.	Y COMP.	Z COMP.
STA. NO. 1	.9367	.1814	.8635
STA. NO. 2	.9926	.5482	2.0505
STA. NO. 3	.9920	.1934	1.5264
STA. NO. 4	2.2410	.1820	1.6695
STA. NO. 5	.9906	.0062	1.2342
STA. NO. 6	.9886	.1305	.9938
STA. NO. 7	.9870	.1810	.8163
STA. NO. 8	.9877	.2012	.7119
STA. NO. 9	.9900	.3452	.6743
STA. NO. 10	.9873	.1812	.8633

RMS VELOCITY 1E-03 IN PER SEC

X COMP.	Y COMP.	Z COMP.
.6584	.0562	.7384
.6607	.1697	1.7304
.6607	.0600	1.3003
.9840	.0564	.9769
.6606	.0040	1.0588
.6605	.0405	.8579
.6604	.0561	.7047
.6604	.0623	.6054
.6605	.1069	.3156
.6604	.0561	.7286

Table 3-12
FUNCTIONAL VALUES, CASE 1-3-3 TN

SERIAL 772352

PEAK ANG. VEL. ARCSEC PER SEC
RESULT. 1.3590 WX 1.0831 WY .8100 WZ .5257

PEAK EULER ANG. ARCSEC
TOTAL .5950 B1 .1707 B2 -.3866 B3 -.4515

PEAK ACCELERATION 1E-05 GS

	RESULT.	X COMP.	Y COMP.	Z COMP.
STA. NO. 1	2.1434	-.2723	1.6060	2.0841
STA. NO. 2	5.1662	-.4226	3.6957	5.0810
STA. NO. 3	3.7256	-.4218	2.8271	3.6473
STA. NO. 4	4.4278	1.7978	1.6062	4.2851
STA. NO. 5	2.9152	-.4200	2.3393	2.8444
STA. NO. 6	2.2472	-.4174	1.9311	2.1809
STA. NO. 7	1.8036	-.4155	1.6059	1.6860
STA. NO. 8	1.5158	-.4163	1.3915	1.3835
STA. NO. 9	1.2067	-.4192	.7322	-1.1952
STA. NO. 10	2.0850	.3449	1.6059	2.0175

PEAK VELOCITY 1E-03 IN PER SEC

	RESULT.	X COMP.	Y COMP.	Z COMP.
	1.6933	.1145	-1.2350	1.6403
	4.1177	.1928	-2.9825	4.0316
	2.9433	.1927	-2.2530	2.8676
	3.0944	-.7882	-1.2351	3.0707
	2.2845	.1922	-1.8423	2.2138
	1.7534	.1915	-1.4986	1.6699
	1.4207	.1910	-1.2350	1.2591
	1.2030	.1912	-1.0635	1.0006
	.5366	.1920	-.5045	.3044
	1.6147	.1237	-1.2350	1.5563

RMS ACCELERATION 1E-05 GS

	X COMP.	Y COMP.	Z COMP.
STA. NO. 1	.1326	.6294	.8224
STA. NO. 2	.1858	1.5712	2.1034
STA. NO. 3	.1854	1.1700	1.5060
STA. NO. 4	.7920	.6294	1.7846
STA. NO. 5	.1844	.9480	1.1714
STA. NO. 6	.1830	.7666	.8928
STA. NO. 7	.1819	.6294	.6817
STA. NO. 8	.1823	.5407	.5505
STA. NO. 9	.1840	.2686	.4995
STA. NO. 10	.1712	.6294	.7906

RMS VELOCITY 1E-03 IN PER SEC

	X COMP.	Y COMP.	Z COMP.
	.0470	.4798	.7227
	.0764	1.1810	1.7995
	.0763	.8871	1.2891
	.3321	.4798	1.2332
	.0760	.7221	1.0023
	.0756	.5848	.7633
	.0754	.4797	.5805
	.0755	.4116	.4613
	.0759	.1900	.1554
	.0539	.4798	.6873

Table 3-13
FUNCTIONAL VALUES, CASE 1-4-4 TNOM

SERIAL 772439

PEAK ANG. VEL. ARCSEC PER SEC
RESULT. .9017 WX .2094 WY -.0191 WZ .8771

PEAK EULER ANG. ARCSEC
TOTAL .4340 B1 -.4221 B2 -.0062 B3 -.1010

PEAK ACCELERATION 1E-05 GS

	RESULT.	X COMP.	Y COMP.	Z COMP.
STA. NO. 1	3.9120	2.0447	3.9115	.0339
STA. NO. 2	2.5044	2.2759	1.5563	.0679
STA. NO. 3	2.6333	2.2734	1.5915	-.0615
STA. NO. 4	6.3630	-6.3549	3.9119	.2614
STA. NO. 5	2.7997	2.2672	2.4819	-.0608
STA. NO. 6	3.3273	2.2583	3.3084	-.0612
STA. NO. 7	3.9210	2.2516	3.9112	-.0618
STA. NO. 8	4.2997	2.2545	4.2919	-.0668
STA. NO. 9	5.6166	2.2645	5.6108	-.0923
STA. NO. 10	3.9117	2.0656	3.9113	-.0172

PEAK VELOCITY 1E-03 IN PER SEC

	RESULT.	X COMP.	Y COMP.	Z COMP.
	3.0640	1.6355	3.0594	.0274
	1.5092	1.4781	.5670	-.0530
	1.6673	1.4783	1.2589	-.0495
	3.0666	2.8909	3.0595	.2077
	2.1126	1.4787	1.9895	-.0484
	2.6583	1.4794	2.6025	-.0486
	3.0994	1.4800	3.0593	-.0495
	3.3869	1.4797	3.3519	-.0502
	4.3620	1.4789	4.3399	.0686
	3.0666	1.5866	3.0593	-.0120

RMS ACCELERATION 1E-05 GS

	X COMP.	Y COMP.	Z COMP.
STA. NO. 1	.9483	1.5717	.0141
STA. NO. 2	1.0493	.6990	.0301
STA. NO. 3	1.0485	.7313	.0250
STA. NO. 4	2.8464	1.5717	.1076
STA. NO. 5	1.0465	1.0341	.0249
STA. NO. 6	1.0437	1.3364	.0264
STA. NO. 7	1.0416	1.5717	.0284
STA. NO. 8	1.0425	1.7237	.0300
STA. NO. 9	1.0456	2.2337	.0366
STA. NO. 10	1.0210	1.5717	.0083

RMS VELOCITY 1E-03 IN PER SEC

	X COMP.	Y COMP.	Z COMP.
	.6484	1.3367	.0126
	.6999	.2378	.0264
	.6998	.5767	.0222
	1.1359	1.3367	.0921
	.6996	.8788	.0214
	.6993	1.1378	.0218
	.6991	1.3367	.0227
	.6992	1.4658	.0235
	.6995	1.8924	.0273
	.6615	1.3367	.0070

Table 3-14
FUNCTIONAL VALUES, CASE 1-4-5 TNOM

SERIAL 772439

PEAK ANG. VEL. ARCSEC PER SEC
RESULT. 1.9695 WX-1.6996 WY -.9951 WZ .1386

PEAK EULER ANG. ARCSEC
TOTAL .9530 B1 .0451 B2 .4858 B3 .8199

PEAK ACCELERATION 1E-05 GS

	RESULT.	X COMP.	Y COMP.	Z COMP.
STA. NO. 1	3.9562	1.9826	-.3980	3.8732
STA. NO. 2	2.0911	2.0536	1.1612	-.4733
STA. NO. 3	2.3979	2.0535	.4359	2.0162
STA. NO. 4	5.0126	-4.6294	-.3987	3.5041
STA. NO. 5	3.1632	2.0532	-.0859	3.0337
STA. NO. 6	3.9667	2.0528	-.2501	3.8938
STA. NO. 7	4.6221	2.0525	-.3974	4.5652
STA. NO. 8	5.0761	2.0526	-.4747	5.0202
STA. NO. 9	6.7891	2.0531	-.8415	6.7273
STA. NO. 10	4.1849	2.0066	-.3976	4.0896

PEAK VELOCITY 1E-03 IN PER SEC

	RESULT.	X COMP.	Y COMP.	Z COMP.
	2.8720	1.5937	.1941	2.7913
	1.6811	1.6314	-.5085	-.1669
	1.7641	1.6315	.2030	1.4857
	2.3862	2.1558	.1943	2.1594
	2.3615	1.6317	-.0680	2.2631
	2.9764	1.6321	.1115	2.9121
	3.4517	1.6323	.1940	3.4005
	3.7582	1.6322	.2431	3.7085
	4.7744	1.6318	.4332	4.7176
	2.9997	1.5940	.1940	2.9146

RMS ACCELERATION 1E-05 GS

	X COMP.	Y COMP.	Z COMP.
STA. NO. 1	.9125	.1730	1.5054
STA. NO. 2	.9787	.5103	.2256
STA. NO. 3	.9782	.1872	.7728
STA. NO. 4	1.9689	.1735	1.7421
STA. NO. 5	.9772	.0358	1.1933
STA. NO. 6	.9756	.1208	1.5477
STA. NO. 7	.9744	.1727	1.8172
STA. NO. 8	.9749	.1979	1.9910
STA. NO. 9	.9767	.3438	2.5837
STA. NO. 10	.9570	.1728	1.5772

RMS VELOCITY 1E-03 IN PER SEC

	X COMP.	Y COMP.	Z COMP.
	.6528	.0738	1.2739
	.6723	.2172	.0824
	.6723	.0900	.6634
	.8837	.0739	.8258
	.6722	.0316	1.0217
	.6722	.0477	1.3198
	.6721	.0737	1.5456
	.6722	.0901	1.6904
	.6722	.1622	2.1612
	.6577	.0737	1.3298

Table 3-15
FUNCTIONAL VALUES, CASE 1-5-1 TNOM

SERIAL 772439

PEAK ANG. VEL. ARCSEC PER SEC
RESULT. 2.7437 WX-2.1028 WY-1.7619 WZ -.1458

PEAK EULER ANG. ARCSEC
TOTAL 1.3106 B1 -.0475 B2 .8385 B3 1.0072

PEAK ACCELERATION 1E-05 GS

	RESULT.	X COMP.	Y COMP.	Z COMP.
STA. NO. 1	4.6383	-2.0344	.3962	4.5718
STA. NO. 2	2.5297	-2.1107	-1.2030	-2.2537
STA. NO. 3	2.1603	-2.1105	-.4665	1.1894
STA. NO. 4	5.7375	4.6187	.3970	5.0918
STA. NO. 5	3.0295	-2.1101	-.1055	2.8611
STA. NO. 6	4.3638	-2.1095	.2501	4.2991
STA. NO. 7	5.4585	-2.1090	.3956	5.4165
STA. NO. 8	6.2019	-2.1092	.4727	6.1637
STA. NO. 9	8.9005	-2.1099	.8501	8.8609
STA. NO. 10	4.9197	-2.0615	.3959	4.8352

PEAK VELOCITY 1E-03 IN PER SEC

RESULT.	X COMP.	Y COMP.	Z COMP.
3.4462	-1.6379	.1936	3.3917
1.9215	-1.6791	.5647	-1.8711
1.7276	-1.6792	.2429	.7628
2.9492	-2.1737	.1938	2.8519
2.2061	-1.6794	.0793	2.1081
3.3093	-1.6797	.1237	3.2587
4.1708	-1.6800	.1933	4.1330
4.7274	-1.6798	.2318	4.6926
6.5695	-1.6795	-.4110	6.5346
3.6071	-1.6398	.1934	3.5494

RMS ACCELERATION 1E-05 GS

	X COMP.	Y COMP.	Z COMP.
STA. NO. 1	.9114	.1753	1.7604
STA. NO. 2	.9797	.5169	.9582
STA. NO. 3	.9792	.1921	.4512
STA. NO. 4	1.9631	.1757	2.5449
STA. NO. 5	.9782	.0422	1.1077
STA. NO. 6	.9766	.1220	1.6905
STA. NO. 7	.9755	.1749	2.1352
STA. NO. 8	.9760	.2015	2.4211
STA. NO. 9	.9777	.3508	3.3877
STA. NO. 10	.9562	.1751	1.8489

RMS VELOCITY 1E-03 IN PER SEC

X COMP.	Y COMP.	Z COMP.
.6442	.0862	1.5145
.6660	.2225	.7791
.6660	.0894	.3360
.8725	.0863	1.0991
.6660	.0315	.9491
.6659	.0560	1.4619
.6659	.0861	1.8501
.6659	.1051	2.0988
.6659	.1832	2.9042
.6497	.0862	1.5812

Table 3-16
FUNCTIONAL VALUES, CASE 1-5-3 TNOM

SERIAL 772439

PEAK ANG. VEL. ARCSEC PER SEC
RESULT. 2.0805 WX-1.3262 WY-1.6089 WZ-1.0645

PEAK EULER ANG. ARCSEC
TOTAL 1.0292 B1 -.3464 B2 .7761 B3 .6734

PEAK ACCELERATION 1E-05 GS

	RESULT.	X COMP.	Y COMP.	Z COMP.
STA. NO. 1	4.6745	.5000	3.1624	4.4900
STA. NO. 2	2.1322	.7871	1.3212	-2.0725
STA. NO. 3	1.1867	.7858	.7205	1.1519
STA. NO. 4	6.0501	-3.3338	3.1621	5.6942
STA. NO. 5	2.7757	.7827	1.6554	2.6999
STA. NO. 6	4.1385	.7782	2.4978	4.0342
STA. NO. 7	5.1957	.7749	3.1626	5.0705
STA. NO. 8	5.9060	.7763	3.5990	5.7605
STA. NO. 9	8.4974	.7814	5.0065	8.2394
STA. NO. 10	4.8722	-.6180	3.1625	4.6844

PEAK VELOCITY 1E-03 IN PER SEC

RESULT.	X COMP.	Y COMP.	Z COMP.
3.5233	-.2155	-2.5412	3.3617
1.6764	-.3736	1.0306	-1.6742
.7762	-.3732	-.4832	.7467
3.5279	1.5137	-2.5412	3.4495
2.0456	-.3724	-1.3071	1.9688
3.1167	-.3712	-2.0051	3.0137
3.9323	-.3703	-2.5413	3.8082
4.4600	-.3707	-2.8899	4.3165
6.2221	-.3720	-4.0349	5.9939
3.6164	-.2247	-2.5413	3.4549

RMS ACCELERATION 1E-05 GS

	X COMP.	Y COMP.	Z COMP.
STA. NO. 1	.2391	1.3452	1.7393
STA. NO. 2	.3377	.6489	.9014
STA. NO. 3	.3370	.2759	.4387
STA. NO. 4	1.4369	1.3452	2.5984
STA. NO. 5	.3352	.6898	1.0532
STA. NO. 6	.3327	1.0623	1.6006
STA. NO. 7	.3309	1.3452	2.0174
STA. NO. 8	.3317	1.5277	2.2836
STA. NO. 9	.3345	2.1361	3.1746
STA. NO. 10	.3060	1.3452	1.8027

RMS VELOCITY 1E-03 IN PER SEC

X COMP.	Y COMP.	Z COMP.
.0879	1.0242	1.5013
.1451	.4111	.7049
.1449	.2017	.3285
.6295	1.0241	1.3049
.1444	.5316	.8960
.1438	.8106	1.3705
.1433	1.0242	1.7294
.1435	1.1627	1.9588
.1442	1.6196	2.6989
.0971	1.0242	1.5440

Table 3-17
FUNCTIONAL VALUES, CASE 1-1-2 TMIN

SERIAL 772439

PEAK ANG. VEL. ARCSEC PER SEC
RESULT. 1.4447 WX .4724 WY 1.3652 WZ -.0047

PEAK EULER ANG. ARCSEC
TOTAL .5565 B1 .0021 B2 -.5259 B3 -.1020

PEAK ACCELERATION 1E-05 GS

	RESULT.	X COMP.	Y COMP.	Z COMP.
STA. NO. 1	2.3566	-2.3407	.2607	1.6543
STA. NO. 2	8.6528	-2.3650	-.7879	8.6000
STA. NO. 3	5.4493	-2.3647	-.2779	5.3753
STA. NO. 4	5.1827	4.8750	.2614	-5.1433
STA. NO. 5	3.6870	-2.3642	.0268	3.5904
STA. NO. 6	2.4595	-2.3633	.1874	2.1721
STA. NO. 7	2.3714	-2.3627	.2600	1.2548
STA. NO. 8	2.3649	-2.3630	.2891	1.0361
STA. NO. 9	3.9616	-2.3639	.4961	-3.8135
STA. NO. 10	2.3747	-2.3639	.2603	1.7647

PEAK VELOCITY 1E-03 IN PER SEC

RESULT.	X COMP.	Y COMP.	Z COMP.
1.9960	-1.9929	-.0888	.5903
5.0478	-1.9594	.2699	4.9907
3.1175	-1.9597	.0953	3.0246
3.0452	-3.0347	-.0891	2.2590
2.1006	-1.9603	.0169	1.9246
1.9897	-1.9612	-.0641	1.0239
1.9643	-1.9619	-.0886	.4401
1.9635	-1.9616	-.0983	-.3003
2.2746	-1.9606	-.1688	-2.1320
1.9649	-1.9625	-.0887	.5976

RMS ACCELERATION 1E-05 GS

	X COMP.	Y COMP.	Z COMP.
STA. NO. 1	1.1421	.1146	.5967
STA. NO. 2	1.1229	.3536	2.8616
STA. NO. 3	1.1230	.1264	1.7730
STA. NO. 4	2.1520	.1149	2.1815
STA. NO. 5	1.1234	.0094	1.1713
STA. NO. 6	1.1239	.0820	.7031
STA. NO. 7	1.1243	.1143	.4606
STA. NO. 8	1.1242	.1273	.4959
STA. NO. 9	1.1235	.2197	1.4659
STA. NO. 10	1.1243	.1145	.6707

RMS VELOCITY 1E-03 IN PER SEC

X COMP.	Y COMP.	Z COMP.
.8740	.0401	.2578
.8636	.1247	1.9045
.8636	.0452	1.1755
1.1876	.0402	.7172
.8639	.0063	.7667
.8642	.0288	.4301
.8644	.0400	.1927
.8643	.0445	.1341
.8640	.0768	.6644
.8645	.0400	.2595

Table 3-18
FUNCTIONAL VALUES, CASE 1-2-2 TMIN

SERIAL 772439

PEAK ANG. VEL. ARCSEC PER SEC
RESULT. 1.2414 WX .0491 WY .0200 WZ-1.2403

PEAK EULER ANG. ARCSEC
TOTAL .4841 B1 .4838 B2 .0067 B3 -.0169

PEAK ACCELERATION 1E-05 GS

	RESULT.	X COMP.	Y COMP.	Z COMP.
STA. NO. 1	2.8407	2.8313	-.9025	.0215
STA. NO. 2	9.2489	2.9980	9.2277	-.0664
STA. NO. 3	5.6253	2.9962	5.5905	-.0264
STA. NO. 4	7.6237	-7.5970	-.9036	.0555
STA. NO. 5	3.6236	2.9917	3.5597	.0104
STA. NO. 6	3.1802	2.9853	1.9536	-.0291
STA. NO. 7	3.0707	2.9804	-.9016	-.0440
STA. NO. 8	3.0162	2.9825	-.6476	-.0537
STA. NO. 9	3.0716	2.9898	-2.4804	-.0856
STA. NO. 10	3.0247	3.0157	-.9020	.0232

PEAK VELOCITY 1E-03 IN PER SEC

RESULT.	X COMP.	Y COMP.	Z COMP.
1.9510	-1.9197	.7053	-.0168
5.0695	-1.6909	4.9877	.0500
3.3021	-1.6917	3.1558	.0218
3.9690	-3.9598	.7055	.0327
2.3779	-1.6937	2.1364	.0080
1.7812	-1.6965	1.3098	-.0179
1.7293	-1.6986	.7051	-.0274
1.7110	-1.6977	.3467	-.0335
1.7027	-1.6945	-1.1736	-.0538
1.8570	-1.8222	.7052	-.0170

RMS ACCELERATION 1E-05 GS

	X COMP.	Y COMP.	Z COMP.
STA. NO. 1	1.2868	.4235	.0106
STA. NO. 2	1.3923	3.0636	.0335
STA. NO. 3	1.3915	1.8538	.0129
STA. NO. 4	3.4317	.4239	.0204
STA. NO. 5	1.3895	1.2023	.0045
STA. NO. 6	1.3866	.7210	.0106
STA. NO. 7	1.3845	.4232	.0177
STA. NO. 8	1.3854	.3183	.0224
STA. NO. 9	1.3886	.8976	.0383
STA. NO. 10	1.3652	.4233	.0119

RMS VELOCITY 1E-03 IN PER SEC

X COMP.	Y COMP.	Z COMP.
.8941	.2656	.0077
.9107	1.8623	.0237
.9106	1.1803	.0095
1.4719	.2657	.0143
.9105	.8011	.0034
.9103	.4927	.0069
.9102	.2655	.0118
.9103	.1358	.0150
.9104	.4405	.0260
.8977	.2656	.0083

Table 3-19
FUNCTIONAL VALUES, CASE 1-3-1 TMIN

SERIAL 772439

PEAK ANG. VEL. ARCSEC PER SEC
RESULT. .6378 WX .2061 WY .6036 WZ -.0023

PEAK EULER ANG. ARCSEC
TOTAL .2419 B1 .0009 B2 -.2289 B3 -.0782

PEAK ACCELERATION 1E-05 GS

	RESULT.	X COMP.	Y COMP.	Z COMP.
STA. NO. 1	2.7177	-2.3553	.2592	2.5816
STA. NO. 2	5.5551	-2.3804	-.7834	5.4827
STA. NO. 3	4.1737	-2.3802	-.2763	4.0909
STA. NO. 4	5.8218	4.8518	.2599	5.7977
STA. NO. 5	3.4140	-2.3796	.0114	3.3221
STA. NO. 6	2.8217	-2.3788	.1863	2.7156
STA. NO. 7	2.4781	-2.3782	.2586	2.3207
STA. NO. 8	2.4410	-2.3784	.2875	2.1561
STA. NO. 9	2.7313	-2.3794	.4933	2.4320
STA. NO. 10	2.8088	-2.3786	.2588	2.7112

PEAK VELOCITY 1E-03 IN PER SEC

	RESULT.	X COMP.	Y COMP.	Z COMP.
2.0230	-2.0008	-.0891	1.0951	
3.1905	-1.9689	.2706	3.1058	
2.3419	-1.9691	.0956	2.2284	
3.0430	-3.0295	-.0894	2.7287	
2.0771	-1.9697	.0075	1.7397	
2.0266	-1.9707	-.0640	1.3346	
2.0006	-1.9713	-.0889	1.0340	
1.9867	-1.9710	-.0989	.8623	
1.9736	-1.9700	-.1700	.7502	
1.9958	-1.9714	-.0890	1.0875	

RMS ACCELERATION 1E-05 GS

	X COMP.	Y COMP.	Z COMP.
STA. NO. 1	1.1399	.1148	.8504
STA. NO. 2	1.1209	.3502	1.8095
STA. NO. 3	1.1211	.1242	1.3378
STA. NO. 4	2.1420	.1151	2.4094
STA. NO. 5	1.1214	.0045	1.0790
STA. NO. 6	1.1220	.0822	.8780
STA. NO. 7	1.1224	.1145	.7555
STA. NO. 8	1.1222	.1274	.7245
STA. NO. 9	1.1216	.2193	1.1958
STA. NO. 10	1.1223	.1146	.9084

RMS VELOCITY 1E-03 IN PER SEC

	X COMP.	Y COMP.	Z COMP.
.8736	.0402	.4736	
.8634	.1232	1.1997	
.8635	.0439	.8794	
1.1843	.0403	.8510	
.8637	.0028	.7001	
.8640	.0288	.5522	
.8642	.0401	.4425	
.8641	.0446	.3774	
.8638	.0769	.3322	
.8642	.0401	.4741	

Table 3-20
FUNCTIONAL VALUES, CASE 1-3-3 TMIN

SERIAL 772439

PEAK ANG. VEL. ARCSEC PER SEC
RESULT. .7052 WX -.1974 WY .5926 WZ .6604

PEAK EULER ANG. ARCSEC
TOTAL .2844 B1 .2592 B2 -.2341 B3 -.0971

PEAK ACCELERATION 1E-05 GS

	RESULT.	X COMP.	Y COMP.	Z COMP.
STA. NO. 1	2.7287	-.1818	1.8863	2.5881
STA. NO. 2	5.7494	-.3732	4.3021	5.4554
STA. NO. 3	4.3255	-.3727	3.3019	4.0866
STA. NO. 4	5.8149	1.6322	1.8865	5.7677
STA. NO. 5	3.5420	-.3714	2.7415	3.3308
STA. NO. 6	2.9207	-.3696	2.2646	2.7351
STA. NO. 7	2.5077	-.3682	1.8862	2.3487
STA. NO. 8	2.3255	-.3688	1.6368	2.1895
STA. NO. 9	2.5315	-.3709	.8475	2.4835
STA. NO. 10	2.8581	-.2428	1.8862	2.7224

PEAK VELOCITY 1E-03 IN PER SEC

	RESULT.	X COMP.	Y COMP.	Z COMP.
	1.5831	-.0722	-1.5738	1.0989
	3.8420	.2319	-3.7372	3.0872
	2.8950	.2317	-2.8359	2.2255
	2.7575	-.9868	-1.5739	2.6989
	2.3672	.2312	-2.3284	1.7453
	1.9289	.2305	-1.9030	1.3471
	1.5938	.2299	-1.5737	1.0508
	1.3778	.2302	-1.3588	.8798
	.7502	.2310	-.6601	.7366
	1.5796	.0798	-1.5738	1.0933

RMS ACCELERATION 1E-05 GS

	X COMP.	Y COMP.	Z COMP.
STA. NO. 1	.0737	.9090	.8513
STA. NO. 2	.1660	2.1339	1.8035
STA. NO. 3	.1658	1.6239	1.3368
STA. NO. 4	.7224	.9091	2.4057
STA. NO. 5	.1652	1.3377	1.0808
STA. NO. 6	.1644	1.0966	.8818
STA. NO. 7	.1637	.9090	.7603
STA. NO. 8	.1640	.7862	.7293
STA. NO. 9	.1650	.3921	1.1959
STA. NO. 10	.1002	.9090	.9099

RMS VELOCITY 1E-03 IN PER SEC

	X COMP.	Y COMP.	Z COMP.
	.0343	.6694	.4738
	.0891	1.6075	1.1983
	.0890	1.2159	.8792
	.3843	.6594	.8500
	.0889	.9956	.7005
	.0886	.8112	.5531
	.0884	.6693	.4438
	.0885	.5770	.3787
	.0888	.2751	.3319
	.0338	.6693	.4744

Table 3-21
FUNCTIONAL VALUES, CASE 1-4-5 TMIN

SERIAL 772439

PEAK ANG. VEL. ARCSEC PER SEC
RESULT. 1.5972 WX-1.3430 WY -.8629 WZ .1720

PEAK EULER ANG. ARCSEC
TOTAL .6203 B1 .0678 B2 .3298 B3 .5245

PEAK ACCELERATION 1E-05 GS

	RESULT.	X COMP.	Y COMP.	Z COMP.
STA. NO. 1	4.4061	2.3173	-.3581	4.3126
STA. NO. 2	2.4356	2.4069	1.0718	.8002
STA. NO. 3	2.4933	2.4067	.4292	2.0927
STA. NO. 4	6.2918	-4.3471	-.3387	-6.2611
STA. NO. 5	3.3141	2.4062	-.0964	3.1987
STA. NO. 6	4.2530	2.4054	-.1888	4.1641
STA. NO. 7	5.0124	2.4049	-.3376	4.9358
STA. NO. 8	5.5544	2.4051	-.4211	5.4846
STA. NO. 9	7.8472	2.4060	-.7787	7.7957
STA. NO. 10	4.6807	2.3523	-.3379	4.6081

PEAK VELOCITY 1E-03 IN PER SEC

	RESULT.	X COMP.	Y COMP.	Z COMP.
2.1823	1.9887	.2213	2.0731	
2.0953	2.0202	-.6477	-.3353	
2.0545	2.0205	-.2635	.9613	
2.7591	2.7732	.2215	2.6734	
2.1004	2.0211	-.0613	1.6209	
2.2918	2.0221	.1154	2.1723	
2.6790	2.0228	.2211	2.5778	
2.9107	2.0225	.2846	2.8217	
3.6092	2.0214	.5253	3.5502	
2.2455	1.9750	.2212	2.1492	

RMS ACCELERATION 1E-05 GS

	X COMP.	Y COMP.	Z COMP.
STA. NO. 1	1.1367	.1529	1.3915
STA. NO. 2	1.1522	.4738	.3334
STA. NO. 3	1.1524	.1898	.6798
STA. NO. 4	1.9181	.1531	2.6702
STA. NO. 5	1.1527	.0416	1.0369
STA. NO. 6	1.1533	.0903	1.3516
STA. NO. 7	1.1537	.1527	1.6017
STA. NO. 8	1.1535	.1888	1.7765
STA. NO. 9	1.1529	.3460	2.5226
STA. NO. 10	1.1270	.1528	1.4903

RMS VELOCITY 1E-03 IN PER SEC

	X COMP.	Y COMP.	Z COMP.
.8685	.0849	.8612	
.8851	.2538	.1067	
.8852	.1064	.4090	
1.0739	.0850	.8552	
.8854	.0283	.6628	
.8857	.0448	.8755	
.8859	.0848	1.0374	
.8859	.1100	1.1423	
.8855	.2048	1.4984	
.8657	.0849	.9019	

Table 3-22
FUNCTIONAL VALUES, CASE 1-4-4 TMIN

SERIAL 772439

PEAK ANG. VEL. ARCSEC PER SEC
RESULT. .0126 WX .1674 WY -.0227 WZ .7951

PEAK EULER ANG. ARCSEC
TOTAL .2664 B1 -.2585 B2 -.0090 B3 -.0643

PEAK ACCELERATION 1E-05 GS

	RESULT.	X COMP.	Y COMP.	Z COMP.
STA. NO. 1	4.2714	-2.4570	4.2379	.0403
STA. NO. 2	2.5865	-2.5671	1.3115	-.0803
STA. NO. 3	2.5717	-2.5666	1.2781	-.0714
STA. NO. 4	5.1083	5.1083	4.2384	.2823
STA. NO. 5	2.6681	-2.5655	2.5115	-.0664
STA. NO. 6	3.6287	-2.5640	3.5159	-.0623
STA. NO. 7	4.3285	-2.5628	4.2374	-.0592
STA. NO. 8	4.7720	-2.5633	4.6911	-.0572
STA. NO. 9	6.3351	-2.5651	6.2754	.0833
STA. NO. 10	4.2678	-2.5146	4.2376	-.0239

PEAK VELOCITY 1E-03 IN PER SEC

RESULT.	X COMP.	Y COMP.	Z COMP.
2.5234	1.9630	2.4467	.0251
2.0026	1.8924	-.7155	-.0533
1.9725	1.8929	.8609	-.0440
3.1354	3.1327	2.4467	.1702
1.9813	1.8940	1.4993	-.0402
2.2300	1.8957	2.0384	-.0370
2.6069	1.8971	2.4466	.0369
2.8549	1.8965	2.7099	.0435
3.6943	1.8946	3.5880	.0662
2.5381	1.9144	2.4466	.0183

RMS ACCELERATION 1E-05 GS

	X COMP.	Y COMP.	Z COMP.
STA. NO. 1	1.1769	1.4084	.0165
STA. NO. 2	1.2430	.6155	.0398
STA. NO. 3	1.2428	.5096	.0267
STA. NO. 4	2.2651	1.4086	.0947
STA. NO. 5	1.2425	.8507	.0224
STA. NO. 6	1.2420	1.1715	.0218
STA. NO. 7	1.2417	1.4083	.0235
STA. NO. 8	1.2418	1.5584	.0253
STA. NO. 9	1.2424	2.0820	.0344
STA. NO. 10	1.1993	1.4083	.0119

RMS VELOCITY 1E-03 IN PER SEC

X COMP.	Y COMP.	Z COMP.
.8743	.9051	.0110
.9011	.2773	.0274
.9011	.3564	.0175
1.1415	.9051	.0621
.9012	.5684	.0146
.9014	.7589	.0149
.9015	.9051	.0168
.9015	.9997	.0186
.9013	1.3179	.0264
.8756	.9051	.0085

Table 3-23
FUNCTIONAL VALUES, CASE 1-5-3 TMIN

SERIAL 772439

PEAK ANG. VEL. ARCSEC PER SEC
RESULT. 2.1571 WX-1.6734 WY-1.2740 WZ-1.3480

PEAK EULER ANG. ARCSEC
TOTAL .7967 B1 -.5285 B2 .4962 B3 .5832

PEAK ACCELERATION 1E-05 GS

	RESULT.	X COMP.	Y COMP.	Z COMP.
STA. NO. 1	5.6153	.3245	3.7789	5.3502
STA. NO. 2	2.4257	.7077	1.5285	-2.3537
STA. NO. 3	2.0263	.7068	.8622	1.9237
STA. NO. 4	10.1990	-3.1081	3.7787	-9.9540
STA. NO. 5	3.5848	.7045	2.0095	3.4347
STA. NO. 6	5.0231	.7012	2.9983	4.8203
STA. NO. 7	6.2220	.6987	3.7792	5.9736
STA. NO. 8	7.1025	.6998	4.2918	6.8266
STA. NO. 9	10.9275	.7035	5.9454	10.6016
STA. NO. 10	6.0714	.4335	3.7791	5.8258

PEAK VELOCITY 1E-03 IN PER SEC

	RESULT.	X COMP.	Y COMP.	Z COMP.
	3.2678	.1409	-3.2342	2.3103
	1.4864	-.4520	1.2349	-1.4222
	.7955	-.4517	-.6539	.6747
	4.0170	1.9249	-3.2341	3.8108
	1.7501	-.4508	-1.6860	1.5186
	2.6322	-.4495	-2.5591	2.3017
	3.3182	-.4485	-3.2343	2.8923
	3.7610	-.4490	-3.6743	3.2528
	5.1874	-.4504	-5.1134	4.4205
	3.2628	-.1424	-3.2342	2.4250

RMS ACCELERATION 1E-05 GS

	X COMP.	Y COMP.	Z COMP.
STA. NO. 1	.1350	1.8657	1.7521
STA. NO. 2	.3142	.6888	.8758
STA. NO. 3	.3138	.3988	.6989
STA. NO. 4	1.3719	1.8656	4.4503
STA. NO. 5	.3128	.9813	1.1138
STA. NO. 6	.3113	1.4791	1.5537
STA. NO. 7	.3102	1.8658	1.9255
STA. NO. 8	.3106	2.1183	2.2020
STA. NO. 9	.3123	2.9413	3.4959
STA. NO. 10	.1773	1.8658	1.9251

RMS VELOCITY 1E-03 IN PER SEC

	X COMP.	Y COMP.	Z COMP.
	.0684	1.3965	.9941
	.1745	.5336	.4678
	.1744	.2768	.2886
	.7544	1.3965	1.3188
	.1741	.7274	.6431
	.1737	1.1057	.9553
	.1733	1.3965	1.1956
	.1735	1.5856	1.3529
	.1740	2.2066	1.9038
	.0604	1.3965	1.0487

Table 3-24
FUNCTIONAL VALUES, CASE 1-5-1 TMIN

SERIAL 772439

PEAK ANG. VEL. ARCSEC PER SEC
RESULT. 2.0367 WX-1.5942 WY-1.2656 WZ -.1870

PEAK EULER ANG. ARCSEC
TOTAL .7973 B1 -.0730 B2 .5001 B3 .6203

PEAK ACCELERATION 1E-05 GS

	RESULT.	X COMP.	Y COMP.	Z COMP.
STA. NO. 1	5.4180	-2.3585	.3905	5.3543
STA. NO. 2	2.6496	-2.4524	-1.0949	-2.3501
STA. NO. 3	2.4733	-2.4522	-.4214	1.9103
STA. NO. 4	10.0981	4.2958	.3910	*****
STA. NO. 5	3.4863	-2.4517	.0987	3.4114
STA. NO. 6	4.8497	-2.4510	.2298	4.7888
STA. NO. 7	5.9891	-2.4505	.3900	5.9359
STA. NO. 8	6.8335	-2.4507	.4809	6.7848
STA. NO. 9	10.5855	-2.4515	.8632	10.5459
STA. NO. 10	5.8682	-2.3944	.3902	5.8207

PEAK VELOCITY 1E-03 IN PER SEC

RESULT.	X COMP.	Y COMP.	Z COMP.
2.3778	-2.0079	-.2300	2.3126
2.1984	-2.0456	.6933	-1.4193
2.0635	-2.0459	.2875	.6689
3.9201	-2.7247	-.2302	3.8805
2.1026	-2.0464	.0777	1.5047
2.3655	-2.0472	-.1180	2.2822
2.9377	-2.0478	-.2298	2.8683
3.2870	-2.0475	-.2977	3.2269
4.4245	-2.0466	-.5551	4.3899
2.4757	-1.9967	-.2299	2.4222

RMS ACCELERATION 1E-05 GS

	X COMP.	Y COMP.	Z COMP.
STA. NO. 1	1.1291	.1740	1.7527
STA. NO. 2	1.1487	.4849	.8752
STA. NO. 3	1.1489	.1885	.6973
STA. NO. 4	1.8973	.1743	4.4550
STA. NO. 5	1.1492	.0397	1.1096
STA. NO. 6	1.1498	.1064	1.5477
STA. NO. 7	1.1502	.1738	1.9183
STA. NO. 8	1.1500	.2134	2.1942
STA. NO. 9	1.1494	.3813	3.4875
STA. NO. 10	1.1206	.1739	1.9244

RMS VELOCITY 1E-03 IN PER SEC

X COMP.	Y COMP.	Z COMP.
.8666	.0952	.9942
.8860	.2685	.4677
.8861	.1115	.2877
1.0635	.0953	1.3190
.8863	.0306	.6418
.8865	.0522	.9538
.8868	.0952	1.1939
.8867	.1226	1.3511
.8863	.2251	1.9017
.8644	.0952	1.0485

Table 3-25
FUNCTIONAL VALUES, CASE 1-2-1 HEARTBEAT

SERIAL 757475

PEAK ANG. VEL. ARCSEC PER SEC
RESULT. .0754 WX .0247 WY .0712 WZ -.0003

PEAK EULER ANG. ARCSEC
TOTAL .0036 B1 -.0000 B2 .0034 B3 .0012

PEAK ACCELERATION 1E-05 GS

	RESULT.	X COMP.	Y COMP.	Z COMP.
STA. NO. 1	1.0401	.9896	.0819	-.3284
STA. NO. 2	1.9629	1.0495	.2657	1.6578
STA. NO. 3	1.4746	1.0489	.0971	1.0635
STA. NO. 4	.3957	-.3735	.0822	.3173
STA. NO. 5	1.2583	1.0476	.0035	.7285
STA. NO. 6	1.1334	1.0456	.0572	.4539
STA. NO. 7	1.0744	1.0441	.0817	-.2552
STA. NO. 8	1.0559	1.0448	.0917	-.1566
STA. NO. 9	1.0787	1.0470	-.1611	.2297
STA. NO. 10	1.0949	1.0448	.0818	-.3438

PEAK VELOCITY 1E-03 IN PER SEC

RESULT.	X COMP.	Y COMP.	Z COMP.
.1706	.1602	-.0139	.0577
.3319	.1704	.0452	.2813
.2489	.1703	.0165	.1811
.1414	-.1260	-.0139	-.0867
.2106	.1700	.0006	.1245
.1870	.1697	-.0097	.0783
.1756	.1694	-.0138	.0445
.1719	.1695	-.0156	.0246
.1748	.1699	-.0274	.0536
.1800	.1696	-.0139	.0596

RMS ACCELERATION 1E-05 GS

	X COMP.	Y COMP.	Z COMP.
STA. NO. 1	.3818	.0340	.1247
STA. NO. 2	.4045	.1088	.5879
STA. NO. 3	.4043	.0395	.3785
STA. NO. 4	.1946	.0341	.1571
STA. NO. 5	.4038	.0012	.2607
STA. NO. 6	.4030	.0239	.1649
STA. NO. 7	.4025	.0339	.0967
STA. NO. 8	.4027	.0380	.0615
STA. NO. 9	.4036	.0665	.1057
STA. NO. 10	.4027	.0340	.1305

RMS VELOCITY 1E-03 IN PER SEC

X COMP.	Y COMP.	Z COMP.
.0546	.0065	.0201
.0581	.0205	.0913
.0580	.0074	.0585
.0617	.0065	.0420
.0579	.0002	.0402
.0578	.0046	.0255
.0577	.0065	.0156
.0578	.0073	.0119
.0579	.0126	.0264
.0578	.0065	.0215

Table 3-26
FUNCTIONAL VALUES, CASE 2-1-7 TNOM

SERIAL 727135

PEAK ANG. VEL. ARCSEC PER SEC
RESULT. 1.9252 WX 1.2010 WY .9582 WZ 1.6743

PEAK EULER ANG. ARCSEC
TOTAL .7638 B1 .5446 B2 -.4142 B3 -.5253

PEAK ACCELERATION 1E-05 GS

	RESULT.	X COMP.	Y COMP.	Z COMP.
STA. NO. 1	2.6867	-.6196	2.1607	-2.3631
STA. NO. 2	2.7910	-.6196	-1.2427	-2.5160
STA. NO. 3	3.1154	-.6196	-.7769	-3.0322
STA. NO. 4	3.5729	-.6196	-1.7501	-3.5543
STA. NO. 5	4.1794	-.6196	-2.8580	-4.1233
STA. NO. 6	5.3267	-.6196	-4.6187	-5.0171
STA. NO. 7	6.8900	-.6196	-6.4211	-5.9395
STA. NO. 8	7.3949	-2.0993	-5.7216	-6.5529
STA. NO. 9	6.1608	.6746	-5.9061	-4.9535
STA. NO. 10	6.4475	2.2276	-5.9061	-4.1019

PEAK VELOCITY 1E-03 IN PER SEC

	RESULT.	X COMP.	Y COMP.	Z COMP.
2.1438	.4832	-1.6195	1.6634	
2.2148	.4832	-1.0193	-2.0056	
2.5005	.4832	.5775	-2.4342	
2.8894	.4832	1.3720	-2.8739	
3.4224	.4832	2.2526	-3.3628	
4.4542	.4832	3.6372	-4.1400	
5.6379	.4832	5.0577	-4.9427	
6.3910	1.6906	4.3382	-5.5841	
4.8443	-.5315	4.6518	-3.9865	
5.0399	-1.7491	4.6518	-3.1176	

RMS ACCELERATION 1E-05 GS

	X COMP.	Y COMP.	Z COMP.
STA. NO. 1	.3145	1.0059	1.0329
STA. NO. 2	.3145	.5473	1.1832
STA. NO. 3	.3145	.3353	1.3552
STA. NO. 4	.3145	.6712	1.5416
STA. NO. 5	.3145	1.1905	1.7559
STA. NO. 6	.3145	2.0473	2.1069
STA. NO. 7	.3145	2.9361	2.4778
STA. NO. 8	.9096	2.7689	2.7373
STA. NO. 9	.3264	2.6816	2.0709
STA. NO. 10	1.0950	2.6816	1.7209

RMS VELOCITY 1E-03 IN PER SEC

	X COMP.	Y COMP.	Z COMP.
.2565	.8682	.7857	
.2565	.4874	.9447	
.2565	.2577	1.1191	
.2565	.4902	1.3026	
.2565	.9072	1.5092	
.2565	1.6009	1.8417	
.2565	2.3213	2.1881	
.7086	2.2166	2.4364	
.2630	2.1150	1.8016	
.8860	2.1150	1.4624	

Table 3-27
FUNCTIONAL VALUES, CASE 2-1-8 TNOM

SERIAL 727135

PEAK ANG. VEL. ARCSEC PER SEC

RESULT. 1.1210 WX .4624 WY .7369 WZ .7208

PEAK EULER ANG. ARCSEC

TOTAL .5018 B1 -.3021 B2 -.3419 B3 -.2094

PEAK ACCELERATION 1E-05 GS

	RESULT.	X COMP.	Y COMP.	Z COMP.
STA. NO. 1	3.1930	2.8044	-1.7282	-2.1727
STA. NO. 2	3.2690	2.8044	-1.3093	-2.5998
STA. NO. 3	3.3591	2.8044	-.8905	-3.0269
STA. NO. 4	3.5031	2.8044	-.4717	-3.4540
STA. NO. 5	3.9367	2.8044	-.0166	-3.9196
STA. NO. 6	4.7133	2.8044	.7011	-4.6500
STA. NO. 7	5.5845	2.8044	1.4341	-5.3974
STA. NO. 8	5.7522	2.4864	1.5084	-5.5534
STA. NO. 9	5.0982	2.9300	1.2246	-4.8786
STA. NO. 10	4.9224	3.0956	1.2246	-4.5132

PEAK VELOCITY 1E-03 IN PER SEC

	RESULT.	X COMP.	Y COMP.	Z COMP.
	2.4530	-2.2021	-1.4437	-1.7004
	2.5008	-2.2021	-1.0942	-2.0533
	2.5586	-2.2021	-.7448	-2.4076
	2.8085	-2.2021	-.3953	-2.7625
	3.1687	-2.2021	-.0149	-3.1503
	3.8169	-2.2021	.5832	-3.7595
	4.5462	-2.2021	1.1948	-4.3830
	4.7216	-1.9428	1.2905	-4.5411
	4.1305	-2.2963	1.0201	-3.9246
	3.9783	-2.4153	1.0201	-3.5884

RMS ACCELERATION 1E-05 GS

	X COMP.	Y COMP.	Z COMP.
STA. NO. 1	1.1293	.7605	.9608
STA. NO. 2	1.1293	.5760	1.1334
STA. NO. 3	1.1293	.3915	1.3077
STA. NO. 4	1.1293	.2070	1.4829
STA. NO. 5	1.1293	.0069	1.6747
STA. NO. 6	1.1293	.3097	1.9766
STA. NO. 7	1.1293	.6326	2.2865
STA. NO. 8	.9949	.6504	2.3513
STA. NO. 9	1.2683	.5403	2.0705
STA. NO. 10	1.4660	.5403	1.9181

RMS VELOCITY 1E-03 IN PER SEC

	X COMP.	Y COMP.	Z COMP.
	.8467	.6793	.7888
	.8467	.5145	.9440
	.8467	.3498	1.0999
	.8467	.1851	1.2562
	.8467	.0063	1.4270
	.8467	.2762	1.6954
	.8467	.5645	1.9705
	.7426	.5853	2.0328
	.9816	.4821	1.7746
	1.1710	.4821	1.6340

Table 3-28
FUNCTIONAL VALUES, CASE 2-2-2 TNOM

SERIAL 727135

PEAK ANG. VEL. ARCSEC PER SEC
RESULT. 1.8268 WX -.1237 WY -.3984 WZ-1.7788

PEAK EULER ANG. ARCSEC
TOTAL .8287 B1 .8066 B2 .1809 B3 .0586

PEAK ACCELERATION 1E-05 GS

	RESULT.	X COMP.	Y COMP.	Z COMP.
STA. NO. 1	8.4233	2.8120	8.2473	-.9639
STA. NO. 2	7.3245	2.8120	7.1501	-.7180
STA. NO. 3	6.2348	2.8120	6.0530	-.4723
STA. NO. 4	5.1599	2.8120	4.9657	-.2267
STA. NO. 5	4.0191	2.8120	3.7827	.0427
STA. NO. 6	3.2884	2.8120	1.9748	.4622
STA. NO. 7	3.2052	2.8120	-1.5744	.8925
STA. NO. 8	3.5711	3.4875	1.5715	.8770
STA. NO. 9	3.3502	2.9324	1.6175	.6800
STA. NO. 10	3.5992	3.2246	1.6175	.5745

PEAK VELOCITY 1E-03 IN PER SEC

	RESULT.	X COMP.	Y COMP.	Z COMP.
	6.6680	-2.2274	6.5043	-.7558
	5.8109	-2.2274	5.6482	-.5626
	4.9621	-2.2274	4.7932	-.3695
	4.1269	-2.2274	3.9427	-.1764
	3.2441	-2.2274	3.0247	.0350
	2.6217	-2.2274	1.6266	.3646
	2.5984	-2.2274	-1.3395	.7024
	2.5795	-2.4524	-1.3235	.6944
	2.6378	-2.2612	-1.3582	.5327
	2.7063	-2.3434	-1.3582	.4451

RMS ACCELERATION 1E-05 GS

	X COMP.	Y COMP.	Z COMP.
STA. NO. 1	1.3254	3.4351	.4027
STA. NO. 2	1.3254	2.9832	.3002
STA. NO. 3	1.3254	2.5345	.1976
STA. NO. 4	1.3254	2.0909	.0951
STA. NO. 5	1.3254	1.6182	.0181
STA. NO. 6	1.3254	.9400	.1924
STA. NO. 7	1.3254	.6262	.3719
STA. NO. 8	1.7034	.6122	.3648
STA. NO. 9	1.1152	.6325	.2844
STA. NO. 10	1.2258	.6325	.2419

RMS VELOCITY 1E-03 IN PER SEC

	X COMP.	Y COMP.	Z COMP.
	1.0599	2.9845	.3544
	1.0599	2.5855	.2642
	1.0599	2.1887	.1739
	1.0599	1.7955	.0838
	1.0599	1.3747	.0156
	1.0599	.7624	.1692
	1.0599	.4843	.3271
	1.4435	.4646	.3205
	.8058	.4808	.2503
	.8696	.4808	.2130

Table 3-29
FUNCTIONAL VALUES, CASE 2-2-9 TNOM

SERIAL 727135

PEAK ANG. VEL. ARCSEC PER SEC
RESULT. 1.9187 WX -.0812 WY -.4097 WZ-1.8728

PEAK EULER ANG. ARCSEC
TOTAL .6985 B1 -.6826 B2 -.1472 B3 -.0259

PEAK ACCELERATION 1E-05 GS

	RESULT.	X COMP.	Y COMP.	Z COMP.
STA. NO. 1	8.1089	4.1982	-7.5054	1.0050
STA. NO. 2	7.0252	4.1982	-6.3634	.7522
STA. NO. 3	5.9780	4.1982	-5.2214	.4995
STA. NO. 4	4.9905	4.1982	-4.0806	.2471
STA. NO. 5	4.2357	4.1982	-2.8587	-.0303
STA. NO. 6	4.5586	4.1982	-2.0408	-.4614
STA. NO. 7	5.1688	4.1982	2.9765	-.9038
STA. NO. 8	5.7117	5.0822	2.6113	-.8528
STA. NO. 9	4.2810	3.3427	2.6426	-.7145
STA. NO. 10	3.5984	2.4496	2.6426	-.6414

PEAK VELOCITY 1E-03 IN PER SEC

	RESULT.	X COMP.	Y COMP.	Z COMP.
	6.3374	3.3714	5.9388	-.7901
	5.4717	3.3714	5.0339	-.5915
	4.6308	3.3714	4.1290	-.3928
	3.8309	3.3714	3.2240	-.1942
	3.4043	3.3714	2.2452	.0228
	3.6885	3.3714	1.6358	.3620
	4.2053	3.3714	2.4993	.7097
	4.6478	4.1192	2.2057	.6684
	3.4912	2.6628	2.2356	.5619
	2.9595	1.9289	2.2356	.5040

RMS ACCELERATION 1E-05 GS

	X COMP.	Y COMP.	Z COMP.
STA. NO. 1	1.8394	2.8155	.4027
STA. NO. 2	1.8394	2.3822	.3026
STA. NO. 3	1.8394	1.9627	.2026
STA. NO. 4	1.8394	1.5681	.1028
STA. NO. 5	1.8394	1.1959	.0142
STA. NO. 6	1.8394	.9193	.1787
STA. NO. 7	1.8394	1.2439	.3537
STA. NO. 8	2.3345	1.0873	.3250
STA. NO. 9	1.4000	1.1011	.2882
STA. NO. 10	1.0668	1.1011	.2730

RMS VELOCITY 1E-03 IN PER SEC

	X COMP.	Y COMP.	Z COMP.
	1.5386	2.0448	.3038
	1.5386	1.7270	.2288
	1.5386	1.4246	.1538
	1.5386	1.1500	.0791
	1.5386	.9121	.0112
	1.5386	.8070	.1323
	1.5386	1.1004	.2635
	1.9076	.9730	.2381
	1.2110	.9870	.2182
	.9450	.9870	.2121

Table 3-30
FUNCTIONAL VALUES, CASE 2-3-2 TNOM

SERIAL 727135

PEAK ANG. VEL. ARCSEC PER SEC
RESULT. 3.0495 WX 1.6152 WY -.1214 WZ-2.5840

PEAK EULER ANG. ARCSEC
TOTAL 1.4391 B1 1.2224 B2 .0613 B3 -.7571

PEAK ACCELERATION 1E-05 GS

	RESULT.	X COMP.	Y COMP.	Z COMP.
STA. NO. 1	10.4202	2.5906	10.2471	-.9083
STA. NO. 2	8.8456	2.5906	8.6511	-.8280
STA. NO. 3	7.2828	2.5906	7.0551	-.7477
STA. NO. 4	5.7413	2.5906	5.4591	-.6674
STA. NO. 5	4.1148	2.5906	3.7203	-.5802
STA. NO. 6	2.7514	2.5906	1.0793	-.4437
STA. NO. 7	3.0302	2.5906	-1.8781	-.3045
STA. NO. 8	4.5877	4.3353	-.7927	-1.8069
STA. NO. 9	3.2601	3.2185	-1.1079	.8763
STA. NO. 10	4.3658	4.2221	-1.1079	2.3386

PEAK VELOCITY 1E-03 IN PER SEC

RESULT.	X COMP.	Y COMP.	Z COMP.
8.2336	-2.0436	8.0839	-.7001
7.0036	-2.0436	6.8320	-.6426
5.7840	-2.0436	5.5825	-.5851
4.5829	-2.0436	4.3330	-.5279
3.3272	-2.0436	2.9745	-.4658
2.2027	-2.0436	.8710	-.3690
2.1657	-2.0436	-1.4155	-.2709
3.6846	-3.3856	-.6789	-1.4725
2.5162	-2.4709	-.8029	.6822
3.1478	-3.0550	-.8029	1.8562

RMS ACCELERATION 1E-05 GS

	X COMP.	Y COMP.	Z COMP.
STA. NO. 1	1.3227	4.3083	.3870
STA. NO. 2	1.3227	3.6420	.3510
STA. NO. 3	1.3227	2.9765	.3153
STA. NO. 4	1.3227	2.3125	.2799
STA. NO. 5	1.3227	1.5925	.2420
STA. NO. 6	1.3227	.5124	.1846
STA. NO. 7	1.3227	.7989	.1319
STA. NO. 8	1.9683	.3055	.7514
STA. NO. 9	1.1957	.5019	.3707
STA. NO. 10	1.6992	.5019	.9794

RMS VELOCITY 1E-03 IN PER SEC

X COMP.	Y COMP.	Z COMP.
1.0822	3.6975	.3250
1.0822	3.1223	.2970
1.0822	2.5477	.2690
1.0822	1.9743	.2412
1.0822	1.3521	.2111
1.0822	.4152	.1647
1.0822	.7001	.1194
1.7294	.2443	.6625
.8511	.4378	.3146
1.2486	.4378	.8463

Table 3-31
FUNCTIONAL VALUES, CASE 2-3-9 TNOM

SERIAL 727135

PEAK ANG. VEL. ARCSEC PER SEC
RESULT. 2.7321 WX 1.3387 WY -.1261 WZ-2.3783

PEAK EULER ANG. ARCSEC
TOTAL .8932 B1 -.7885 B2 -.0443 B3 .4338

PEAK ACCELERATION 1E-05 GS

	RESULT.	X COMP.	Y COMP.	Z COMP.
STA. NO. 1	9.2197	4.0336	-8.6955	.7801
STA. NO. 2	7.8640	4.0336	-7.2494	.7105
STA. NO. 3	6.5534	4.0336	-5.8052	.6410
STA. NO. 4	5.3241	4.0336	-4.3699	.5715
STA. NO. 5	4.1606	4.0336	-2.8060	.4957
STA. NO. 6	4.2407	4.0336	-1.3732	.3768
STA. NO. 7	4.5471	4.0336	2.2817	.2552
STA. NO. 8	5.4641	5.2295	1.7200	1.5399
STA. NO. 9	3.9638	3.5245	1.8708	-.7517
STA. NO. 10	3.5346	-3.1687	1.8708	-2.0017

PEAK VELOCITY 1E-03 IN PER SEC

RESULT.	X COMP.	Y COMP.	Z COMP.
7.2757	3.2438	6.9121	-.6362
6.1848	3.2438	5.7591	-.5751
5.1219	3.2438	4.6060	-.5139
4.1130	3.2438	3.4563	-.4528
3.2713	3.2438	2.2038	-.3861
3.4193	3.2438	1.1829	-.2815
3.6962	3.2438	-1.8099	-.1745
4.1021	-3.8884	1.4794	-1.1786
3.2030	2.8171	1.5688	.6062
2.8728	2.4969	1.5688	1.5797

RMS ACCELERATION 1E-05 GS

	X COMP.	Y COMP.	Z COMP.
STA. NO. 1	1.8019	3.2918	.2975
STA. NO. 2	1.8019	2.7585	.2700
STA. NO. 3	1.8019	2.2306	.2427
STA. NO. 4	1.8019	1.7131	.2154
STA. NO. 5	1.8019	1.1770	.1860
STA. NO. 6	1.8019	.6110	.1407
STA. NO. 7	1.8019	1.0640	.0967
STA. NO. 8	2.3763	.7165	.5759
STA. NO. 9	1.4671	.8545	.2852
STA. NO. 10	1.4359	.8545	.7537

RMS VELOCITY 1E-03 IN PER SEC

X COMP.	Y COMP.	Z COMP.
1.4898	2.4025	.2203
1.4898	2.0174	.1990
1.4898	1.6383	.1778
1.4898	1.2705	.1567
1.4898	.8987	.1340
1.4898	.5469	.0992
1.4898	.8574	.0665
1.8667	.6437	.4110
1.2815	.7154	.2097
1.2655	.7154	.5470

Table 3-32
FUNCTIONAL VALUES, CASE 2-1-7 TMIN

SERIAL 727135

PEAK ANG. VEL. ARCSEC PER SEC
RESULT. 2.5217 WX -.8945 WY .5637 WZ 2.3555

PEAK EULER ANG. ARCSEC
TOTAL .9626 B1 .8921 B2 -.1326 B3 -.3588

PEAK ACCELERATION 1E-05 GS

	RESULT.	X COMP.	Y COMP.	Z COMP.
STA. NO. 1	3.1590	-.8674	2.5346	-2.0320
STA. NO. 2	2.9154	-.8674	-1.4276	-2.4765
STA. NO. 3	3.0197	-.8674	.7010	-2.9211
STA. NO. 4	3.4403	-.8674	1.8399	-3.3657
STA. NO. 5	4.1457	-.8674	-3.3557	-3.8503
STA. NO. 6	5.9091	-.8674	-5.8056	-4.6105
STA. NO. 7	8.4319	-.8674	-8.3128	-5.3886
STA. NO. 8	7.5385	-2.7430	-7.0155	-5.0633
STA. NO. 9	7.8140	.9269	-7.5964	-5.2521
STA. NO. 10	8.5075	3.0801	-7.5964	-5.3550

PEAK VELOCITY 1E-03 IN PER SEC

	RESULT.	X COMP.	Y COMP.	Z COMP.
2.2254	.6858	-1.8587	1.4575	
1.7448	.6858	-.8938	1.4603	
1.7866	.6858	.5518	-1.7227	
2.1328	.6858	1.6198	-1.9960	
3.0591	.6858	2.8495	-2.2939	
4.8741	.6858	4.7958	-2.7612	
6.8323	.6858	6.7912	-3.2395	
6.2108	2.2694	5.6904	-3.0102	
6.2682	-.7420	6.2202	-3.1800	
6.7419	-2.4550	6.2202	-3.2726	

RMS ACCELERATION 1E-05 GS

	X COMP.	Y COMP.	Z COMP.
STA. NO. 1	.4373	1.3269	.8881
STA. NO. 2	.4373	.6351	.9784
STA. NO. 3	.4373	.2993	1.0867
STA. NO. 4	.4373	.9052	1.2080
STA. NO. 5	.4373	1.6744	1.3511
STA. NO. 6	.4373	2.9009	1.5910
STA. NO. 7	.4373	4.1614	1.8494
STA. NO. 8	1.3703	3.5166	1.7936
STA. NO. 9	.4658	3.8010	1.8131
STA. NO. 10	1.5493	3.8010	1.9200

RMS VELOCITY 1E-03 IN PER SEC

	X COMP.	Y COMP.	Z COMP.
.3167	.9304	.6492	
.3167	.4285	.6972	
.3167	.2276	.7577	
.3167	.6858	.8279	
.3167	1.2463	.9130	
.3167	2.1376	1.0592	
.3167	3.0532	1.2198	
1.0104	2.5727	1.2198	
.3390	2.7915	1.1815	
1.1258	2.7515	1.2472	

Table 3-33
FUNCTIONAL VALUES, CASE 2-1-8 TMIN

SERIAL 727135

PEAK ANG. VEL. ARCSEC PER SEC
RESULT. .7544 WX -.2679 WY .4685 WZ .5828

PEAK EULER ANG. ARCSEC
TOTAL .2179 B1 .1354 B2 -.1771 B3 -.1060

PEAK ACCELERATION 1E-05 GS

	RESULT.	X COMP.	Y COMP.	Z COMP.
STA. NO. 1	3.4162	3.1337	-1.8552	-2.3961
STA. NO. 2	3.3086	3.1337	-1.4033	-2.7746
STA. NO. 3	3.4825	3.1337	-.9514	-3.1531
STA. NO. 4	3.7420	3.1337	-.4995	-3.5316
STA. NO. 5	4.1034	3.1337	.0096	-3.9441
STA. NO. 6	4.7904	3.1337	.7658	-4.5913
STA. NO. 7	5.5949	3.1337	1.5567	-5.2537
STA. NO. 8	5.4728	2.7177	1.4407	-5.1976
STA. NO. 9	5.4022	3.5444	1.3307	-4.9535
STA. NO. 10	5.5353	4.0416	1.3307	-4.8203

PEAK VELOCITY 1E-03 IN PER SEC

RESULT.	X COMP.	Y COMP.	Z COMP.
2.8595	-2.7127	-1.1596	-1.4304
2.8213	-2.7127	-.8771	-1.6575
2.8017	-2.7127	-.5945	-1.8847
2.7997	-2.7127	-.3119	-2.1118
2.8158	-2.7127	.0076	-2.3594
2.9052	-2.7127	.4793	-2.7478
3.3913	-2.7127	.9738	-3.1453
3.2991	-2.3657	.8927	-3.1040
3.2987	-2.9617	.8325	-2.9715
3.4095	-3.2710	.8325	-2.8992

RMS ACCELERATION 1E-05 GS

	X COMP.	Y COMP.	Z COMP.
STA. NO. 1	1.5652	.8100	.8344
STA. NO. 2	1.5652	.6119	.9639
STA. NO. 3	1.5652	.4138	1.0936
STA. NO. 4	1.5652	.2157	1.2233
STA. NO. 5	1.5652	.0041	1.3649
STA. NO. 6	1.5652	.3389	1.5870
STA. NO. 7	1.5652	.6856	1.8144
STA. NO. 8	1.3579	.5742	1.8076
STA. NO. 9	1.7691	.5865	1.7041
STA. NO. 10	2.0266	.5865	1.6539

RMS VELOCITY 1E-03 IN PER SEC

X COMP.	Y COMP.	Z COMP.
1.1724	.5445	.5605
1.1724	.4112	.6462
1.1724	.2780	.7319
1.1724	.1447	.8178
1.1724	.0031	.9114
1.1724	.2284	1.0585
1.1724	.4616	1.2090
1.0190	.3792	1.2128
1.3092	.3950	1.1297
1.4814	.3950	1.0897

Table 3-34
FUNCTIONAL VALUES, CASE 2-2-9 TMIN

SERIAL 727135

PEAK ANG. VEL. ARCSEC PER SEC
RESULT. 2.0535 WX -.1020 WY -.4390 WZ-2.0038

PEAK EULER ANG. ARCSEC
TOTAL .8258 B1 -.8058 B2 -.1766 B3 -.0396

PEAK ACCELERATION 1E-05 GS

	RESULT.	X COMP.	Y COMP.	Z COMP.
STA. NO. 1	8.2272	4.0887	7.8688	-1.0237
STA. NO. 2	7.0802	4.0887	6.6973	-.7661
STA. NO. 3	5.9569	4.0887	5.5259	-.5086
STA. NO. 4	4.8735	4.0887	4.3669	-.2511
STA. NO. 5	4.3298	4.0887	-3.3385	-.0348
STA. NO. 6	4.5426	4.0887	1.9811	.4700
STA. NO. 7	4.8191	4.0887	2.5425	.9206
STA. NO. 8	5.0584	4.4926	2.3430	.8687
STA. NO. 9	4.3922	3.6849	2.3810	.7278
STA. NO. 10	3.9970	3.2028	2.3810	.6509

PEAK VELOCITY 1E-03 IN PER SEC

	RESULT.	X COMP.	Y COMP.	Z COMP.
	6.9224	2.4237	6.7258	-.8434
	5.9607	2.4237	5.7625	-.6306
	5.0109	2.4237	4.8052	-.4178
	4.0811	2.4237	3.8539	-.2052
	3.1128	2.4237	2.8331	.0287
	2.7297	2.4237	1.3304	.3909
	2.8629	2.4237	1.5211	.7634
	3.0392	-2.9310	1.4192	.7275
	2.6623	2.2337	1.4451	.5986
	2.4756	2.0057	1.4451	.5298

RMS ACCELERATION 1E-05 GS

	X COMP.	Y COMP.	Z COMP.
STA. NO. 1	1.4710	3.6099	.4388
STA. NO. 2	1.4710	3.1199	.3280
STA. NO. 3	1.4710	2.6359	.2172
STA. NO. 4	1.4710	2.1617	.1066
STA. NO. 5	1.4710	1.6658	.0174
STA. NO. 6	1.4710	1.0106	.2044
STA. NO. 7	1.4710	.8796	.3983
STA. NO. 8	1.8635	.8096	.3822
STA. NO. 9	1.2758	.8274	.3113
STA. NO. 10	1.4276	.8274	.2753

RMS VELOCITY 1E-03 IN PER SEC

	X COMP.	Y COMP.	Z COMP.
	1.0095	2.7736	.3404
	1.0095	2.3901	.2544
	1.0095	2.0099	.1685
	1.0095	1.6354	.0827
	1.0095	1.2396	.0128
	1.0095	.6982	.1584
	1.0095	.5872	.3088
	1.3460	.5273	.2957
	.8304	.5380	.2415
	.9634	.5380	.2134

Table 3-35
FUNCTIONAL VALUES, CASE 2-2-2 TMIN

SERIAL 727135

PEAK ANG. VEL. ARCSEC PER SEC
RESULT. 1.6443 WX -.0824 WY -.3938 WZ-1.7999

PEAK EULER ANG. ARCSEC
TOTAL .3781 B1 .3673 B2 .0827 B3 .0345

PEAK ACCELERATION 1E-05 GS

	RESULT.	X COMP.	Y COMP.	Z COMP.
STA. NO. 1	10.0173	3.8161	9.6765	-1.2259
STA. NO. 2	8.6228	3.8161	8.2645	-.9167
STA. NO. 3	7.2482	3.8161	6.8526	-.6075
STA. NO. 4	5.9075	3.8161	5.4406	-.2982
STA. NO. 5	4.5203	3.8161	3.9015	.0388
STA. NO. 6	3.9095	3.8161	-1.7862	.5675
STA. NO. 7	4.4421	3.8161	2.1977	1.1087
STA. NO. 8	5.1716	4.8261	-1.8838	1.0546
STA. NO. 9	3.5332	-2.9643	-1.9188	.8703
STA. NO. 10	3.3558	-2.7768	-1.9188	.7698

PEAK VELOCITY 1E-03 IN PER SEC

	RESULT.	X COMP.	Y COMP.	Z COMP.
	6.1466	-3.0784	5.9060	-.7577
	5.2898	-3.0784	5.0333	-.5668
	4.4473	-3.0784	4.1607	-.3759
	3.6292	-3.0784	3.2881	-.1850
	3.1056	-3.0784	2.3369	.0231
	3.2825	-3.0784	-1.3907	.3496
	3.6037	-3.0784	-1.8532	.6836
	3.9766	-3.6375	-1.6508	.6481
	3.0914	-2.5924	-1.6709	.5382
	2.7486	-2.2135	-1.6709	.4783

RMS ACCELERATION 1E-05 GS

	X COMP.	Y COMP.	Z COMP.
STA. NO. 1	1.9146	3.4447	.4777
STA. NO. 2	1.9146	2.9109	.3584
STA. NO. 3	1.9146	2.3845	.2391
STA. NO. 4	1.9146	1.8715	.1199
STA. NO. 5	1.9146	1.3460	.0136
STA. NO. 6	1.9146	.7784	.2147
STA. NO. 7	1.9146	1.0965	.4235
STA. NO. 8	2.4854	.9158	.3923
STA. NO. 9	1.4330	.9182	.3410
STA. NO. 10	1.1687	.9182	.3150

RMS VELOCITY 1E-03 IN PER SEC

	X COMP.	Y COMP.	Z COMP.
	1.3978	2.2368	.3142
	1.3978	1.8900	.2358
	1.3978	1.5500	.1575
	1.3978	1.2225	.0793
	1.3978	.8957	.0092
	1.3978	.5850	.1405
	1.3978	.8142	.2775
	1.7632	.6956	.2560
	1.0808	.6997	.2245
	.8986	.6997	.2091

Table 3-36
FUNCTIONAL VALUES, CASE 2-3-9 TMIN

SERIAL 727135

PEAK ANG. VEL. ARCSEC PER SEC
RESULT. 3.1362 WX 1.5322 WY -.1679 WZ-2.7322

PEAK EULER ANG. ARCSEC
TOTAL 1.2617 B1-1.0997 B2 -.0667 B3 .6150

PEAK ACCELERATION 1E-05 GS

	RESULT.	X COMP.	Y COMP.	Z COMP.
STA. NO. 1	9.6657	3.8488	9.3394	-.8822
STA. NO. 2	8.1761	3.8488	7.8031	-.7907
STA. NO. 3	6.7118	3.8488	6.2669	-.6993
STA. NO. 4	5.2942	3.8488	-4.8004	-.6081
STA. NO. 5	4.1020	3.8488	-3.2876	-.5089
STA. NO. 6	4.0613	3.8488	1.2972	-.3534
STA. NO. 7	4.0236	3.8488	-2.3565	-.1947
STA. NO. 8	4.9859	-4.7329	1.3433	-1.5228
STA. NO. 9	4.1213	3.9373	-1.5996	.8302
STA. NO. 10	4.2359	4.0498	-1.5996	2.1128

PEAK VELOCITY 1E-03 IN PER SEC

RESULT.	X COMP.	Y COMP.	Z COMP.
8.3462	2.2682	8.1754	-.7741
7.0463	2.2682	6.8523	-.6929
5.7596	2.2682	5.5338	-.6117
4.4997	2.2682	4.2154	-.5305
3.2038	2.2682	2.7859	-.4420
2.4088	2.2682	.8104	-.3034
2.6940	2.2682	-1.8941	-.1625
3.9195	-3.6961	.8053	-1.3159
2.4963	2.3985	-1.2550	.7269
3.1703	2.5549	-1.2550	1.8412

RMS ACCELERATION 1E-05 GS

	X COMP.	Y COMP.	Z COMP.
STA. NO. 1	1.4385	4.5269	.4305
STA. NO. 2	1.4385	3.8159	.3843
STA. NO. 3	1.4385	3.1067	.3382
STA. NO. 4	1.4385	2.4008	.2922
STA. NO. 5	1.4385	1.6404	.2420
STA. NO. 6	1.4385	.5628	.1638
STA. NO. 7	1.4385	.9907	.0852
STA. NO. 8	2.0484	.4627	.7165
STA. NO. 9	1.3884	.6871	.4027
STA. NO. 10	1.9661	.6871	1.0127

RMS VELOCITY 1E-03 IN PER SEC

X COMP.	Y COMP.	Z COMP.
1.0050	3.4406	.3267
1.0050	2.8946	.2919
1.0050	2.3496	.2572
1.0050	1.8066	.2225
1.0050	1.2201	.1847
1.0050	.3779	.1256
1.0050	.7651	.0660
1.5452	.3073	.5478
.9014	.5206	.3060
1.3474	.5206	.7715

Table 3-37
FUNCTIONAL VALUES, CASE 2-3-2 TMIN

SERIAL 727135

PEAK ANG. VEL. ARCSEC PER SEC
RESULT. 2.7388 WX 1.3282 WY -.1419 WZ-2.3910

PEAK EULER ANG. ARCSEC
TOTAL .7966 B1 .6832 B2 .0499 B3 -.4065

PEAK ACCELERATION 1E-05 GS

	RESULT.	X COMP.	Y COMP.	Z COMP.
STA. NO. 1	11.9422	3.7649	11.6125	-1.0976
STA. NO. 2	10.0909	3.7649	9.7106	-.9835
STA. NO. 3	8.2641	3.7649	7.8088	-.8693
STA. NO. 4	6.4826	3.7649	5.9069	-.7552
STA. NO. 5	4.6539	3.7649	3.8339	-.6308
STA. NO. 6	3.8269	3.7649	-1.1160	-.4356
STA. NO. 7	4.2538	3.7649	-2.7478	-.2358
STA. NO. 8	5.6261	-5.2814	1.1414	-1.8831
STA. NO. 9	3.3133	-3.1920	-1.7985	1.0323
STA. NO. 10	4.1499	-3.5941	-1.7985	2.6225

PEAK VELOCITY 1E-03 IN PER SEC

RESULT.	X COMP.	Y COMP.	Z COMP.
7.2669	-2.9630	7.0368	-.6646
6.1442	-2.9630	5.8777	-.5957
5.0389	-2.9630	4.7185	-.5269
3.9658	-2.9630	3.5593	-.4581
2.9835	-2.9630	2.2958	-.3831
3.0614	-2.9630	-.8948	-.2655
3.2140	-2.9630	-1.7149	-.1450
3.5676	-3.4311	-.9731	-1.1454
2.9113	-2.7443	-1.1353	.6255
2.9339	-2.8238	-1.1353	1.5914

RMS ACCELERATION 1E-05 GS

	X COMP.	Y COMP.	Z COMP.
STA. NO. 1	1.9010	4.0167	.3789
STA. NO. 2	1.9010	3.3498	.3399
STA. NO. 3	1.9010	2.6855	.3009
STA. NO. 4	1.9010	2.0264	.2620
STA. NO. 5	1.9010	1.3233	.2198
STA. NO. 6	1.9010	.4691	.1539
STA. NO. 7	1.9010	1.1788	.0883
STA. NO. 8	2.6433	.5697	.6595
STA. NO. 9	1.4842	.8792	.3570
STA. NO. 10	1.5409	.8792	.9108

RMS VELOCITY 1E-03 IN PER SEC

X COMP.	Y COMP.	Z COMP.
1.3740	2.6152	.2469
1.3740	2.1837	.2214
1.3740	1.7546	.1959
1.3740	1.3302	.1704
1.3740	.8812	.1428
1.3740	.3619	.0999
1.3740	.7898	.0577
1.8207	.4245	.4284
1.1374	.6032	.2324
1.1690	.6032	.5923

Table 3-38
FUNCTIONAL VALUES, CASE 2-1-7 PPNOM

SERIAL 727135

PEAK ANG. VEL. ARCSEC PER SEC
RESULT. 1.9074 WX -.6014 WY .3596 WZ 1.7957

PEAK EULER ANG. ARCSEC
TOTAL .4244 B1 .4003 B2 -.0799 B3 -.1232

PEAK ACCELERATION 1E-05 GS

	RESULT.	X COMP.	Y COMP.	Z COMP.
STA. NO. 1	3.5459	-1.1266	3.3467	-2.6326
STA. NO. 2	2.9457	-1.1266	1.6066	2.8733
STA. NO. 3	3.2649	-1.1266	-.9261	3.1647
STA. NO. 4	3.6145	-1.1266	-2.5154	3.4561
STA. NO. 5	4.7447	-1.1266	-4.4864	3.7737
STA. NO. 6	7.7258	-1.1266	-7.6374	4.2719
STA. NO. 7	10.9801	-1.1266	*****	4.8028
STA. NO. 8	9.8631	-3.6102	-9.1726	5.0706
STA. NO. 9	10.1500	1.2058	-9.9658	4.7477
STA. NO. 10	11.0472	4.0021	-9.9658	5.0075

PEAK VELOCITY 1E-03 IN PER SEC

RESULT.	X COMP.	Y COMP.	Z COMP.
1.6555	.5259	-1.5419	-1.3910
1.6045	.5259	-.7037	-1.5572
1.7751	.5259	-.4253	-1.7234
1.9457	.5259	1.1132	-1.8895
2.1316	.5259	2.0514	-2.0706
3.5873	.5259	3.5370	-2.3548
5.1144	.5259	5.0574	-2.6456
4.5789	1.6715	4.2629	-2.7776
4.7383	-.5623	4.6230	-2.3832
5.1575	-1.8682	4.6230	-2.1681

RMS ACCELERATION 1E-05 GS

	X COMP.	Y COMP.	Z COMP.
STA. NO. 1	.3693	1.1120	1.2616
STA. NO. 2	.3693	.5713	1.3913
STA. NO. 3	.3693	.4073	1.5298
STA. NO. 4	.3693	.8690	1.6749
STA. NO. 5	.3693	1.5005	1.8388
STA. NO. 6	.3693	2.5286	2.1046
STA. NO. 7	.3693	3.5920	2.3844
STA. NO. 8	1.1962	3.0180	2.4635
STA. NO. 9	.3962	3.2877	2.2056
STA. NO. 10	1.3145	3.2877	2.1362

RMS VELOCITY 1E-03 IN PER SEC

X COMP.	Y COMP.	Z COMP.
.1709	.5493	.5247
.1709	.2914	.5921
.1709	.1629	.6639
.1709	.3559	.7390
.1709	.6452	.8234
.1709	1.1180	.9597
.1709	1.6072	1.1024
.5280	1.3608	1.0956
.1810	1.4672	1.0469
.6032	1.4672	1.0473

Table 3-39
FUNCTIONAL VALUES, CASE 2-1-7 PPMIN, RR4-2

SERIAL 727135

PEAK ANG. VEL. ARCSEC PER SEC
RESULT. 1.3177 WX .4829 WY -.3362 WZ-1.2254

PEAK EULER ANG. ARCSEC
TOTAL .4820 B1 -.4487 B2 .0635 B3 .1744

PEAK ACCELERATION 1E-05 GS

	RESULT.	X COMP.	Y COMP.	Z COMP.
STA. NO. 1	2.2071	.6085	-1.9728	-1.1595
STA. NO. 2	1.6401	.6085	-1.0541	-1.2246
STA. NO. 3	1.5390	.6085	-.4056	-1.4295
STA. NO. 4	1.9542	.6085	1.2021	-1.7202
STA. NO. 5	2.7436	.6085	2.2956	-2.0371
STA. NO. 6	4.2192	.6085	4.0110	-2.5342
STA. NO. 7	5.9059	.6085	5.7687	-3.0430
STA. NO. 8	5.2658	1.8941	4.8817	-2.6373
STA. NO. 9	5.4990	-.6477	5.2662	-3.1146
STA. NO. 10	5.9886	-2.1551	5.2662	-3.3799

PEAK VELOCITY 1E-03 IN PER SEC

	RESULT.	X COMP.	Y COMP.	Z COMP.
1.2035	-.3559	1.0409	-.9899	
1.0757	-.3559	.5726	-1.0632	
1.1926	-.3559	-.3372	-1.1438	
1.3466	-.3559	-.8705	-1.2294	
1.6672	-.3559	-1.5129	-1.3261	
2.5924	-.3559	-2.5282	-1.4847	
3.6033	-.3559	-3.5679	1.7615	
3.2956	-1.1969	-2.9815	-1.7916	
3.2948	.3869	-3.2708	1.7830	
3.5212	1.2780	-3.2708	1.9067	

RMS ACCELERATION 1E-05 GS

	X COMP.	Y COMP.	Z COMP.
STA. NO. 1	.3095	.9781	.5036
STA. NO. 2	.3095	.4816	.5824
STA. NO. 3	.3095	.1608	.6754
STA. NO. 4	.3095	.5817	.7777
STA. NO. 5	.3095	1.1268	.8959
STA. NO. 6	.3095	1.9931	1.0902
STA. NO. 7	.3095	2.8824	1.2958
STA. NO. 8	.9404	2.4483	1.1734
STA. NO. 9	.3271	2.6282	1.3164
STA. NO. 10	1.0909	2.6282	1.4387

RMS VELOCITY 1E-03 IN PER SEC

	X COMP.	Y COMP.	Z COMP.
.1434	.4327	.3888	
.1434	.2132	.4282	
.1434	.1275	.4720	
.1434	.3156	.5190	
.1434	.5645	.5731	
.1434	.9653	.6620	
.1434	1.3784	.7567	
.4563	1.1617	.7656	
.1532	1.2602	.7150	
.5091	1.2602	.7181	

Table 3-40
FUNCTIONAL VALUES, CASE 2-1-1 HEARTBEAT

SERIAL 157475

PEAK ANG. VEL. ARCSEC PER SEC
RESULT. .1563 WX .0827 WY .0122 WZ -.1321

PEAK EULER ANG. ARCSEC
TOTAL .0122 B1 -.0106 B2 -.0008 B3 .0061

PEAK ACCELERATION 1E-05 GS

	RESULT.	X COMP.	Y COMP.	Z COMP.
STA. NO. 1	.9509	-.2390	.5276	-.7650
STA. NO. 2	.8362	-.2390	-.1418	-.7985
STA. NO. 3	.9089	-.2390	-.2870	-.8319
STA. NO. 4	1.1195	-.2390	-.6920	-.8654
STA. NO. 5	1.4529	-.2390	-1.1335	-.9019
STA. NO. 6	2.0618	-.2390	-1.8260	-.9591
STA. NO. 7	2.7275	-.2390	-2.5348	-1.0176
STA. NO. 8	2.5791	-.8831	-2.0207	-1.3643
STA. NO. 9	2.4364	.2672	-2.3323	-.7090
STA. NO. 10	2.5064	.8747	-2.3323	-.4059

PEAK VELOCITY 1E-03 IN PER SEC

	RESULT.	X COMP.	Y COMP.	Z COMP.
	.1561	-.0377	.0806	-.1286
	.1404	-.0377	-.0213	-.1343
	.1527	-.0377	-.0480	-.1400
	.1876	-.0377	-.1121	-.1456
	.2399	-.0377	-.1819	-.1518
	.3354	-.0377	-.2915	-.1615
	.4401	-.0377	-.4036	-.1715
	.4189	-.1409	-.3214	-.2288
	.3923	.0423	-.3716	-.1198
	.4008	.1384	-.3716	-.0633

RMS ACCELERATION 1E-05 GS

	X COMP.	Y COMP.	Z COMP.
STA. NO. 1	.0946	.2154	.2815
STA. NO. 2	.0946	.0582	.2915
STA. NO. 3	.0946	.1074	.3017
STA. NO. 4	.0946	.2662	.3119
STA. NO. 5	.0946	.4402	.3233
STA. NO. 6	.0946	.7135	.3413
STA. NO. 7	.0946	.9933	.3601
STA. NO. 8	.3447	.7944	.4935
STA. NO. 9	.1053	.9133	.2428
STA. NO. 10	.3452	.9133	.1273

RMS VELOCITY 1E-03 IN PER SEC

	X COMP.	Y COMP.	Z COMP.
	.0135	.0303	.0423
	.0135	.0081	.0440
	.0135	.0159	.0458
	.0135	.0385	.0476
	.0135	.0632	.0496
	.0135	.1021	.0527
	.0135	.1420	.0560
	.0493	.1135	.0748
	.0150	.1306	.0392
	.0492	.1306	.0229

Table 3-41
FUNCTIONAL VALUES, CASE 2-1-1 COUGH

SERIAL 757475

PEAK ANG. VEL. ARCSEC PER SEC
RESULT. 4.2619 WX 2.6373 WY .7869 WZ-3.3230

PEAK EULER ANG. ARCSEC
TOTAL .4044 B1 .3508 B2 .0582 B3 -.1983

PEAK ACCELERATION 1E-05 GS

	RESULT.	X COMP.	Y COMP.	Z COMP.
STA. NO. 1	16.2564	-4.2613	-6.7837	14.7602
STA. NO. 2	16.0019	-4.2613	3.3115	15.9693
STA. NO. 3	18.0259	-4.2613	5.4090	17.1783
STA. NO. 4	21.7000	-4.2613	11.4982	18.3874
STA. NO. 5	26.7914	-4.2613	18.1355	19.7053
STA. NO. 6	35.9115	-4.2613	28.5482	21.7728
STA. NO. 7	45.9155	-4.2613	39.2044	23.8887
STA. NO. 8	44.4400	11.6697	29.7361	30.9925
STA. NO. 9	40.4810	-7.5426	36.1597	17.1195
STA. NO. 10	40.5800	*****	36.1597	14.5831

PEAK VELOCITY 1E-03 IN PER SEC

	RESULT.	X COMP.	Y COMP.	Z COMP.
	3.8047	-1.1576	2.0719	-3.1905
	3.4477	-1.1576	-.9208	-3.4163
	3.8198	-1.1576	-1.1525	-3.6421
	4.7527	-1.1576	-2.7611	-3.8679
	6.1101	-1.1576	-4.5172	-4.1140
	8.5520	-1.1576	-7.2720	-4.5001
	11.2161	-1.1576	*****	-4.8952
	10.5341	-2.7179	-7.6933	-6.6933
	10.0344	2.1489	-9.2858	-4.2283
	10.3921	4.5140	-9.2858	-3.7790

RMS ACCELERATION 1E-05 GS

	X COMP.	Y COMP.	Z COMP.
STA. NO. 1	1.8072	2.7733	5.7067
STA. NO. 2	1.8072	1.0214	6.2194
STA. NO. 3	1.8072	2.0824	6.7409
STA. NO. 4	1.8072	4.1917	7.2691
STA. NO. 5	1.8072	6.5816	7.8510
STA. NO. 6	1.8072	10.3686	8.7738
STA. NO. 7	1.8072	14.2582	9.7276
STA. NO. 8	4.8160	11.1058	11.9180
STA. NO. 9	2.4895	13.1462	7.4777
STA. NO. 10	5.4971	13.1462	5.3148

RMS VELOCITY 1E-03 IN PER SEC

	X COMP.	Y COMP.	Z COMP.
	.4404	.7911	1.2812
	.4404	.3305	1.3978
	.4404	.4644	1.5187
	.4404	.9722	1.6429
	.4404	1.5652	1.7813
	.4404	2.5104	2.0032
	.4404	3.4829	2.2346
	1.1273	2.7552	2.7289
	.6638	3.2048	1.7331
	1.4218	3.2048	1.2948

Table 3-42
FUNCTIONAL VALUES, CASE 3-1-11 TNOM, RR5-3

SERIAL 727135

PEAK ANG. VEL. ARCSEC PER SEC
RESULT. 1.7705 WX .0000 WY 1.7705 WZ .0000

PEAK EULER ANG. ARCSEC
TOTAL .6872 B1 .0000 B2 -.6872 B3 .0000

PEAK ACCELERATION 1E-05 GS

	RESULT.	X COMP.	Y COMP.	Z COMP.
STA. NO. 1	7.6919	-5.6842	.0000	5.9328
STA. NO. 2	7.5663	-5.6842	.0000	6.2526
STA. NO. 3	7.3850	-5.6842	.0000	6.7243
STA. NO. 4	7.2405	-5.6842	.0000	7.1241
STA. NO. 5	7.6354	-5.6842	.0000	7.5239
STA. NO. 6	8.3415	-5.6842	.0000	8.2385
STA. NO. 7	8.5539	-5.6842	.0000	8.4535
STA. NO. 8	9.0697	-5.6842	.0000	8.9751
STA. NO. 9	9.0697	-5.6842	.0000	8.9751
STA. NO. 10	9.0697	-5.6842	.0000	8.9751

PEAK VELOCITY 1E-03 IN PER SEC

RESULT.	X COMP.	Y COMP.	Z COMP.
5.5756	4.4644	.0000	4.4631
5.5322	4.4644	.0000	4.7594
5.4693	4.4644	.0000	5.2124
5.7186	4.4644	.0000	5.6103
6.1311	4.4644	.0000	6.0162
6.8736	4.4644	.0000	6.7548
7.0975	4.4644	.0000	6.9787
7.6416	4.4644	.0000	7.5247
7.6416	4.4644	.0000	7.5247
7.6416	4.4644	.0000	7.5247

RMS ACCELERATION 1E-05 GS

	X COMP.	Y COMP.	Z COMP.
STA. NO. 1	2.3790	.0000	2.7652
STA. NO. 2	2.3790	.0000	2.8424
STA. NO. 3	2.3790	.0000	2.9701
STA. NO. 4	2.3790	.0000	3.0899
STA. NO. 5	2.3790	.0000	3.2190
STA. NO. 6	2.3790	.0000	3.4692
STA. NO. 7	2.3790	.0000	3.5487
STA. NO. 8	2.3790	.0000	3.7487
STA. NO. 9	2.3790	.0000	3.7487
STA. NO. 10	2.3790	.0000	3.7487

RMS VELOCITY 1E-03 IN PER SEC

X COMP.	Y COMP.	Z COMP.
1.8147	.0000	2.1473
1.8147	.0000	2.2589
1.8147	.0000	2.4300
1.8147	.0000	2.5802
1.8147	.0000	2.7343
1.8147	.0000	3.0170
1.8147	.0000	3.1036
1.8147	.0000	3.3161
1.8147	.0000	3.3161
1.8147	.0000	3.3161

Table 3-43
FUNCTIONAL VALUES, CASE 3-2-10 TNOM, RR5-1

SERIAL 727135

PEAK ANG. VEL. ARCSEC PER SEC
RESULT. 13.7971 WX***** WY-1.6926 WZ 1.2646

PEAK EULER ANG. ARCSEC
TOTAL 5.3751 D1 .4112 D2 .8134 D3 5.3135

PEAK ACCELERATION 1E-05 GS

	RESULT.	X COMP.	Y COMP.	Z COMP.
STA. NO. 1	9.7083	-.0000	-7.2376	9.5660
STA. NO. 2	9.2916	-.0000	-6.9253	9.1555
STA. NO. 3	8.6770	-.0000	-6.4648	8.5501
STA. NO. 4	8.1562	-.0000	-6.0745	8.0370
STA. NO. 5	7.6354	.0000	-5.6842	7.5239
STA. NO. 6	7.0985	.2810	-4.9879	5.3364
STA. NO. 7	6.4271	.0000	-4.7787	6.3334
STA. NO. 8	5.7500	.0000	-4.2714	5.6664
STA. NO. 9	10.6752	-.6245	-4.2714	10.6289
STA. NO. 10	7.4804	.6245	-4.2714	6.2111

PEAK VELOCITY 1E-03 IN PER SEC

	RESULT.	X COMP.	Y COMP.	Z COMP.
	7.7957	.0000	5.6845	7.6492
	7.4611	.0000	5.4392	7.3209
	6.9676	.0000	5.0775	6.8368
	6.5493	.0000	4.7710	6.4265
	6.1311	.0000	4.4644	6.0162
	5.0144	-.2207	3.9176	-3.2471
	5.1607	.0000	3.7533	5.0643
	4.6170	.0000	3.3548	4.5309
	9.8392	.4905	3.3548	9.7753
	4.7768	-.4905	3.3548	-3.4198

RMS ACCELERATION 1E-05 GS

	X COMP.	Y COMP.	Z COMP.
STA. NO. 1	.0000	3.0291	4.0927
STA. NO. 2	.0000	2.8984	3.9171
STA. NO. 3	.0000	2.7057	3.6580
STA. NO. 4	.0000	2.5423	3.4385
STA. NO. 5	.0000	2.3790	3.2190
STA. NO. 6	.1176	2.0876	2.2736
STA. NO. 7	.0000	2.0000	2.7097
STA. NO. 8	.0000	1.7877	2.4243
STA. NO. 9	.2614	1.7877	4.5468
STA. NO. 10	.2614	1.7877	2.1604

RMS VELOCITY 1E-03 IN PER SEC

	X COMP.	Y COMP.	Z COMP.
	.0000	2.3106	3.4764
	.0000	2.2109	3.3272
	.0000	2.0639	3.1072
	.0000	1.9393	2.9207
	.0000	1.8147	2.7343
	.0897	1.5924	1.6220
	.0000	1.5256	2.3017
	.0000	1.3636	2.0592
	.1994	1.3636	4.1554
	.1994	1.3636	1.1779

Table 3-44
FUNCTIONAL VALUES, CASE 3-3-1 TNOM, RR5-2

SERIAL 727135

PEAK ANG. VEL. ARCSEC PER SEC
RESULT. 18.8089 WX18.6429 WY-3.2227 WZ 1.8014

PEAK EULER ANG. ARCSEC
TOTAL 9.0606 B1 .5857 B2-1.3517 B3-8.9594

PEAK ACCELERATION 1E-05 GS

	RESULT.	X COMP.	Y COMP.	Z COMP.
STA. NO. 1	6.1345	5.6842	-2.2128	4.1327
STA. NO. 2	5.9631	5.6842	-1.7680	4.8029
STA. NO. 3	6.0378	5.6842	-1.1119	5.8090
STA. NO. 4	6.8057	5.6842	-.5560	6.6659
STA. NO. 5	7.6354	5.6842	.0000	7.5239
STA. NO. 6	13.1964	6.0845	.9919	13.1361
STA. NO. 7	9.6047	5.6842	1.2899	9.5305
STA. NO. 8	10.7213	5.6842	2.0126	10.6549
STA. NO. 9	6.1520	4.7947	2.0126	3.4443
STA. NO. 10	19.7443	6.5738	2.0126	19.6976

PEAK VELOCITY 1E-03 IN PER SEC

	RESULT.	X COMP.	Y COMP.	Z COMP.
	4.7918	-4.4644	1.7379	3.7570
	4.7021	-4.4644	1.3886	4.1938
	5.0801	-4.4644	.8733	4.8520
	5.5927	-4.4644	.4367	5.4271
	6.1311	-4.4644	.0000	6.0162
	10.3986	-4.7788	-.7790	10.3492
	7.4824	-4.4644	-1.0131	7.4348
	8.2842	-4.4644	-1.5807	8.2507
	4.6071	-3.7658	-1.5807	-2.1913
	15.4815	-5.1631	-1.5807	15.4468

RMS ACCELERATION 1E-05 GS

	X COMP.	Y COMP.	Z COMP.
STA. NO. 1	2.3790	.9261	1.8047
STA. NO. 2	2.3790	.7399	2.0199
STA. NO. 3	2.3790	.4654	2.4186
STA. NO. 4	2.3790	.2327	2.8050
STA. NO. 5	2.3790	.0000	3.2190
STA. NO. 6	2.5465	.4151	5.7330
STA. NO. 7	2.3790	.5398	4.2402
STA. NO. 8	2.3790	.8423	4.8340
STA. NO. 9	2.0067	.8423	1.2420
STA. NO. 10	2.7513	.8423	8.6676

RMS VELOCITY 1E-03 IN PER SEC

	X COMP.	Y COMP.	Z COMP.
	1.8147	.7064	1.6371
	1.8147	.5644	1.8295
	1.8147	.3550	2.1456
	1.8147	.1775	2.4337
	1.8147	.0000	2.7343
	1.9425	.3167	4.7658
	1.8147	.4118	3.4612
	1.8147	.6425	3.8799
	1.5307	.6425	.7845
	2.0987	.6425	7.1477

Table 3-45
FUNCTIONAL VALUES, CASE 3-1-11 TMIN, RR6-3

SERIAL 727135

PEAK ANG. VEL. ARCSEC PER SEC					PEAK EULER ANG. ARCSEC										
RESULT.	.0000	WX	.0000	WY	.0000	WZ	.0000	TOTAL	.0000	B1	.0000	B2	.0000	B3	.0000

PEAK ACCELERATION 1E-05 GS					PEAK VELOCITY 1E-03 IN PER SEC			
	RESULT.	X COMP.	Y COMP.	Z COMP.	RESULT.	X COMP.	Y COMP.	Z COMP.
STA. NO. 1	8.2620	-6.6414	.0000	7.7592	5.7593	5.6348	.0000	4.6474
STA. NO. 2	8.2620	-6.6414	.0000	7.7592	5.7593	5.6348	.0000	4.6474
STA. NO. 3	8.2620	-6.6414	.0000	7.7592	5.7593	5.6348	.0000	4.6474
STA. NO. 4	8.2620	-6.6414	.0000	7.7592	5.7593	5.6348	.0000	4.6474
STA. NO. 5	8.2620	-6.6414	.0000	7.7592	5.7593	5.6348	.0000	4.6474
STA. NO. 6	8.2620	-6.6414	.0000	7.7592	5.7593	5.6348	.0000	4.6474
STA. NO. 7	8.2620	-6.6414	.0000	7.7592	5.7593	5.6348	.0000	4.6474
STA. NO. 8	8.2620	-6.6414	.0000	7.7592	5.7593	5.6348	.0000	4.6474
STA. NO. 9	8.2620	-6.6414	.0000	7.7592	5.7593	5.6348	.0000	4.6474
STA. NO. 10	8.2620	-6.6414	.0000	7.7592	5.7593	5.6348	.0000	4.6474

RMS ACCELERATION 1E-05 GS				RMS VELOCITY 1E-03 IN PER SEC		
	X COMP.	Y COMP.	Z COMP.	X COMP.	Y COMP.	Z COMP.
STA. NO. 1	3.3139	.0000	2.6770	2.4658	.0000	1.7816
STA. NO. 2	3.3139	.0000	2.6770	2.4658	.0000	1.7816
STA. NO. 3	3.3139	.0000	2.6770	2.4658	.0000	1.7816
STA. NO. 4	3.3139	.0000	2.6770	2.4658	.0000	1.7816
STA. NO. 5	3.3139	.0000	2.6770	2.4658	.0000	1.7816
STA. NO. 6	3.3139	.0000	2.6770	2.4658	.0000	1.7816
STA. NO. 7	3.3139	.0000	2.6770	2.4658	.0000	1.7816
STA. NO. 8	3.3139	.0000	2.6770	2.4658	.0000	1.7816
STA. NO. 9	3.3139	.0000	2.6770	2.4658	.0000	1.7816
STA. NO. 10	3.3139	.0000	2.6770	2.4658	.0000	1.7816

Table 3-46
FUNCTIONAL VALUES, CASE 3-2-10 TMIN, RR6-1

SERIAL 727135

PEAK ANG. VEL. ARCSEC PER SEC
RESULT. 1.6307 WX .0000 WY-1.3075 WZ 1.5961

PEAK EULER ANG. ARCSEC
TOTAL .6552 B1 .6261 B2 .5097 B3 .0000

PEAK ACCELERATION 1E-05 GS

	RESULT.	X COMP.	Y COMP.	Z COMP.
STA. NO. 1	10.5063	-.0000	-8.4564	9.8653
STA. NO. 2	10.0552	-.0000	-8.0915	9.4419
STA. NO. 3	9.3898	-.0000	-7.5534	8.8175
STA. NO. 4	8.8259	-.0000	-7.0974	8.2884
STA. NO. 5	8.2620	.0000	-6.6414	7.7592
STA. NO. 6	7.2574	.3283	-5.8279	6.8152
STA. NO. 7	6.9538	.0000	-5.5835	6.5316
STA. NO. 8	6.2207	.0000	-4.9906	5.8437
STA. NO. 9	6.2285	-.7296	-4.9906	5.8437
STA. NO. 10	6.2285	.7296	-4.9906	5.8437

PEAK VELOCITY 1E-03 IN PER SEC

RESULT.	X COMP.	Y COMP.	Z COMP.
7.3325	.0000	7.1747	5.9088
7.0163	.0000	6.8652	5.6553
6.5498	.0000	6.4086	5.2813
6.1546	.0000	6.0217	4.9643
5.7593	.0000	5.6348	4.6474
5.0616	-.2786	4.9446	4.0820
4.8422	.0000	4.7372	3.9121
4.3283	.0000	4.2342	3.5001
4.3716	.6190	4.2342	3.5001
4.3716	-.6190	4.2342	3.5001

RMS ACCELERATION 1E-05 GS

	X COMP.	Y COMP.	Z COMP.
STA. NO. 1	.0000	4.2195	3.4036
STA. NO. 2	.0000	4.0375	3.2575
STA. NO. 3	.0000	3.7690	3.0421
STA. NO. 4	.0000	3.5415	2.8595
STA. NO. 5	.0000	3.3139	2.6770
STA. NO. 6	.1638	2.9080	2.3513
STA. NO. 7	.0000	2.7860	2.2534
STA. NO. 8	.0000	2.4902	2.0161
STA. NO. 9	.3641	2.4902	2.0161
STA. NO. 10	.3641	2.4902	2.0161

RMS VELOCITY 1E-03 IN PER SEC

X COMP.	Y COMP.	Z COMP.
.0000	3.1397	2.2652
.0000	3.0042	2.1680
.0000	2.8044	2.0246
.0000	2.6351	1.9031
.0000	2.4658	1.7816
.1219	2.1638	1.5648
.0000	2.0730	1.4997
.0000	1.8529	1.3418
.2709	1.8529	1.3418
.2709	1.8529	1.3418

Table 3-47
FUNCTIONAL VALUES, CASE 3-3-1 TMIN, RR6-2

SERIAL 727135

PEAK ANG. VEL. ARCSEC PER SEC
RESULT.14.7397 WX14.4013 WY 3.0367 WZ 2.2736

PEAK EULER ANG. ARCSEC
TOTAL 5.8057 D1 .8919 D2-1.4291 D3-5.6147

PEAK ACCELERATION 1E-05 GS

	RESULT.	X COMP.	Y COMP.	Z COMP.
STA. NO. 1	7.2371	6.6414	-2.5854	2.8022
STA. NO. 2	7.0617	6.6414	-2.0657	3.7986
STA. NO. 3	6.8673	6.6414	-1.2992	5.2682
STA. NO. 4	7.1106	6.6414	-.6496	6.5137
STA. NO. 5	8.2620	6.6414	.0000	7.7592
STA. NO. 6	14.5080	7.1091	1.1589	14.1777
STA. NO. 7	11.0393	6.6414	1.5071	10.6488
STA. NO. 8	12.6320	6.6414	2.3515	12.2679
STA. NO. 9	6.0877	5.6021	2.3515	2.9424
STA. NO. 10	21.8646	7.6808	2.3515	21.5934

PEAK VELOCITY 1E-03 IN PER SEC

RESULT.	X COMP.	Y COMP.	Z COMP.
6.0668	-5.6348	2.1935	1.7176
5.9043	-5.6348	1.7526	2.3065
5.7493	-5.6348	1.1023	3.1752
5.7053	-5.6348	.5511	3.9113
5.7593	-5.6348	.0000	4.6474
8.7426	-6.0317	-.9832	8.4741
6.6723	-5.6348	-1.2786	6.3552
7.6085	-5.6348	-1.9951	7.3122
5.2868	-4.7530	-1.9951	1.7266
13.1186	-6.5167	-1.9951	12.8977

RMS ACCELERATION 1E-05 GS

	X COMP.	Y COMP.	Z COMP.
STA. NO. 1	3.3139	1.2901	1.0237
STA. NO. 2	3.3139	1.0307	1.3221
STA. NO. 3	3.3139	.6483	1.8075
STA. NO. 4	3.3139	.3241	2.2379
STA. NO. 5	3.3139	.0000	2.6770
STA. NO. 6	3.5473	.5783	4.9174
STA. NO. 7	3.3139	.7520	3.7117
STA. NO. 8	3.3139	1.1734	4.2966
STA. NO. 9	2.7953	1.1734	1.1367
STA. NO. 10	3.8325	1.1734	7.5055

RMS VELOCITY 1E-03 IN PER SEC

X COMP.	Y COMP.	Z COMP.
2.4658	.9599	.6662
2.4658	.7670	.8594
2.4658	.4824	1.1860
2.4658	.2412	1.4800
2.4658	.0000	1.7816
2.6395	.4303	3.2913
2.4658	.5595	2.4951
2.4658	.8731	2.8993
2.0799	.8731	.8041
2.8517	.8731	5.0334

Table 3-48
FUNCTIONAL VALUES, CASE 3-1-11 PPNOM, RR8-3

SERIAL 727135

PEAK ANG. VEL. ARCSEC PER SEC
RESULT. .0000 WX .0000 WY .0000 WZ .0000

PEAK EULER ANG. ARCSEC
TOTAL .0000 B1 .0000 B2 .0000 B3 .0000

PEAK ACCELERATION 1E-05 GS

	RESULT.	X COMP.	Y COMP.	Z COMP.
STA. NO. 1	8.9284	-8.8746	.0000	-7.1808
STA. NO. 2	8.9284	-8.8746	.0000	-7.1808
STA. NO. 3	8.9284	-8.8746	.0000	-7.1808
STA. NO. 4	8.9284	-8.8746	.0000	-7.1808
STA. NO. 5	8.9284	-8.8746	.0000	-7.1808
STA. NO. 6	8.9284	-8.8746	.0000	-7.1808
STA. NO. 7	8.9284	-8.8746	.0000	-7.1808
STA. NO. 8	8.9284	-8.8746	.0000	-7.1808
STA. NO. 9	8.9284	-8.8746	.0000	-7.1808
STA. NO. 10	8.9284	-8.8746	.0000	-7.1808

PEAK VELOCITY 1E-03 IN PER SEC

RESULT.	X COMP.	Y COMP.	Z COMP.
4.0896	4.0597	.0000	3.9586
4.0896	4.0597	.0000	3.9586
4.0896	4.0597	.0000	3.9586
4.0896	4.0597	.0000	3.9586
4.0896	4.0597	.0000	3.9586
4.0896	4.0597	.0000	3.9586
4.0896	4.0597	.0000	3.9586
4.0896	4.0597	.0000	3.9586
4.0896	4.0597	.0000	3.9586
4.0896	4.0597	.0000	3.9586

RMS ACCELERATION 1E-05 GS

	X COMP.	Y COMP.	Z COMP.
STA. NO. 1	2.9670	.0000	3.5387
STA. NO. 2	2.9670	.0000	3.5387
STA. NO. 3	2.9670	.0000	3.5387
STA. NO. 4	2.9670	.0000	3.5387
STA. NO. 5	2.9670	.0000	3.5387
STA. NO. 6	2.9670	.0000	3.5387
STA. NO. 7	2.9670	.0000	3.5387
STA. NO. 8	2.9670	.0000	3.5387
STA. NO. 9	2.9670	.0000	3.5387
STA. NO. 10	2.9670	.0000	3.5387

RMS VELOCITY 1E-03 IN PER SEC

X COMP.	Y COMP.	Z COMP.
1.2768	.0000	1.6143
1.2768	.0000	1.6143
1.2768	.0000	1.6143
1.2768	.0000	1.6143
1.2768	.0000	1.6143
1.2768	.0000	1.6143
1.2768	.0000	1.6143
1.2768	.0000	1.6143
1.2768	.0000	1.6143
1.2768	.0000	1.6143

Table 3-49
FUNCTIONAL VALUES, CASE 3-2-10 PPNOM, RR8-1

SERIAL 727135

PEAK ANG. VEL. ARCSEC PER SEC
RESULT. 1.1583 WX -.0000 WY-1.1137 WZ 1.1499

PEAK EULER ANG. ARCSEC
TOTAL .2740 D1 .2475 D2 .2639 D3 -.0000

PEAK ACCELERATION 1E-05 GS

	RESULT.	X COMP.	Y COMP.	Z COMP.
STA. NO. 1	11.3672	-.0000	*****	-9.1299
STA. NO. 2	10.8770	-.0000	*****	-8.7381
STA. NO. 3	10.1540	-.0000	*****	-8.1602
STA. NO. 4	9.5412	-.0000	-9.4840	-7.6705
STA. NO. 5	8.9284	.0000	-8.8746	-7.1808
STA. NO. 6	7.8468	.4387	-7.7275	-6.3072
STA. NO. 7	7.5068	.0000	-7.4609	-6.0447
STA. NO. 8	6.7103	.0000	-6.6688	-5.4081
STA. NO. 9	6.7766	-.9750	-6.6688	-5.4081
STA. NO. 10	6.7766	.9750	-6.6688	-5.4081

PEAK VELOCITY 1E-03 IN PER SEC

	RESULT.	X COMP.	Y COMP.	Z COMP.
	5.2070	.0000	5.1692	5.0330
	4.9824	.0000	4.9462	4.8171
	4.6511	.0000	4.6172	4.4985
	4.3703	.0000	4.3385	4.2286
	4.0896	.0000	4.0597	3.9586
	3.5943	-.2007	3.5624	3.4770
	3.4382	.0000	3.4130	3.3323
	3.0732	.0000	3.0507	2.9813
	3.1054	.4460	3.0507	2.9813
	3.1054	-.4460	3.0507	2.9813

RMS ACCELERATION 1E-05 GS

	X COMP.	Y COMP.	Z COMP.
STA. NO. 1	.0000	3.7779	4.4992
STA. NO. 2	.0000	3.6149	4.3061
STA. NO. 3	.0000	3.3745	4.0213
STA. NO. 4	.0000	3.1708	3.7800
STA. NO. 5	.0000	2.9670	3.5387
STA. NO. 6	.1467	2.6036	3.1081
STA. NO. 7	.0000	2.4944	2.9788
STA. NO. 8	.0000	2.2296	2.6651
STA. NO. 9	.3260	2.2296	2.6651
STA. NO. 10	.3260	2.2296	2.6651

RMS VELOCITY 1E-03 IN PER SEC

	X COMP.	Y COMP.	Z COMP.
	.0000	1.6257	2.0524
	.0000	1.5556	1.9644
	.0000	1.4521	1.8345
	.0000	1.3645	1.7244
	.0000	1.2768	1.6143
	.0631	1.1204	1.4179
	.0000	1.0734	1.3589
	.0000	.9594	1.2158
	.1403	.9594	1.2158
	.1403	.9594	1.2158

Table 3-50
FUNCTIONAL VALUES, CASE 3-1-11 PPMIN, RR7-3

SERIAL 727135

PEAK ANG. VEL. ARCSEC PER SEC
RESULT. .0000 WX .0000 WY .0000 WZ .0000

PEAK EULER ANG. ARCSEC
TOTAL .0000 B1 .0000 B2 .0000 B3 .0000

PEAK ACCELERATION 1E-05 GS

	RESULT.	X COMP.	Y COMP.	Z COMP.
STA. NO. 1	5.5075	4.5446	.0000	4.2682
STA. NO. 2	5.5075	4.5446	.0000	4.2682
STA. NO. 3	5.5075	4.5446	.0000	4.2682
STA. NO. 4	5.5075	4.5446	.0000	4.2682
STA. NO. 5	5.5075	4.5446	.0000	4.2682
STA. NO. 6	5.5075	4.5446	.0000	4.2682
STA. NO. 7	5.5075	4.5446	.0000	4.2682
STA. NO. 8	5.5075	4.5446	.0000	4.2682
STA. NO. 9	5.5075	4.5446	.0000	4.2682
STA. NO. 10	5.5075	4.5446	.0000	4.2682

PEAK VELOCITY 1E-03 IN PER SEC

RESULT.	X COMP.	Y COMP.	Z COMP.
3.1218	-2.9910	.0000	2.4950
3.1218	-2.9910	.0000	2.4950
3.1218	-2.9910	.0000	2.4950
3.1218	-2.9910	.0000	2.4950
3.1218	-2.9910	.0000	2.4950
3.1218	-2.9910	.0000	2.4950
3.1218	-2.9910	.0000	2.4950
3.1218	-2.9910	.0000	2.4950
3.1218	-2.9910	.0000	2.4950
3.1218	-2.9910	.0000	2.4950

RMS ACCELERATION 1E-05 GS

	X COMP.	Y COMP.	Z COMP.
STA. NO. 1	2.2315	.0000	1.8355
STA. NO. 2	2.2315	.0000	1.8355
STA. NO. 3	2.2315	.0000	1.8355
STA. NO. 4	2.2315	.0000	1.8355
STA. NO. 5	2.2315	.0000	1.8355
STA. NO. 6	2.2315	.0000	1.8355
STA. NO. 7	2.2315	.0000	1.8355
STA. NO. 8	2.2315	.0000	1.8355
STA. NO. 9	2.2315	.0000	1.8355
STA. NO. 10	2.2315	.0000	1.8355

RMS VELOCITY 1E-03 IN PER SEC

X COMP.	Y COMP.	Z COMP.
1.1168	.0000	1.1134
1.1168	.0000	1.1134
1.1168	.0000	1.1134
1.1168	.0000	1.1134
1.1168	.0000	1.1134
1.1168	.0000	1.1134
1.1168	.0000	1.1134
1.1168	.0000	1.1134
1.1168	.0000	1.1134
1.1168	.0000	1.1134

Table 3-51
FUNCTIONAL VALUES, CASE 3-3-1 PPNOM, RR8-2

SERIAL 727135

PEAK ANG. VEL. ARCSEC PER SEC
RESULT.12.6283 WX12.2668 WY 2.9733 WZ 1.6381

PEAK EULER ANG. ARCSEC
TOTAL 2.9933 B1 .3525 B2 -.7082 B3-2.9064

PEAK ACCELERATION 1E-05 GS

PEAK VELOCITY 1E-03 IN PER SEC

	RESULT.	X COMP.	Y COMP.	Z COMP.
STA. NO. 1	9.5864	8.8746	-3.4547	-2.6638
STA. NO. 2	9.3273	8.8746	-2.7603	-3.4603
STA. NO. 3	9.0489	8.8746	-1.7361	-4.7121
STA. NO. 4	8.9172	8.8746	-.8680	-5.8593
STA. NO. 5	8.9284	8.8746	.0000	-7.1808
STA. NO. 6	13.6329	9.4996	1.5485	*****
STA. NO. 7	10.4926	8.8746	2.0138	*****
STA. NO. 8	12.1906	8.8746	3.1423	*****
STA. NO. 9	8.2409	7.4858	3.1423	-3.3344
STA. NO. 10	20.7666	10.2635	3.1422	*****

RESULT.	X COMP.	Y COMP.	Z COMP.
4.4153	-4.0597	1.5804	1.0901
4.3045	-4.0597	1.2627	1.6666
4.1809	-4.0597	.7942	2.5171
4.1160	-4.0597	.3971	3.2378
4.0896	-4.0597	.0000	3.9586
7.4632	-4.3456	-.7084	7.3853
5.7217	-4.0597	-.9212	5.6307
6.6513	-4.0597	-1.4374	6.5677
3.7300	-3.4244	-1.4374	1.8100
11.3886	-4.6951	-1.4374	11.3253

RMS ACCELERATION 1E-05 GS

RMS VELOCITY 1E-03 IN PER SEC

	X COMP.	Y COMP.	Z COMP.
STA. NO. 1	2.9670	1.1550	1.1052
STA. NO. 2	2.9670	.9229	1.5665
STA. NO. 3	2.9670	.5804	2.2860
STA. NO. 4	2.9670	.2902	2.9095
STA. NO. 5	2.9670	.0000	3.5387
STA. NO. 6	3.1760	.5177	6.5806
STA. NO. 7	2.9670	.6733	5.0081
STA. NO. 8	2.9670	1.0505	5.8344
STA. NO. 9	2.5027	1.0505	1.6127
STA. NO. 10	3.4314	1.0505	10.0824

X COMP.	Y COMP.	Z COMP.
1.2768	.4970	.5468
1.2768	.3971	.7513
1.2768	.2498	1.0668
1.2768	.1249	1.3394
1.2768	.0000	1.6143
1.3667	.2228	2.9801
1.2768	.2897	2.2560
1.2768	.4521	2.6169
1.0770	.4521	.6908
1.4766	.4521	4.5549

Table 3-52
FUNCTIONAL VALUES, CASE 3-2-10 PPMIN, RR7-1

SERIAL 727135

PEAK ANG. VEL. ARCSEC PER SEC
RESULT. .6836 WX .0000 WY -.7019 WZ -.8472

PEAK EULER ANG. ARCSEC
TOTAL .3484 B1 -.3085 B2 -.2809 B3 .0000

PEAK ACCELERATION 1E-05 GS

	RESULT.	X COMP.	Y COMP.	Z COMP.
STA. NO. 1	7.0065	-.0000	5.7865	5.4267
STA. NO. 2	6.7052	-.0000	5.5369	5.1939
STA. NO. 3	6.2607	-.0000	5.1687	4.8504
STA. NO. 4	5.8841	-.0000	4.8566	4.5593
STA. NO. 5	5.5075	.0000	4.5446	4.2682
STA. NO. 6	4.8387	-.2247	3.9879	3.7489
STA. NO. 7	4.6337	.0000	3.8207	3.5929
STA. NO. 8	4.1440	.0000	3.4150	3.2145
STA. NO. 9	4.1620	.4993	3.4150	3.2145
STA. NO. 10	4.1620	-.4993	3.4150	3.2145

PEAK VELOCITY 1E-03 IN PER SEC

	RESULT.	X COMP.	Y COMP.	Z COMP.
	3.9742	.0000	-3.8084	3.1722
	3.8029	.0000	-3.6441	3.0361
	3.5501	.0000	-3.4018	2.8353
	3.3360	.0000	-3.1964	2.6652
	3.1218	.0000	-2.9910	2.4950
	2.7435	.1479	-2.6246	2.1915
	2.6249	.0000	-2.5146	2.1003
	2.3465	.0000	-2.2476	1.8791
	2.3686	-.3286	-2.2476	1.8791
	2.3686	.3286	-2.2476	1.8791

RMS ACCELERATION 1E-05 GS

	X COMP.	Y COMP.	Z COMP.
STA. NO. 1	.0000	2.8413	2.3337
STA. NO. 2	.0000	2.7187	2.2336
STA. NO. 3	.0000	2.5379	2.0859
STA. NO. 4	.0000	2.3847	1.9607
STA. NO. 5	.0000	2.2315	1.8355
STA. NO. 6	.1103	1.9581	1.6122
STA. NO. 7	.0000	1.8760	1.5451
STA. NO. 8	.0000	1.6768	1.3824
STA. NO. 9	.2451	1.6768	1.3824
STA. NO. 10	.2451	1.6768	1.3824

RMS VELOCITY 1E-03 IN PER SEC

	X COMP.	Y COMP.	Z COMP.
	.0000	1.4219	1.4156
	.0000	1.3606	1.3549
	.0000	1.2701	1.2653
	.0000	1.1934	1.1893
	.0000	1.1168	1.1134
	.0552	.9800	.9780
	.0000	.9389	.9373
	.0000	.8392	.8385
	.1227	.8392	.8385
	.1227	.8392	.8385

Table 3-53

FUNCTIONAL VALUES, CASE 3-3-1 PPMIN, RR7-2

SERIAL 727135

PEAK ANG. VEL. ARCSEC PER SEC

RESULT. 7.9845 WX 7.7316 WY 1.9567 WZ-1.2069

PEAK EULER ANG. ARCSEC

TOTAL 3.2125 B1 -.4395 B2 .8165 B3 3.0941

PEAK ACCELERATION 1E-05 GS

	RESULT.	X COMP.	Y COMP.	Z COMP.
STA. NO. 1	4.9838	-4.5446	1.7691	1.8045
STA. NO. 2	4.8796	-4.5446	1.4135	2.2960
STA. NO. 3	4.7762	-4.5446	.8890	3.0278
STA. NO. 4	5.0634	-4.5446	.4445	3.6480
STA. NO. 5	5.5075	-4.5446	.0000	4.2682
STA. NO. 6	8.5306	-4.8646	-.7930	7.6831
STA. NO. 7	6.7093	-4.5446	-1.0313	5.7071
STA. NO. 8	7.4545	-4.5446	-1.6091	6.5133
STA. NO. 9	4.1576	-3.8334	-1.6091	1.4020
STA. NO. 10	12.3553	-5.2558	-1.6091	11.6432

PEAK VELOCITY 1E-03 IN PER SEC

RESULT.	X COMP.	Y COMP.	Z COMP.
3.2147	2.9910	-1.1644	-1.0128
3.1325	2.9910	-.9303	-1.3089
3.0646	2.9910	-.5851	-1.7456
3.0610	2.9910	-.2926	-2.1157
3.1218	2.9910	.0000	2.4950
4.8718	3.2017	.5219	4.6849
3.8591	2.9910	.6787	3.5880
4.4400	2.9910	1.0591	4.2004
2.8304	2.5229	1.0591	1.2227
7.3389	3.4591	1.0591	7.1991

RMS ACCELERATION 1E-05 GS

	X COMP.	Y COMP.	Z COMP.
STA. NO. 1	2.2315	.8687	.7720
STA. NO. 2	2.2315	.6941	.9711
STA. NO. 3	2.2315	.4365	1.2838
STA. NO. 4	2.2315	.2183	1.5576
STA. NO. 5	2.2315	.0000	1.8355
STA. NO. 6	2.3886	.3894	3.3290
STA. NO. 7	2.2315	.5064	2.4888
STA. NO. 8	2.2315	.7901	2.8577
STA. NO. 9	1.8822	.7901	.6864
STA. NO. 10	2.5807	.7901	5.0591

RMS VELOCITY 1E-03 IN PER SEC

X COMP.	Y COMP.	Z COMP.
1.1168	.4347	.3765
1.1168	.3474	.5131
1.1168	.2185	.7304
1.1168	.1092	.9207
1.1168	.0000	1.1134
1.1954	.1949	2.0621
1.1168	.2534	1.5652
1.1168	.3954	1.8197
.9420	.3954	.4966
1.2915	.3954	3.1555

Table 3-54
FUNCTIONAL VALUES, CASE 3-1-11 HEARTBEAT

SERIAL 757415

PEAK ANG. VEL. ARCSEC PER SEC
RESULT. .0286 WX .0000 WY .0286 WZ .0000

PEAK EULER ANG. ARCSEC
TOTAL .0022 B1 .0000 B2 .0022 B3 .0000

PEAK ACCELERATION 1E-05 GS

	RESULT.	X COMP.	Y COMP.	Z COMP.
STA. NO. 1	2.5700	-2.2316	.0000	1.3396
STA. NO. 2	2.5879	-2.2316	.0000	1.3740
STA. NO. 3	2.6150	-2.2316	.0000	1.4248
STA. NO. 4	2.6386	-2.2316	.0000	1.4678
STA. NO. 5	2.6628	-2.2316	.0000	1.5108
STA. NO. 6	2.7072	-2.2316	.0000	1.5875
STA. NO. 7	2.7208	-2.2316	.0000	1.6106
STA. NO. 8	2.7545	-2.2316	.0000	1.6665
STA. NO. 9	2.7545	-2.2316	.0000	1.6665
STA. NO. 10	2.7545	-2.2316	.0000	1.6665

PEAK VELOCITY 1E-03 IN PER SEC

RESULT.	X COMP.	Y COMP.	Z COMP.
.4243	-.3582	.0000	.2281
.4273	-.3582	.0000	.2334
.4318	-.3582	.0000	.2413
.4358	-.3582	.0000	.2488
.4398	-.3582	.0000	.2551
.4471	-.3582	.0000	.2673
.4493	-.3582	.0000	.2713
.4548	-.3582	.0000	.2803
.4548	-.3582	.0000	.2803
.4548	-.3582	.0000	.2803

RMS ACCELERATION 1E-05 GS

	X COMP.	Y COMP.	Z COMP.
STA. NO. 1	.8668	.0000	.4712
STA. NO. 2	.8668	.0000	.4840
STA. NO. 3	.8668	.0000	.5030
STA. NO. 4	.8668	.0000	.5192
STA. NO. 5	.8668	.0000	.5354
STA. NO. 6	.8668	.0000	.5644
STA. NO. 7	.8668	.0000	.5732
STA. NO. 8	.8668	.0000	.5945
STA. NO. 9	.8668	.0000	.5945
STA. NO. 10	.8668	.0000	.5945

RMS VELOCITY 1E-03 IN PER SEC

X COMP.	Y COMP.	Z COMP.
.1245	.0000	.0745
.1245	.0000	.0762
.1245	.0000	.0788
.1245	.0000	.0811
.1245	.0000	.0833
.1245	.0000	.0873
.1245	.0000	.0885
.1245	.0000	.0915
.1245	.0000	.0915
.1245	.0000	.0915

Table 3-55
FUNCTIONAL VALUES, CASE 3-1-11 COUGH

SERIAL 757415

PEAK ANG. VEL. ARCSEC PER SEC
RESULT. 1.8594 WX-1.4784 WY 1.4643 WZ -.5249

PEAK EULER ANG. ARCSEC
TOTAL .2454 B1 .7465 B2 .1987 B3 -.2276

PEAK ACCELERATION 1E-05 G'S

	RESULT.	X COMP.	Y COMP.	Z COMP.
STA. NO. 1	45.3382	35.5617	-7.1197	*****
STA. NO. 2	46.7342	35.5617	-7.4743	*****
STA. NO. 3	47.7919	35.5617	-7.8692	*****
STA. NO. 4	48.7156	35.5617	-8.2759	*****
STA. NO. 5	48.9629	35.5617	-8.6826	*****
STA. NO. 6	51.2172	35.2157	-9.4776	*****
STA. NO. 7	51.2443	35.5617	-9.7183	*****
STA. NO. 8	52.5694	35.5617	*****	*****
STA. NO. 9	51.4338	36.3284	*****	*****
STA. NO. 10	53.7948	34.7937	*****	*****

PEAK VELOCITY 1E-03 IN PER SEC

RESULT.	X COMP.	Y COMP.	Z COMP.
17.4435	-8.8588	1.9742	6.7188
17.6717	-8.8588	1.9933	6.1337
17.8434	-8.8588	2.1332	6.3716
11.7579	-8.8588	2.2517	6.4444
11.2872	-8.8588	2.3772	6.6921
11.7361	-8.7715	2.5816	7.4771
11.8233	-8.8588	2.6467	7.4919
12.1429	-8.8588	2.8776	7.9471
12.7445	-9.7529	2.8776	7.5624
12.2552	-8.6647	2.8776	8.3179

RMS ACCELERATION 1E-05 G'S

	X COMP.	Y COMP.	Z COMP.
STA. NO. 1	12.9284	2.7717	12.1575
STA. NO. 2	12.9284	2.8767	12.4627
STA. NO. 3	12.9284	2.9669	12.9255
STA. NO. 4	12.9284	3.1797	13.3216
STA. NO. 5	12.9284	3.2556	13.7276
STA. NO. 6	12.8355	3.5265	14.7677
STA. NO. 7	12.9284	3.6799	14.6558
STA. NO. 8	12.9284	3.8157	15.1857
STA. NO. 9	13.1374	3.8157	14.4927
STA. NO. 10	12.7229	3.8157	15.9337

RMS VELOCITY 1E-03 IN PER SEC

X COMP.	Y COMP.	Z COMP.
3.7773	.7224	2.7584
3.7773	.7488	2.8269
3.7773	.7894	2.9316
3.7773	.8257	3.0236
3.7773	.8617	3.1182
3.7577	.9293	3.3625
3.7773	.9571	3.3469
3.7773	1.0712	3.4798
3.1215	1.0712	3.3344
3.7342	1.0712	3.6369

Input Data for Figures 3-33 to 3-60, Case 1-2-1 Heartbeat

SERIAL 757475

I1= .54640+07 I2= .41699+08 I3= .38819+08 MASS= .27322+03 CELT= .40000-02 TF=

TRANSFORMATION FROM CREW STA. TO CRAFT AXES

.10000000+01	.00000000	.00000000
.00000000	.00000000	-.10000000+01
.00000000	.10000000+01	.00000000

CREW STATION ORIGIN .130299+04 .480000+02 .000000

INPUT POINT .000000 .000000 .000000

VEHICLE C.C. .182900+04 .476500+02 .679000+01

OUTPUT STATION COORDINATES

STA. NO. 1	.200700+04	.735000+02	.000000
STA. NO. 2	.130299+04	.000000	.000000
STA. NO. 3	.159799+04	.000000	.000000
STA. NO. 4	.200700+04	.252299+03	.000000
STA. NO. 5	.176400+04	.000000	.000000
STA. NO. 6	.190199+04	.000000	.000000
STA. NO. 7	.200700+04	.000000	.000000
STA. NO. 8	.207500+04	.000000	.000000
STA. NO. 9	.230000+04	.000000	.000000
STA. NO. 10	.200700+04	.575000+02	.000000

FORCE COSINE COEF

.31852881-01	-.63437041-01	.11266874+00	-.46431033-01	-.24807210-00	.37126835-00	-.15784980-00
.10203394-01	-.60476211-01	.94055591-01	-.45709430-01	-.16789360-00	.20576835-00	-.35948086-01
.00000000	.00000000	.00000000	.00000000	.00000000	.00000000	.00000000

FORCE SINE COEF

-.19534352-01	-.29521543-01	.12166239-01	.10018206+00	-.19748025-01	.11470724-01	.50624093-01
-.80339524-02	-.66578465-02	-.28314630-01	.92583655-01	-.31451491-02	-.39119639-01	.33628991-01
.00000000	.00000000	.00000000	.00000000	.00000000	.00000000	.00000000

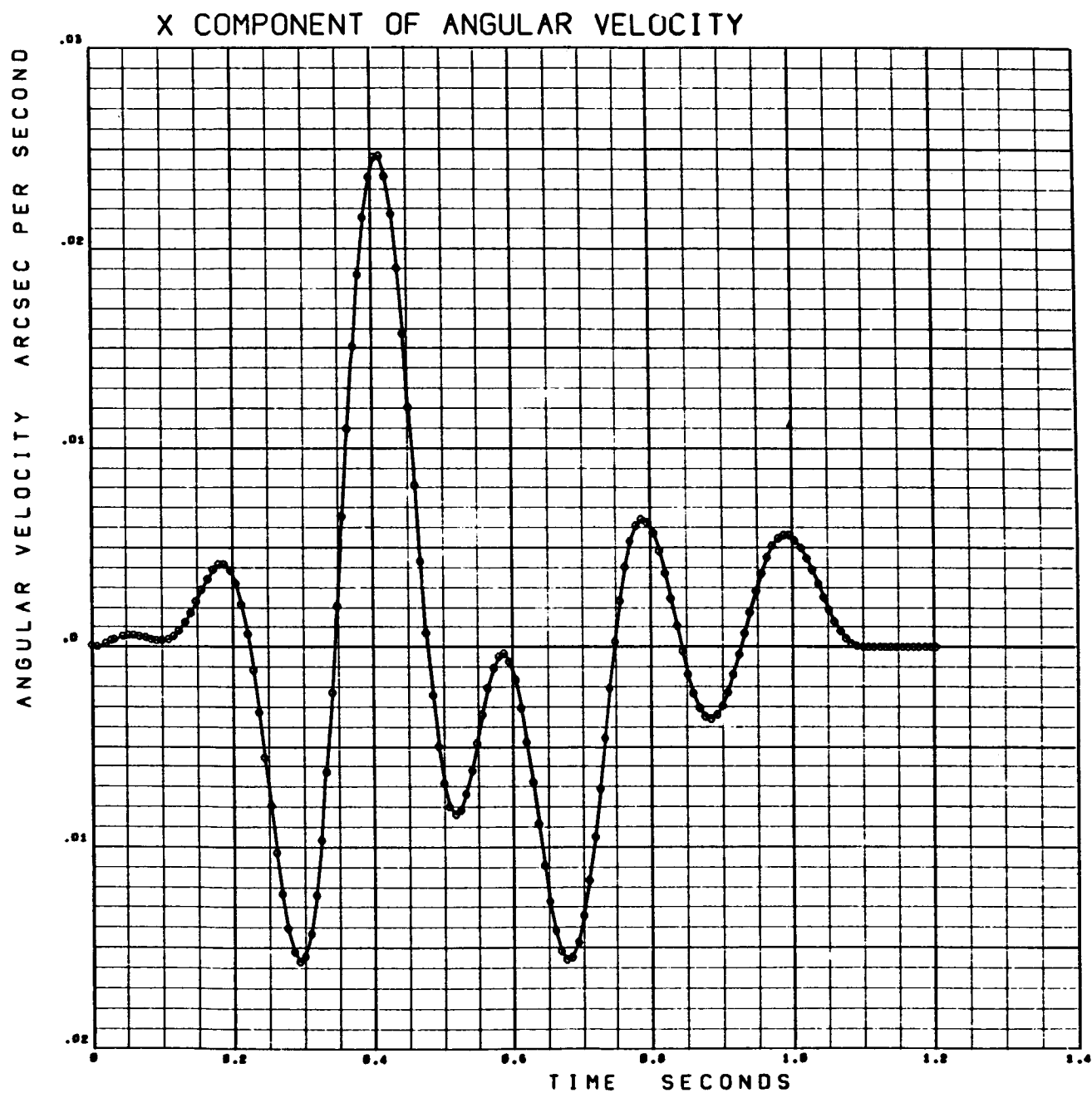


Figure 3-33. Heartbeat (X Component of Angular Velocity)

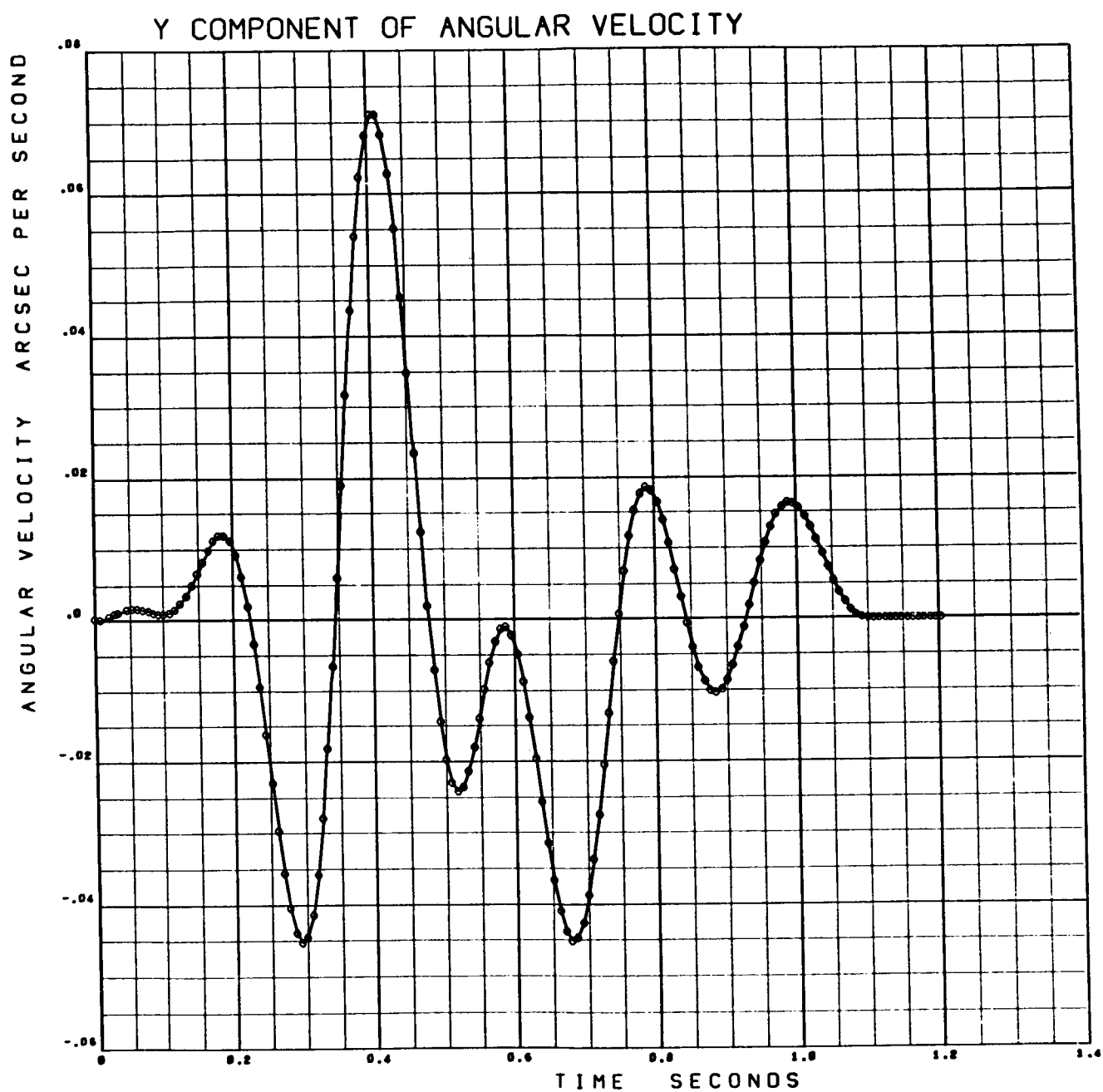


Figure 3-34. Heartbeat (Y Component of Angular Velocity)

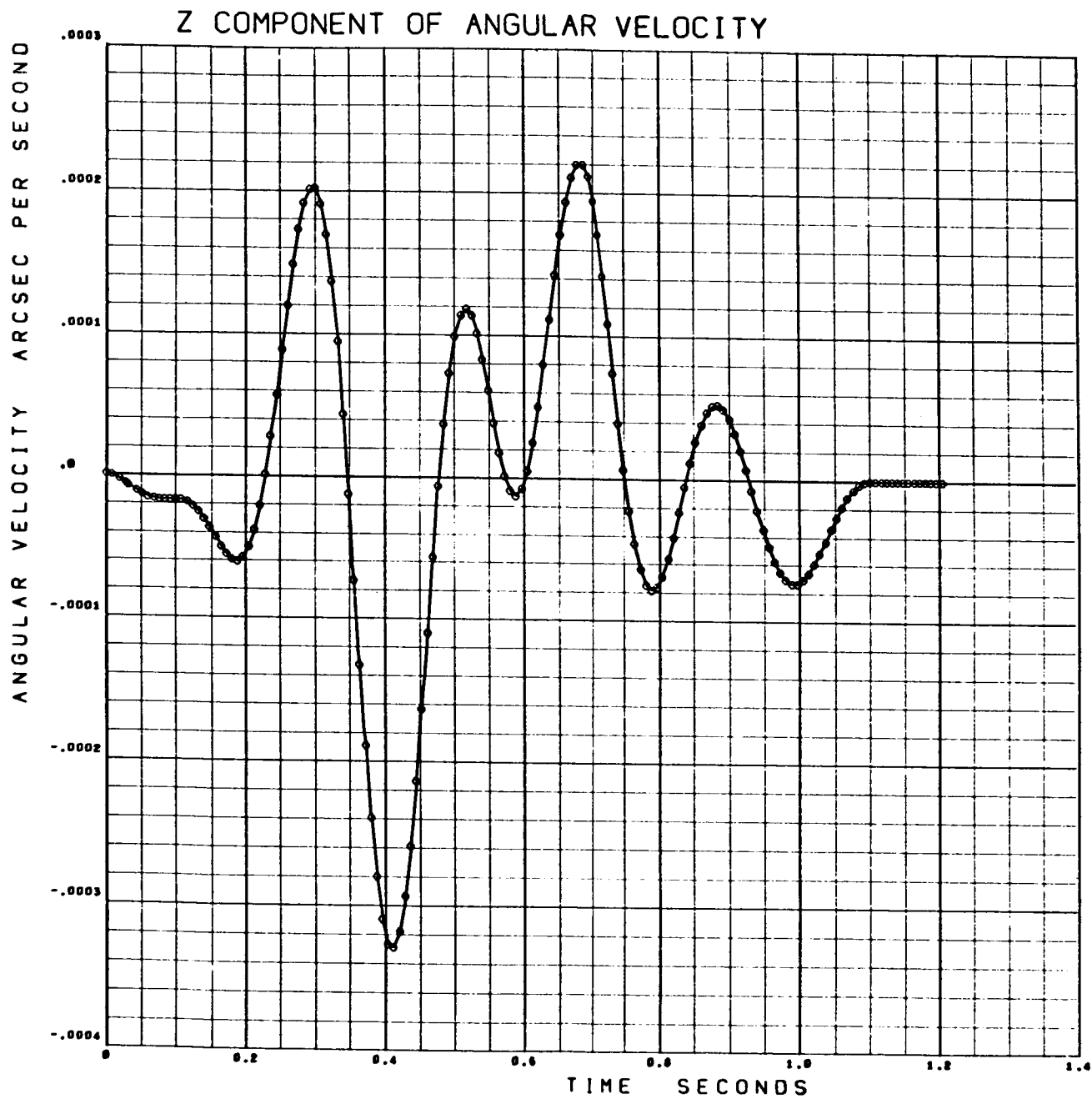


Figure 3-35. Heartbeat (Z Component of Angular Velocity)

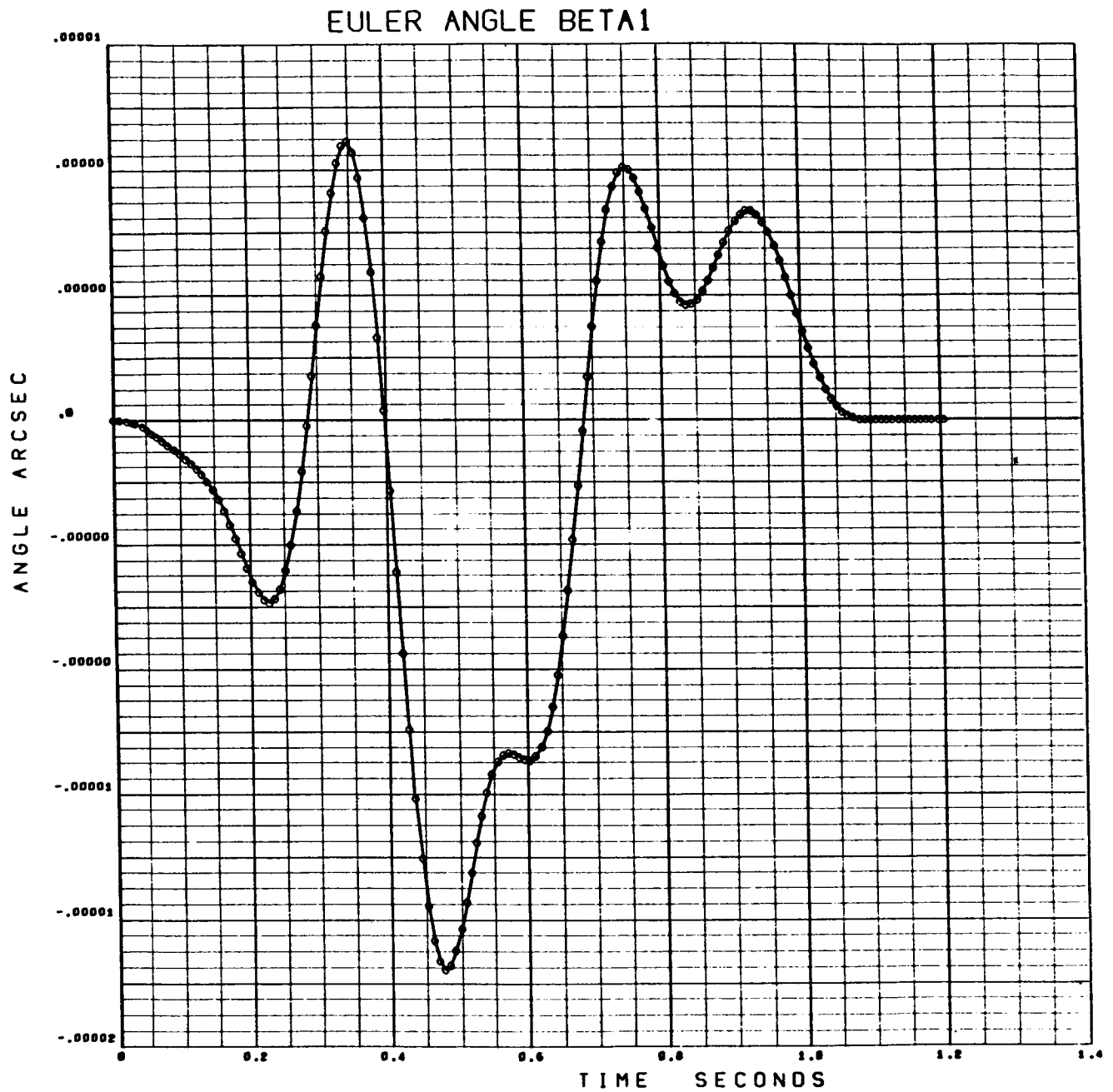


Figure 3-36. Heartbeat (Euler Angle Beta 1)

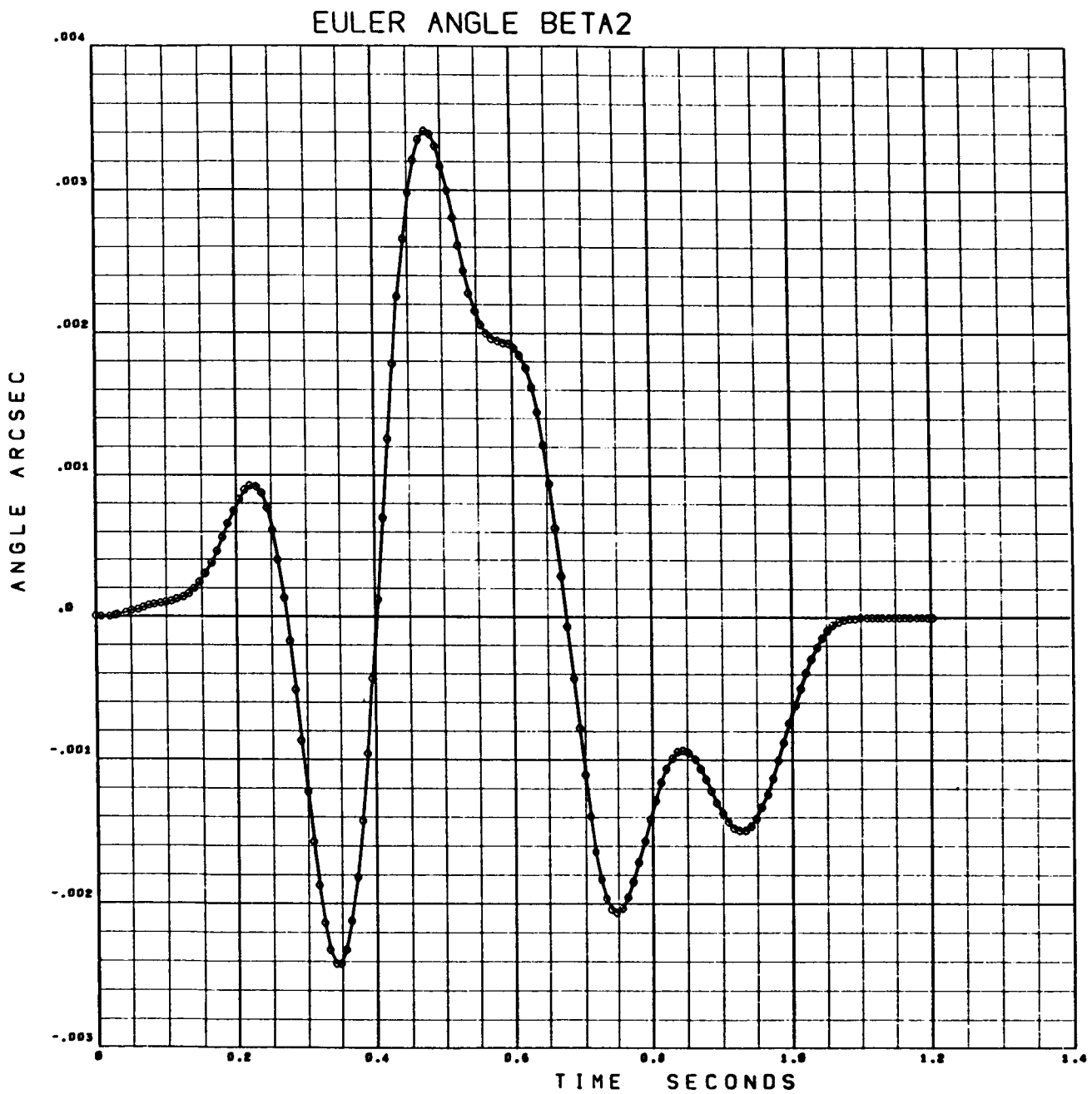


Figure 3-37. Heartbeat (Euler Angle Beta 2)

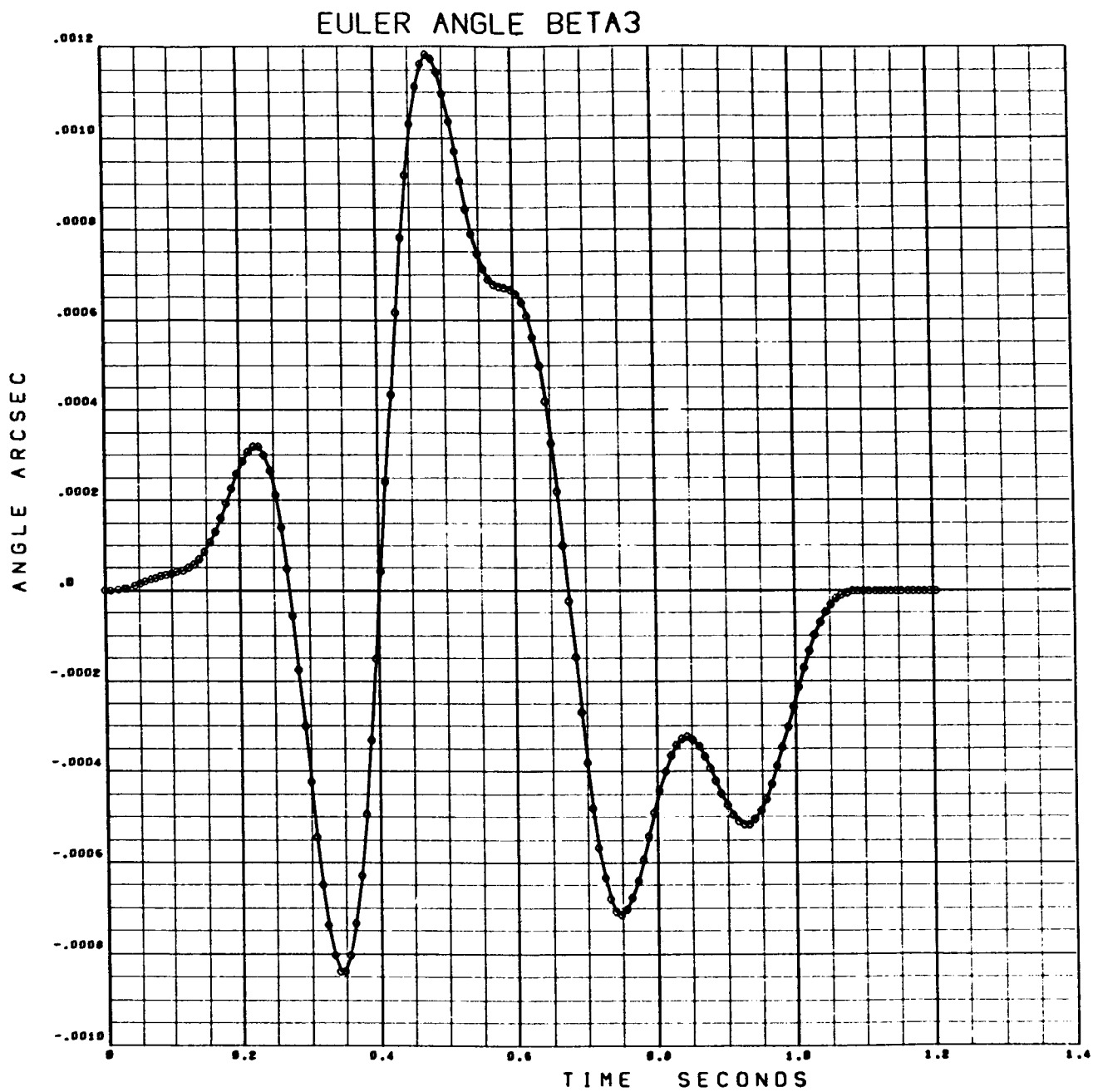


Figure 3-38. Heartbeat (Euler Angle Beta 3)

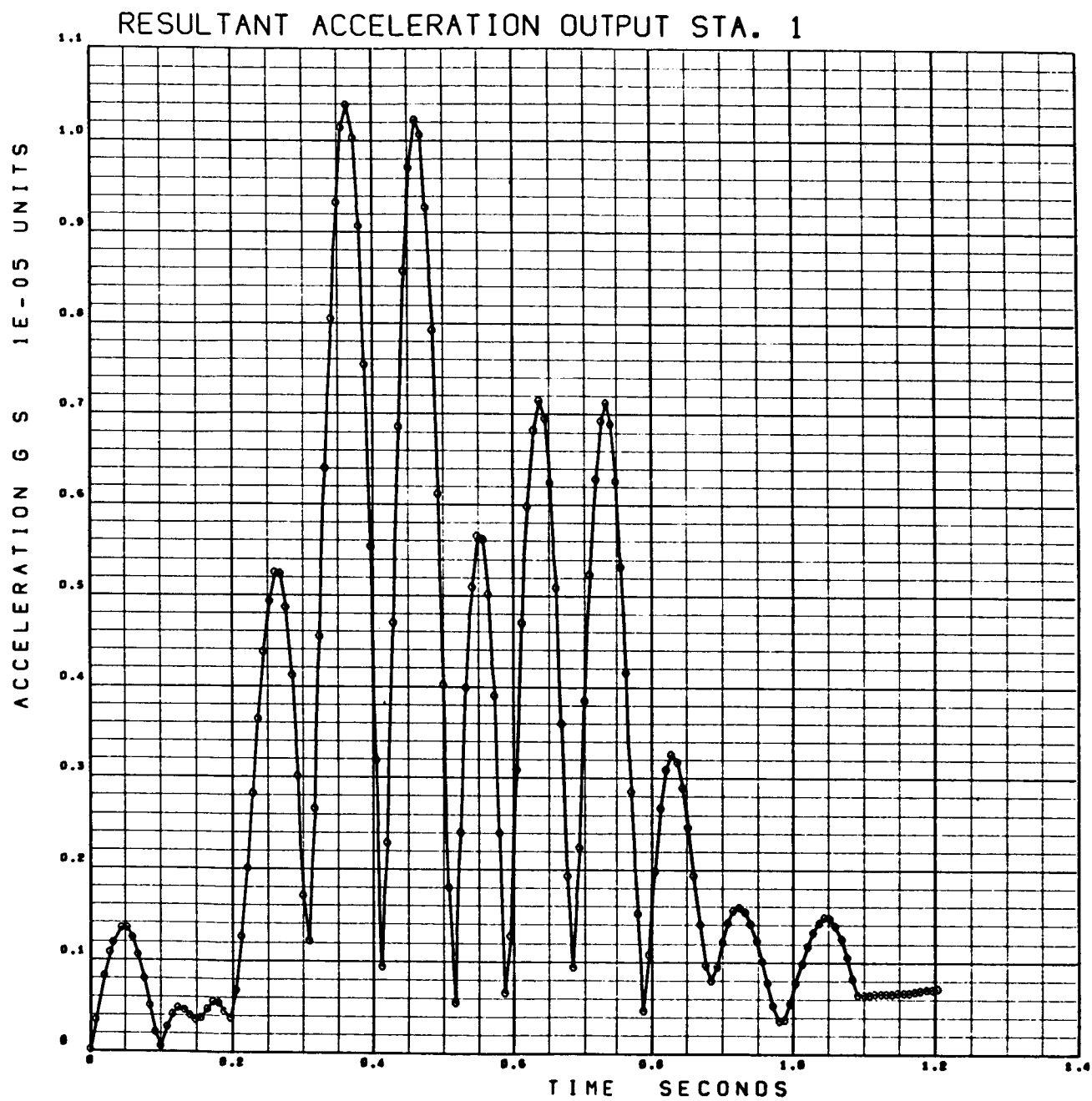


Figure 3-39. Heartbeat – Resultant Acceleration Output Station 1

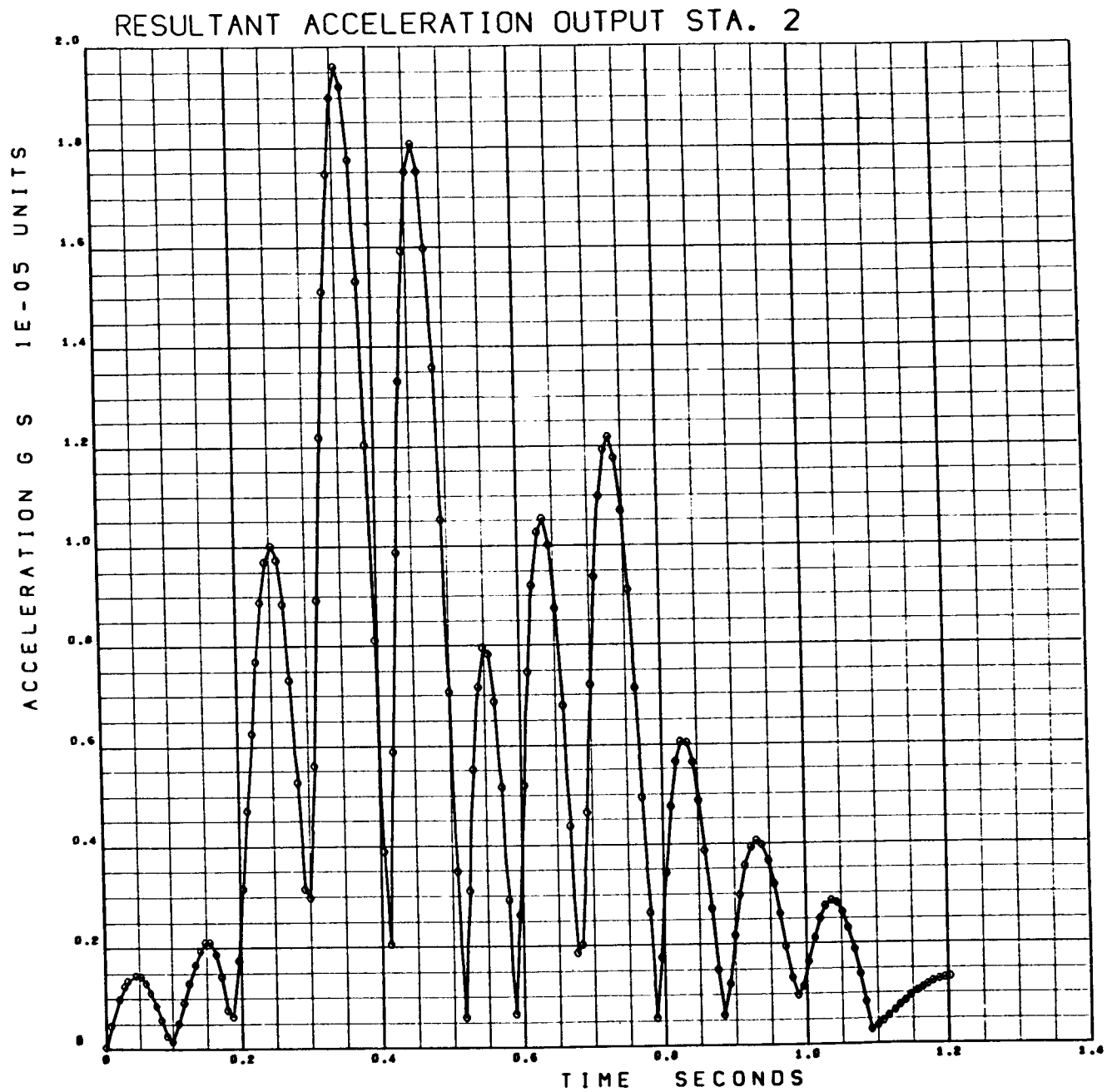


Figure 3-40. Heartbeat – Resultant Acceleration Output Station 2

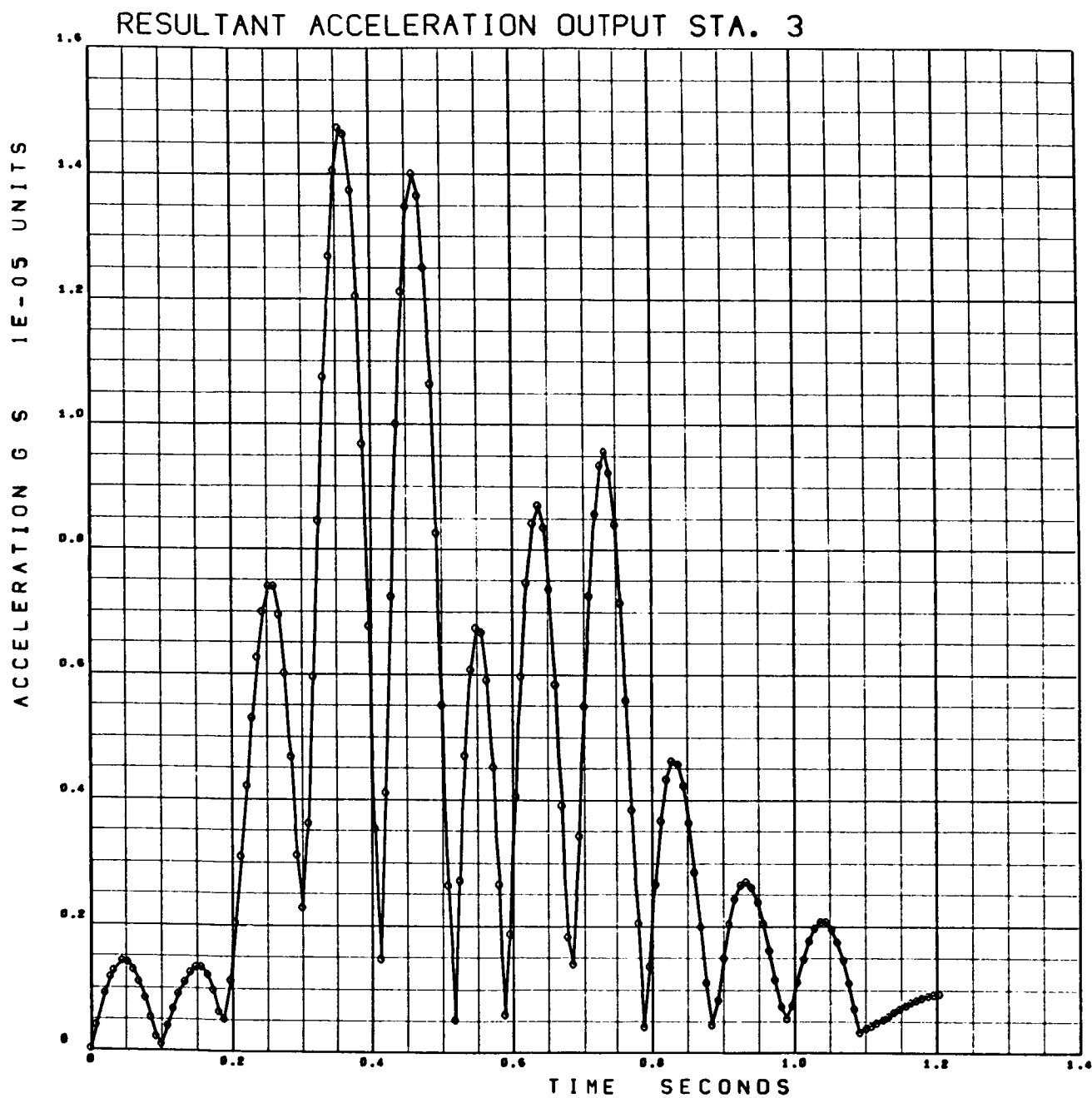


Figure 3-41. Heartbeat – Resultant Acceleration Output Station 3

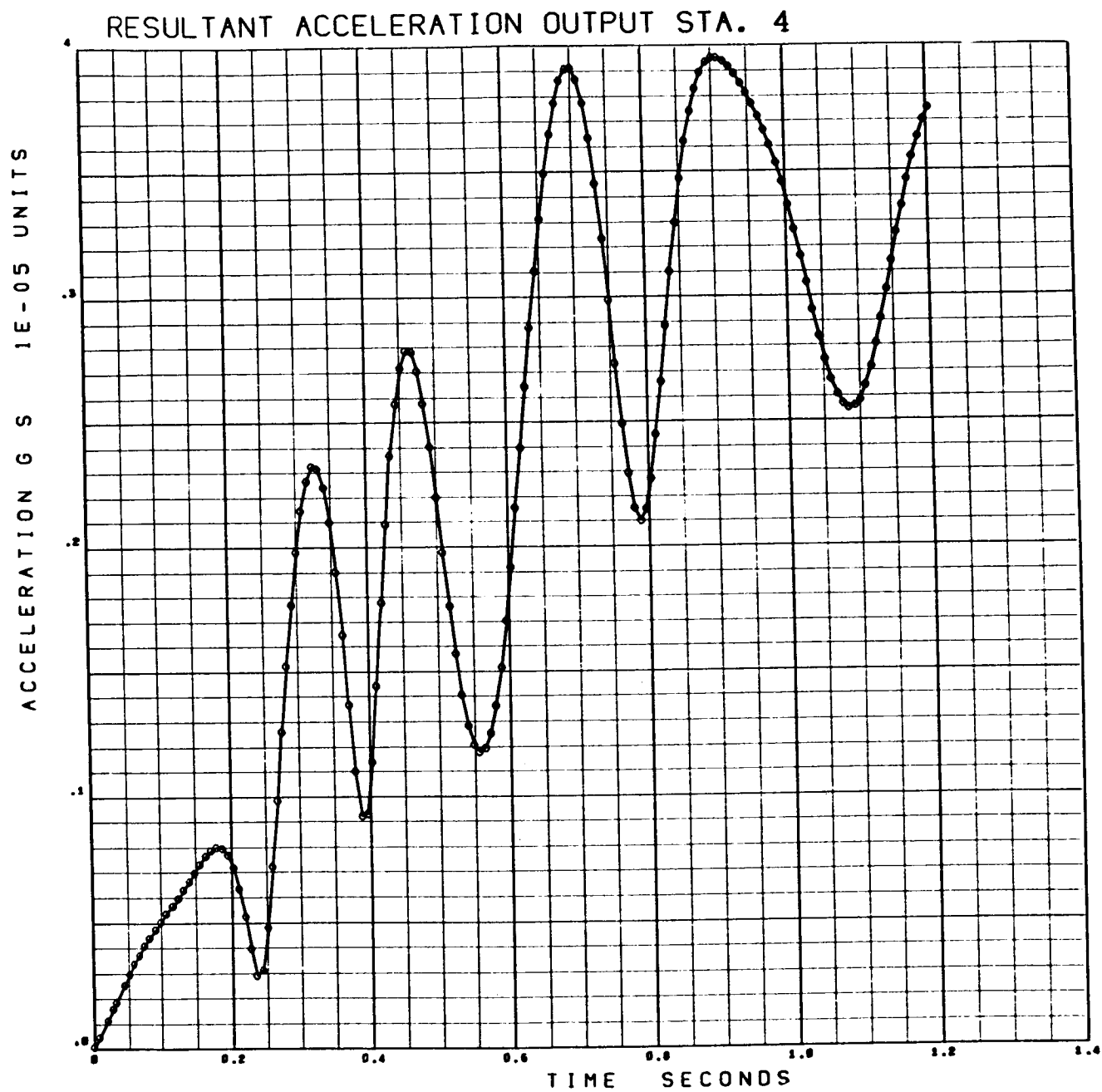


Figure 3-42. Heartbeat – Resultant Acceleration Output Station 4

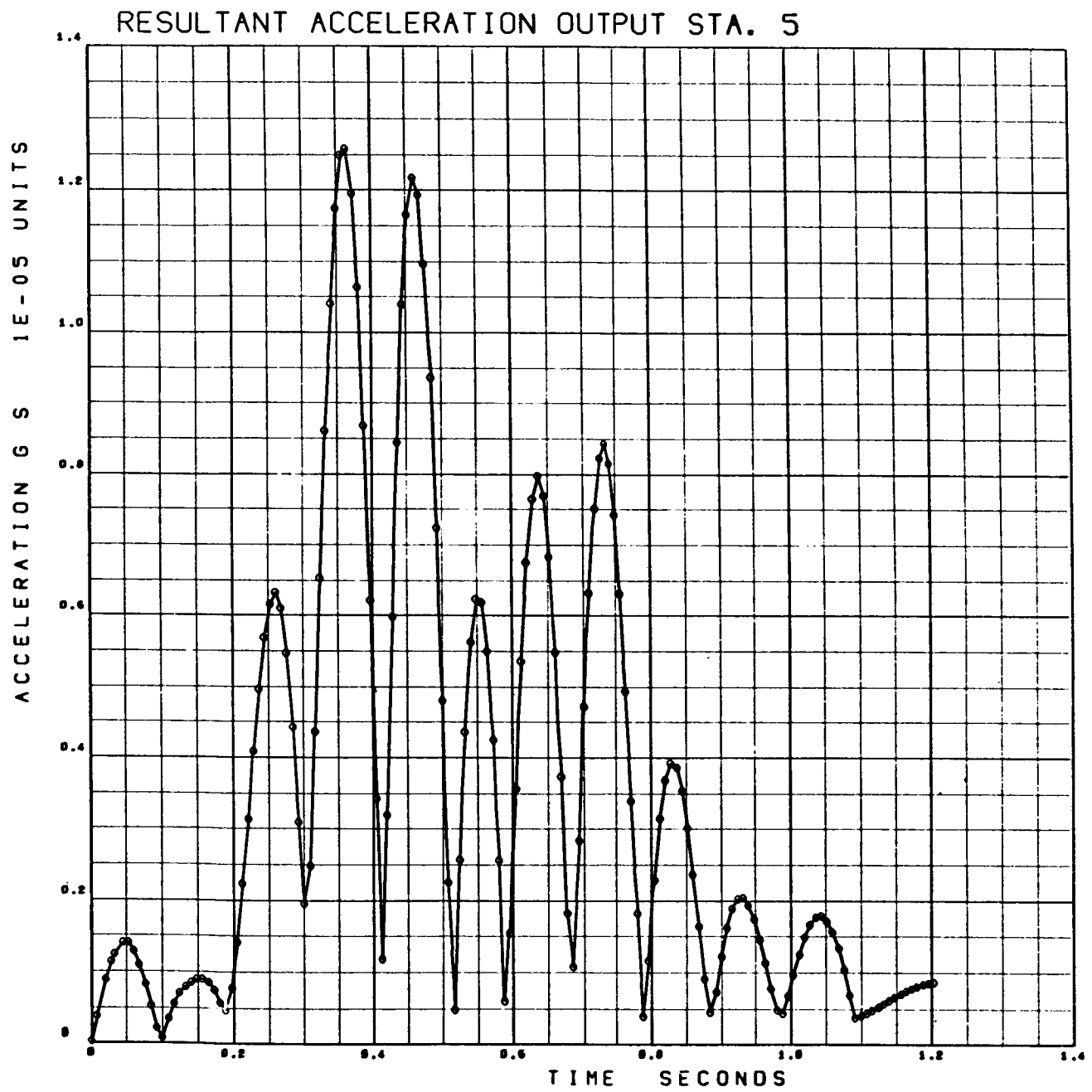


Figure 3-43. Heartbeat – Resultant Acceleration Output Station 5

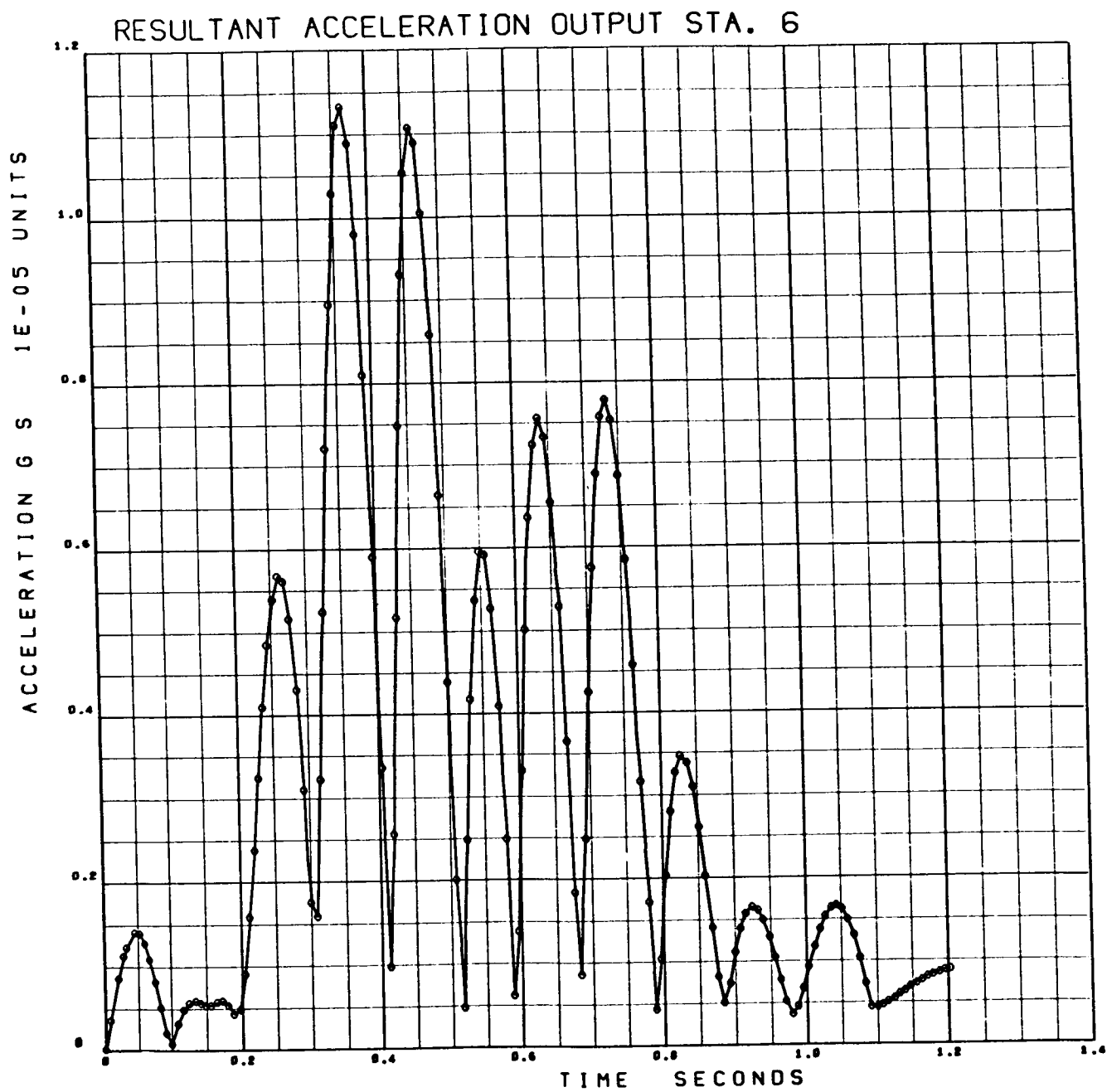


Figure 3-44. Heartbeat – Resultant Acceleration Output Station 6

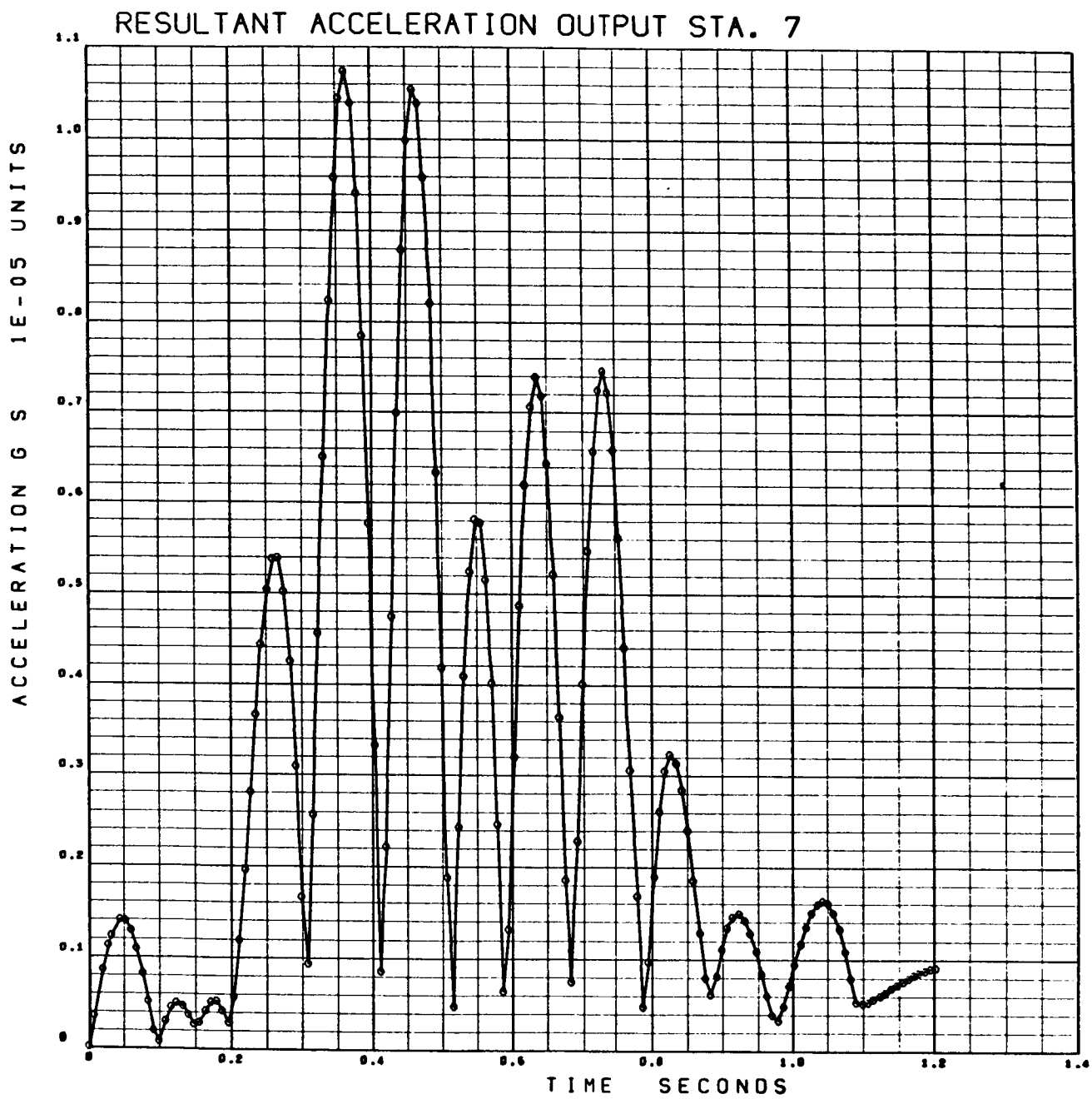


Figure 3-45. Heartbeat – Resultant Acceleration Output Station 7

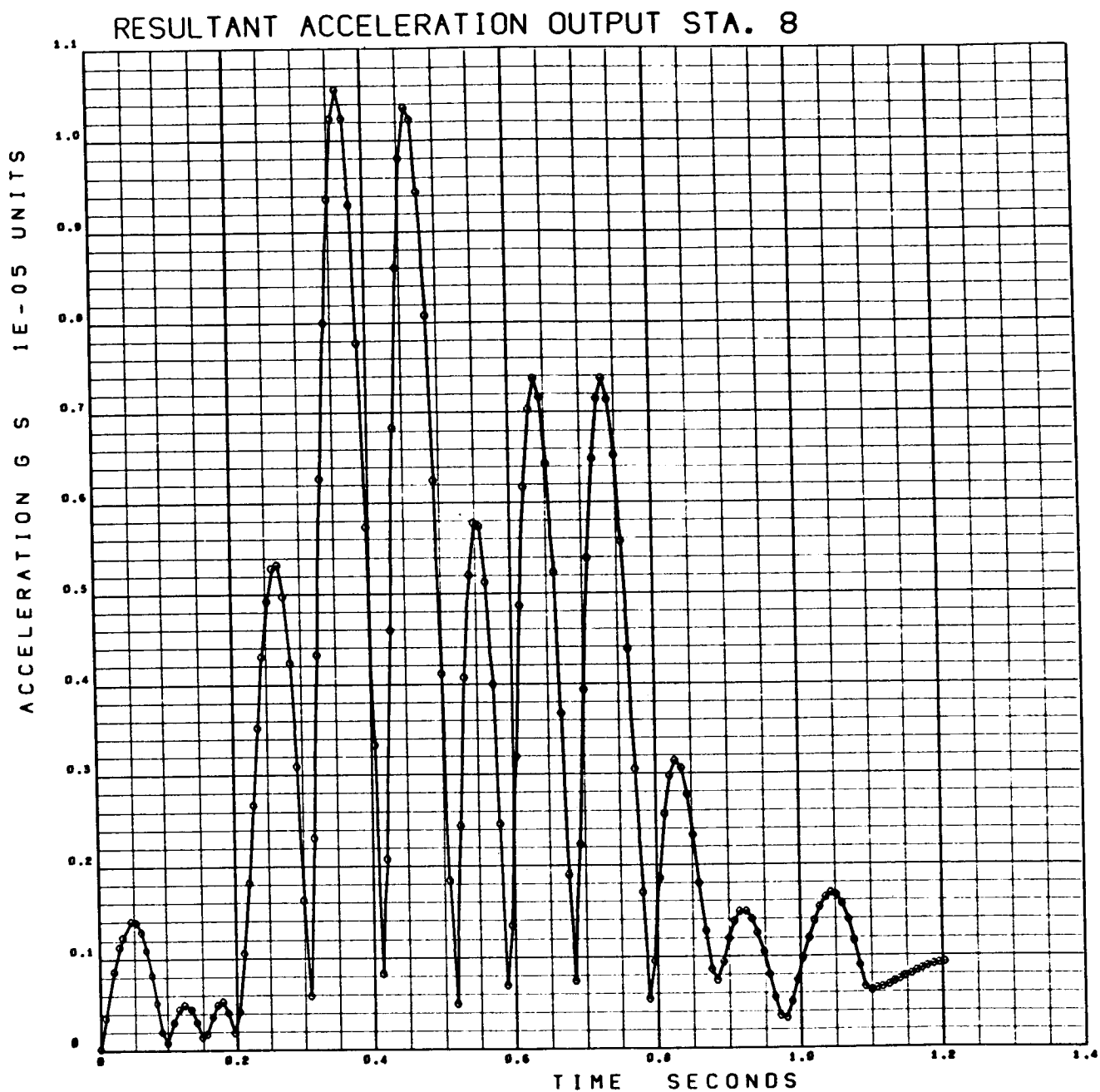


Figure 3-46. Heartbeat – Resultant Acceleration Output Station 8

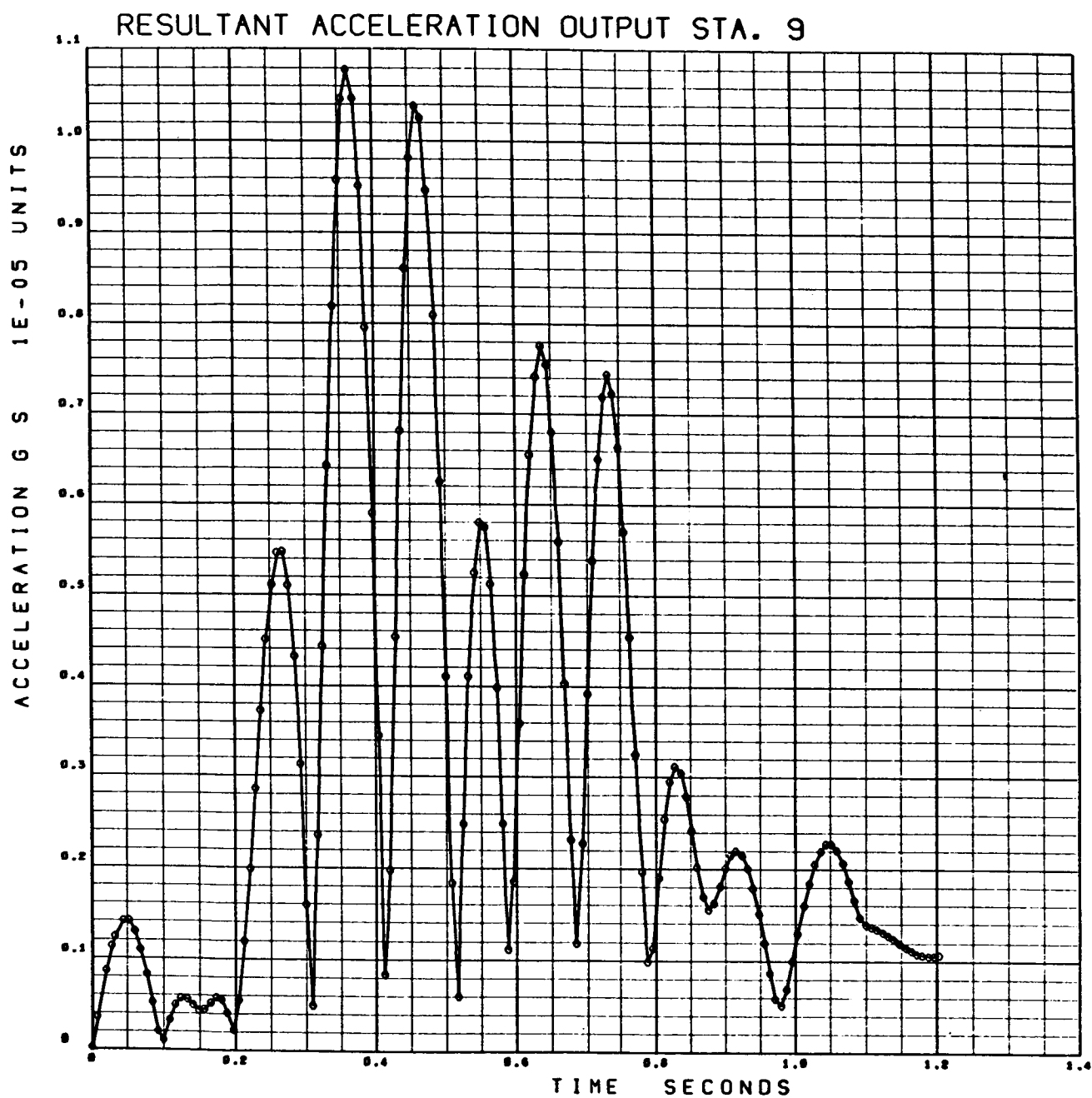


Figure 3-47. Heartbeat – Resultant Acceleration Output Station 9

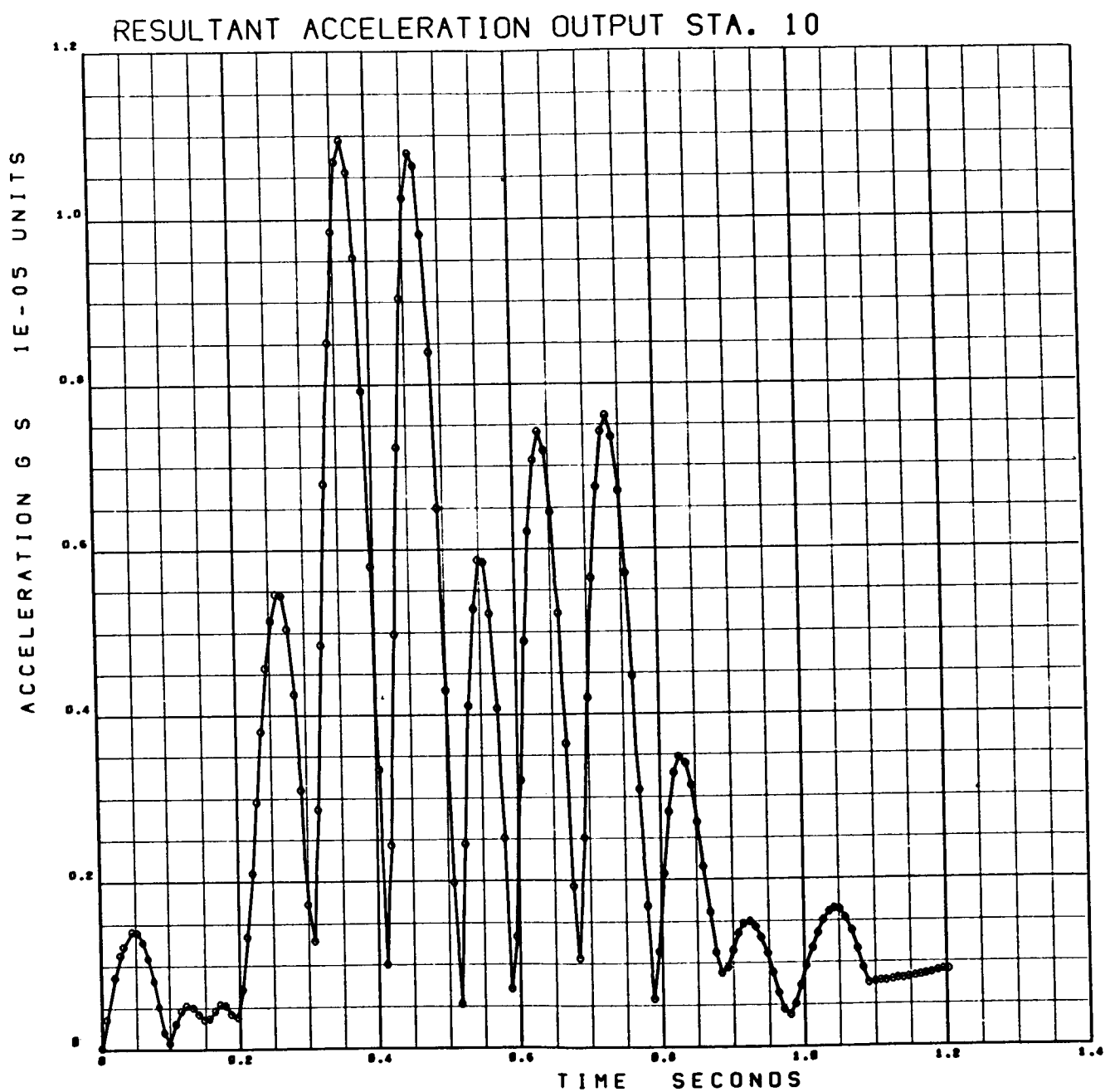


Figure 3-48. Heartbeat – Resultant Acceleration Output Station 10

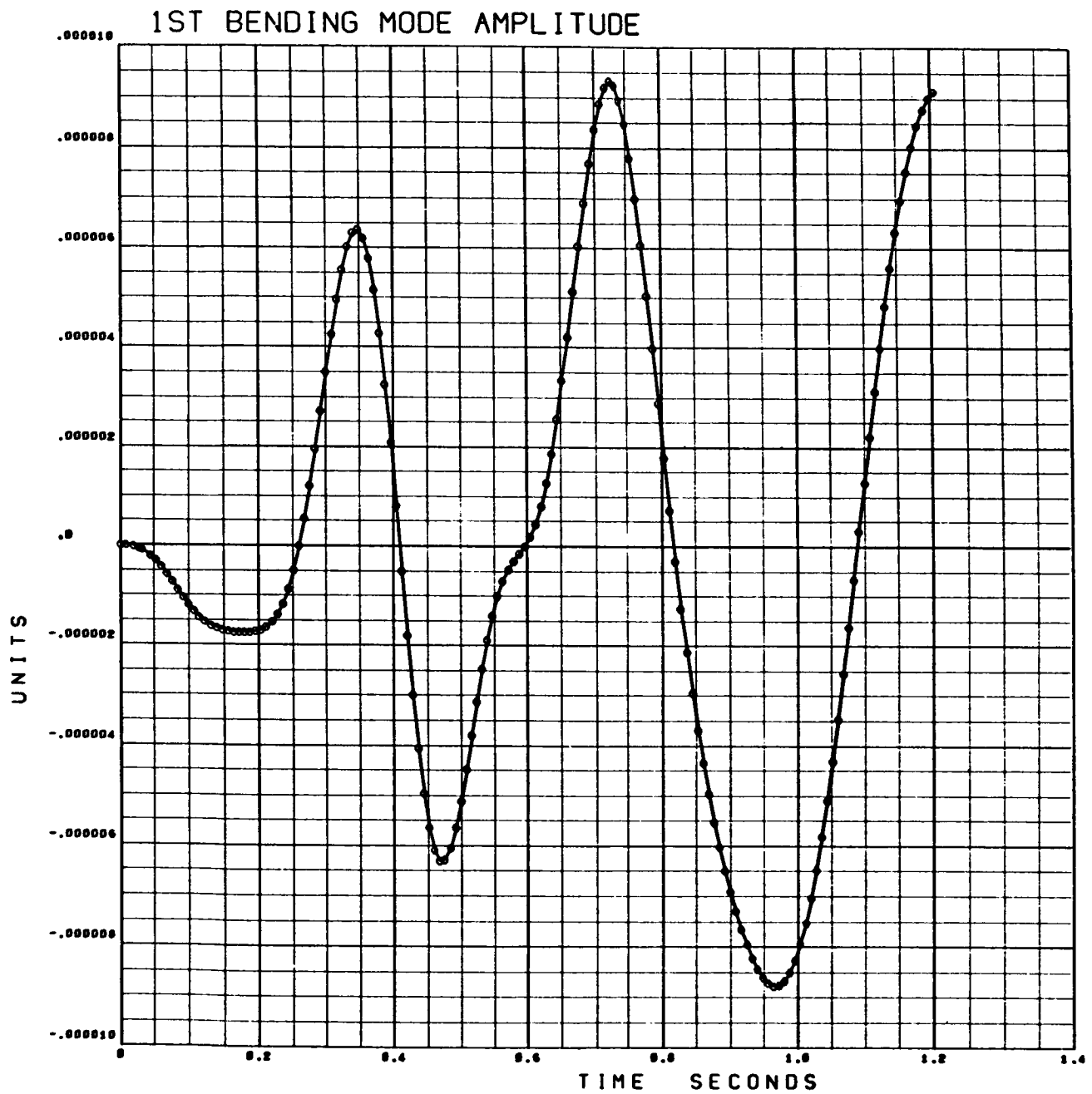


Figure 3-49. Heartbeat – First Bending Mode Amplitude



Figure 3-50. Heartbeat – Second Bending Mode Amplitude

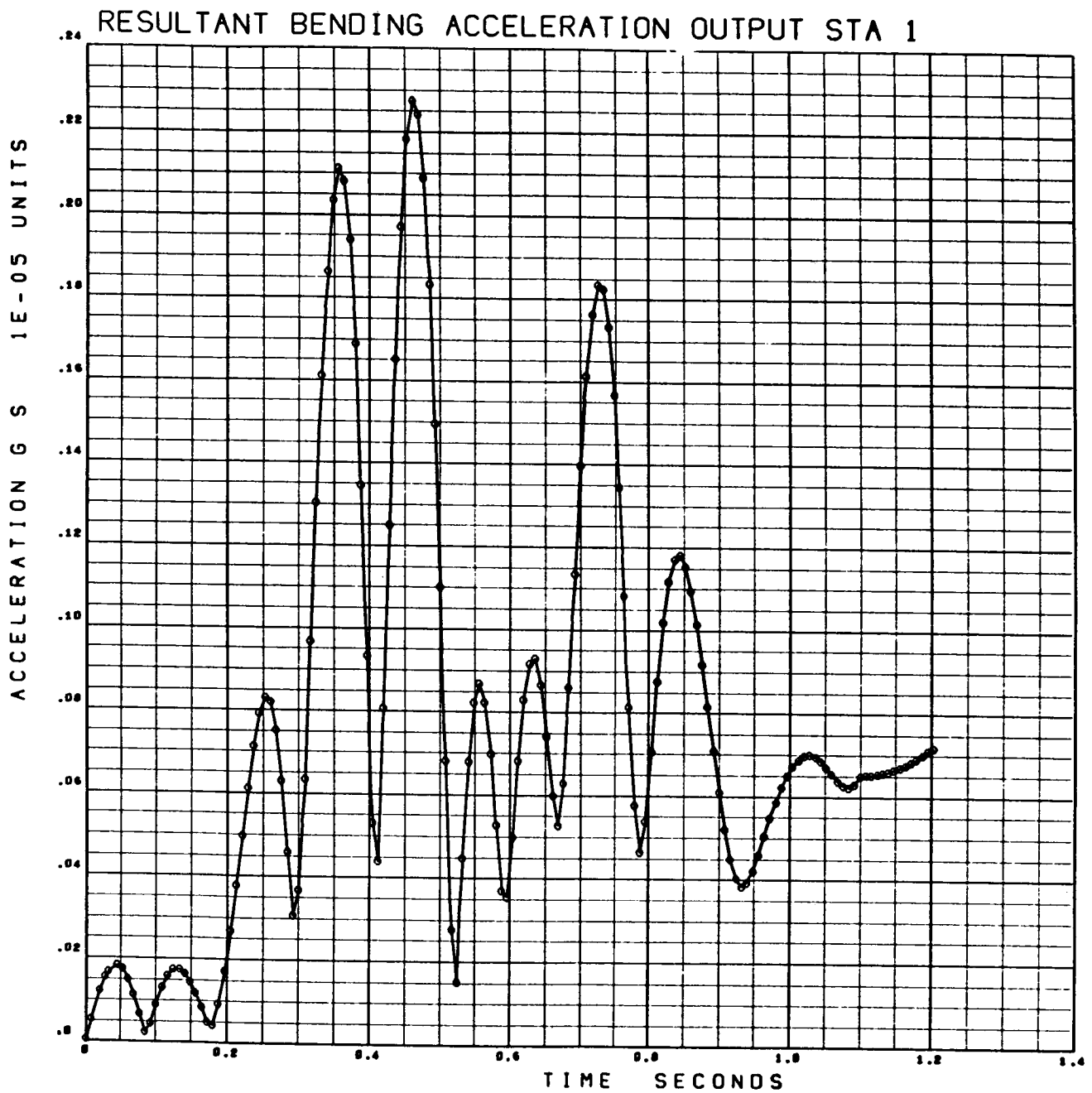


Figure 3-51. Heartbeat – Resultant Bending Acceleration Output Station 1

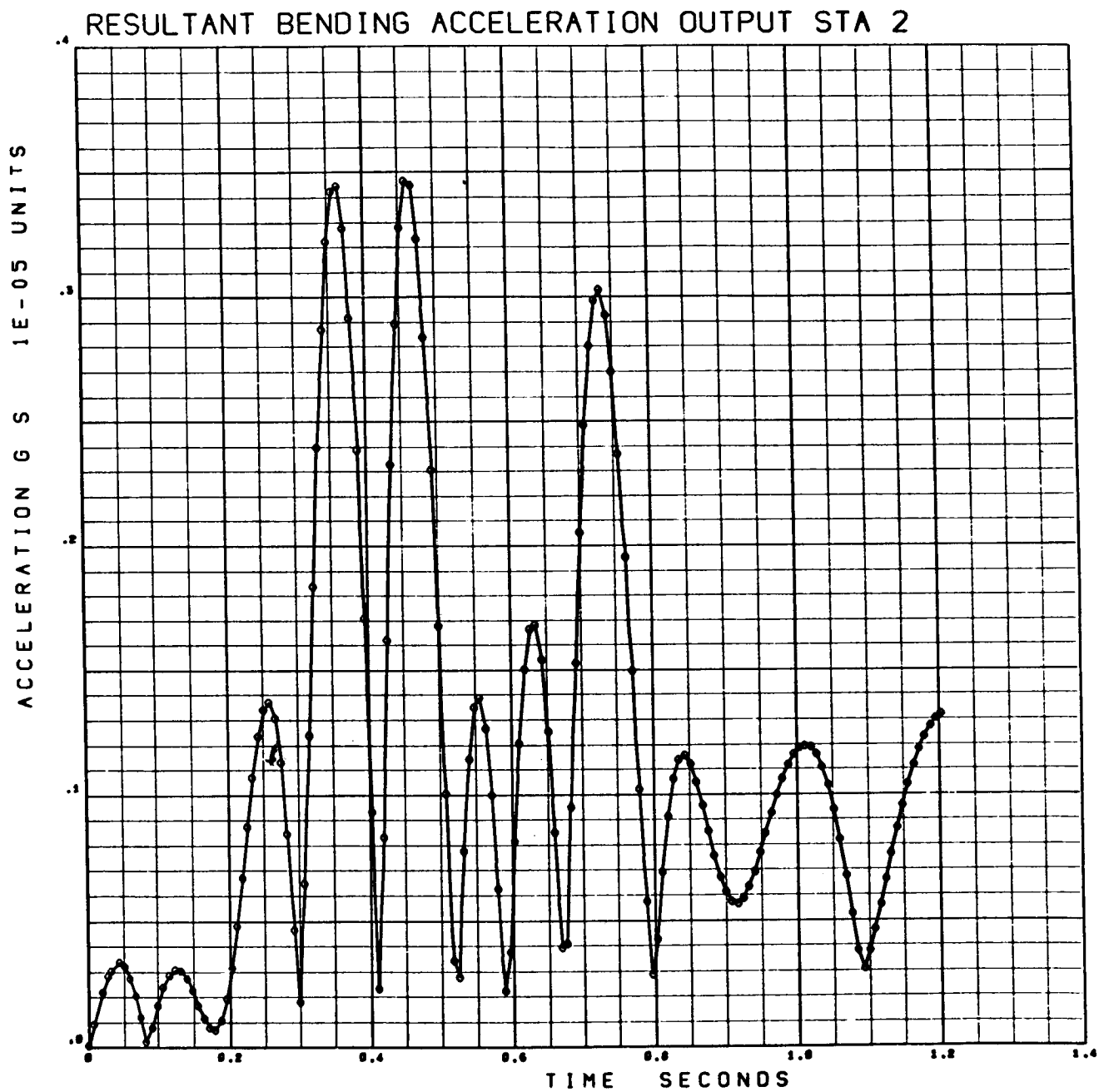


Figure 3-52. Heartbeat – Resultant Bending Acceleration Output Station 2

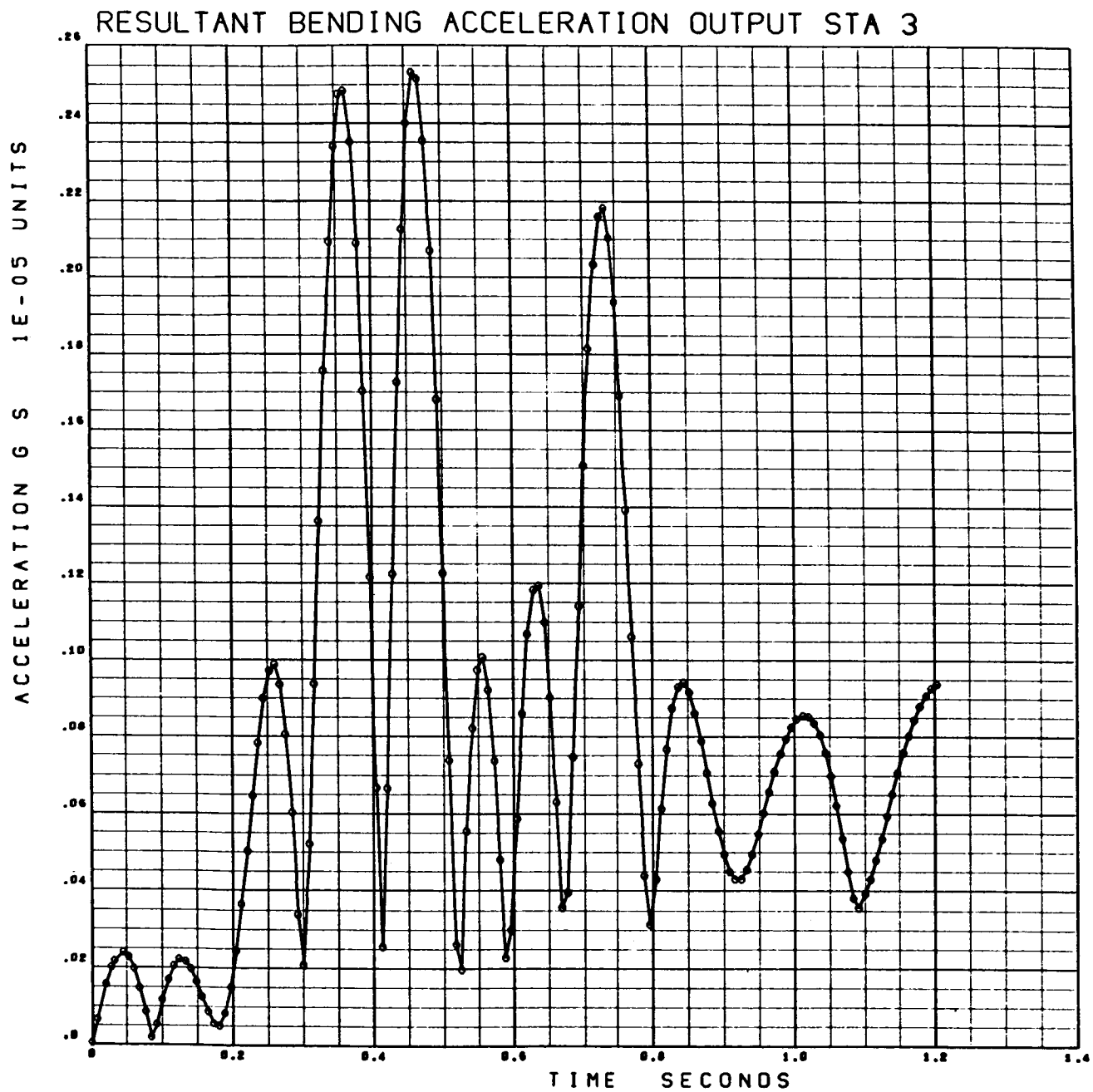


Figure 3-53. Heartbeat – Resultant Bending Acceleration Output Station 3

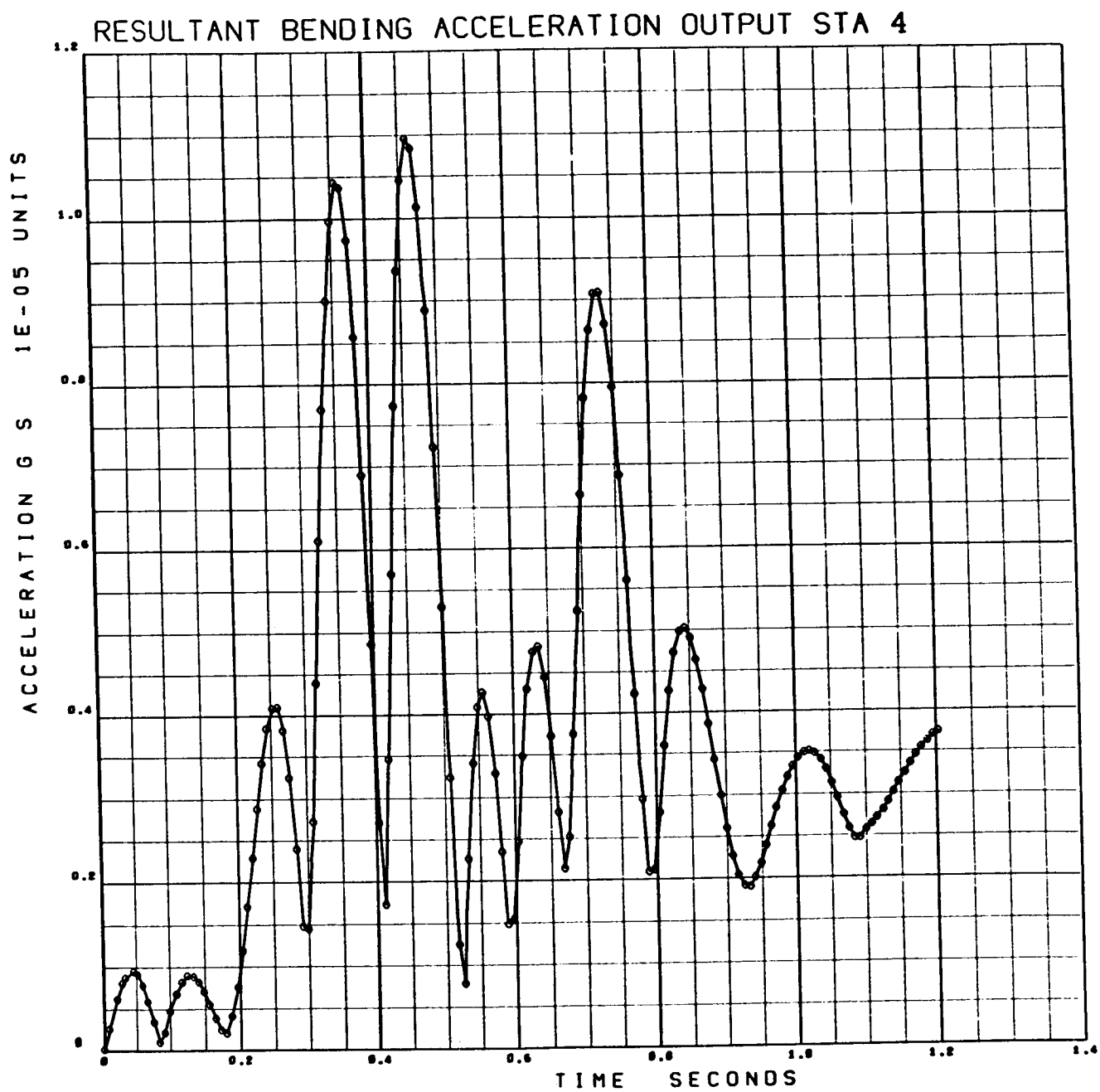


Figure 3-54. Heartbeat – Resultant Bending Acceleration Output Station 4

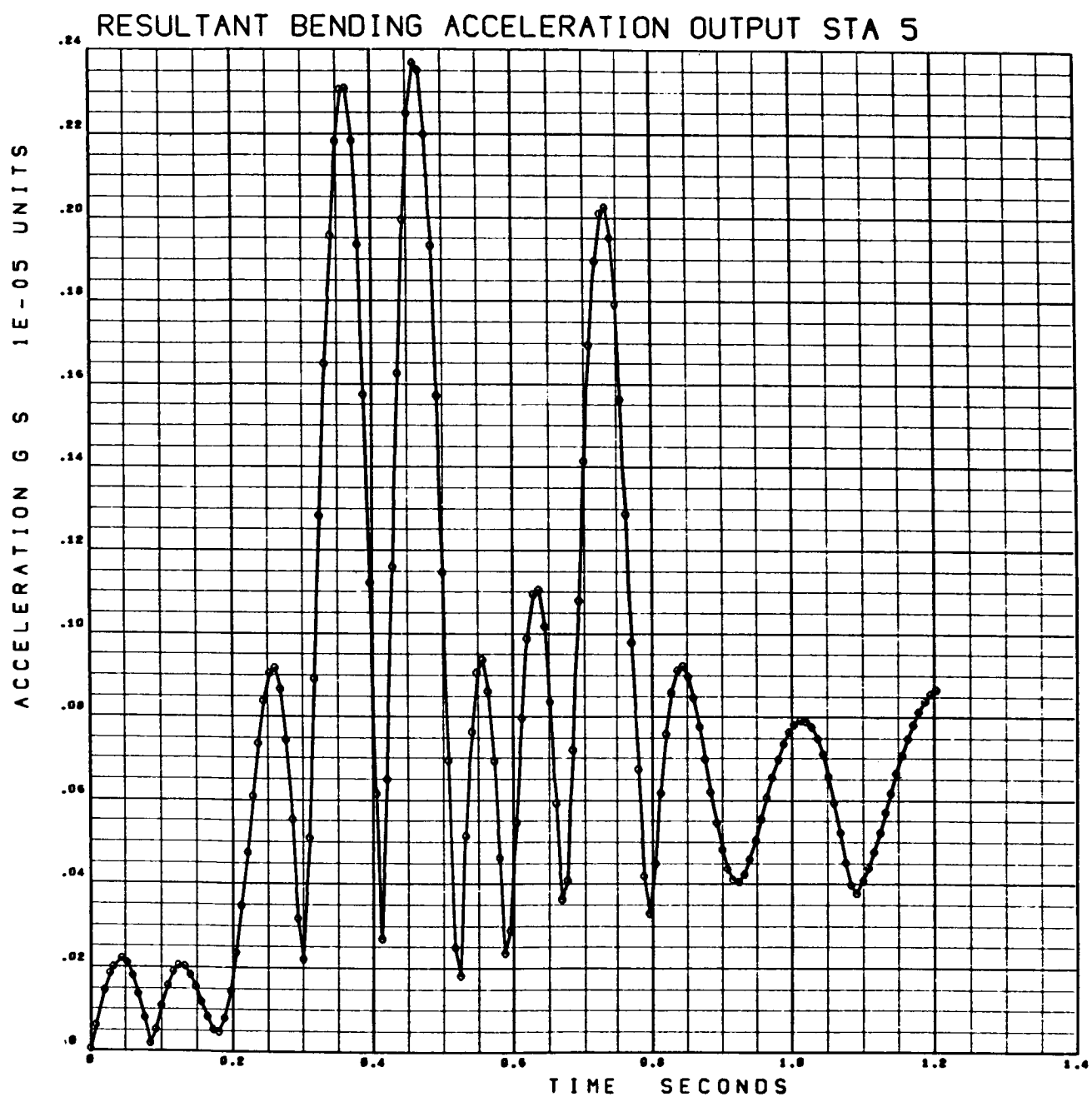


Figure 3-55. Heartbeat – Resultant Bending Acceleration Output Station 5

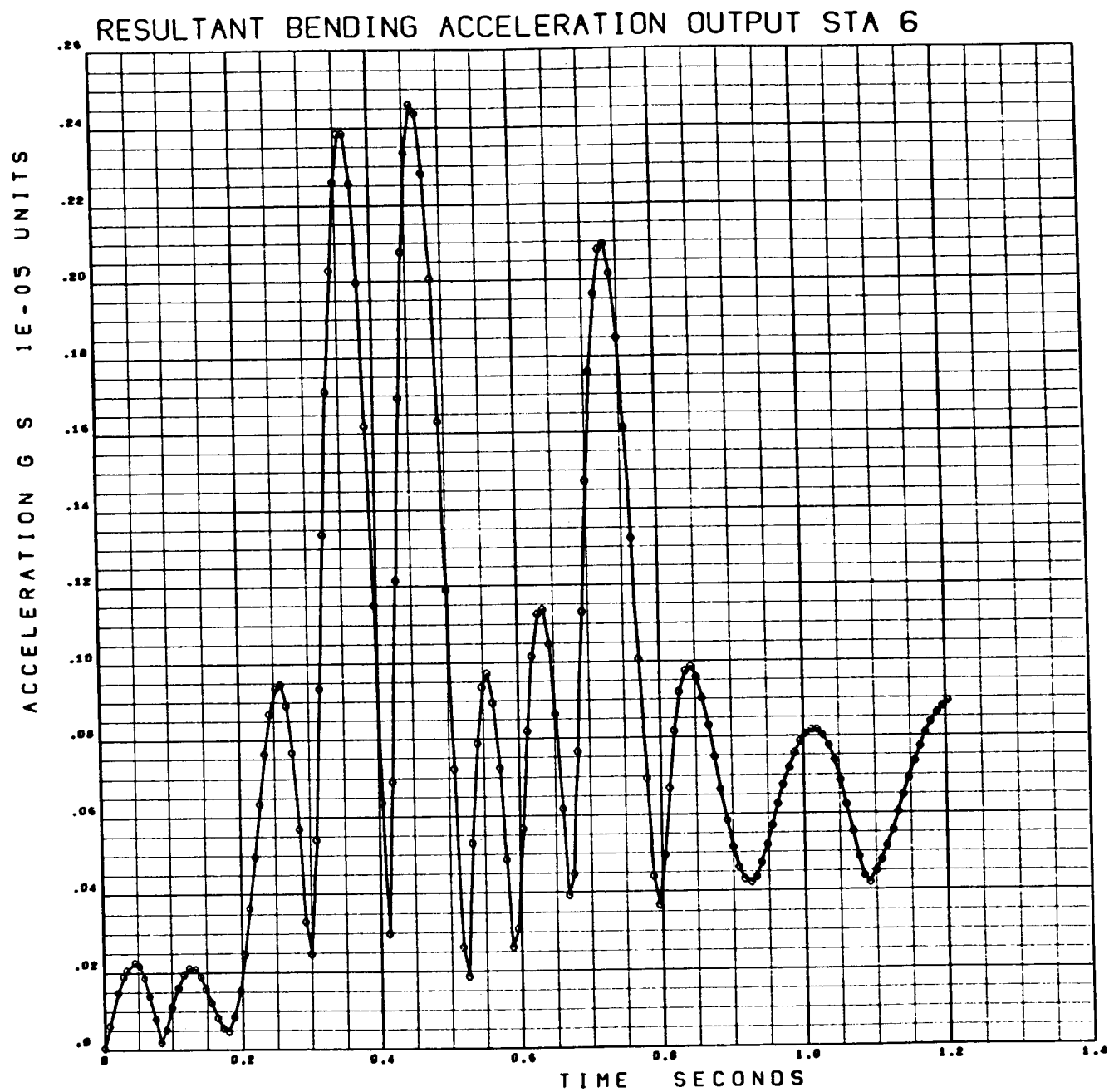


Figure 3-56. Heartbeat – Resultant Bending Acceleration Output Station 6

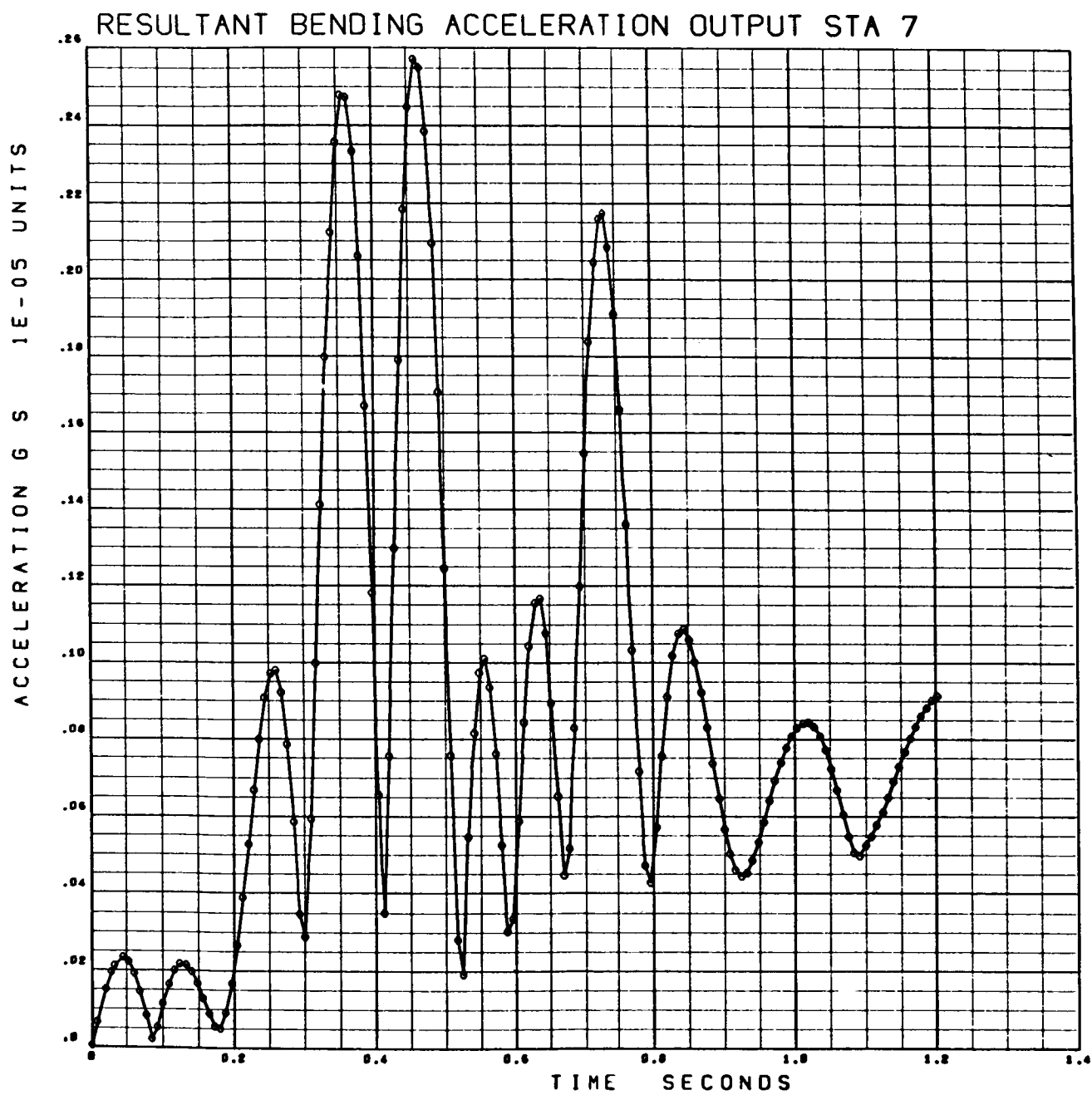


Figure 3-57. Heartbeat – Resultant Bending Acceleration Output Station 7

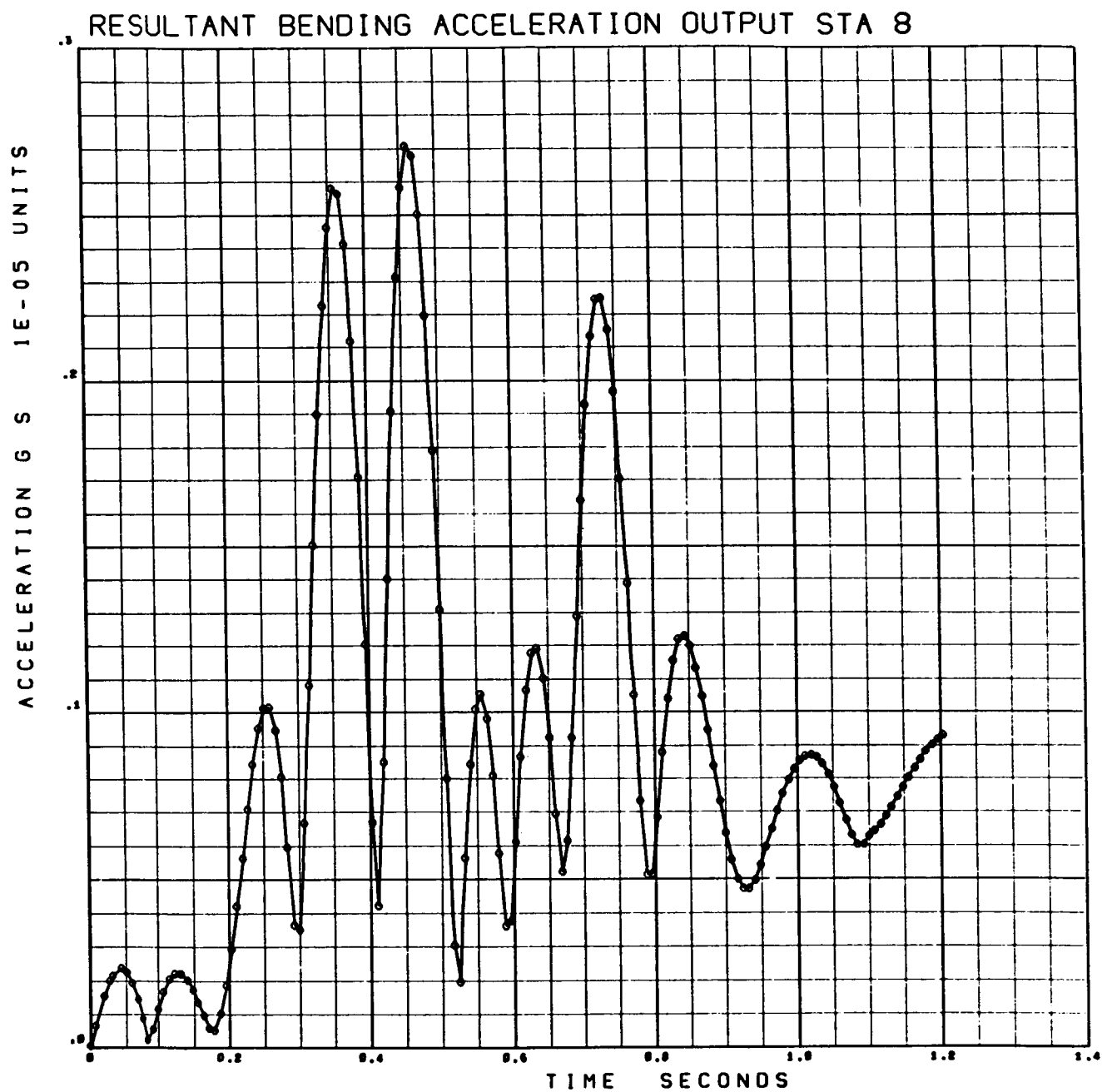


Figure 3-58. Heartbeat – Resultant Bending Acceleration Output Station 8

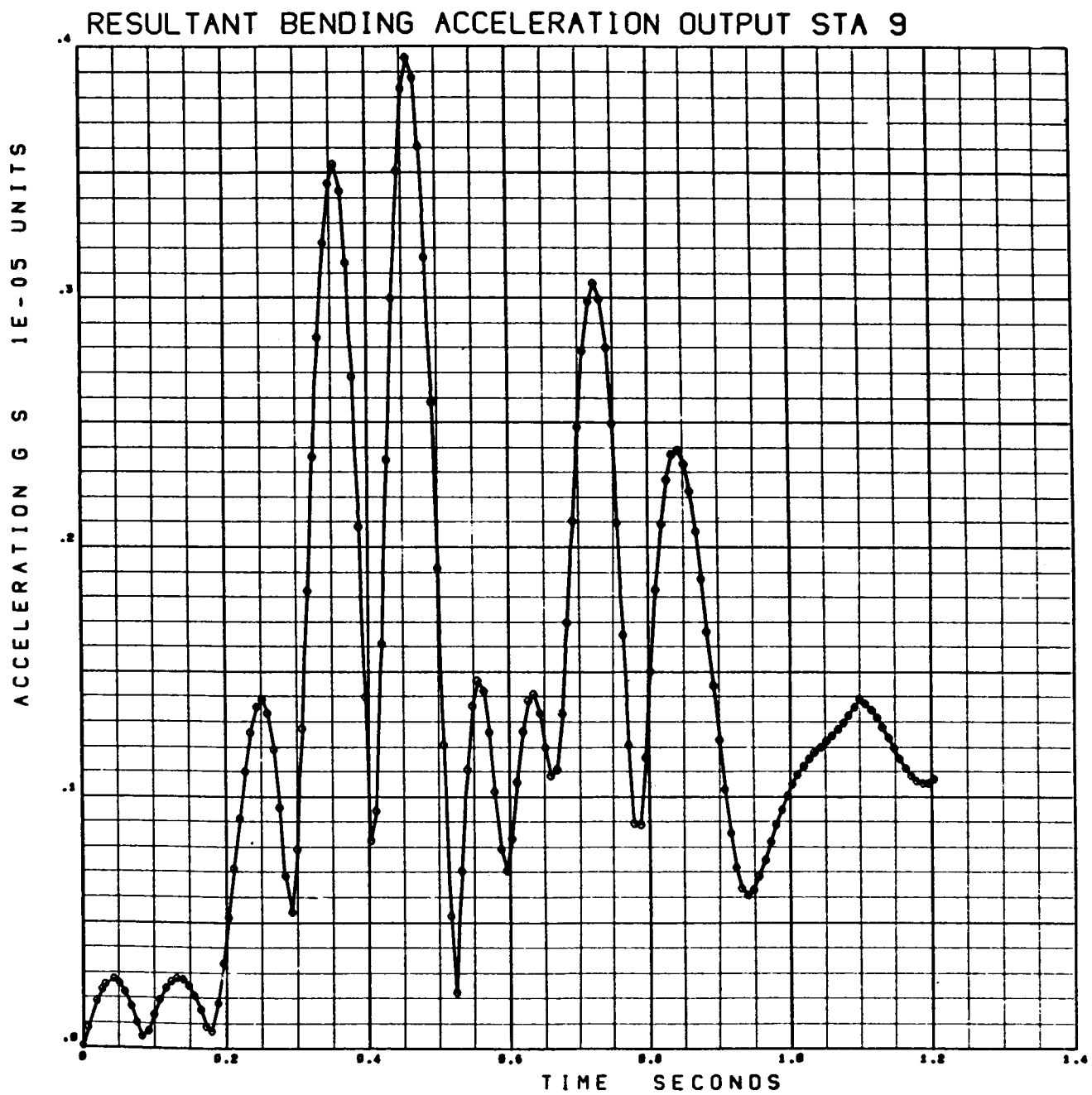


Figure 3-59. Heartbeat – Resultant Bending Acceleration Output Station 9

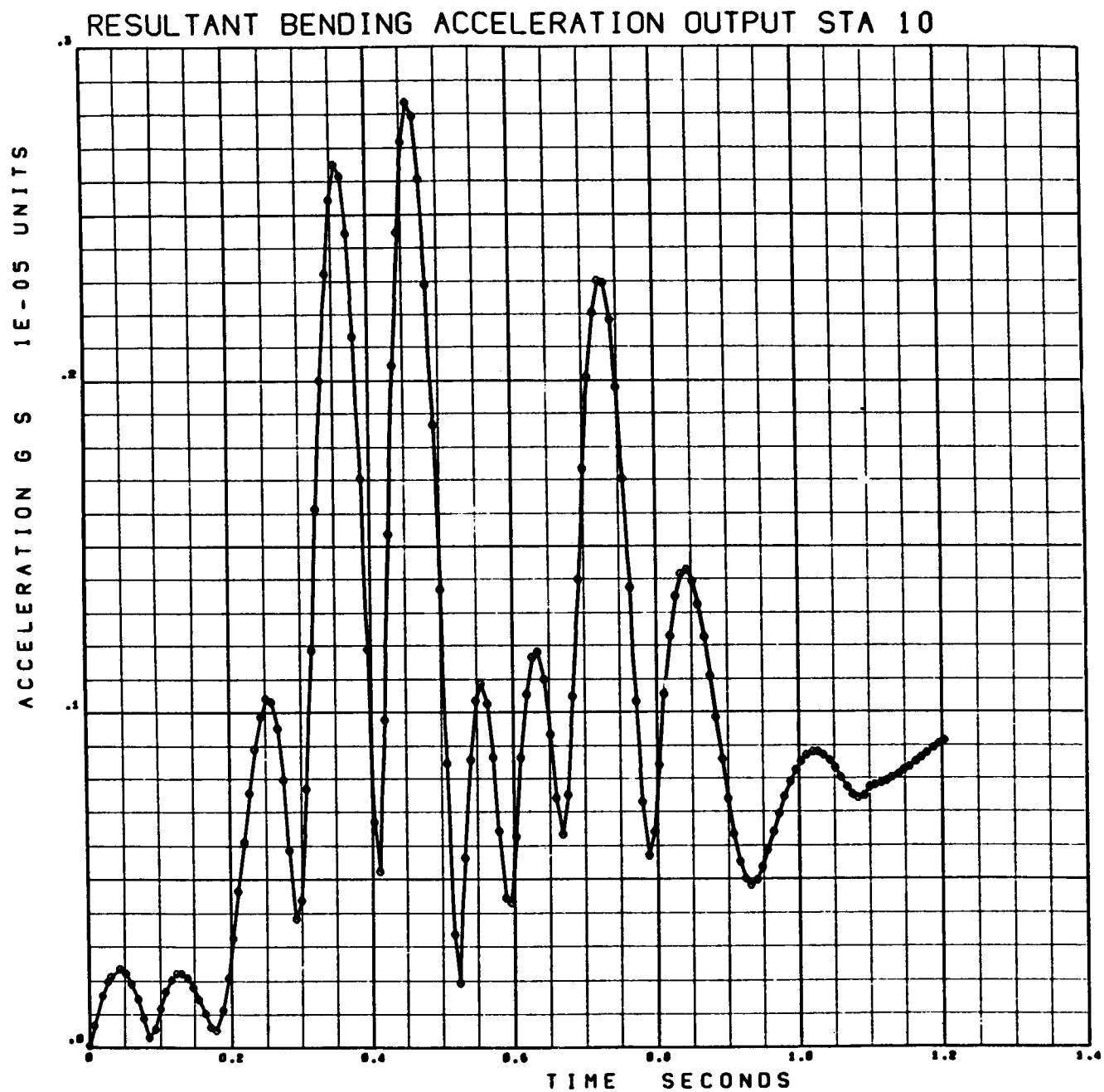


Figure 3-60. Heartbeat – Resultant Bending Acceleration Output Station 10

Input Data for Figures 3-61 to 3-76, Case 2-1-1 Cough

SERIAL 757475

I1= .37963+07 I2= .24223+08 I3= .22079+08 MASS= .20440+03 DELT= .40000-02 TF=

TRANSFORMATION FROM CREW STA. TO CRAFT AXES

.00000000	.00000000	.10000000+01
-.10000000+01	.00000000	.00000000
.00000000	-.10000000+01	.00000000

CREW STATION ORIGIN .198500+04 .125000+03 .180000+02

INPUT POINT .000000 .000000 .000000

VEHICLE C.G. .168934+04 .594600+02 -.614999+01

OUTPUT STATION COORDINATES

STA. NO. 1	.128000+04	.000000	.000000
STA. NO. 2	.138000+04	.000000	.000000
STA. NO. 3	.147999+04	.000000	.000000
STA. NO. 4	.158000+04	.000000	.000000
STA. NO. 5	.168900+04	.000000	.000000
STA. NO. 6	.186000+04	.000000	.000000
STA. NO. 7	.203500+04	.000000	.000000
STA. NO. 8	.198500+04	-.150000+03	-.125000+03
STA. NO. 9	.198500+04	.125000+03	.000000
STA. NO. 10	.198500+04	.275000+03	.000000

FORCE COSINE COEF

.76516327-01	-.14716666+01	-.14946462+01	.11679597+01	.13365398+01	-.29208211+01	.33061182+01
-.34879414-00	-.30294502-00	-.15123076-00	.41767413-00	-.13050494+01	-.24912848+01	.41816300+01
.52426851-01	-.26226359-00	-.40526506-01	.10179601+01	-.12618987+01	.94301330-01	.40000053-00

FORCE SINE COEF

.15946499-00	.10080934+00	-.96027109-00	-.18850627+01	.42810690+01	-.16121931+01	-.42199945-01
.21548027-00	.34402652-00	-.15594341+01	-.34899589+01	.42698295+01	.30025782-00	.55906940-02
-.70904400-01	.31886502-00	-.27874383-00	-.14332246-00	.41600960-00	-.27766767-00	.23051954-01

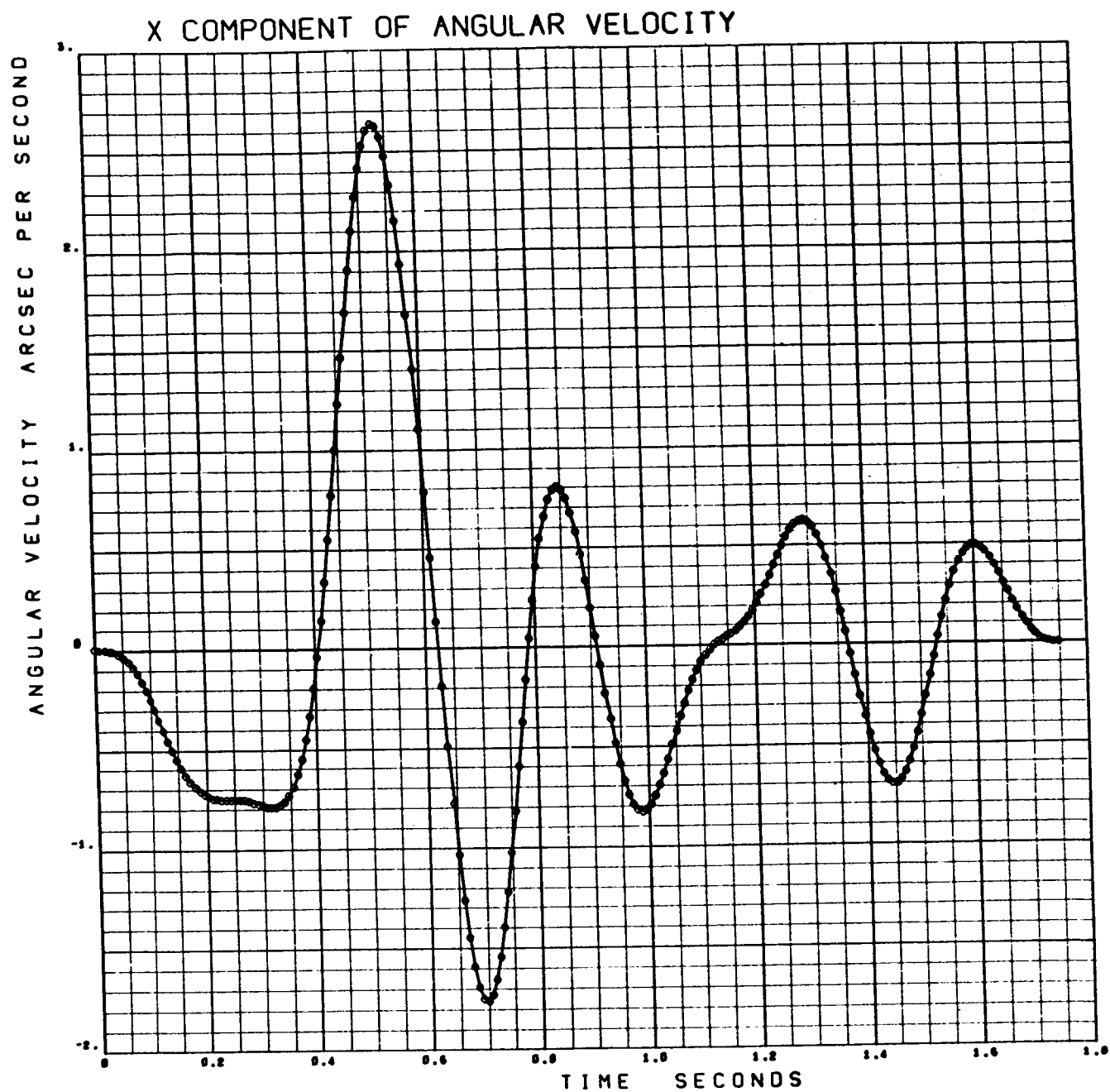


Figure 3-61. Cough (X Component of Angular Velocity)

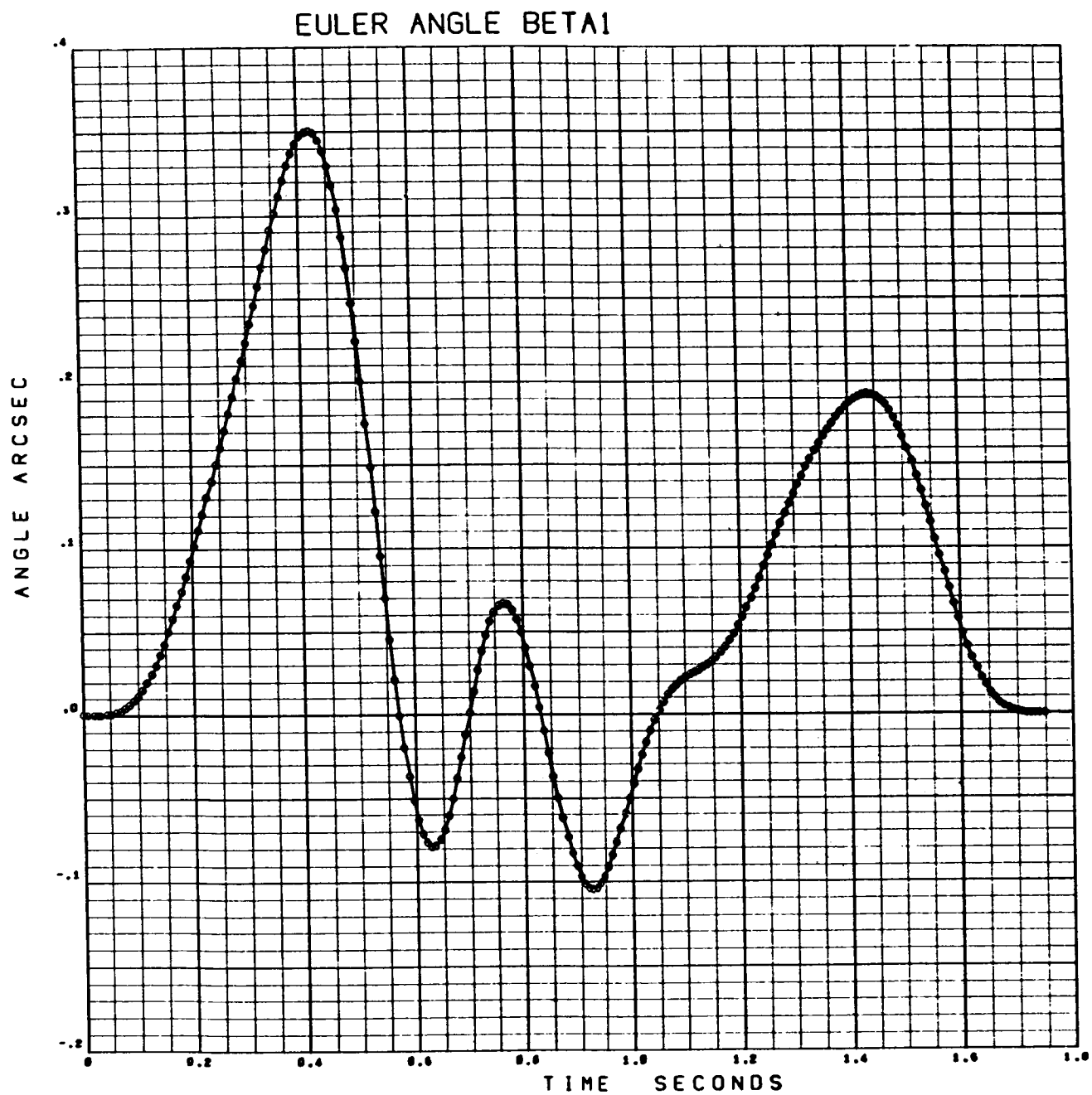


Figure 3-62. Cough (Euler Angle Beta 1)

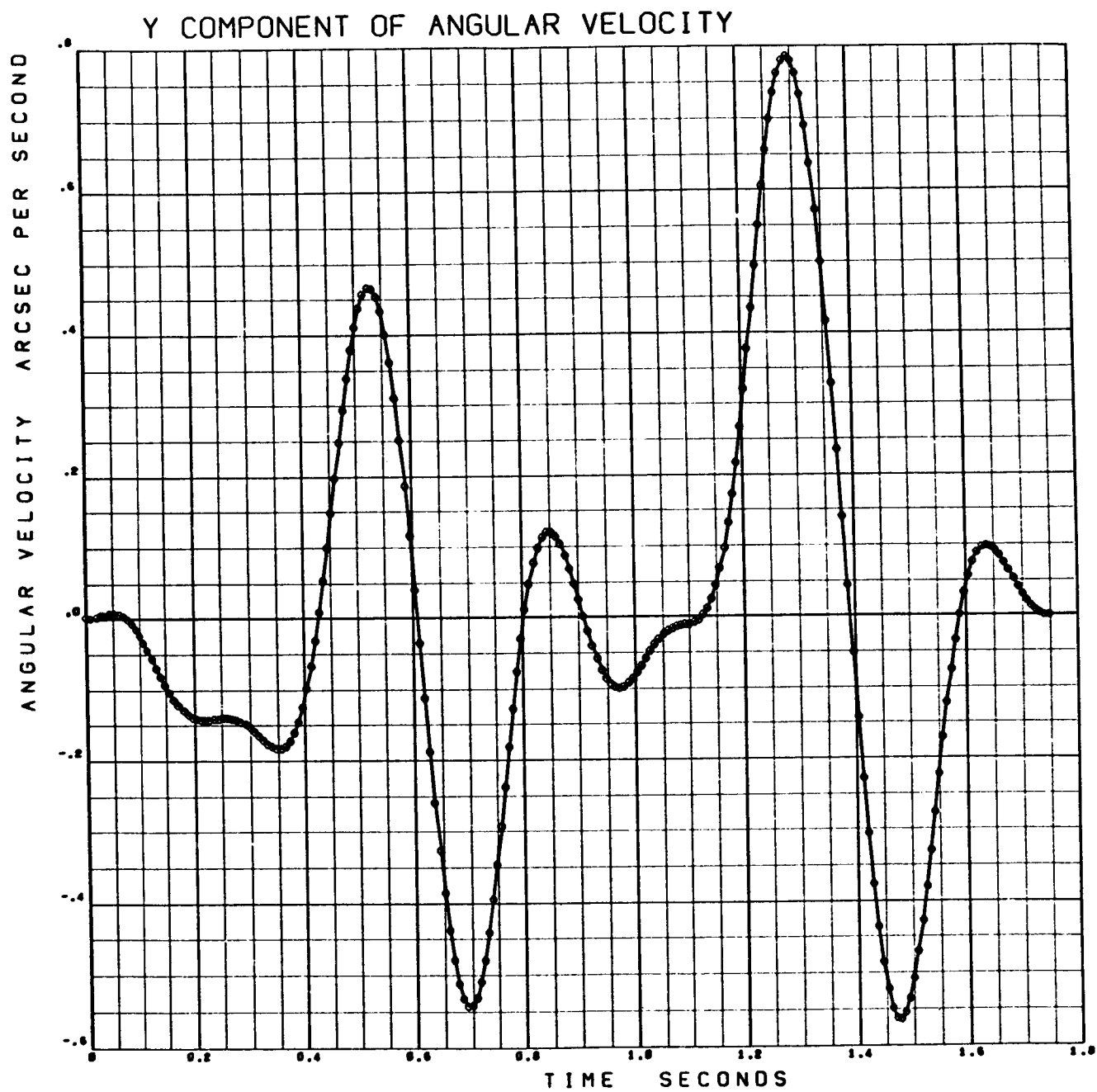


Figure 3-63. Cough (Y Component of Angular Velocity)

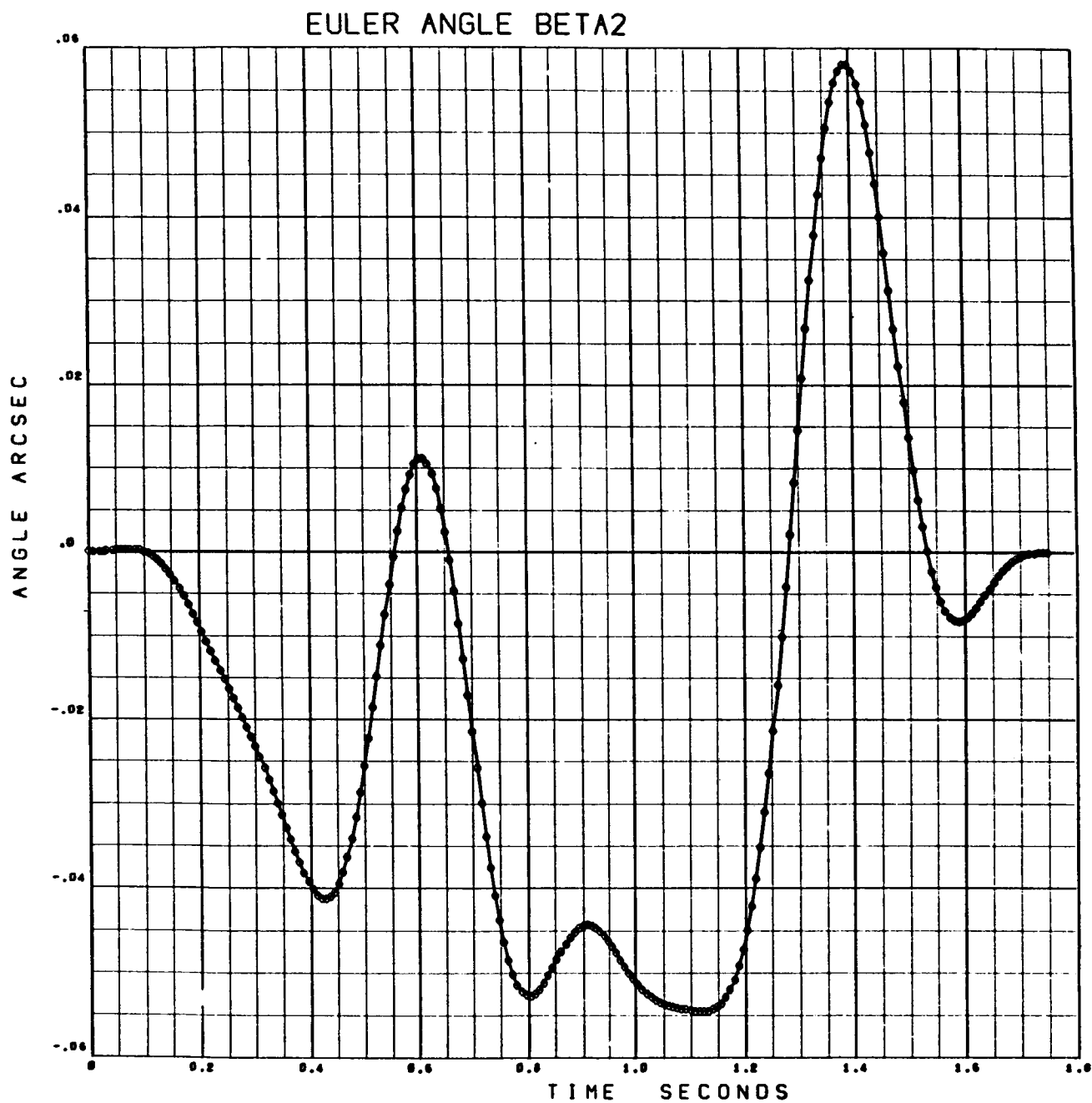


Figure 3-64. Cough (Euler Angle Beta 2)

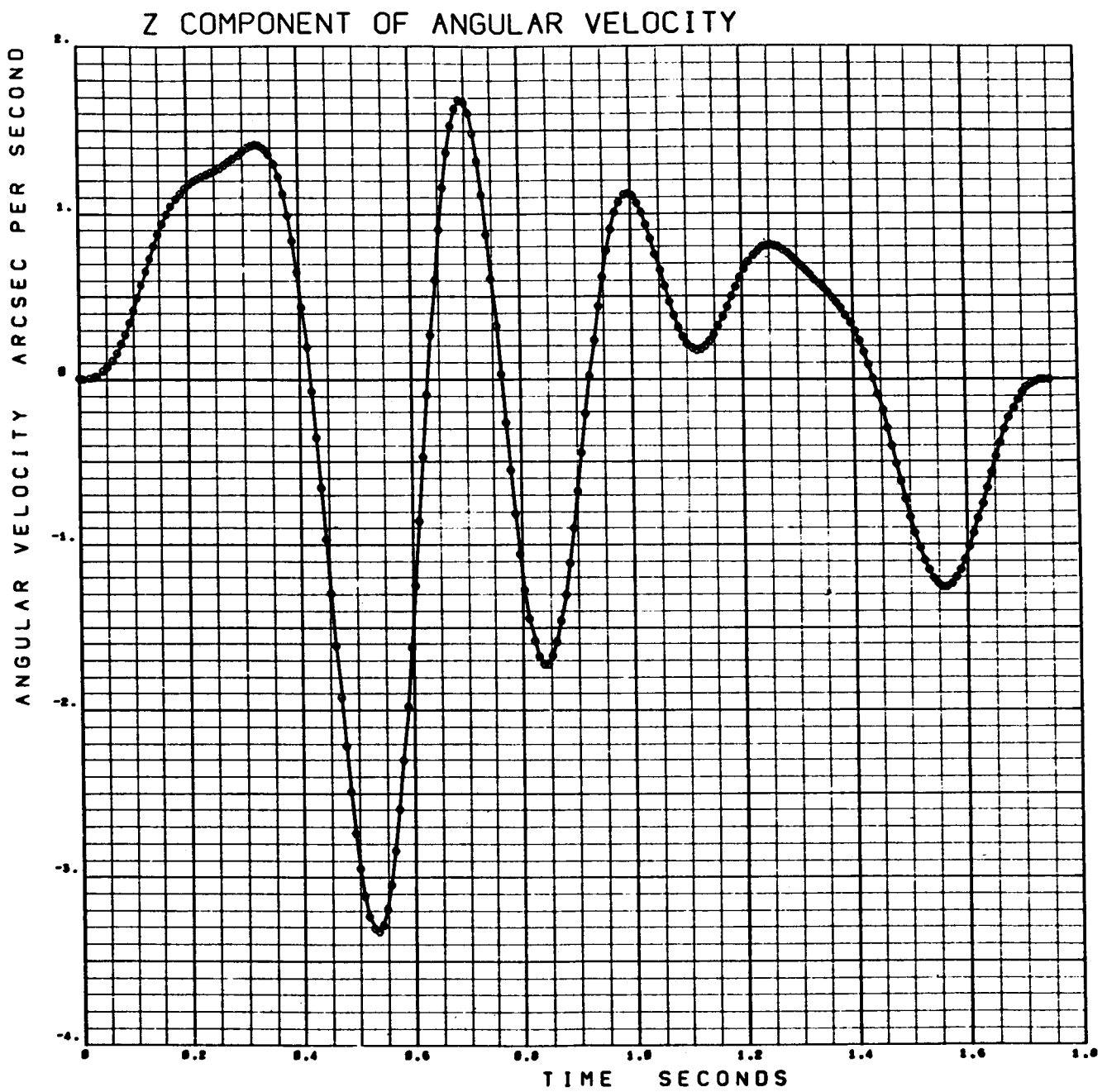


Figure 3-65. Cough (Z Component of Angular Velocity)

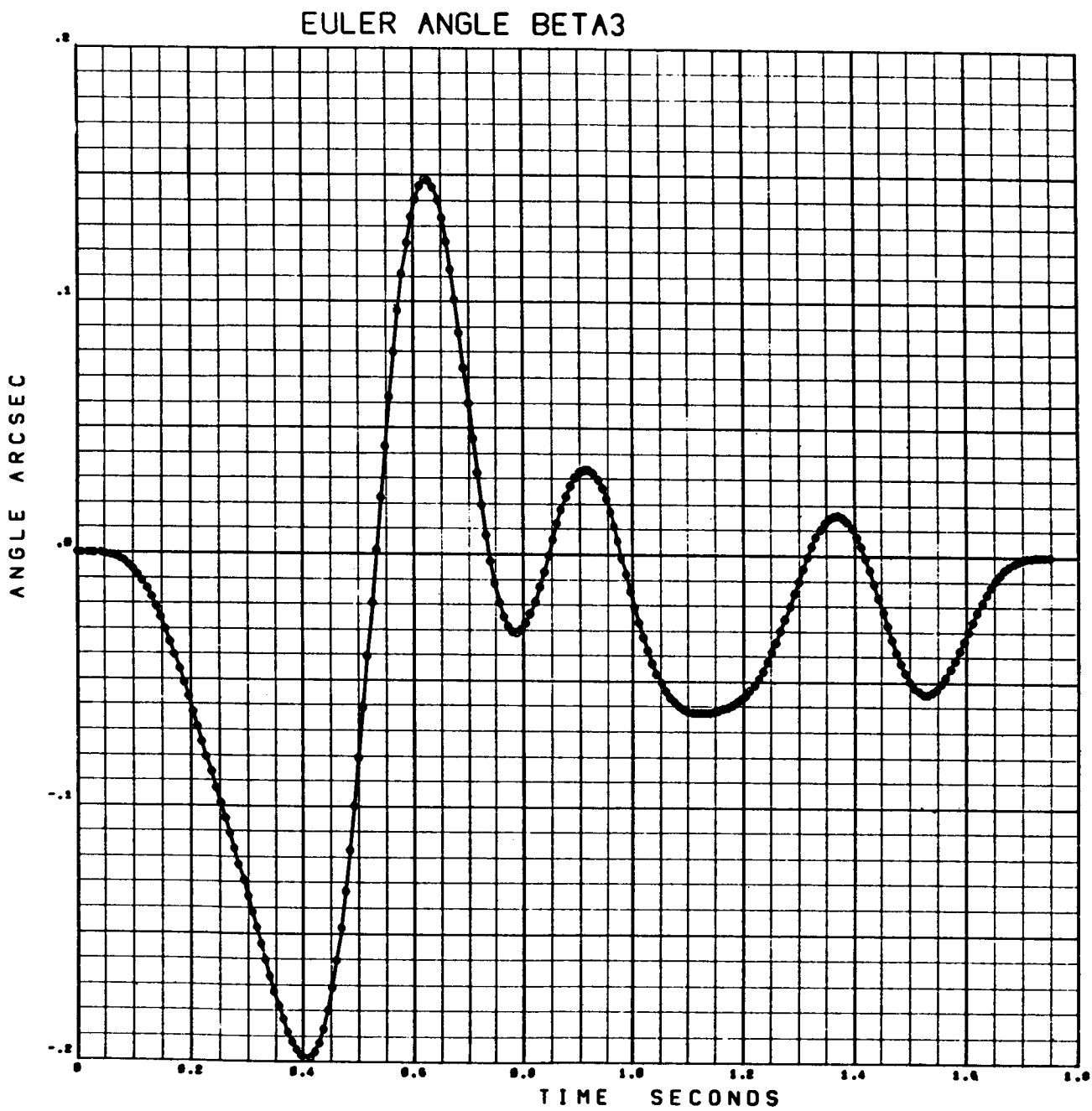


Figure 3-66. Cough (Euler Angle Beta 3)

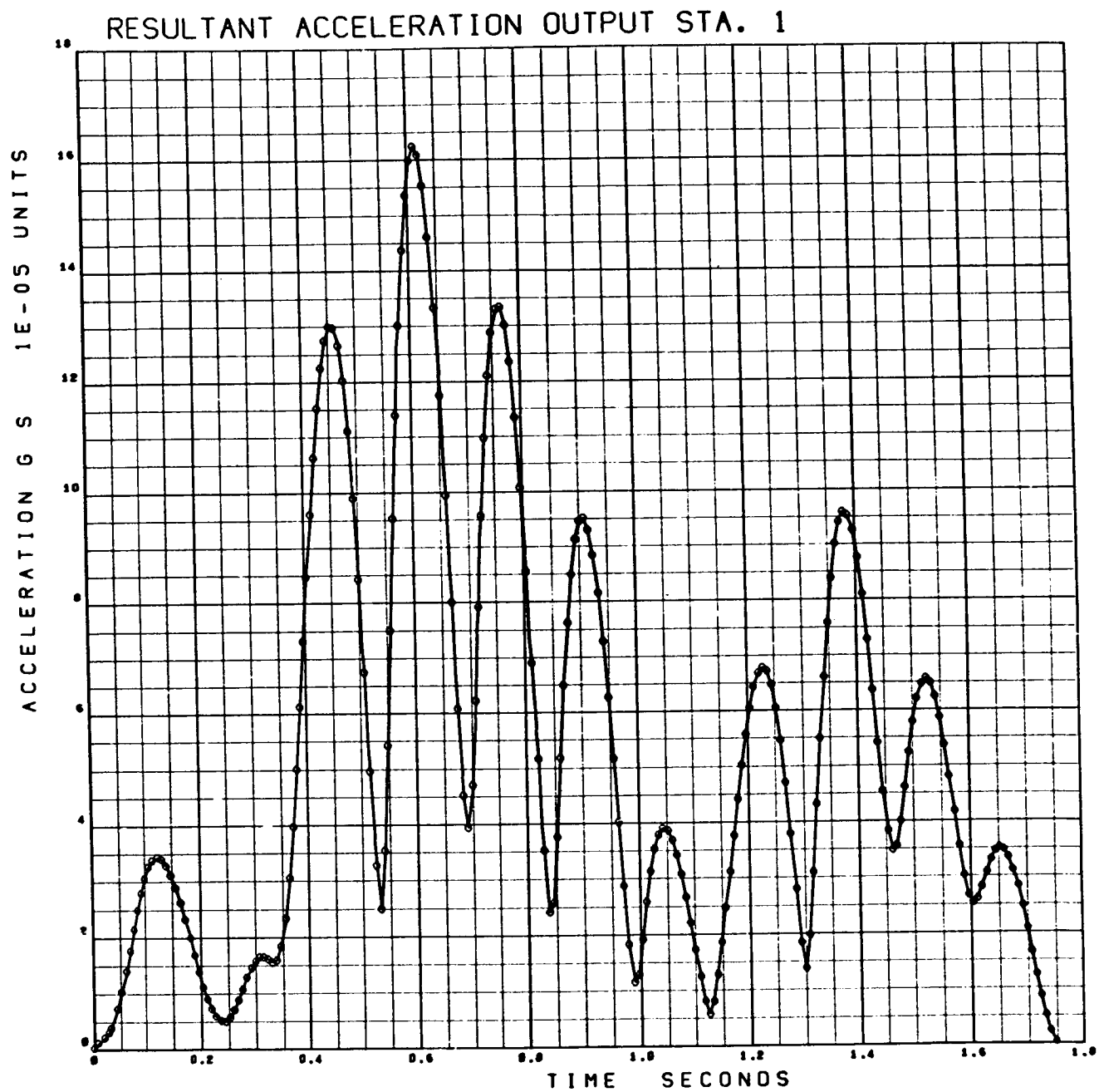


Figure 3-67. Cough — Resultant Acceleration Output Station 1

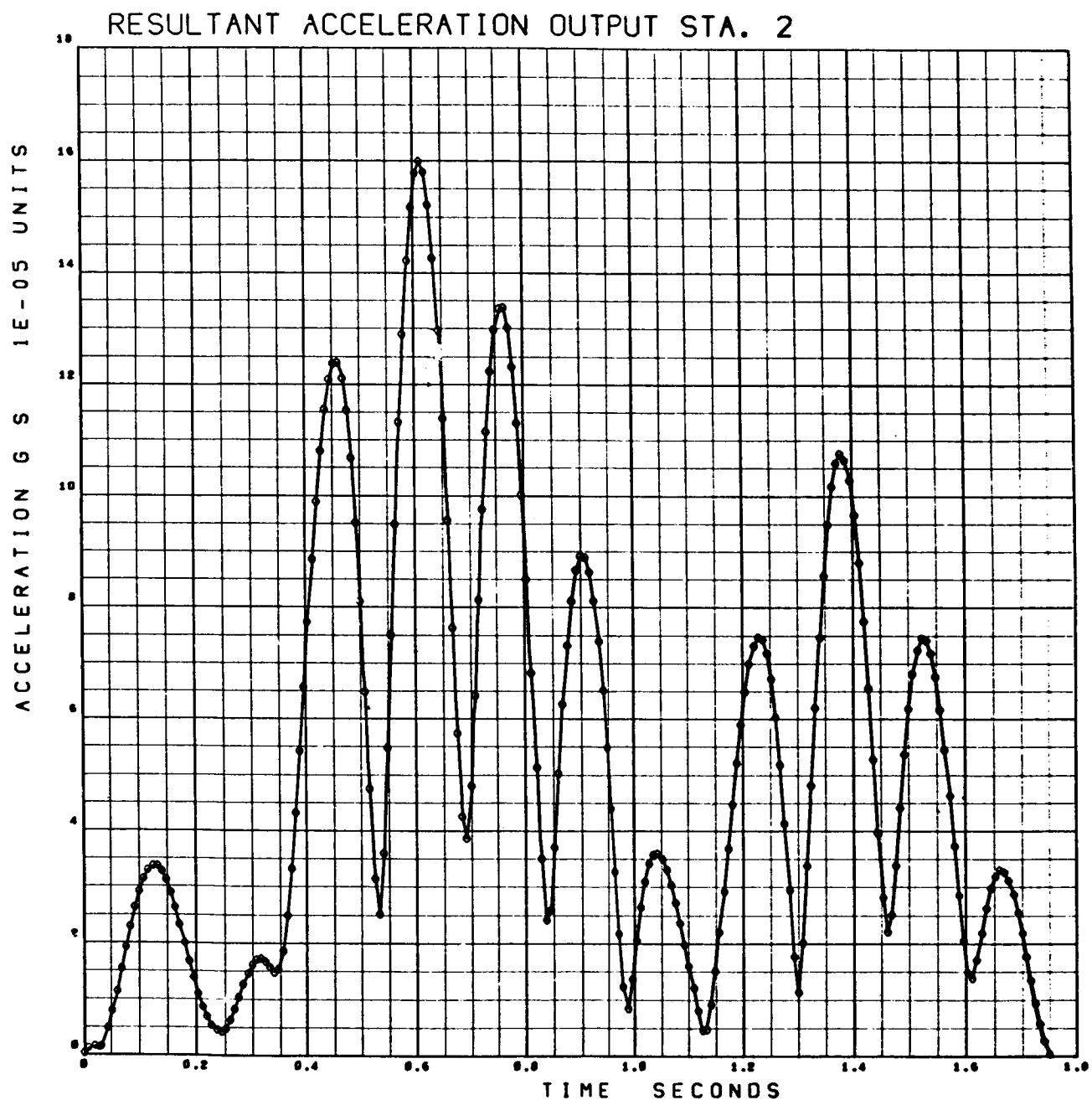


Figure 3-68. Cough – Resultant Acceleration Output Station 2

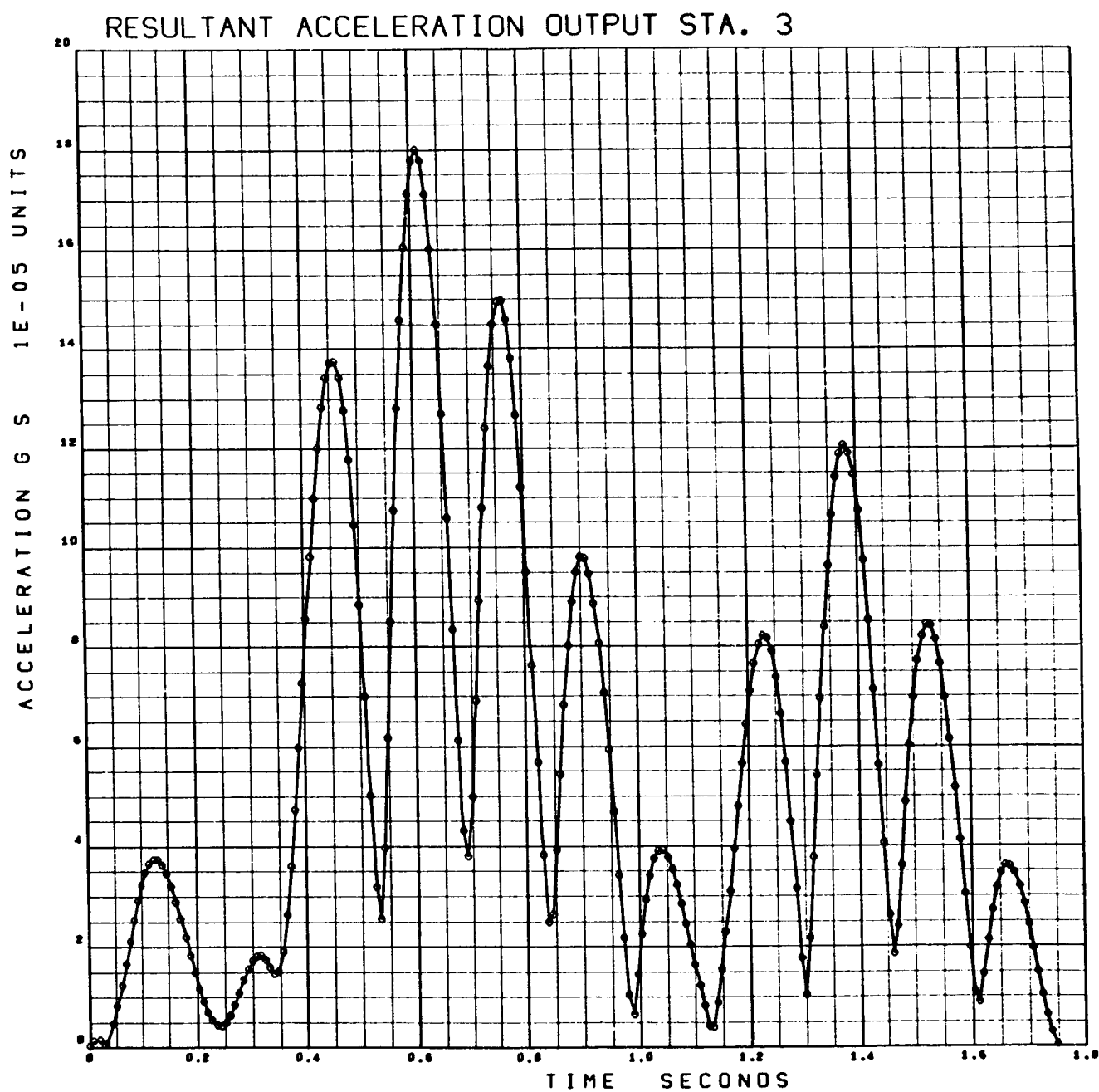


Figure 3-69. Cough — Resultant Acceleration Output Station 3

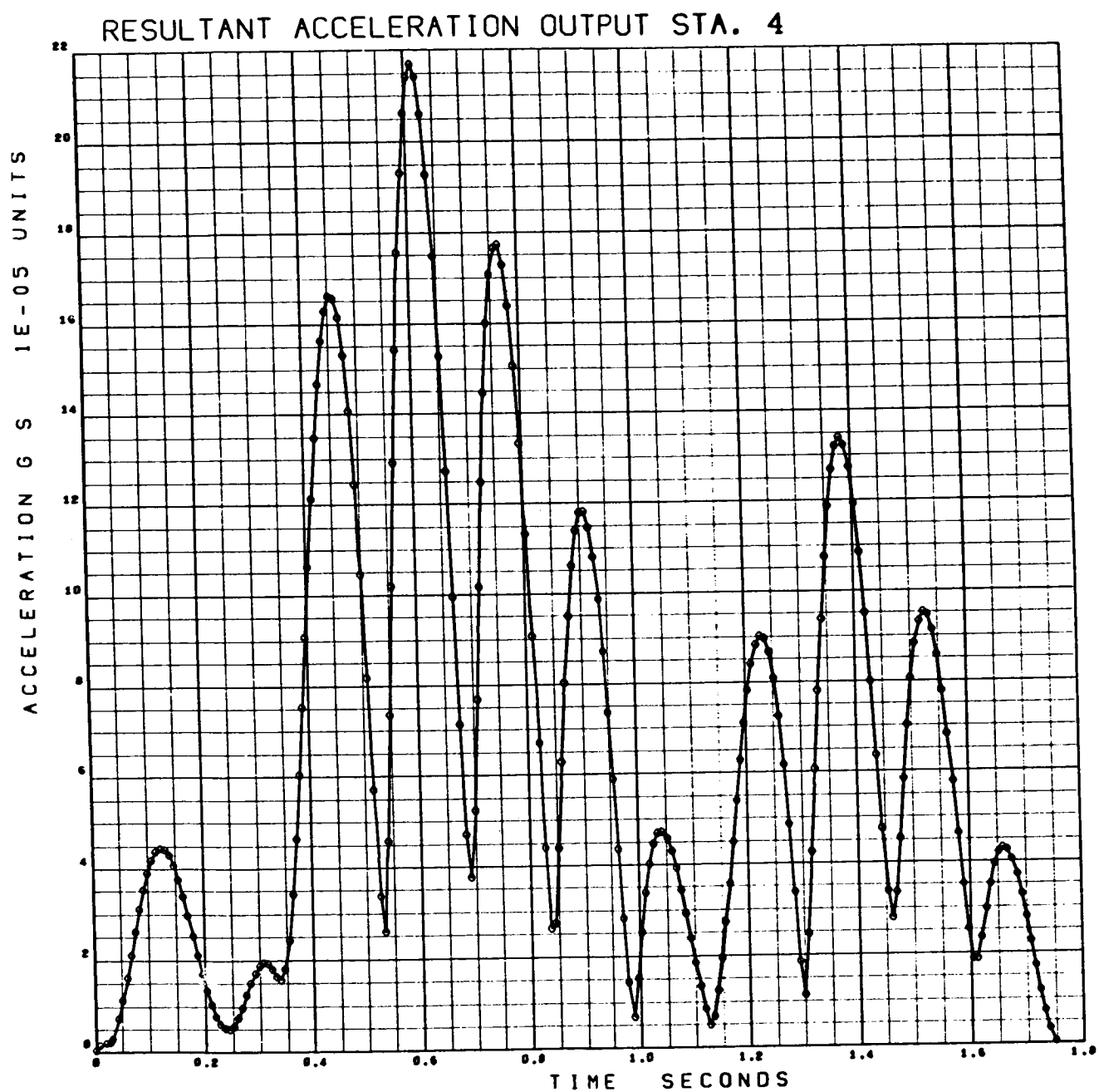


Figure 3-70. Cough — Resultant Acceleration Output Station 4

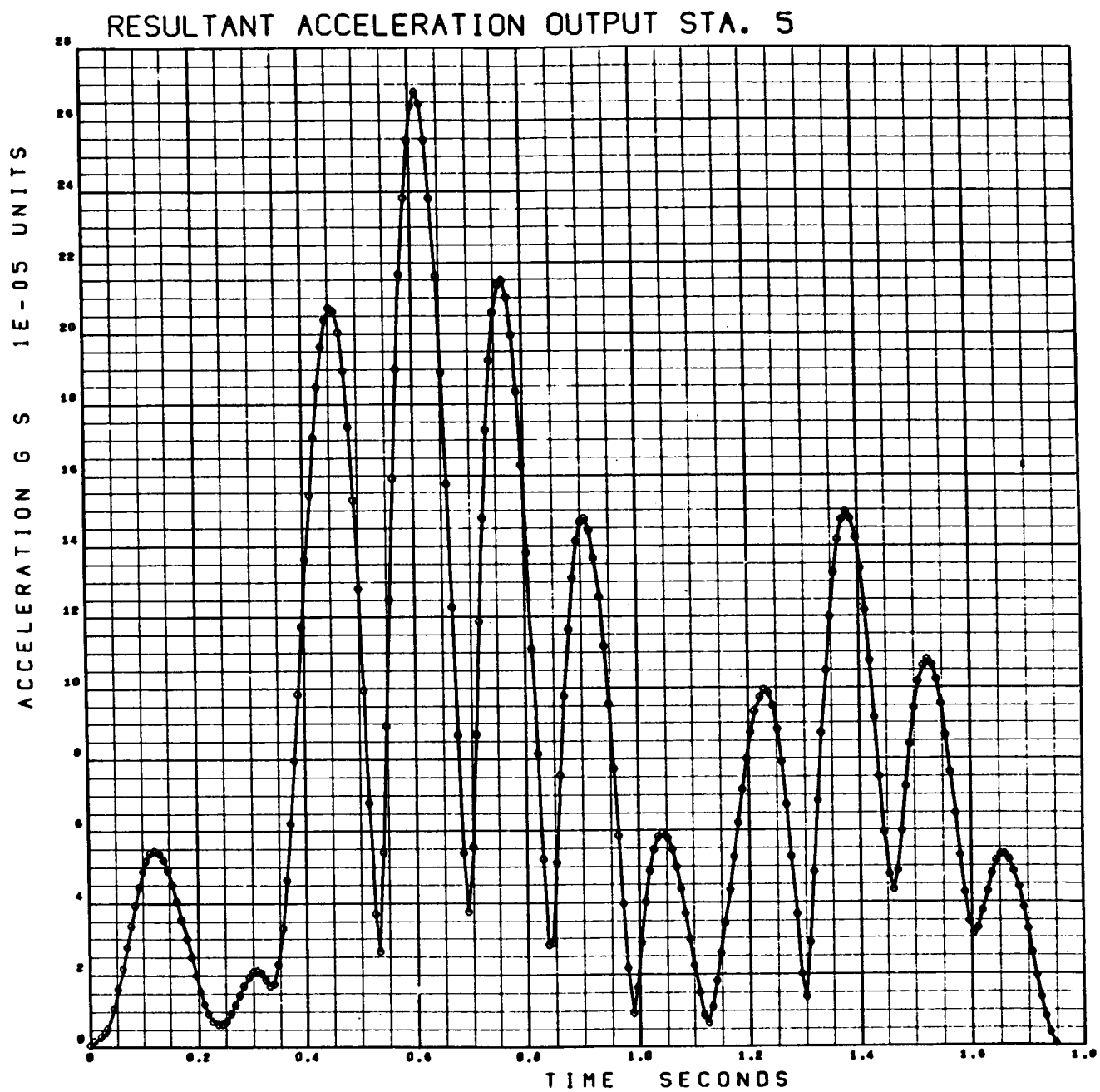


Figure 3-71. Cough – Resultant Acceleration Output Station 5

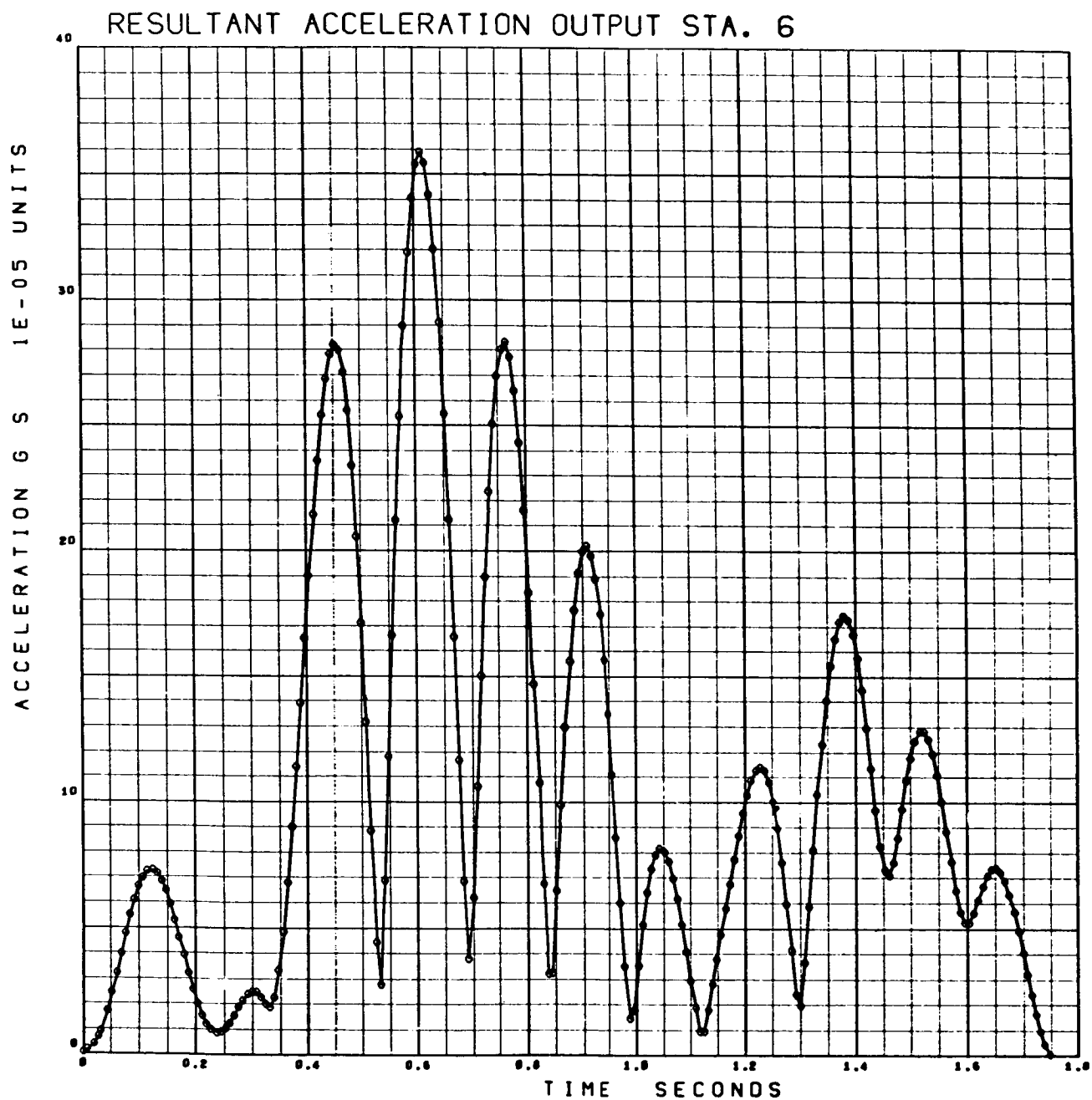


Figure 3-72. Cough – Resultant Acceleration Output Station 6

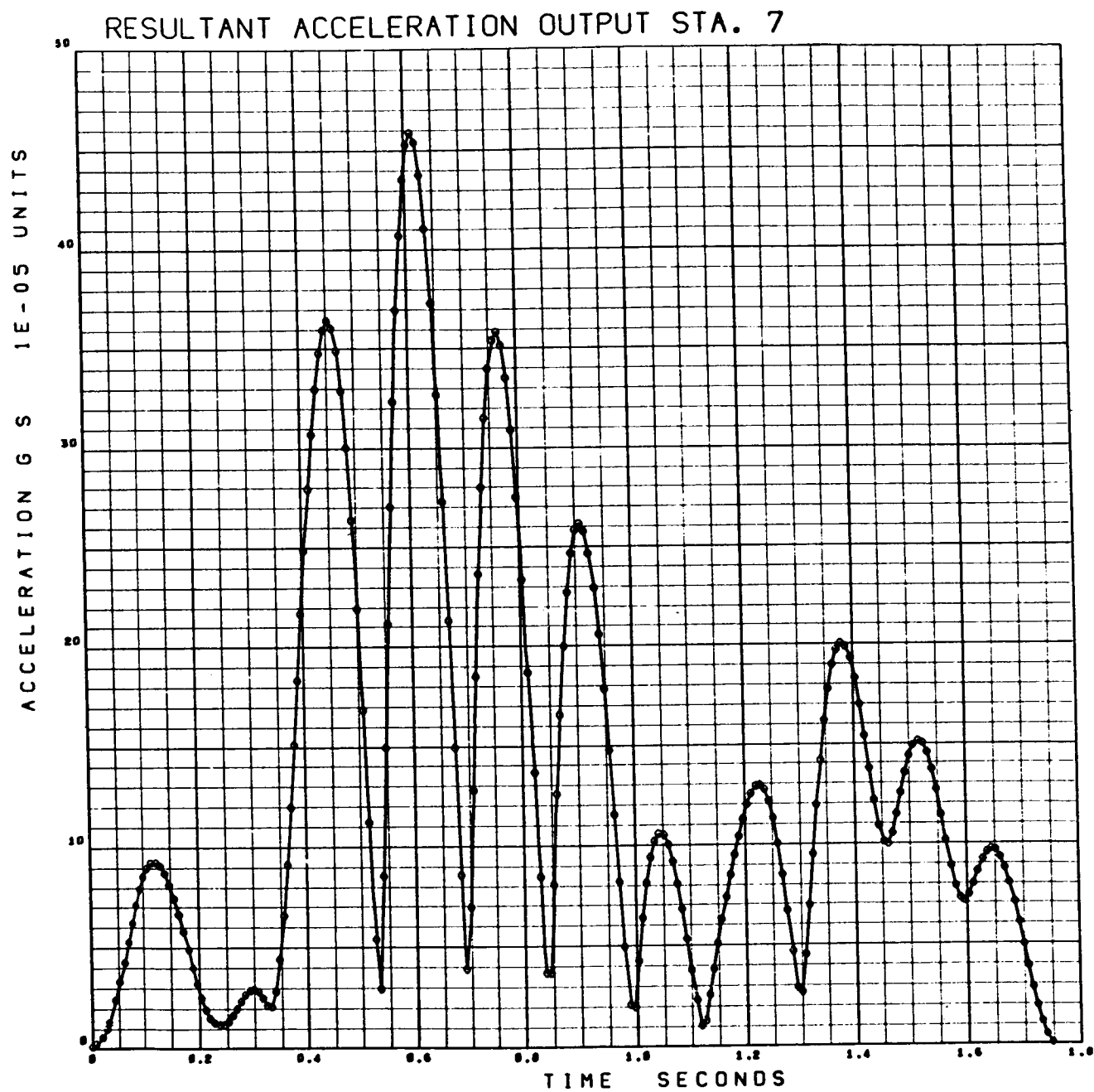


Figure 3-73. Cough — Resultant Acceleration Output Station 7

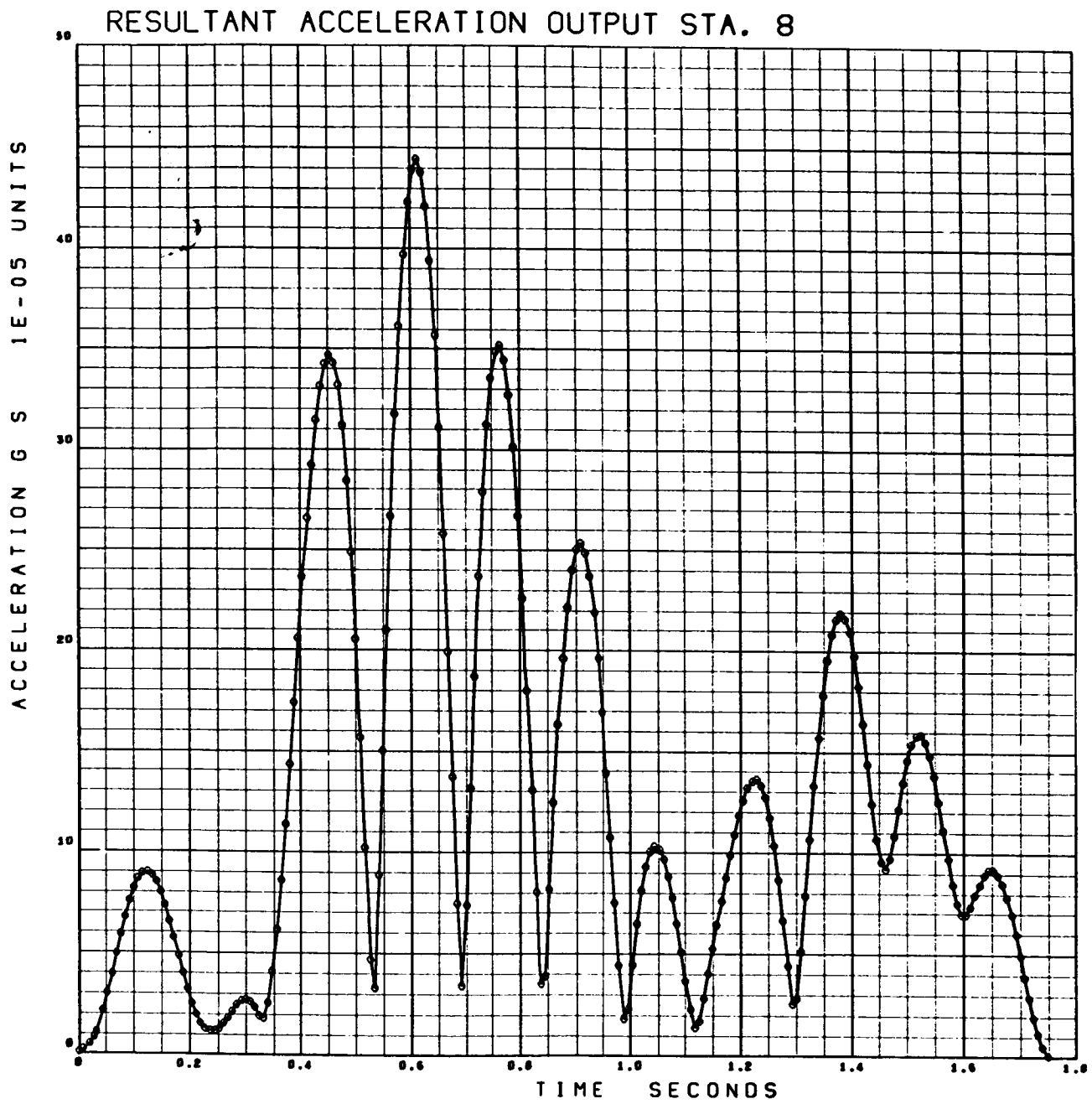


Figure 3-74. Cough – Resultant Acceleration Output Station 8

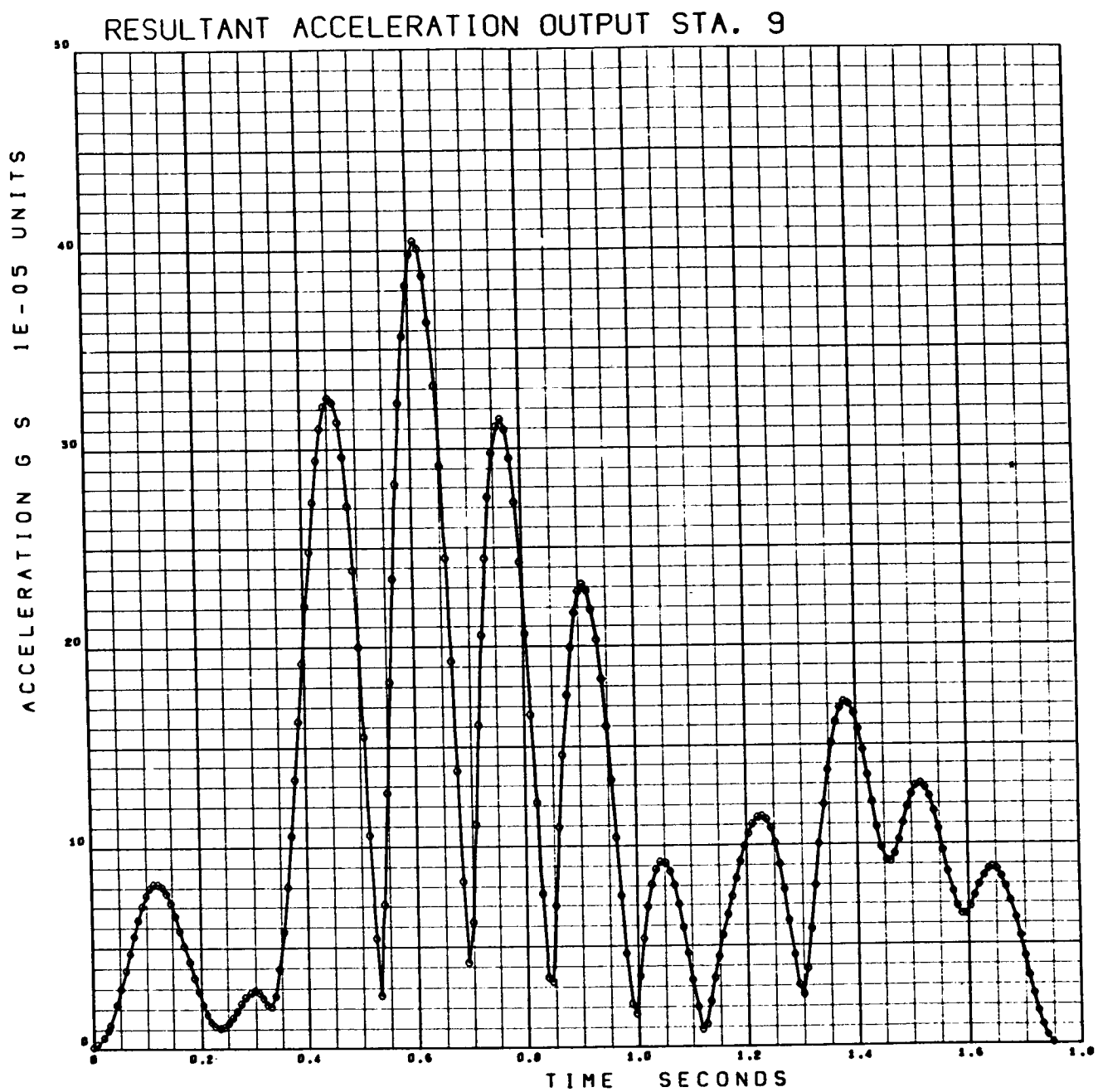


Figure 3-75. Cough — Resultant Acceleration Output Station 9

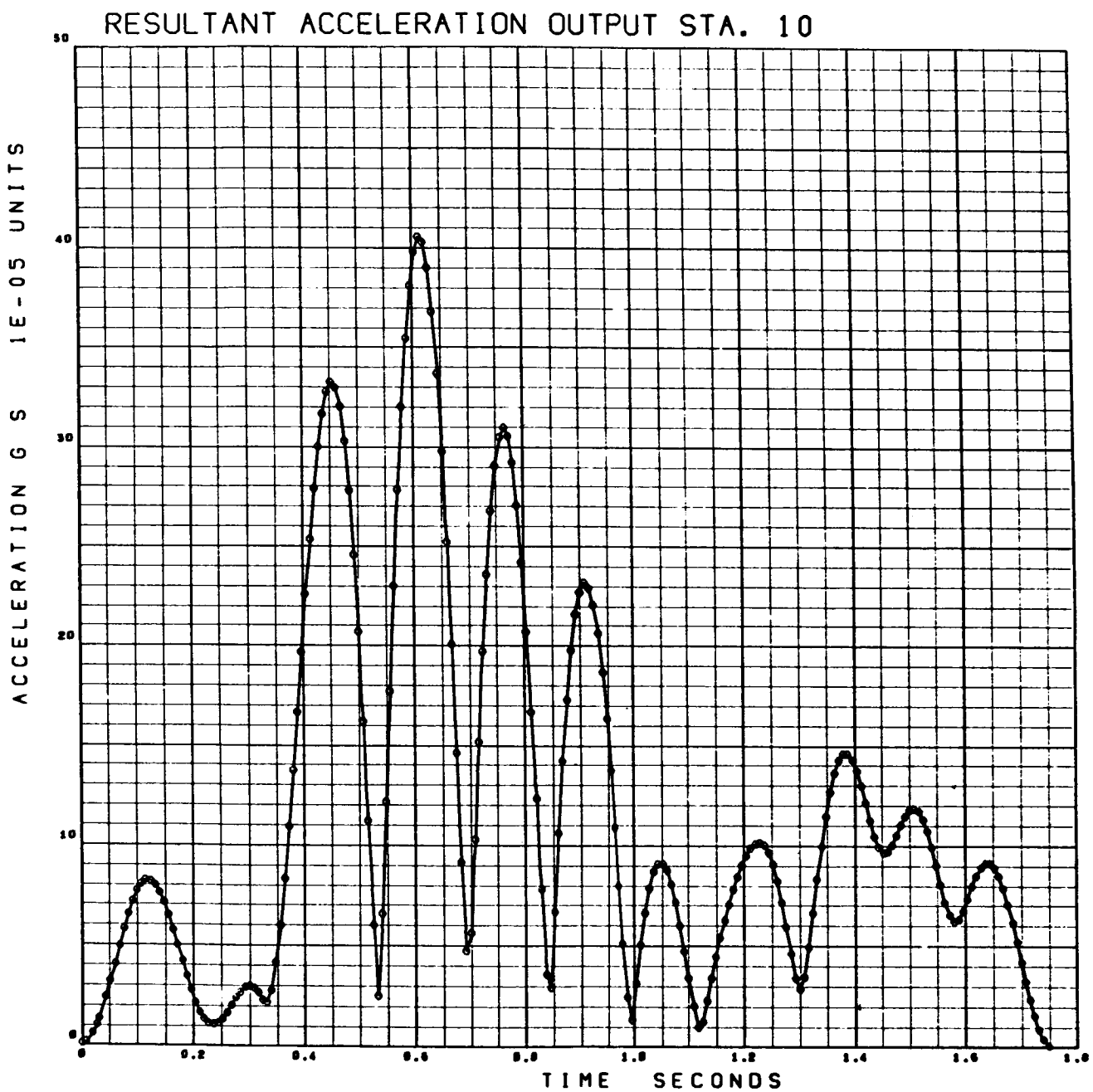


Figure 3-76. Cough – Resultant Acceleration Output Station 10

Input Data for Figures 3-77 to 3-92, Case 3-1-11 Cough

SERIAL 757415

11= .34128+06 12= .26389+07 13= .26210+07 MASS= .10254+03 DELT= .40000-02 TF=

TRANSFORMATION FROM CREW ST. TO CRAFT AXLS

-.10000000+01 .00000000 .00000000
 .00000000 .00000000 .10000000+01
 .00000000 .10000000+01 .00000000

CREW STATION ORIGIN .194100+04 .000000 .000000

INPUT POINT .000000 .000000 .000000

VEHICLE C.G. .194100+04 .000000 .000000

OUTPUT STATION COORDINATES

STA. NO. 1 .214000+04 .000000 .000000
 STA. NO. 2 .210000+04 .000000 .000000
 STA. NO. 3 .204100+04 .000000 .000000
 STA. NO. 4 .199100+04 .000000 .000000
 STA. NO. 5 .194100+04 .000000 .000000
 STA. NO. 6 .185100+04 .360000+02 .000000
 STA. NO. 7 .182500+04 .000000 .000000
 STA. NO. 8 .176000+04 .000000 .000000
 STA. NO. 9 .176000+04 -.800000+01 .000000
 STA. NO. 10 .176000+04 .800000+02 .000000

FORCE COSINE COEF

.76516327-01 -.14716666+01 -.14146462+01 .11679597+01 .13365398+01 -.29208211+01 .33061182+01
 -.34878414-00 -.30294503-00 -.15123076-00 .41767413-00 -.13050494+01 -.24912848+01 .41816300+01
 .52426851-00 -.26226359-00 -.40526507-01 .10179601+01 -.12618987+01 .94301330-01 .40000053-00

FORCE SINE COEF

.15946499-00 .10000934+00 -.06027109-00 -.18850627+01 .42810690+01 -.16121931+01 -.40199945-01
 .21348027-00 .54402650-00 -.15594341+01 -.34899589+01 .42690296+01 .30075782-00 .55906940-02
 -.70906400-01 .31886500-00 -.27874383-00 -.14332246-00 .41600960-00 -.27766767-00 .23051854-01

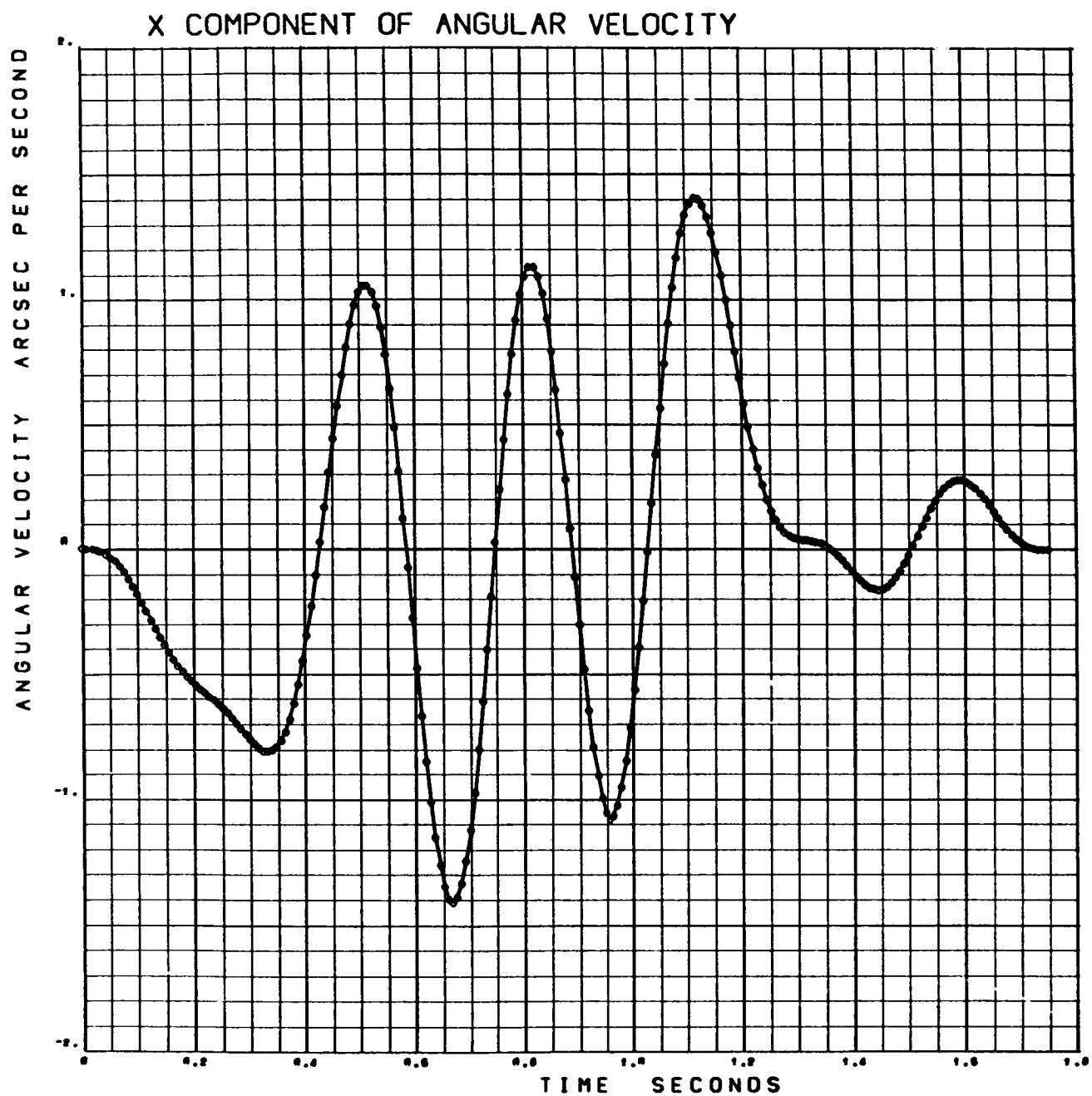


Figure 3-77. Cough (X Component of Angular Velocity)

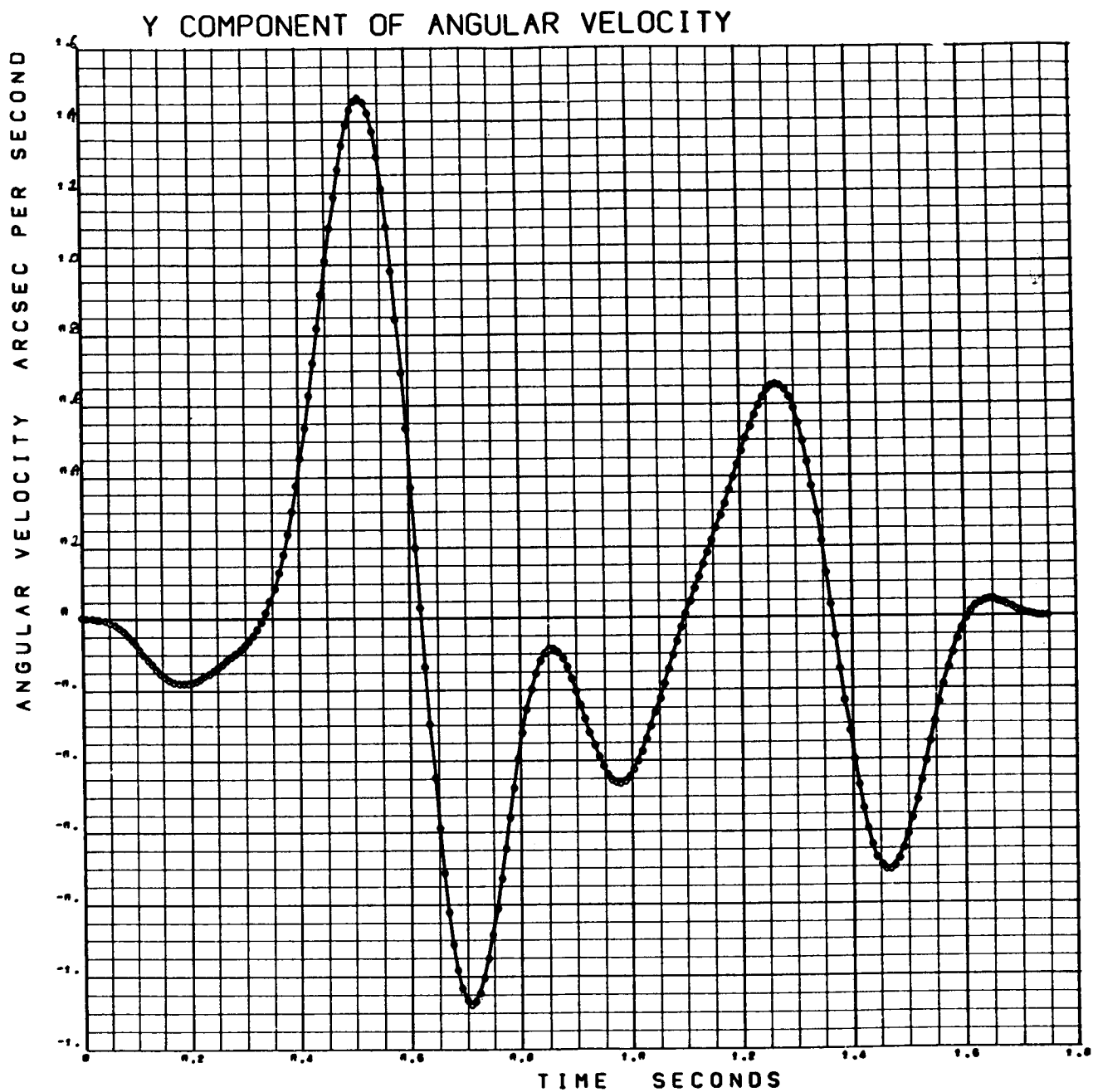


Figure 3-78. Cough (Y Component of Angular Velocity)

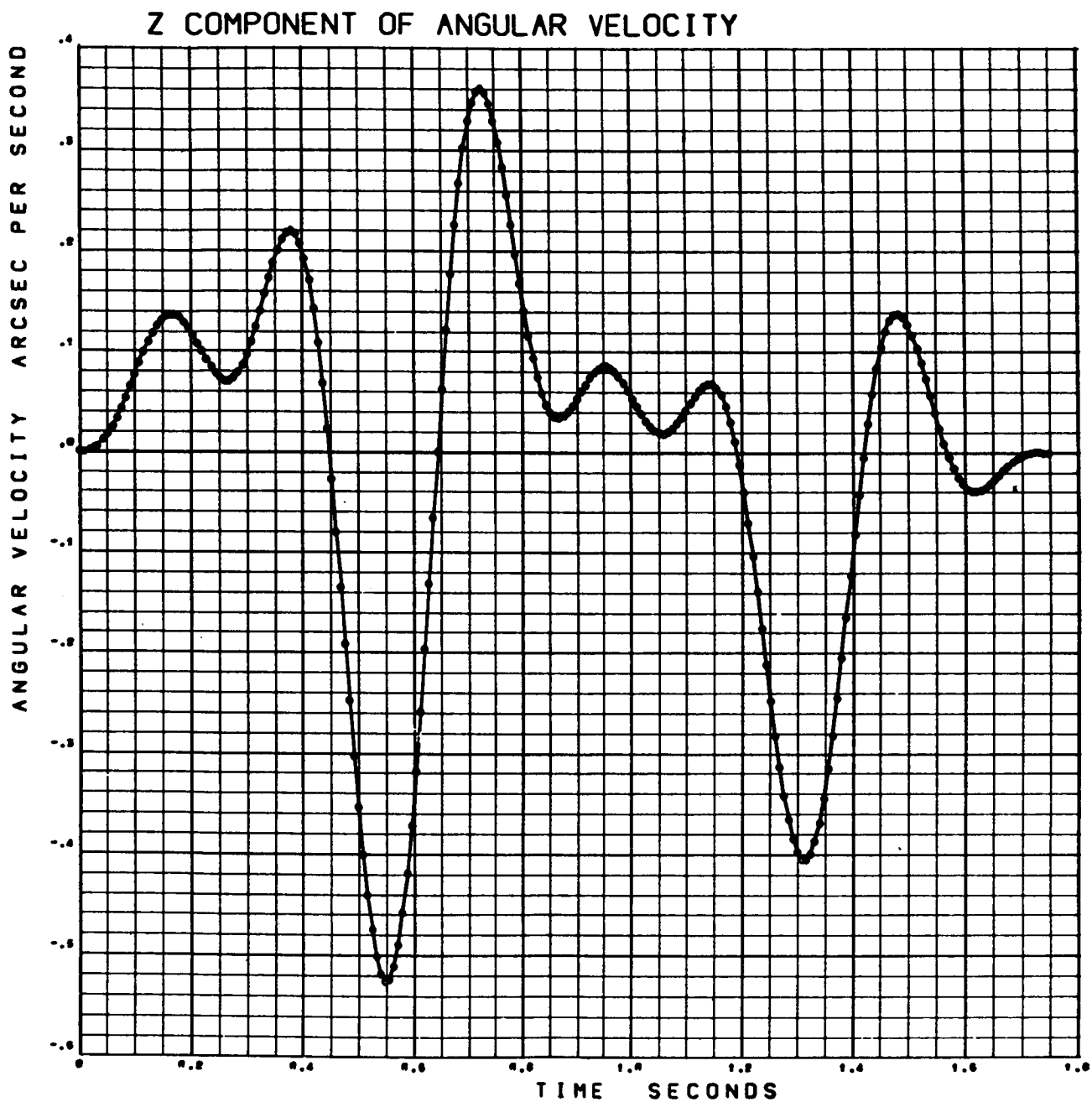


Figure 3-79. Cough (Z Component of Angular Velocity)

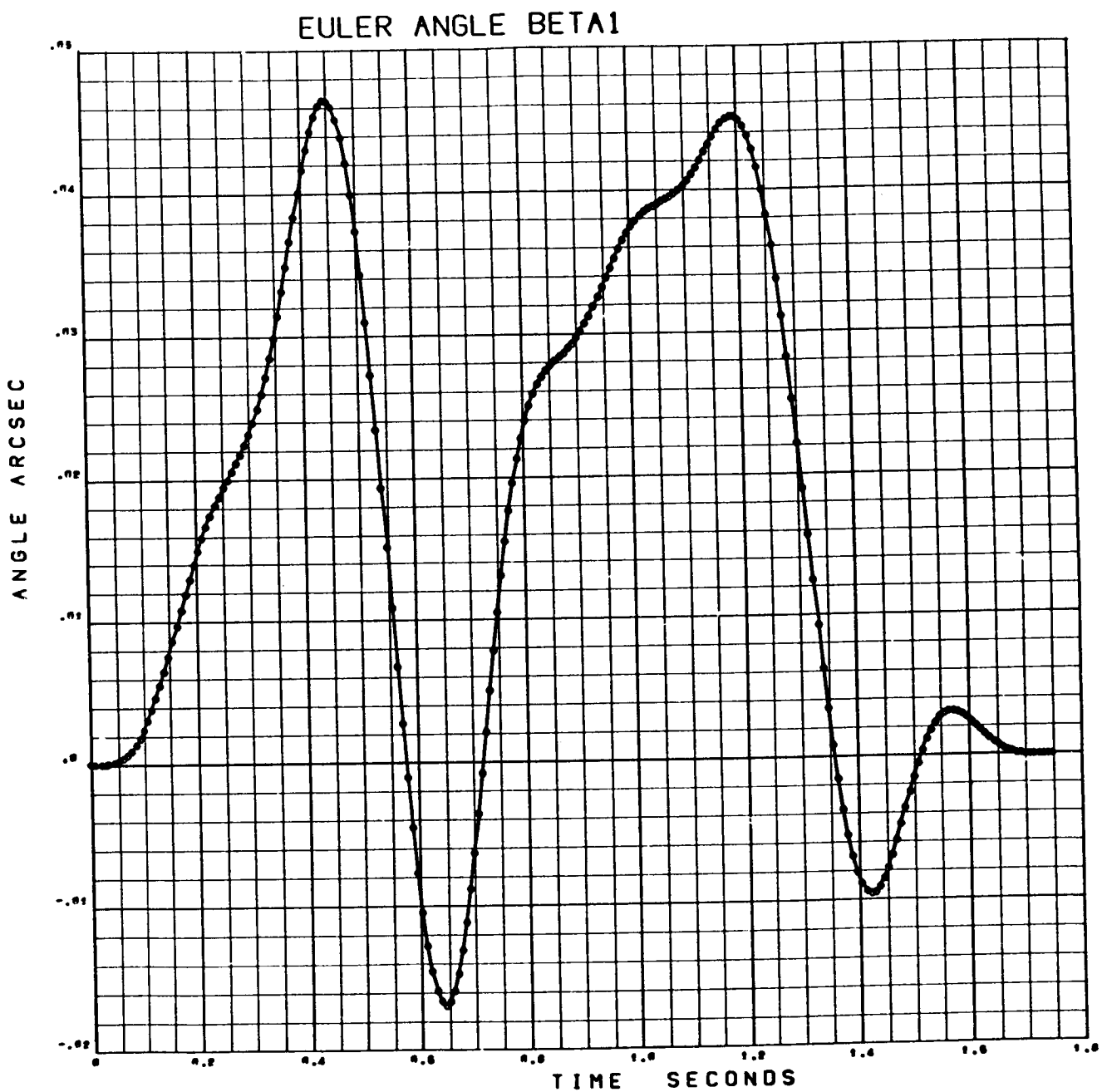


Figure 3-80. Cough (Euler Angle Beta 1)

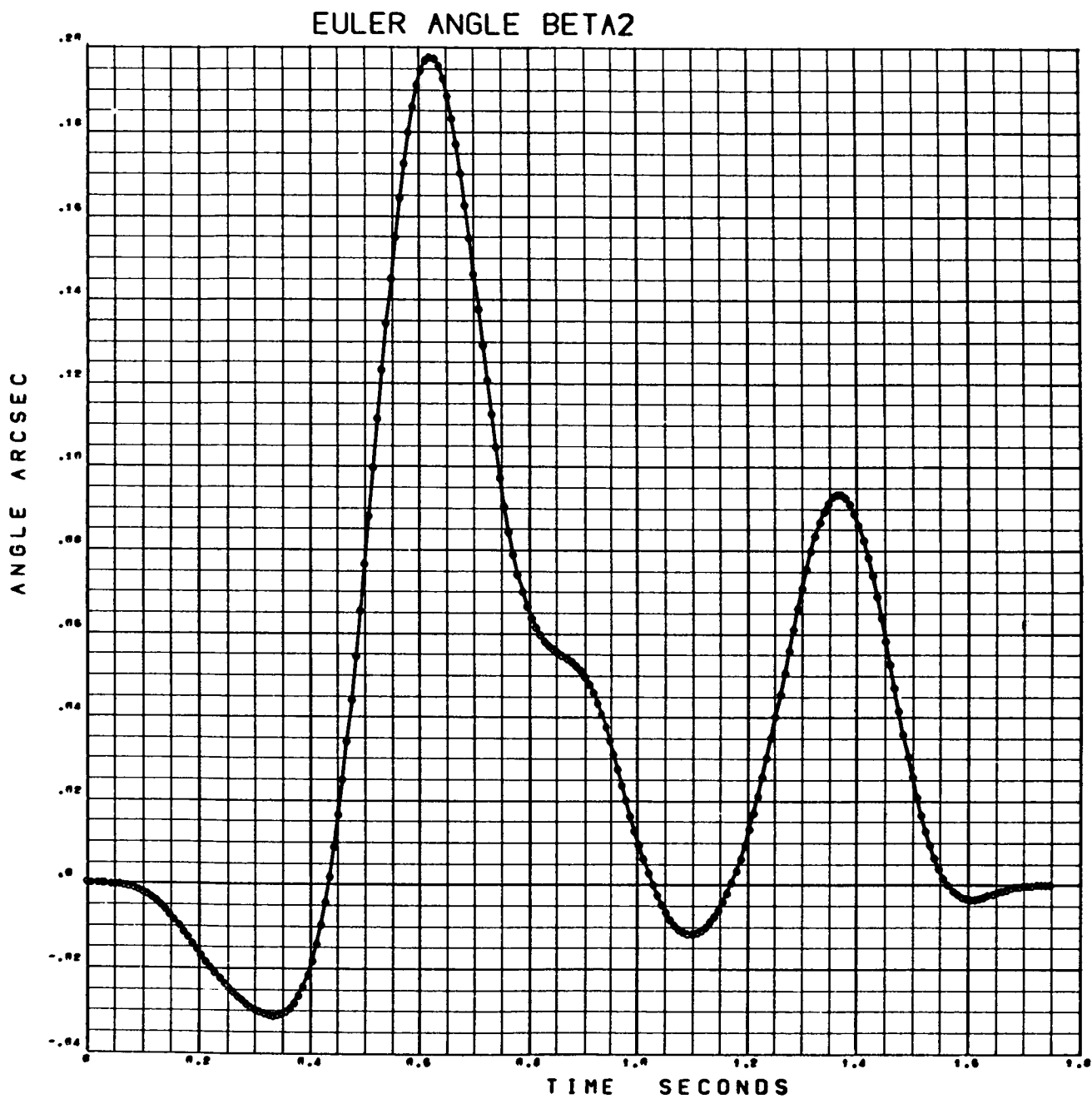


Figure 3-81. Cough (Euler Angle Beta 2)

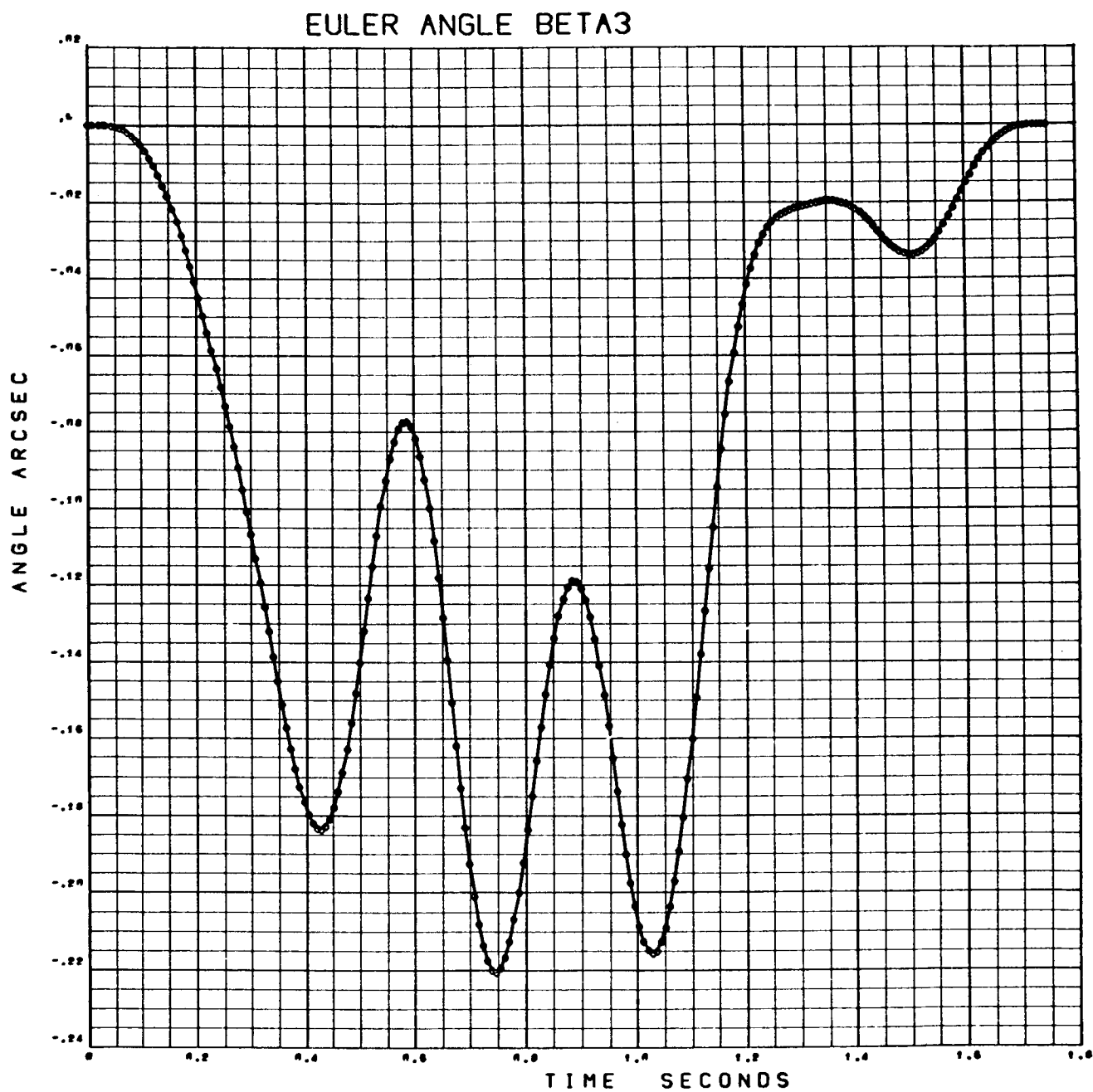


Figure 3-82. Cough (Euler Angle Beta 3)

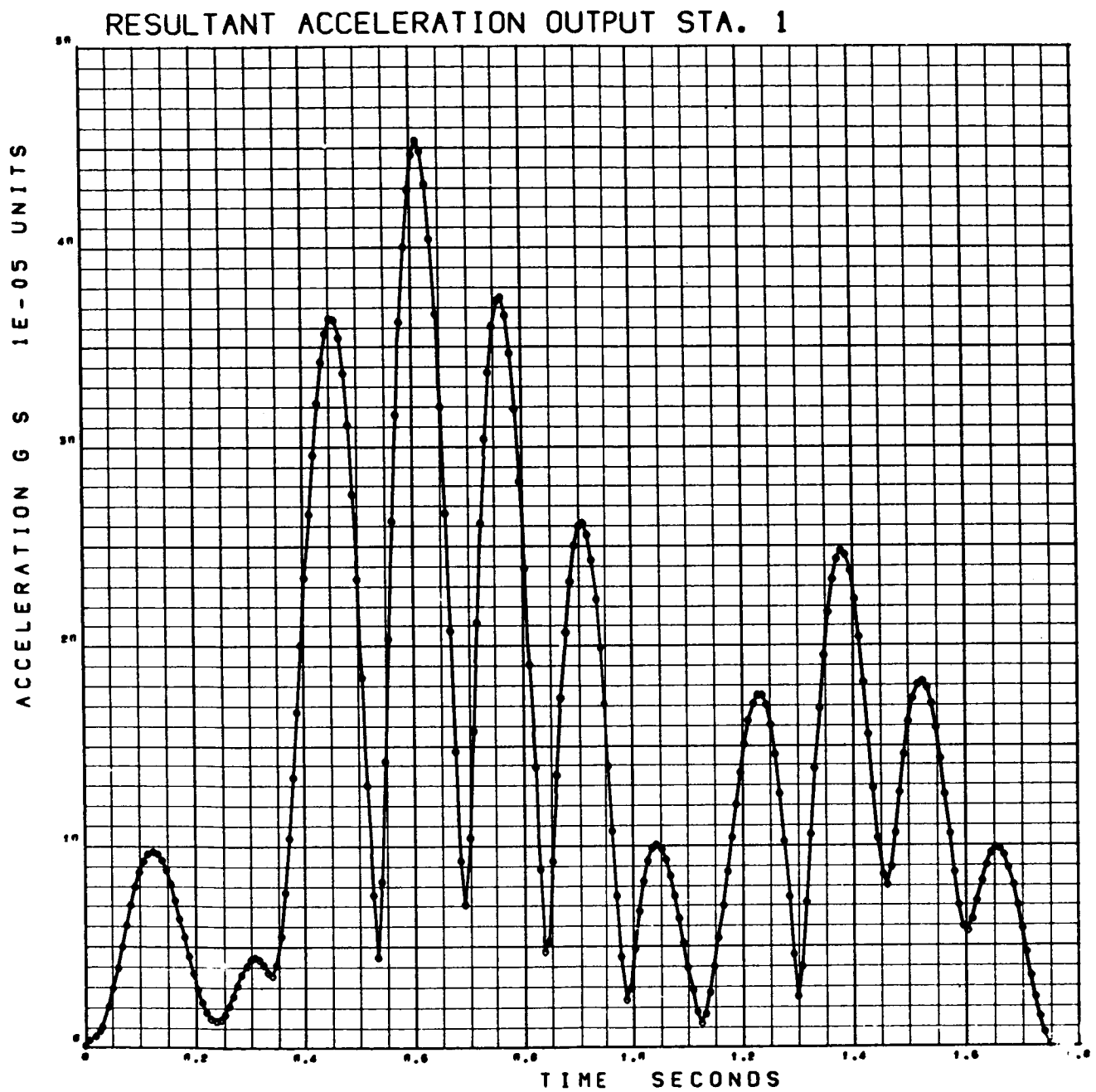


Figure 3-83. Cough – Resultant Acceleration Output Station 1

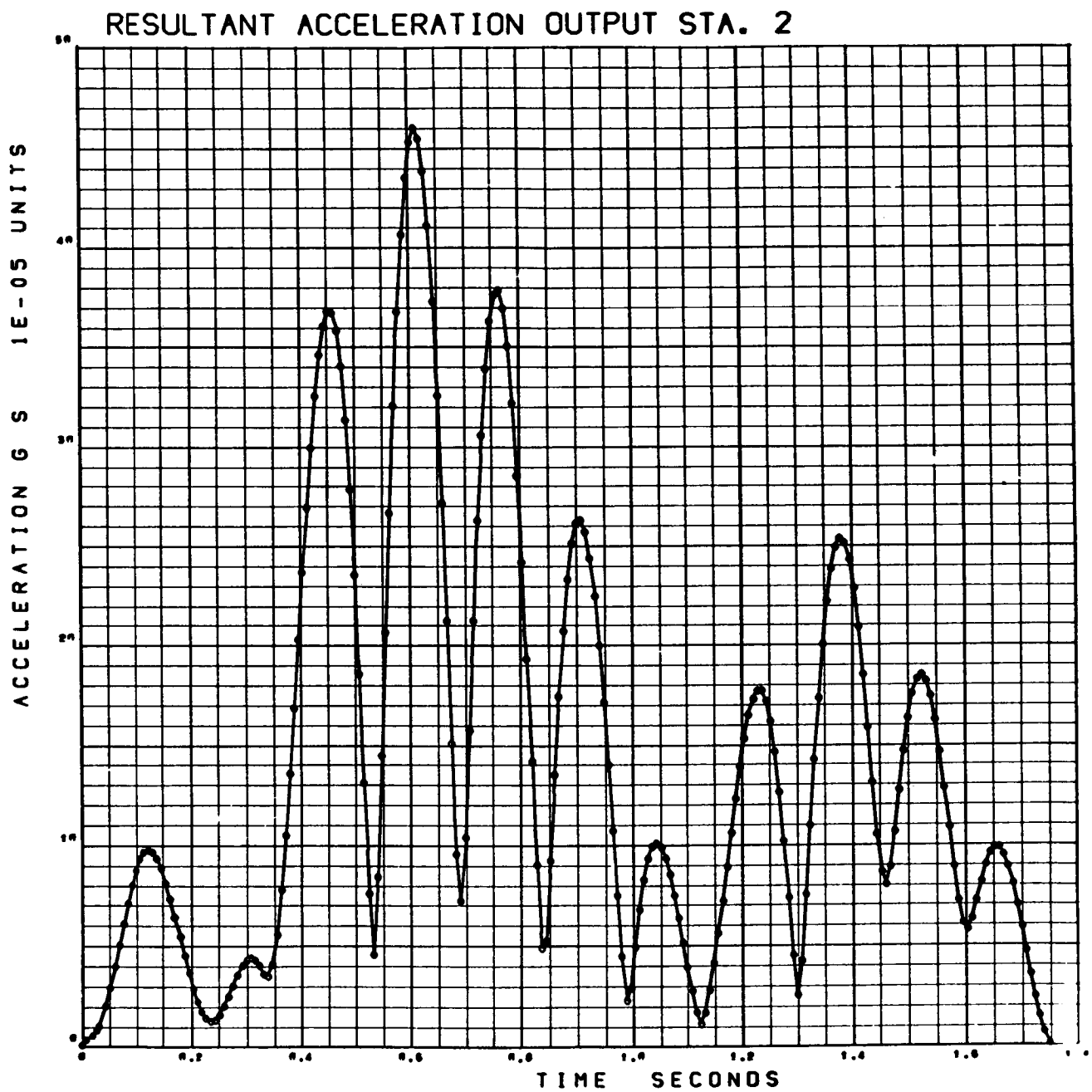


Figure 3-84. Cough — Resultant Acceleration Output Station 2

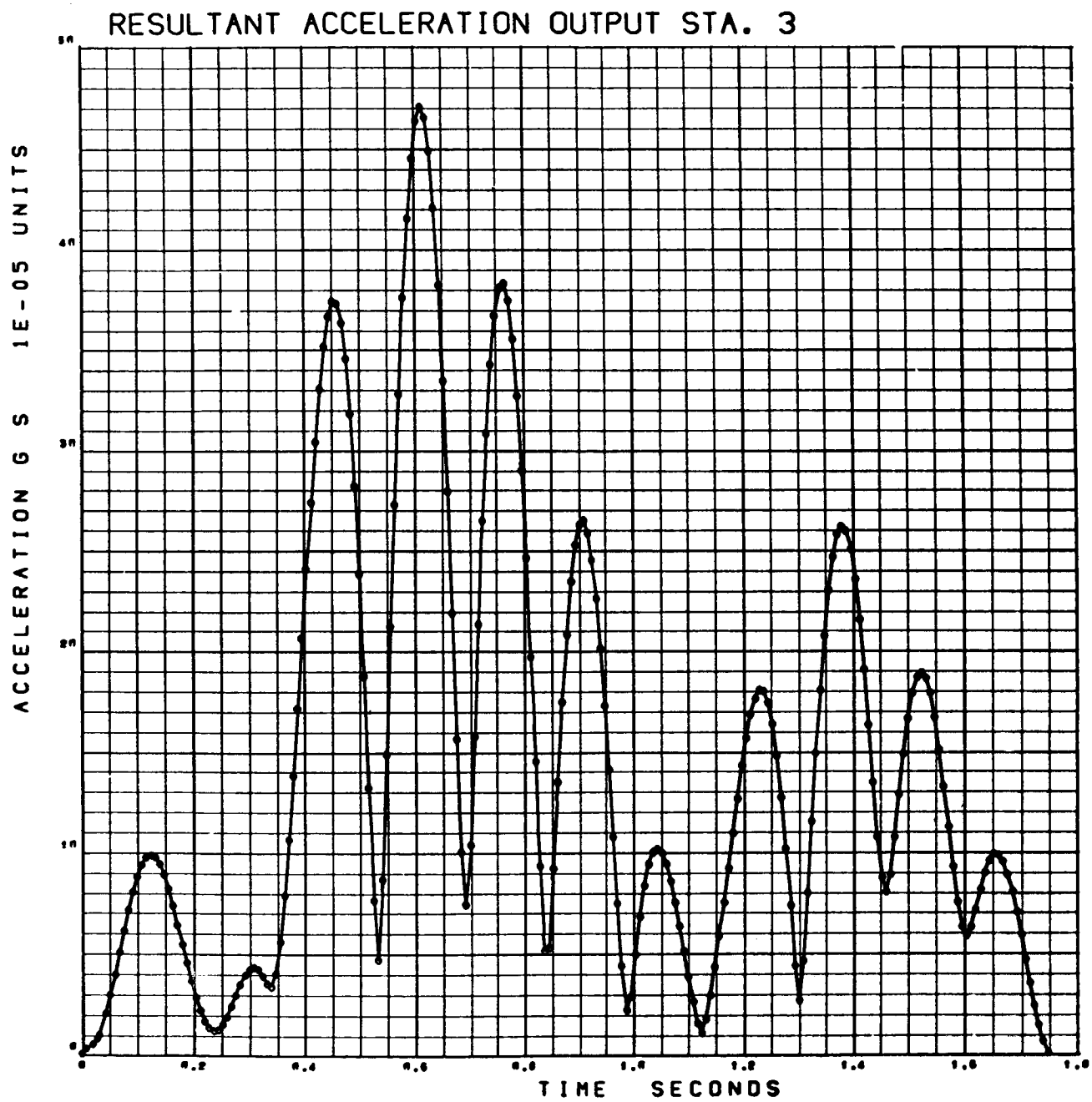


Figure 3-85. Cough — Resultant Acceleration Output Station 3

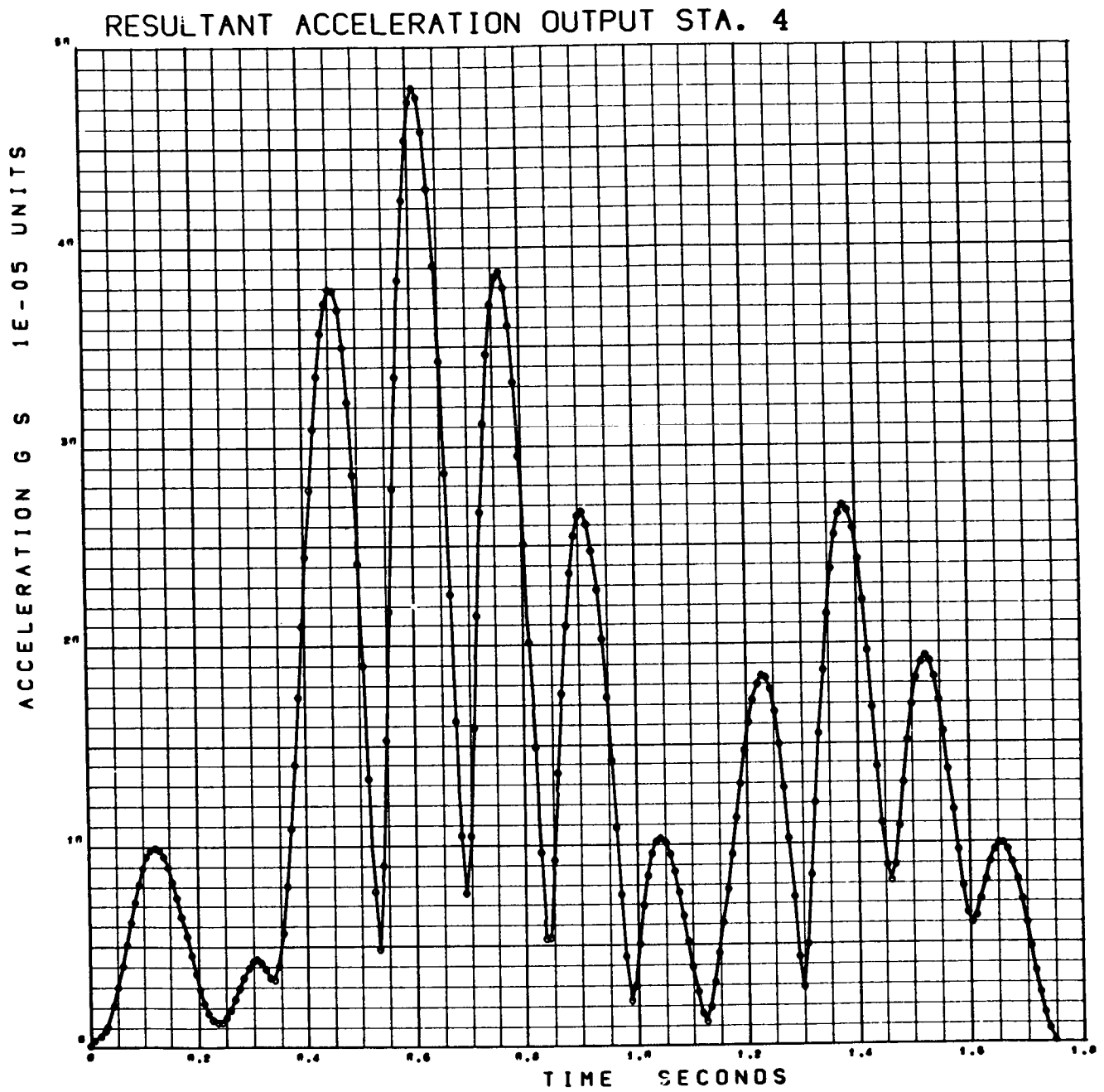


Figure 3-86. Cough – Resultant Acceleration Output Station 4

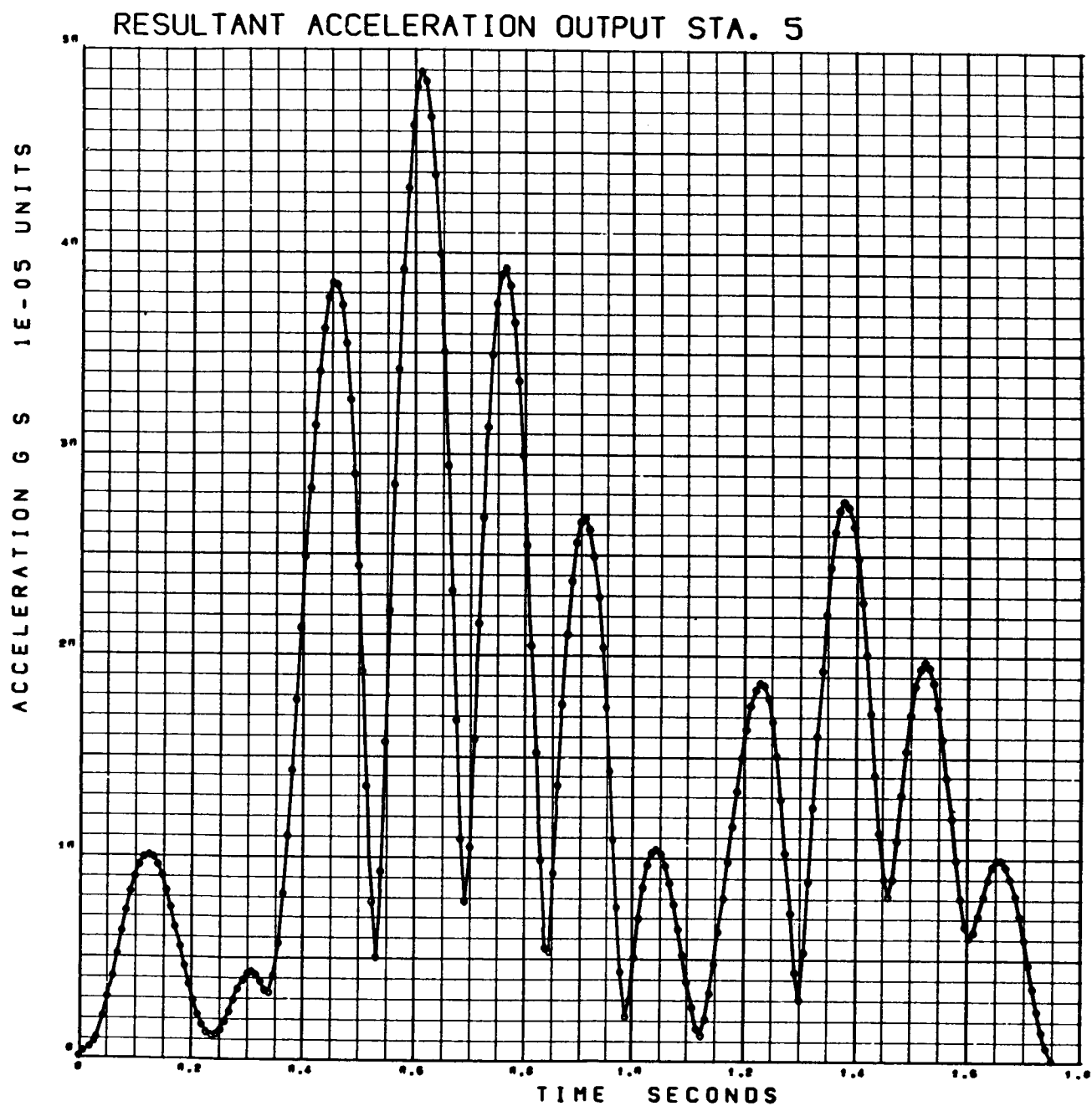


Figure 3-87. Cough – Resultant Acceleration Output Station 5

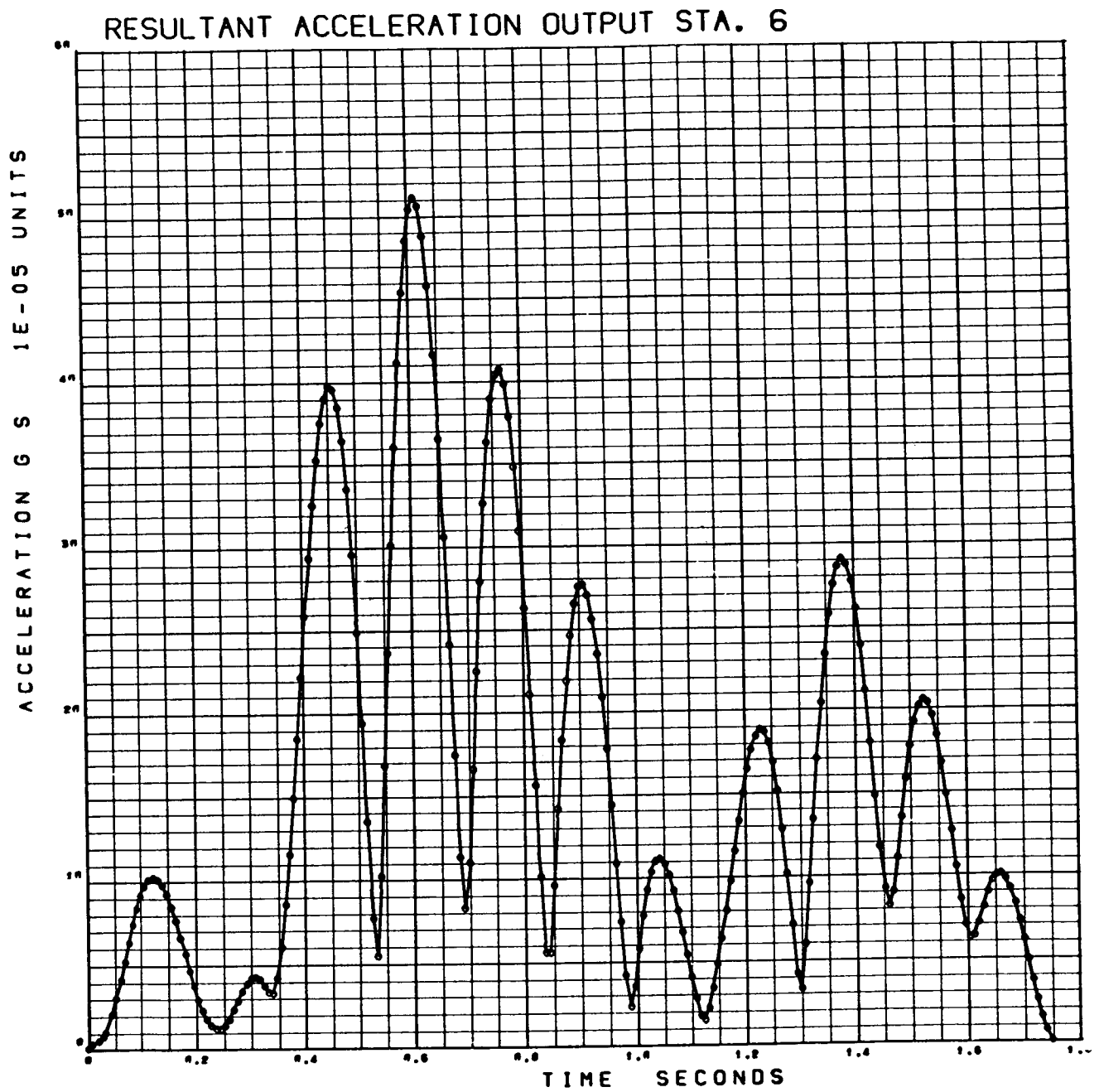


Figure 3-88. Cough – Resultant Acceleration Output Station 6

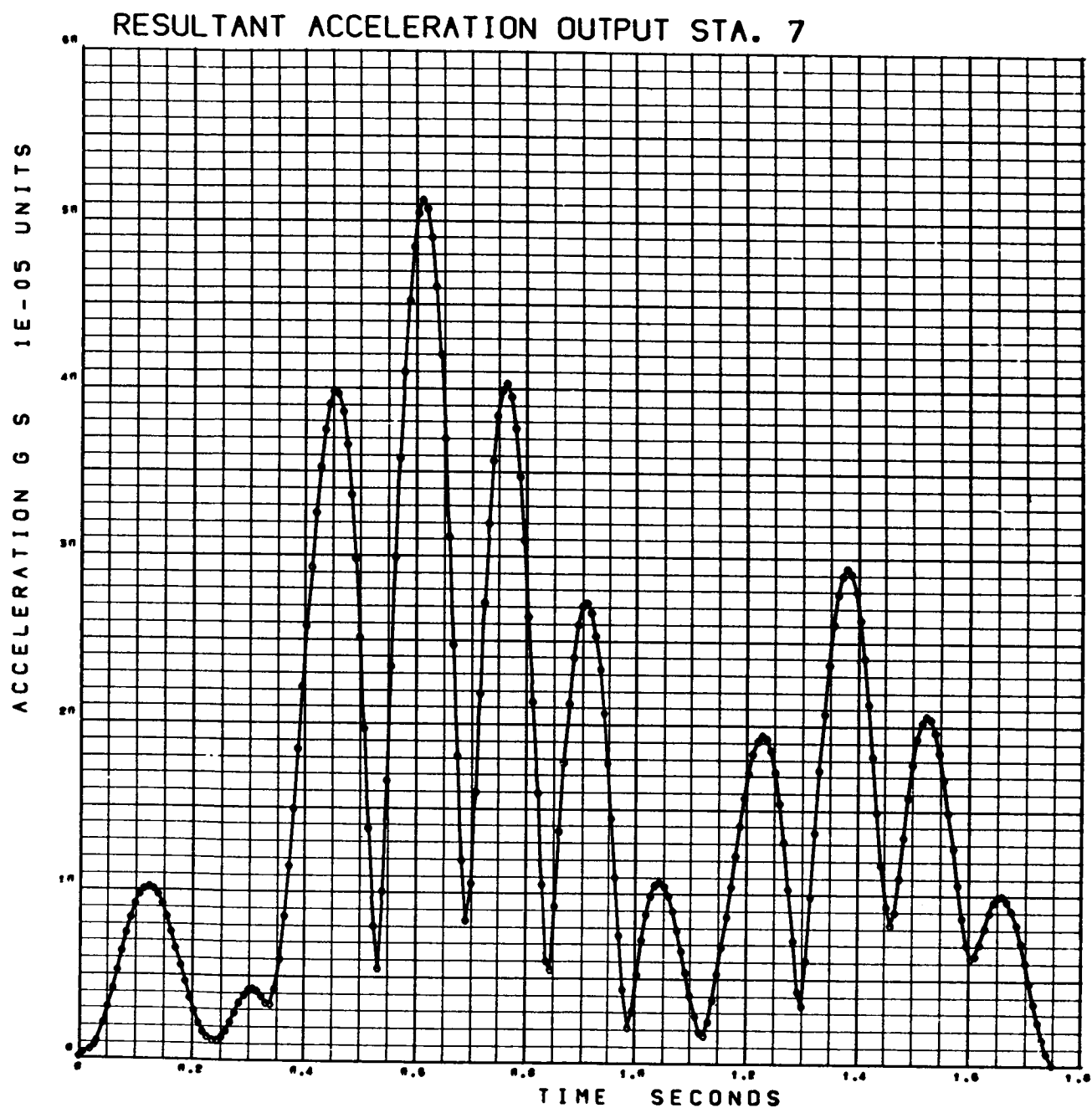


Figure 3-89. Cough – Resultant Acceleration Output Station 7

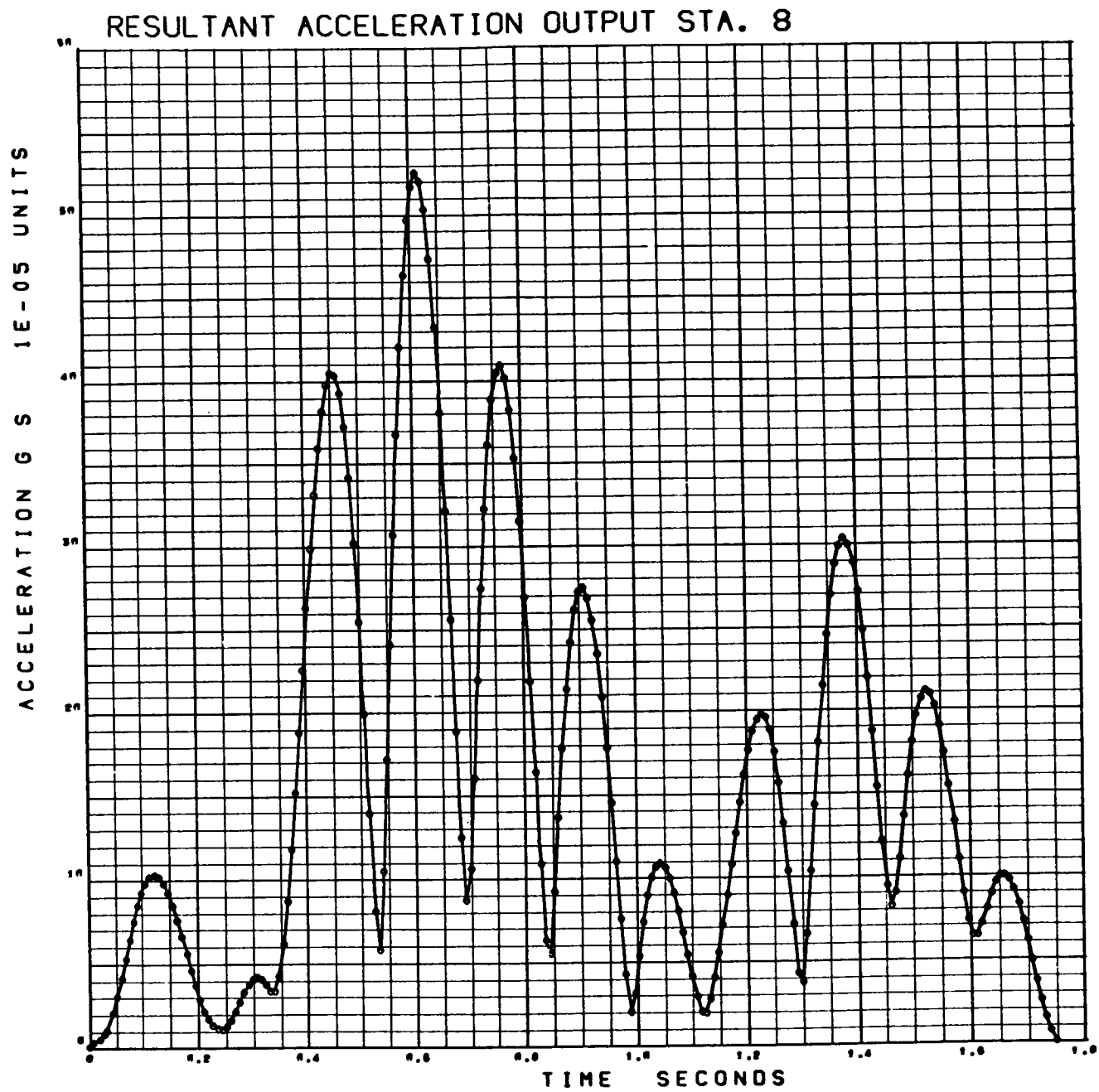


Figure 3-90. Cough — Resultant Acceleration Output Station 8

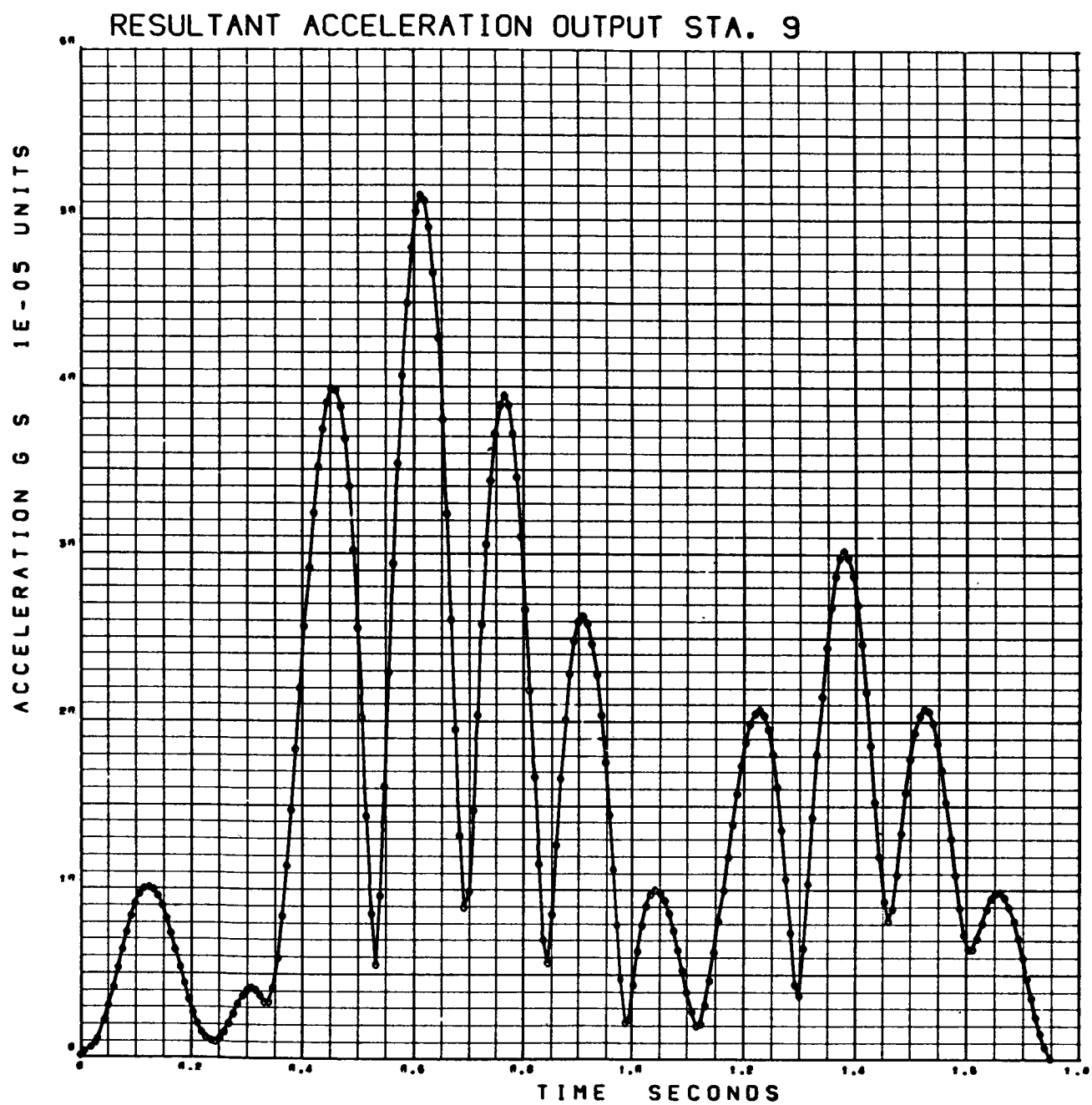


Figure 3-91. Cough – Resultant Acceleration Output Station 9

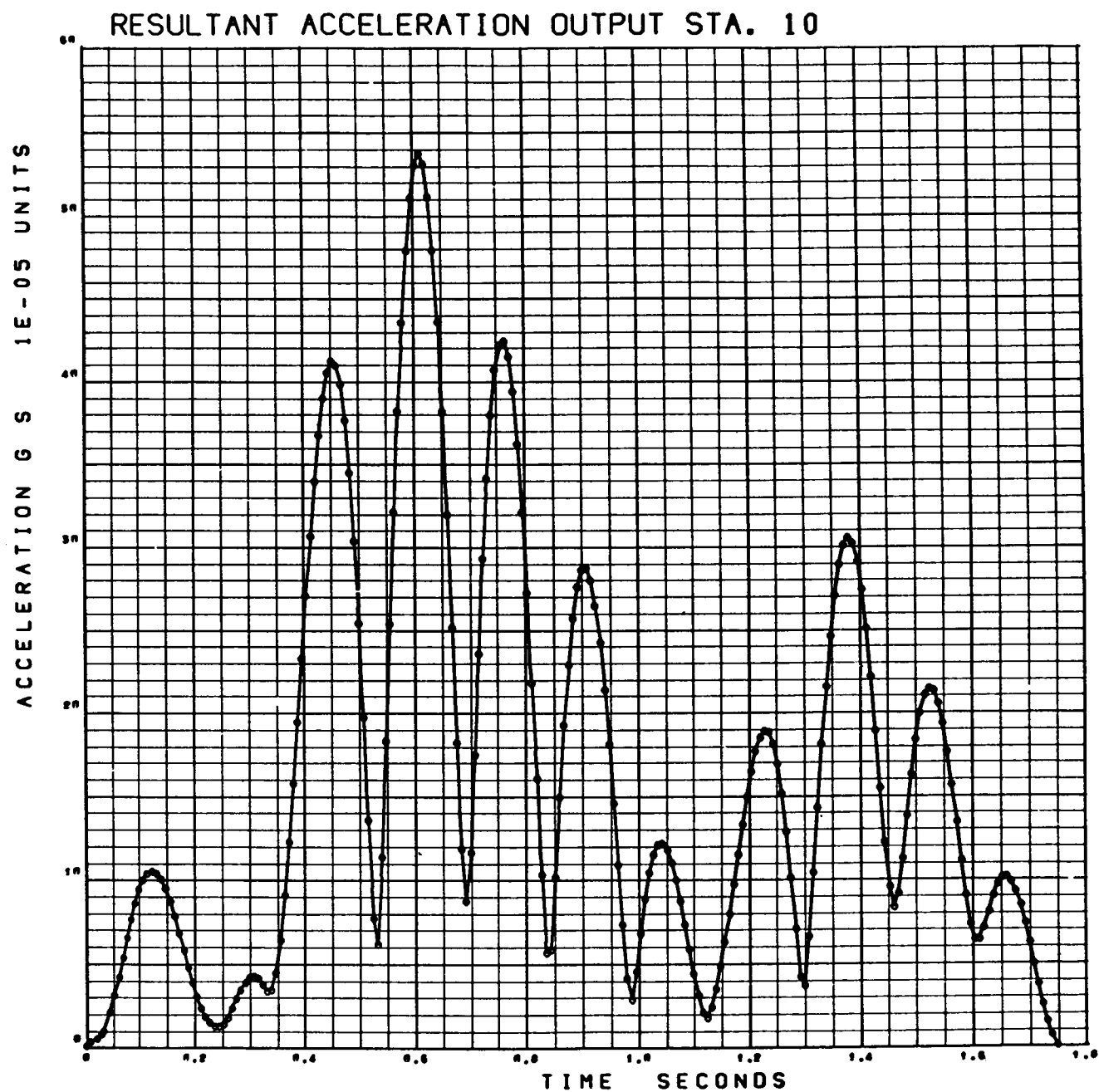


Figure 3-92. Cough — Resultant Acceleration Output Station 10

For Configuration 2, the peak accelerations ranged from about 3×10^{-5} g's to 9×10^{-5} g's for the console operation motions, with heartbeat producing 2.7×10^{-5} g's and a cough 46×10^{-5} g's. A peak angular excursion of 1.44 arc sec was observed.

For Configuration 3, the accelerations ranged from about 5 to 22×10^{-5} g's for the console operation motion. Heartbeat produced 2.8×10^{-5} g's and a cough 54×10^{-5} g's. The maximum peak angular excursion for Configuration 3 was about 9 arc sec. About 94% of the zero-g experiments have an acceleration tolerance of 10^{-4} g's specified, 80% a tolerance of 5×10^{-5} g's, and about 60% a tolerance of 10^{-5} g's. Thus about 60% of the experiment tolerances would be exceeded by heartbeat-induced vehicle accelerations, and about 80% by various console-operation induced accelerations.

It should be noted that in the larger laboratories the peak acceleration resulting from a cough is about four times the next largest peak acceleration (11.94×10^{-5} g's for 2-3-2 T. Min.). If the probability of a cough occurring is low enough, it might be possible to accept an occasional disturbance from this source.

The angular excursions computed also exceed pointing stability requirements for many proposed experiments; however, these experiments will use the ATM stabilization control system and will thus be isolated from vehicle angular motions. The angular excursion data obtained serve mainly to define the dynamic environment in which the ATM stabilization control system will operate.

Section 4

CREW-MOTION ISOLATION DEVICES

The results of Section 3 indicate that the dynamic environment tolerances of a majority of the low acceleration experiments and some of the fine-pointing experiments would be exceeded by the effects of crew motion. A crew-motion isolator with an attenuation of one order of magnitude would improve the dynamic environment sufficiently to include all of the fine-pointing experiments and about one-fifth of the low-acceleration experiments. An isolator of one order of magnitude, attached to the experiments, would result in about one-half of the low-acceleration experiments being feasible. Five types of crew-motion isolators were investigated. In the first scheme, counterweights were attached to the astronauts' limbs to reduce the inertial forces. The second scheme was a simple spring mounting of the astronauts' chair. The third, fourth, and fifth schemes were variations of the tuned spring-mass isolator commonly used in vibration isolation. The fourth and fifth schemes showed the most promise.

4.1 MASS BALANCE

Due to the long lever arms possible in the large orbiting laboratories, the vehicle dynamics are much more sensitive to crew-induced forces than to crew-induced couples, since the moments caused by crew-generated forces and the lever arm from the vehicle center of mass to the crew station are much larger than the couples. The crew-generated forces arise because the center of mass of the astronauts' limbs are not located at the centers of rotation. The mass balance scheme employs counterweights attached to the various limb elements to move the center of mass of the limb towards the pivot point and hence reduce the inertially induced forces.

In the following analysis the astronaut is assumed to be composed of three rigid elements: a forearm, an upper arm, and the remainder of the body. A schematic of the mass balance scheme for one arm is shown in Figure 4-1. The vector location of the four mass elements m_u , \hat{m}_u , m_f , \hat{m}_f are given in the x-iy plane by

$$\vec{\hat{u}} = -\hat{l}_u e^{i\psi}, \quad (4-1)$$

$$\vec{u} = -l_u e^{i\psi}, \quad (4-2)$$

$$\vec{\hat{f}} = l_{se} e^{i\psi} - \hat{l}_f e^{i(\psi+\theta)}, \quad (4-3)$$

$$\vec{f} = l_{se} e^{i\psi} + \hat{l}_f e^{i(\psi+\theta)}. \quad (4-4)$$

The reactive force \vec{F}_r is given by Newton's law as

$$\vec{F}_r = \hat{m}_u \ddot{\vec{u}} + m_u \ddot{\vec{u}} + \hat{m}_f \ddot{\vec{f}} + m_f \ddot{\vec{f}}. \quad (4-5)$$

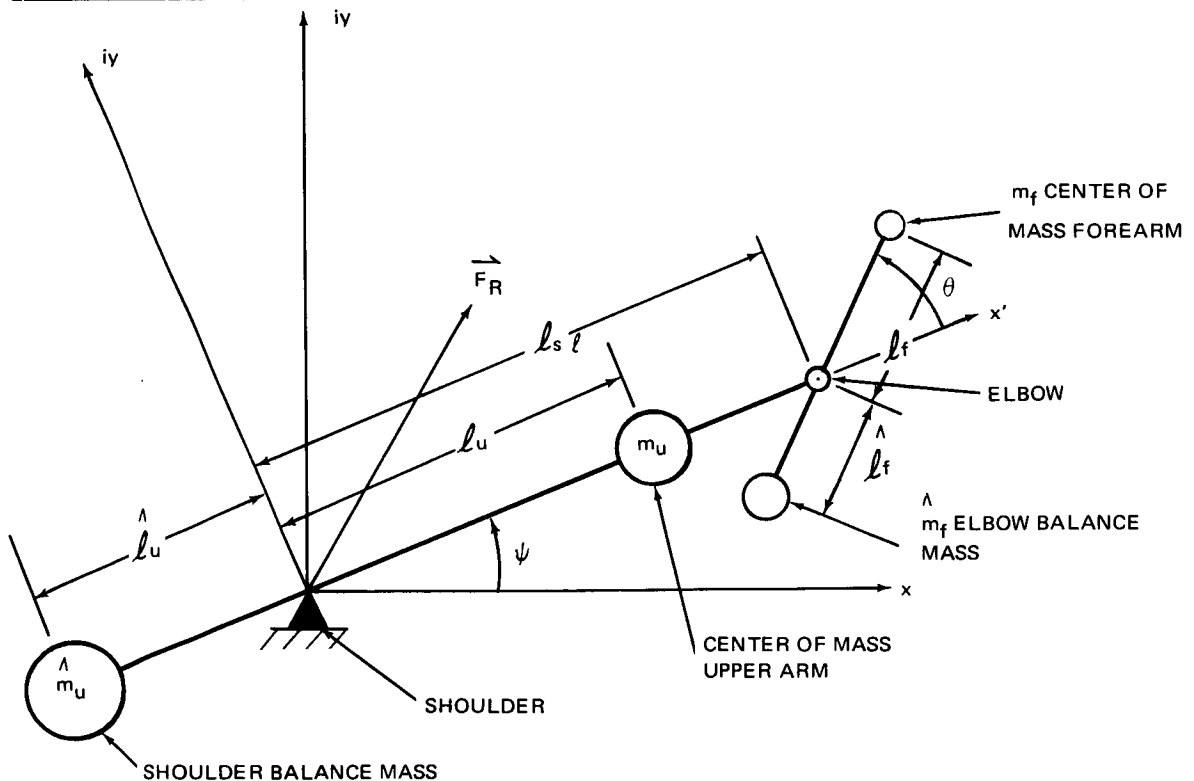


Figure 4-1. Schematic of Arm Mass Balance

Differentiating Equations 4-1 to 4-4 and substituting into Equation 4-5 yield

$$\begin{aligned}\vec{F}_r = & \left\{ \left[\hat{m}_u \hat{\ell}_u - m_u \ell_u - \ell_{se} (m_f + \hat{m}_f) \right] (\dot{\psi}^2 - i\ddot{\psi}) \right. \\ & \left. + (\hat{m}_f \hat{\ell}_f - m_f \ell_f) \left[(\dot{\psi} + \dot{\theta})^2 - i(\ddot{\psi} + \ddot{\theta}) \right] e^{i\theta} \right\} e^{i\psi}.\end{aligned}\quad (4-6)$$

In the rotating coordinate system $x' - iy'$, this merely becomes

$$\begin{aligned}\vec{F}_{r'} = & \left[\hat{m}_u \hat{\ell}_u - m_u \ell_u - \ell_{se} (m_f + \hat{m}_f) \right] (\dot{\psi}^2 - i\ddot{\psi}) \\ & + (\hat{m}_f \hat{\ell}_f - m_f \ell_f) \left[(\dot{\psi} + \dot{\theta})^2 - i(\ddot{\psi} + \ddot{\theta}) \right] e^{i\theta}.\end{aligned}\quad (4-7)$$

The magnitude of the force vector is given by

$$F_{r'} = \left| \vec{F}_{r'} \right| = \sqrt{\vec{F}_{r'} \vec{F}_{r'}^*} \quad (4-8)$$

where the superscript * indicates the complex conjugate. The magnitude will be maximum with respect to θ when

$$\frac{\partial F_{r'}}{\partial \theta} = 0. \quad (4-9)$$

This occurs when

$$\theta = \tan^{-1} \frac{\ddot{\theta} \dot{\psi}^2 - \ddot{\psi} \dot{\theta}^2}{\dot{\psi}^2 (\dot{\psi} + \dot{\theta})^2 + \ddot{\psi} (\ddot{\psi} + \ddot{\theta})}. \quad (4-10)$$

Then

$$\begin{aligned}F_{r' \max} = & \left[m_u \ell_u - \hat{m}_u \hat{\ell}_u + \ell_{se} (m_f + \hat{m}_f) \right] \sqrt{\dot{\psi}^4 + \ddot{\psi}^2} \\ & + (m_f \ell_f - \hat{m}_f \hat{\ell}_f) \sqrt{(\dot{\theta} + \dot{\psi})^4 + (\ddot{\theta} + \ddot{\psi})^2}.\end{aligned}\quad (4-11)$$

Since the angular rate and acceleration histories are not predictable, Equation 4-11 cannot be used as a design equation directly. The following approach is used to generate design equations. It is assumed that the elbow system is exactly balanced; i. e., $\hat{m}_f \ell_f = \hat{m}_f \ell_f$. Then Equation 4-11 becomes

$$F_{r' \max} = \left[m_u \ell_u - \hat{m}_u \hat{\ell}_u + \ell_{se} (m_f + \hat{m}_f) \right] \sqrt{\dot{\psi}^4 + \ddot{\psi}^2} . \quad (4-12)$$

The system transmissibility T_r is defined as the ratio of the transmitted force with the shoulder balance mass to the transmitted force without the shoulder balance mass:

$$T_r = \frac{m_u \ell_u - \hat{m}_u \hat{\ell}_u + \ell_{se} (m_f + \hat{m}_f)}{m_u \ell_u + \ell_{se} m_f} , \quad (4-13)$$

$$= 1 - \frac{1}{1 + \rho} \left(\frac{\hat{m}_u \hat{\ell}_u}{m_u \ell_u} \right) + \frac{\rho}{1 + \rho} \left(\frac{\hat{m}_f}{m_f} \right) , \quad (4-14)$$

where

$$\rho = \frac{\ell_{se} m_f}{\ell_u m_u} . \quad (4-15)$$

The elbow balance mass and lever arm are plotted in Figure 4-2 as ratios of the forearm mass and lever arm respectively. Equation 4-14 is plotted in Figure 4-3. It should be noted that, for a given individual, ρ is a known constant. Then, the design procedure is as follows. Determine a reasonable lever arm for the elbow balance mass and find the corresponding mass ratio from Figure 4-2. Using this mass ratio and the desired transmissibility, find the shoulder moment ratio from Figure 4-3. The choice of a lever arm for the shoulder balance mass will allow the necessary balance mass to be calculated.

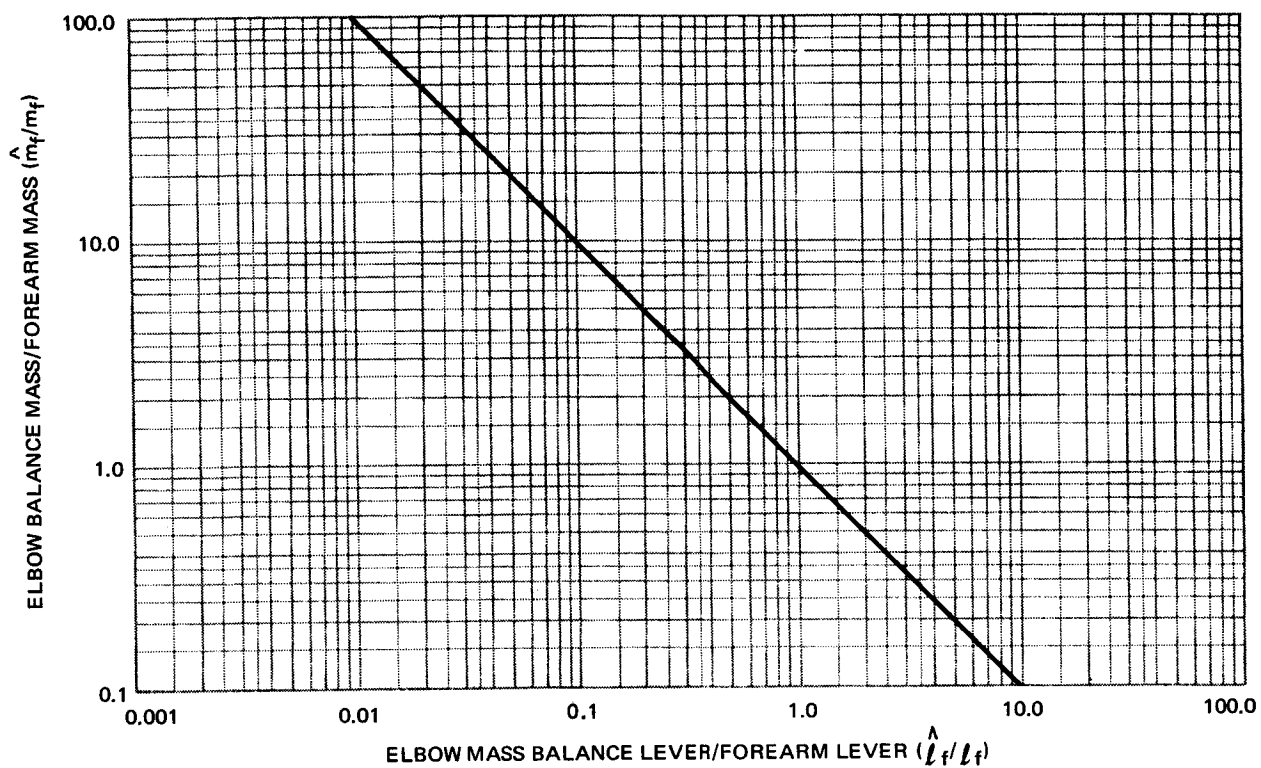


Figure 4-2. Balance Mass vs Lever Arm Fully Balanced Elbow

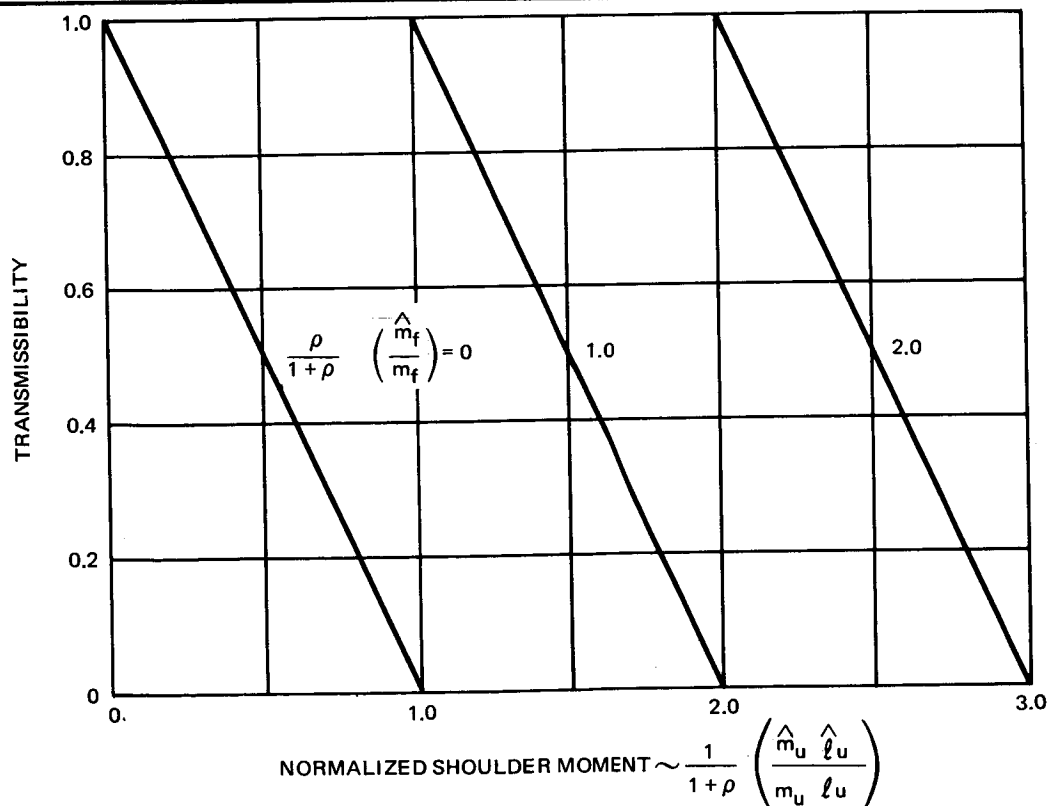


Figure 4-3. Transmissibility for Fully Balanced Elbow

Since the mass balance systems will be donned and doffed as required, an important design parameter is the sensitivity of transmissibility to the lever arms $\hat{\ell}_u$ and $\hat{\ell}_f$. This will tell how carefully the mounting devices must be designed. From Equation 4-14,

$$\frac{\partial T_y}{\partial \hat{\ell}_u} = - \frac{1}{(1 + \rho)} \frac{\hat{m}_u}{m_u \ell_u} . \quad (4-16)$$

For a given shoulder moment ratio this becomes

$$\frac{\partial T_y}{\partial \hat{\ell}_u} = - \left[\frac{1}{1 + \rho} \left(\frac{\hat{m}_u \hat{\ell}_u}{m_u \ell_u} \right) \right] \frac{1}{\hat{\ell}_u} . \quad (4-17)$$

Hence, the longer $\hat{\ell}_u$ the less sensitive the transmissibility is to errors in attaching the shoulder balance mass. The sensitivity of transmissibility to $\hat{\ell}_f$ is undefined; however, Equation 4-11 indicates that

$$\frac{\partial F_{r' \max}}{\partial \hat{\ell}_f} \approx -\hat{m}_f = - \frac{\hat{m}_f \hat{\ell}_f}{\hat{\ell}_f} . \quad (4-18)$$

Again a longer lever arm implies a less sensitive system.

The choice of lever arms will depend on design considerations such as interference envelope, mounting bracket design, materials used (implies volume required), ease of attachment, storage geometry, etc. Many of these quantities can only be determined empirically or are very strongly dependent on vehicle characteristics. Therefore, reasonable lever arms will be arbitrarily selected to allow a discussion of feasibility. A 5-in. elbow lever arm will allow a comfortable posture while seated in an arm chair, and a 10-in. shoulder lever arm would allow approximately 30° of arm motion in the frontal plane, assuming the distance from the shoulder to head is about 5 in. In the following discussion it is assumed that an order of magnitude reduction

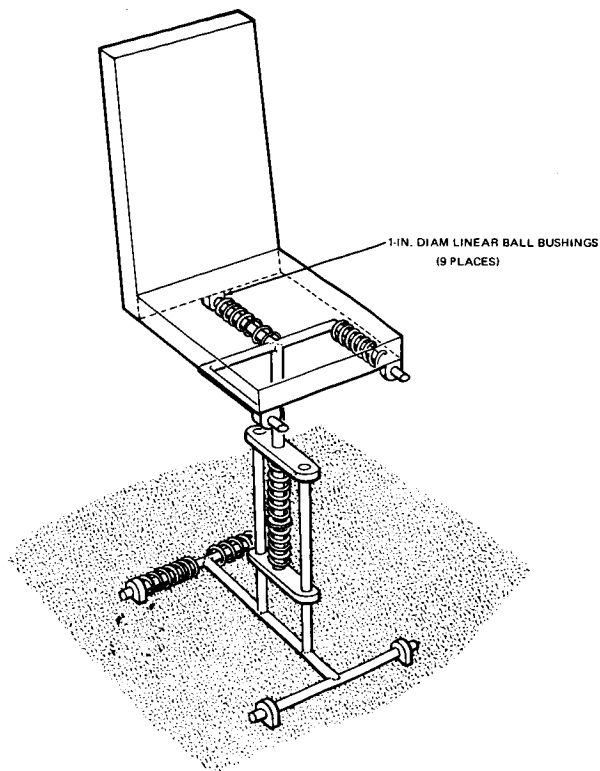


Figure 4-4. Crew Isolation Device (Seated)

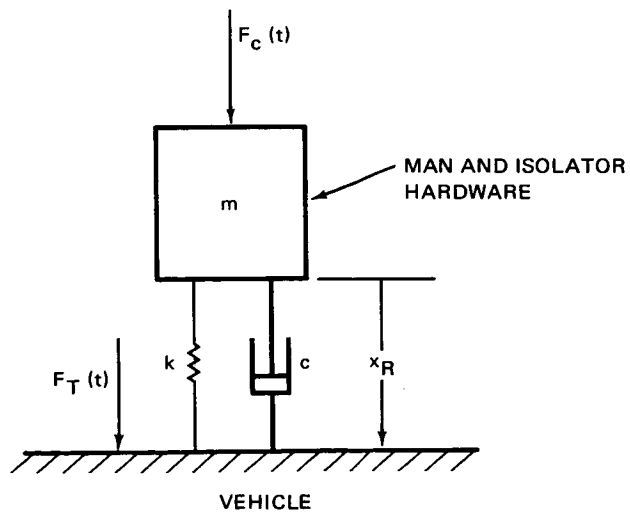


Figure 4-5. Simplified Model Used in Analysis of Shock Mount Scheme

where

$$\omega_n = \sqrt{\frac{k}{m}} = \text{system natural frequency} , \quad (4-23)$$

$$\zeta = \frac{c}{2\sqrt{km}} = \text{system damping ratio} , \quad (4-24)$$

$$\omega_d = \sqrt{1 - \zeta^2} \omega_n = \text{system damped natural frequency} , \quad (4-25)$$

$$D = \sqrt{(\omega_n^2 - \omega^2)^2 + 4\zeta^2 \omega_n^2 \omega^2} , \quad (4-26)$$

$$\alpha = \tan^{-1} \frac{2\zeta \sqrt{1 - \zeta^2}}{2\zeta^2 - 1 + \lambda^2} \quad (4-27)$$

$$\beta = \tan^{-1} \frac{2\zeta}{\lambda^2 - 1} \quad (4-28)$$

$$\lambda = \omega/\omega_n \quad (4-29)$$

The transmitted force is

$$F_T(t) = \frac{F_c \omega \omega_n}{D} \left[\frac{\omega_n}{\omega_d} e^{-\zeta \omega_n t} \sin(\omega_d t + \alpha_2) \right] + \frac{1}{\omega} \sqrt{(2\zeta \omega)^2 + \omega_n^2} \sin(\omega t + \beta_2) \quad (4-30)$$

where

$$\alpha_2 = \tan^{-1} \frac{2\zeta \lambda^2 \sqrt{1 - \zeta^2}}{\lambda^2 (1 - 2\zeta^2) - 1} , \quad (4-31)$$

$$\beta_2 = \tan^{-1} \frac{2\zeta\lambda^3}{\lambda^2(1 - 4\zeta^2) - 1} . \quad (4-32)$$

In an ordinary vibration analysis the transient terms (the first terms inside the brackets of Equations 4-22 and 4-30) would be ignored. However, since the crew motion only involves at most a few cycles of the fundamental frequency, the transient terms become extremely important. The maximum values of the transient portions of Equations 4-22 and 4-30 will occur at

$$t_x = \frac{1}{\omega_d} \tan^{-1} \left[\frac{\sqrt{1 - \zeta^2}}{\zeta} \left(\frac{\lambda^2 - 1}{\lambda^2 + 1} \right) \right] , \quad (4-33)$$

$$t_F = \frac{1}{\omega_d} \tan^{-1} \frac{\sqrt{1 - \zeta^2}}{\zeta} \left[\frac{\lambda^2 - 4\zeta^2\lambda^2 - 1}{3\lambda^2 - 4\zeta^2\lambda^2 - 1} \right] . \quad (4-34)$$

The corresponding values of the transient terms will be

$$X_{RT}(t_x) = \frac{\lambda F_c}{k\sqrt{(\lambda^2 - 1)^2 + 4\zeta^2\lambda^2}} \exp - \left\{ \frac{\zeta}{\sqrt{1 - \zeta^2}} \cdot \tan^{-1} \left[\frac{\sqrt{1 - \zeta^2}}{\zeta} \left(\frac{\lambda^2 - 1}{\lambda^2 + 1} \right) \right] \right\} , \quad (4-35)$$

$$F_{TT}(t_f) = \frac{\lambda F_c}{\sqrt{(\lambda^2 - 1)^2 + 4\zeta^2\lambda^2}} \exp - \left\{ \frac{\zeta}{\sqrt{1 - \zeta^2}} \cdot \tan^{-1} \left[\frac{\sqrt{1 - \zeta^2}}{\zeta} \frac{(\lambda^2 - 4\zeta^2\lambda^2 - 1)}{(3\lambda^2 - 4\zeta^2\lambda^2 - 1)} \right] \right\} . \quad (4-36)$$

The peak values of the driven terms will be

$$X_{RD} = \frac{F_c}{k} \frac{1}{\sqrt{(\lambda^2 - 1)^2 + 4\zeta^2\lambda^2}} , \quad (4-37)$$

$$F'_{TD} = \frac{F_c \sqrt{1 + 4\zeta^2 \lambda^2}}{\sqrt{(\lambda^2 - 1)^2 + 4\zeta^2 \lambda^2}}. \quad (4-38)$$

The sum of the transient and driven peak values yields a conservative estimate or upper bound of the actual peak value. The estimated maximum transmitted force and relative displacement are plotted in Figure 4-6 as functions of the frequency ratio λ , for two values of damping. The displacement bound is normalized by the static deflection F_c/k and the transmitted force, by the magnitude of the crew-induced force F_c . The expressions for the normalized estimates are identical when $\zeta = 0$; hence, there are only three curves in Figure 4-6. It can be seen from this figure that the upper bounds approach asymptotes as λ gets large, and that large values of λ will be required to achieve significant reductions in transmitted force and relative displacement. Therefore, the dependence of the upper bounds on the damping ratio is illustrated by plotting the asymptotic value versus the damping ratio in Figure 4-7. Since it is desired to operate at small deflections and transmissibilities, it can be seen from this figure that the best value of damping is zero, although a value of slightly above $1/2$ appears to be favorable also. It can be determined from Figure 4-6 that reductions of one and two orders of magnitude will require frequency ratios of 10 and 100 respectively. Since the fundamental frequency of crew-motion forces is typically 1 cps, the aforementioned frequency ratios will correspond to 0.1 and 0.01 cps. The latter frequency is very close to the control system natural frequency for the large orbiting laboratories (0.0067 cps for the Manual Orbiting Research Laboratory) (Reference 1). This will lead to control system isolator coupling problems. This coupling is termed base drive and is of such a nature, that the relationship between isolator relative displacement X_R , and the base motion X_V (movement of the vehicle caused by the attitude control system) is given by

$$\frac{X_R}{X_V} = \frac{S^2}{S^2 + 2\zeta\omega_n S + \omega_n^2}. \quad (4-39)$$

If the vehicle natural frequency is very near the isolator natural frequency, the lightly damped system will exhibit violent reactions. As an example, if the vehicle control system were controlling to within $\pm 1^\circ$ and if the crew station were located 30 ft from the center of mass, the resulting base motion would be ± 6.3 in. The peak-to-peak relative displacement corresponding to the frequencies and damping ratios mentioned previously are given in Table 4-1.

Table 4-1
PEAK-TO-PEAK DISPLACEMENT CAUSED BY BASE DRIVING

Isolator Natural Frequency	Damping Ratio	
	0.0	0.707
0.01 cps	12.1 in.	5.5 in.
0.1 cps	0.06 in.	0.06 in.

It is questionable if any of the displacements for the transmissibility of two order of magnitude are reasonable. However, if the vehicle is controlled to well inside 1° , 0.01 transmissibility may be achievable.

4.3 TUNED SPRING MASS ISOLATORS

A tuned spring mass isolator is one in which a small auxiliary mass is coupled to the main mass through a spring and damper. By adjusting the natural frequency of the coupling network the isolator mass can be made to move so that the force transmitted to the main mass through the coupling network is out of phase (acting in an opposite direction) with the crew motion force. The resulting cancellation reduces the force applied to the vehicle.

The isolating mass can be mechanized in two ways, these are shown schematically in Figures 4-8 and 4-9. In Figure 4-8 the mass is attached in the traditional manner, whereas in Figure 4-9, it is mounted between the chair and vehicle.

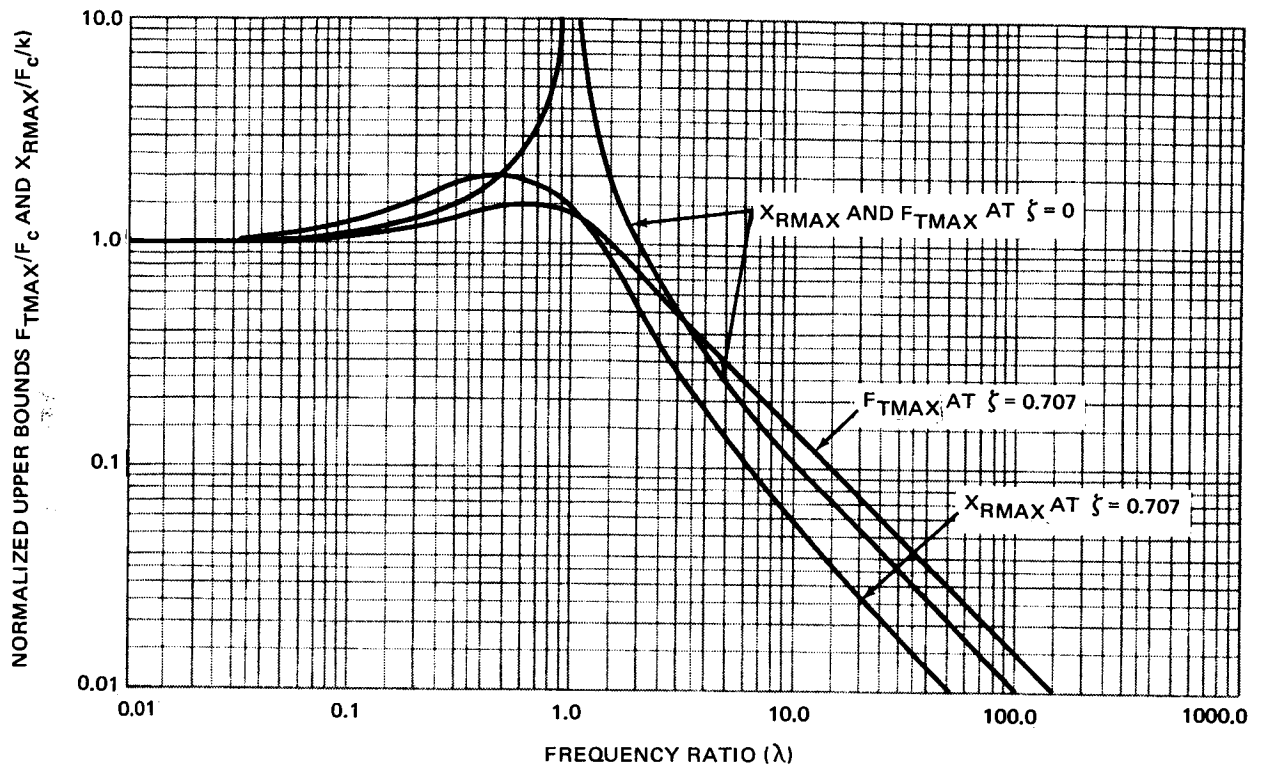


Figure 4-6. Normalized Upper Bounds vs Frequency Ratio

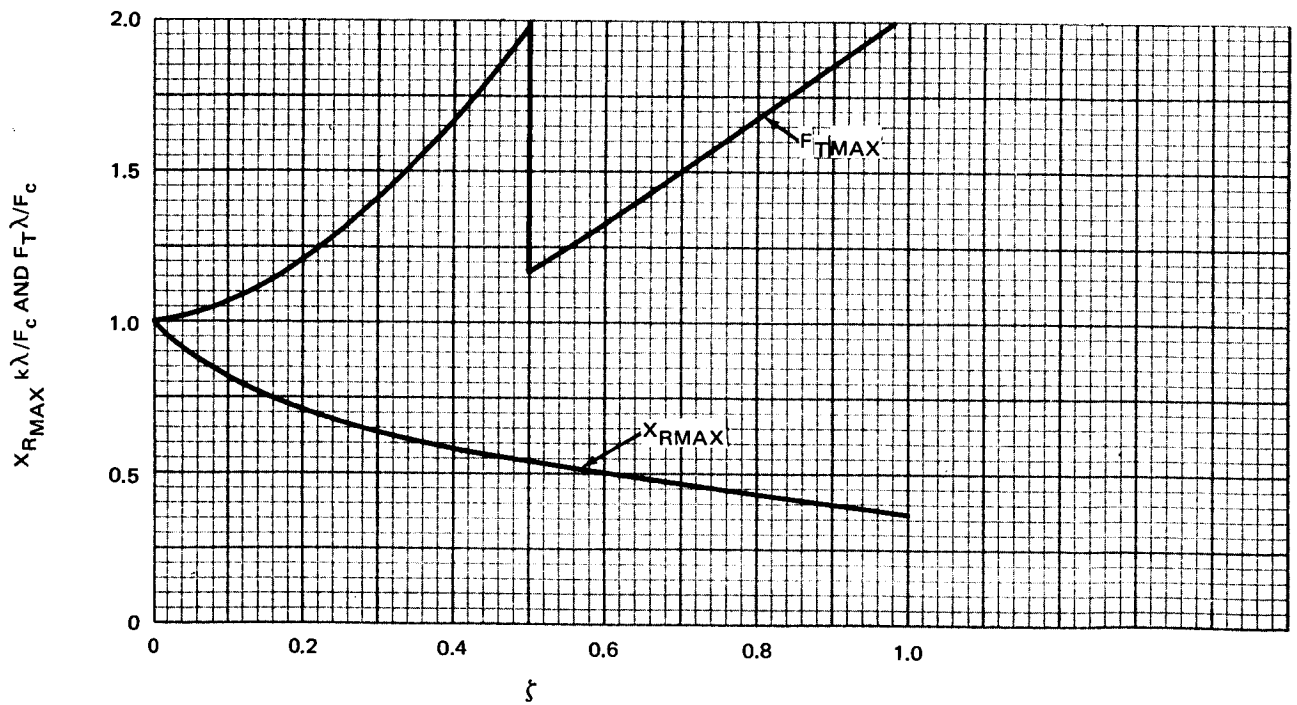


Figure 4-7. Variation of Displacement and Transmitted Force with Damping Ratio

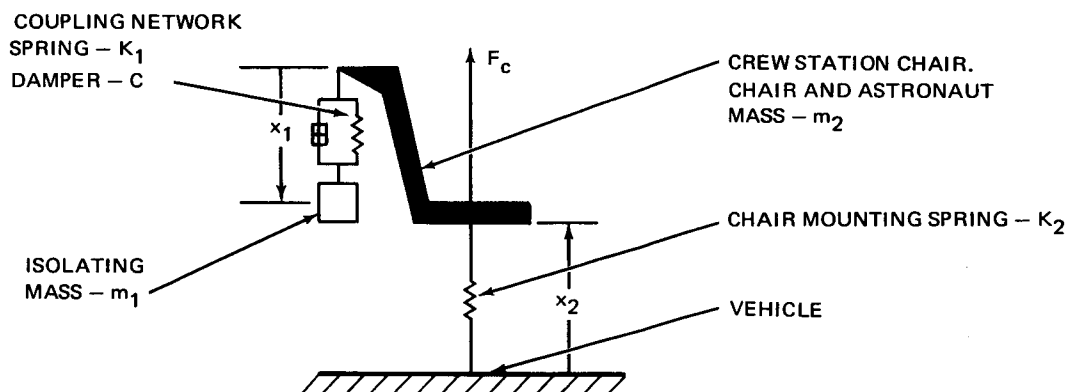


Figure 4-8. Traditional Mounting Arrangement

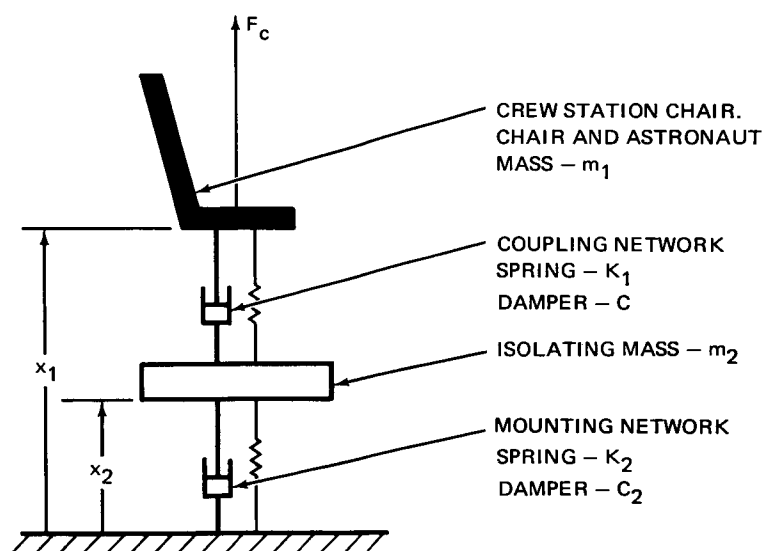


Figure 4-9. Alternate Mounting Arrangement

The equations of motion for the configuration of Figure 4-8 are given by

$$m_1 \ddot{x}_1 + c \dot{x}_1 + k_1 x_1 - m_1 \ddot{x}_2 = 0 , \quad (4-40)$$

$$m_2 \ddot{x}_2 + k_2 x_2 + c \dot{x}_1 + k_1 x_1 = F_c . \quad (4-41)$$

The transmitted force to the vehicle is

$$F_T = k_2 x_2 . \quad (4-42)$$

Equation 4-42 indicates that this scheme has the advantage of simultaneously reducing both the transmitted force and the relative displacement of the astronaut. The transfer functions relating the various independent variables are

$$\frac{X_1}{X_S} = \frac{\omega_2^2 S^2}{S^4 + 2\zeta\omega_1(1+\rho)S^3 + \left[\omega_1^2 - (1+\rho) + \omega_2^2\right]S^2 + 2\zeta\omega_1\omega_2^2 S + \omega_1^2\omega_2^2} , \quad (4-43)$$

$$\frac{X_2}{X_S} = \frac{(S^2 + 2\zeta\omega_1 S + \omega_1^2)\omega_2^2}{S^4 + 2\zeta\omega_1(1+\rho)S^3 + \left[\omega_1^2(1+\rho) + \omega_2^2\right]S^2 + 2\omega_1\omega_2^2 S + \omega_1^2\omega_2^2} , \quad (4-44)$$

$$\frac{F_T}{F_c} = \frac{X_2}{X_S} , \quad (4-45)$$

where

$$X_S = \frac{1}{k_2} F_c , \quad (4-46)$$

$$\omega_1^2 = k_1/m_1 , \quad (4-47)$$

$$\zeta = c/2 \sqrt{k_1 m_1} , \quad (4-48)$$

$$\omega_2^2 = k_2/m_2 , \quad (4-49)$$

$$\rho = m_1/m_2 . \quad (4-50)$$

The denominator of these functions can be factored into the form

$$\left(S^2 + 2\eta_1 \Omega_1 S + \Omega_1^2 \right) \left(S^2 + 2\eta_2 \Omega_2 S + \Omega_2^2 \right) . \quad (4-51)$$

It can be shown that, if the damping ratio ζ and mass ratio ρ are small and the two frequencies ω_1 and ω_2 are well separated, the factored frequencies Ω_1 and Ω_2 are given to a close approximation by

$$\Omega_1 = \left[1 - \frac{\rho \omega_1^2}{2(\omega_2^2 - \omega_1^2)} \right] \omega_1 , \quad (4-52)$$

$$\Omega_2 = \left[1 + \frac{\rho \omega_1^2}{2(\omega_2^2 - \omega_1^2)} \right] \omega_2 . \quad (4-53)$$

If ω_2 is chosen greater than ω_1 , the magnitude of Equation 4-44 will take on the form of Figure 4-10. This figure exhibits a notch isolation characteristic in the vicinity of Ω_B . The first peak in the graph is caused by the resonance at Ω_1 , the trough by the numerator resonance at ω_1 , and the second peak and high-frequency characteristics by the resonance at Ω_2 . Since the high frequency characteristics resemble those of the shock isolator scheme and since the latter was shown to be unfeasible, it is the notch isolation characteristic of this system that must be used to attenuate the crew-motion forces.

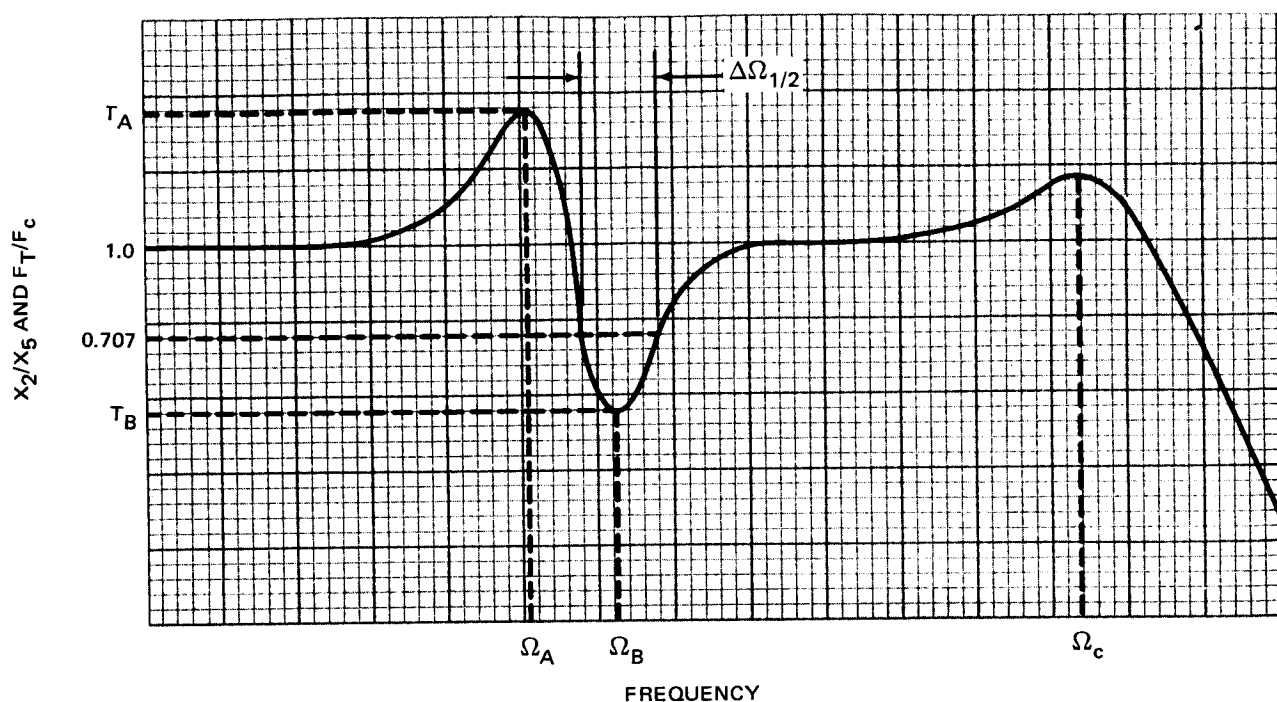


Figure 4-10. Notch Isolation Characteristics Definitions

It is now possible to justify the assumptions made previously. The magnitude of attenuation at the notch frequency Ω_B is inversely proportional to the damping ratio; hence, small damping ratios are again required. The mass ratio was chosen small to insure a practical design. The frequencies ω_1 and ω_2 were assumed separated to make sure that the resonance at Ω_B could not affect the notch attenuation.

Referring to Figure 4-10, the important characteristics of this curve are the magnitude T_A of the unwanted resonance at Ω_A , the attenuation T_B at the notch frequency Ω_B , and the width of the notch $\Delta\Omega$ at the half power point, where $|F_T/F_C| = 0.707$. This latter characteristic is important since the energy of a particular crew motion is not concentrated at one frequency but spread over a small range of frequencies. A parameterization study was conducted to determine how the system parameters ζ , ρ , ω_1 , ω_3 affect these characteristics. Figures 4-11 and 4-12 indicate the effect of the system parameters on T_A and T_B , whereas Table 4-2 summarizes the effect on the notch width $\Delta\Omega$.

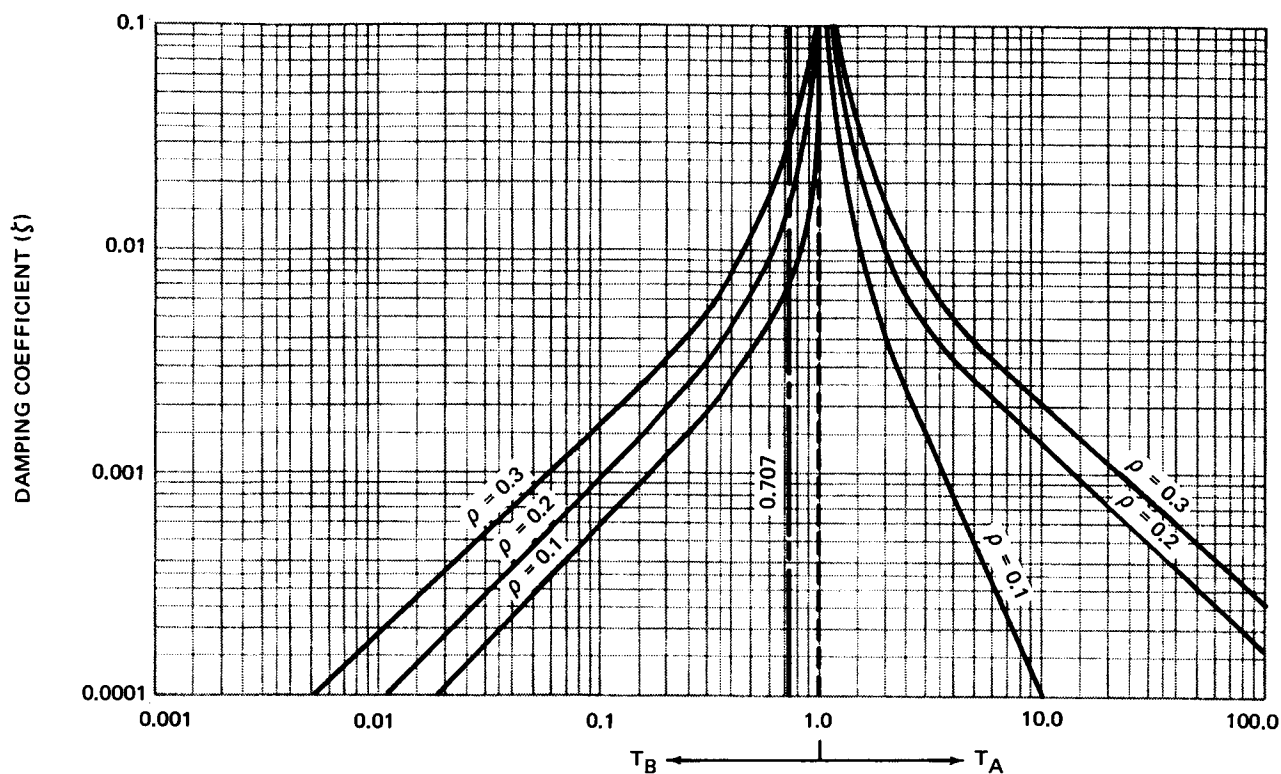


Figure 4-11. Values of T_A and T_B vs ζ and ρ with $\omega_2/\omega_1 = 3.0$

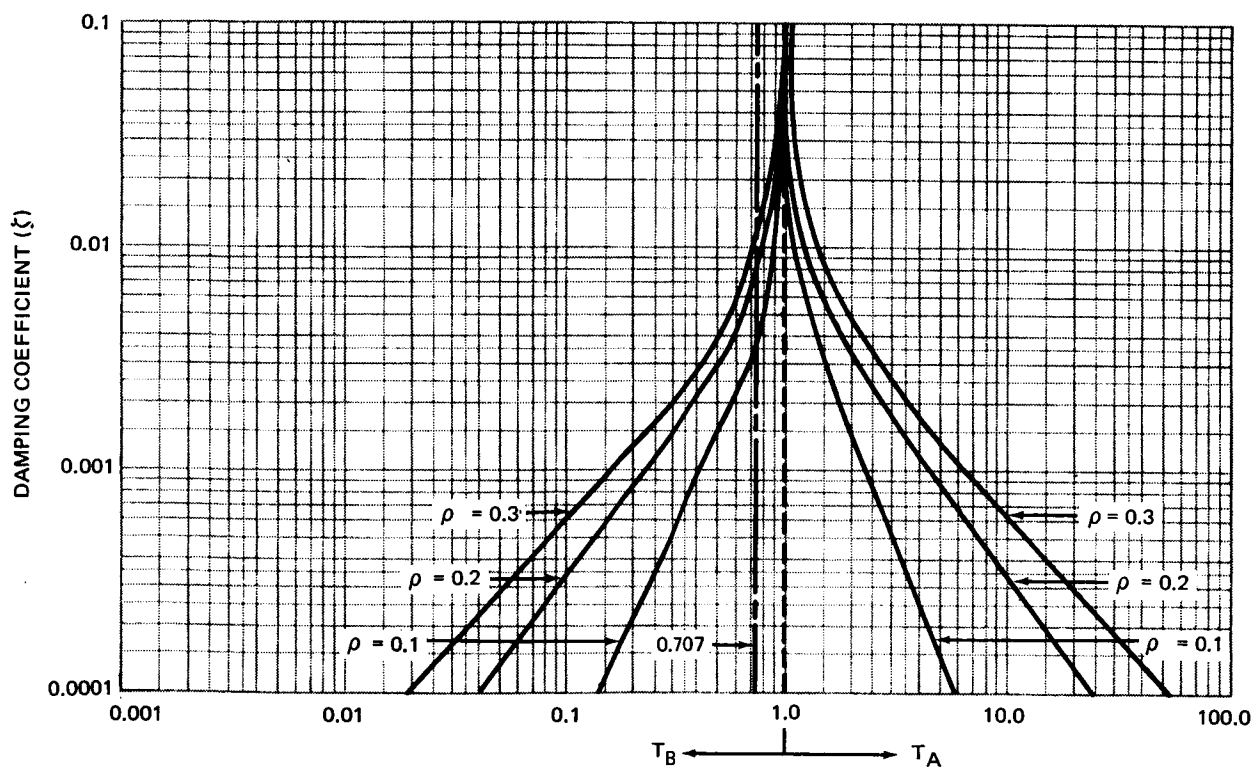


Figure 4-12. Values of T_A and T_B vs ζ and ρ with $\omega_2/\omega_1 = 5.0$

The dash marks in Table 4-2 indicate that for the particular combination of system parameters the amplitude ratio at the notch frequency was not less than 0.707, and hence the notch width was undefined.

Table 4-2
EFFECT OF SYSTEM PARAMETERS ON NORMALIZED
NOTCH WIDTH $\Delta\Omega/\omega_1$

	$\frac{\omega_2}{\omega_1} = 3.0$			$\frac{\omega_2}{\omega_1} = 5.0$		
	$\zeta = 0.1$	$\zeta = 0.01$	$\zeta = 0.001$	$\zeta = 0.1$	$\zeta = 0.01$	$\zeta = 0.001$
$\rho = 0.1$	—	—	0.00302	—	—	0.00485
$\rho = 0.2$	—	0.015	0.02625	—	—	0.01038
$\rho = 0.3$	—	0.0343	0.04015	—	—	0.01575

There are two basic problems with the scheme. From Figures 4-11 and 4-12, it is apparent that extremely low values of damping are required and that the system is quite sensitive to changes in damping. It is questionable if such a low value of damping could be designed to a very tight tolerance. The other problem area is in the notch width. Table 4-2 indicates that the notch width is less than about 4% of the isolator frequency ω_1 , which is approximately equal to the notch frequency Ω_B . Since the fundamental frequencies of the crew-motion forces vary by more than $\pm 2\%$, it is doubtful that a satisfactory system of this nature could be designed.

The equations of motion for the configuration of Figure 4-9 are given by

$$m_1 \ddot{x}_1 + c_1 \dot{x}_1 + k_1 x_1 - c_1 \dot{x}_2 - k_1 x_2 = F_c, \quad (4-54)$$

$$m_2 \ddot{x}_2 + (c_1 + c_2) \dot{x}_2 + (k_1 + k_2) x_2 - c_1 \dot{x}_1 - k_1 x_1 = 0. \quad (4-55)$$

The force transmitted to the vehicle is given by

$$F_T = c_2 \dot{x}_2 + k_2 x_2 . \quad (4-56)$$

The corresponding transfer functions are

$$\frac{X_2}{X_S} = \frac{[S^2 + 2(\zeta_1 \omega_1 + \zeta_2 \omega_2)S + \omega_1^2 + \omega_2^2]}{D(S)} \frac{\omega_2^2}{\rho} , \quad (4-57)$$

$$\frac{X_2}{X_S} = \frac{2\zeta_1 \omega_1 S + \omega_1^2}{D(S)} , \quad (4-58)$$

$$\frac{F_T}{F_c} = \left(\frac{2\zeta_2}{\omega_2} S + 1 \right) \frac{X_2}{X_S} , \quad (4-59)$$

where

$$\begin{aligned} D(S) = & S^4 + 2[(1 + \rho)\zeta_1 \omega_1 + \zeta_2 \omega_2]S^3 \\ & + [(1 + \rho)\omega_1^2 + \omega_2^2 + 2\zeta_1 \omega_1 2\zeta_2 \omega_2]S^2 + 2\omega_1 \omega_2 (\zeta_1 \omega_2 + \zeta_2 \omega_1)S + \omega_1^2 \omega_2^2 . \end{aligned} \quad (4-60)$$

A trial-and-error procedure was used to find a set of system parameters which would yield a reduction of two order of magnitude in crew-motion force at $f = 1$ cps. The parameters found to give the desired system characteristic are given in Table 4-3.

The resulting frequency curves are shown in Figures 4-13, 4-14, and 4-15. These indicate that this system has promise. Future analysis will have to be performed to investigate the transient response characteristics and any coupling phenomena which may exist.

Table 4-3
PARAMETER VALUES

Parameter	Value
m_1	7.0 slugs
k_1	2.0 lb/ft
d_1	6.0 lb/ft/sec
m_2	1.4 slugs
k_2	5.0 lb/ft
d_2	0.083 lb/ft/sec

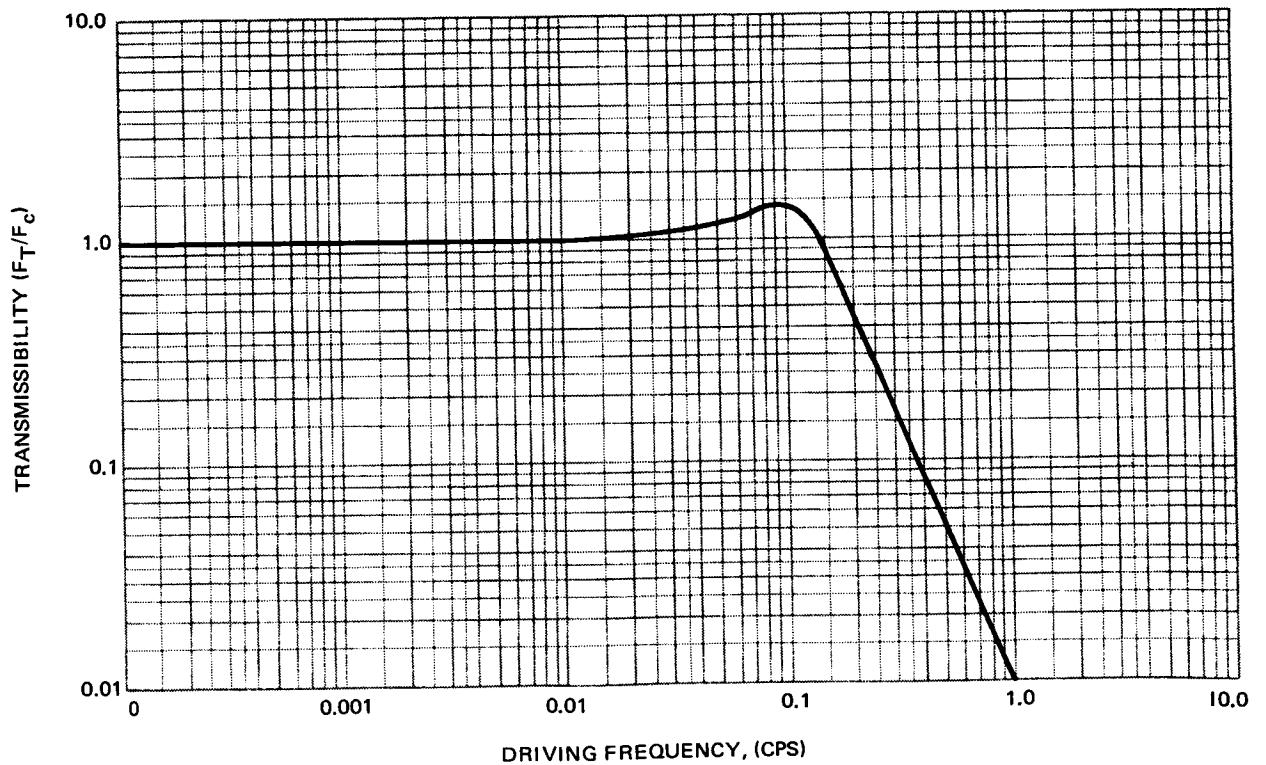


Figure 4-13. Transmissibility vs Driving Frequency

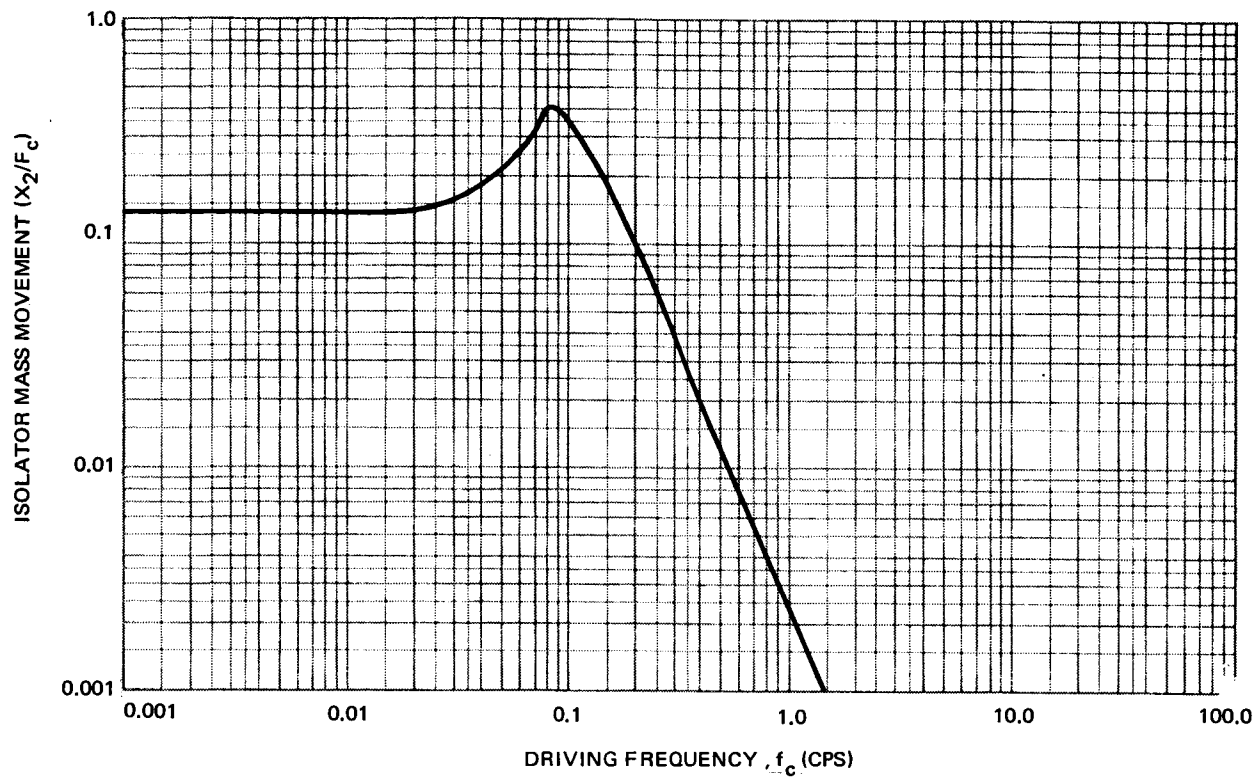


Figure 4-14. Isolator Mass Movement vs Driving Frequency

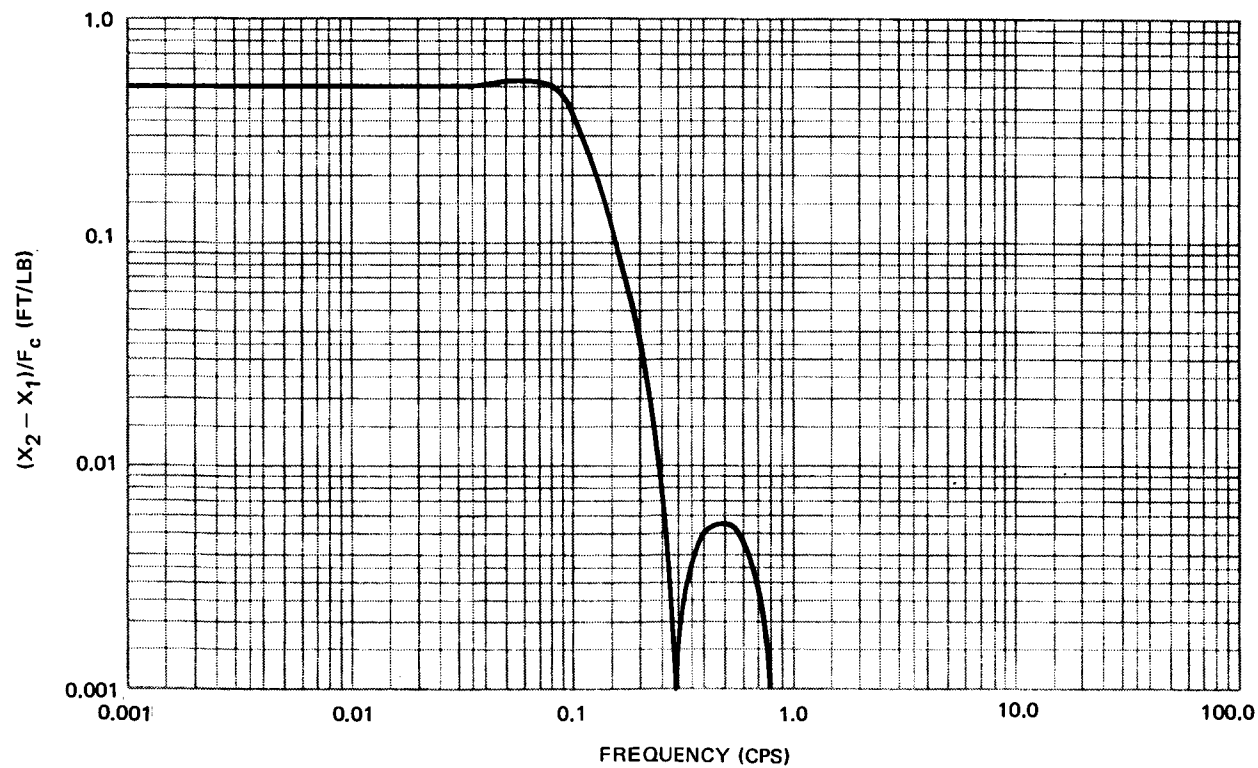


Figure 4-15. Isolator Chair Separation vs Frequency

4.4 PIVOTED TUNED ISOLATOR

The pivoted tuned isolator is described in Reference 13. In this scheme the isolator mass is mounted on a pivot so that it moves in a direction opposite to the main mass. In Reference 13 the concept is applied to the problem of helicopter vibration isolation. It is claimed that the device works well for a large range of occupant weights and for low values of driving frequency.

The model used for this analysis is shown in Figure 4-16. The equations of motion are given by

$$(m_1 + \Lambda^2 m_3) \ddot{x}_1 + c_1 \dot{x}_1 + k_1 + (m_1 - m_3 \Lambda) \ddot{x}_2 = F, \quad (4-61)$$

$$(m_1 - m_3 \Lambda) \ddot{x}_1 + (m_1 + m_2 + m_3) \ddot{x}_2 + c_2 \dot{x}_2 + k_2 x_2 = F, \quad (4-62)$$

where $\Lambda = a/b$. The transmitted force is given by

$$F_T = c_2 \dot{x}_2 + k_2 x_2 \quad (4-63)$$

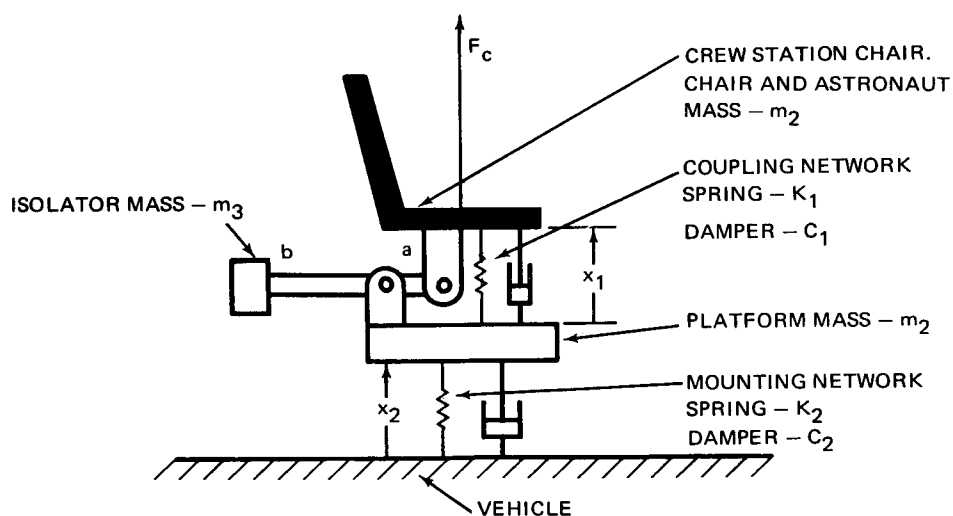


Figure 4-16. Pivoted Tuned Isolator

The transfer functions corresponding to these equations are

$$\frac{X_1}{F_c} = \frac{[m_2 + (1 + \Lambda)m_3]S^2 + c_2S + k_2}{D(S)}, \quad (4-64)$$

$$\frac{X_2}{F_c} = \frac{(1 + \Lambda)\Lambda m_3 S^2 + c_1S + k_1}{D(S)}, \quad (4-65)$$

$$\frac{F_T}{F_c} = (c_2S + k_2) \frac{X_2}{F_c}, \quad (4-66)$$

where

$$\begin{aligned} D(S) = & \left[m_2(m_1 + \Lambda^2 m_3) + m_1 m_3 (1 + \Lambda)^2 \right] S^4 + \left[(m_1 + \Lambda^2 m_3)c_2 + m_T c_1 \right] S^3 \\ & + \left[(m_1 + \Lambda^2 m_3)k_2 + m_T k_1 + c_1 c_2 \right] S^2 + (c_1 k_2 + c_2 k_1)S + k_1 k_2. \end{aligned} \quad (4-67)$$

A trial-and-error approach was again used to determine a set of parameters which would yield a reduction of two order of magnitude at 1 cps. The set of parameters is given in Table 4-4.

The transfer functions of Equations 4-64, 4-65, and 4-66 are plotted in Figures 4-17, 4-18, and 4-19. These figures indicate that the transmitted force and relative displacement of the astronaut will be quite small if the frequency content of crew motion below 1 cps is negligible. The parameters of Table 4-1 were varied to determine the sensitivity of the transmissibility function to each parameter. The motion of the resonance peak and the notch frequency as a function of parameter variations are shown in Figure 4-20. This figure indicates that the unwanted peak of the transmissibility function is insensitive to small changes in m_2 , m_3 , and a/b . Hence, if more attenuation is desired at the notch frequency, changes in m_2 , m_3 , or a/b will serve without raising the undesirable peak; conversely, if less attenuation is

Table 4-4
NOMINAL PARAMETERS FOR PIVOTED TUNED ISOLATOR

Parameter	Value
Λ	0.6
m_1	5.28 slugs
c_1	0.8 lb/ft/sec
k_1	35 lb/ft
m_2	1.5 slugs
c_2	3.5 lb/ft/sec
k_2	18 lb/ft
m_3	0.2 slug

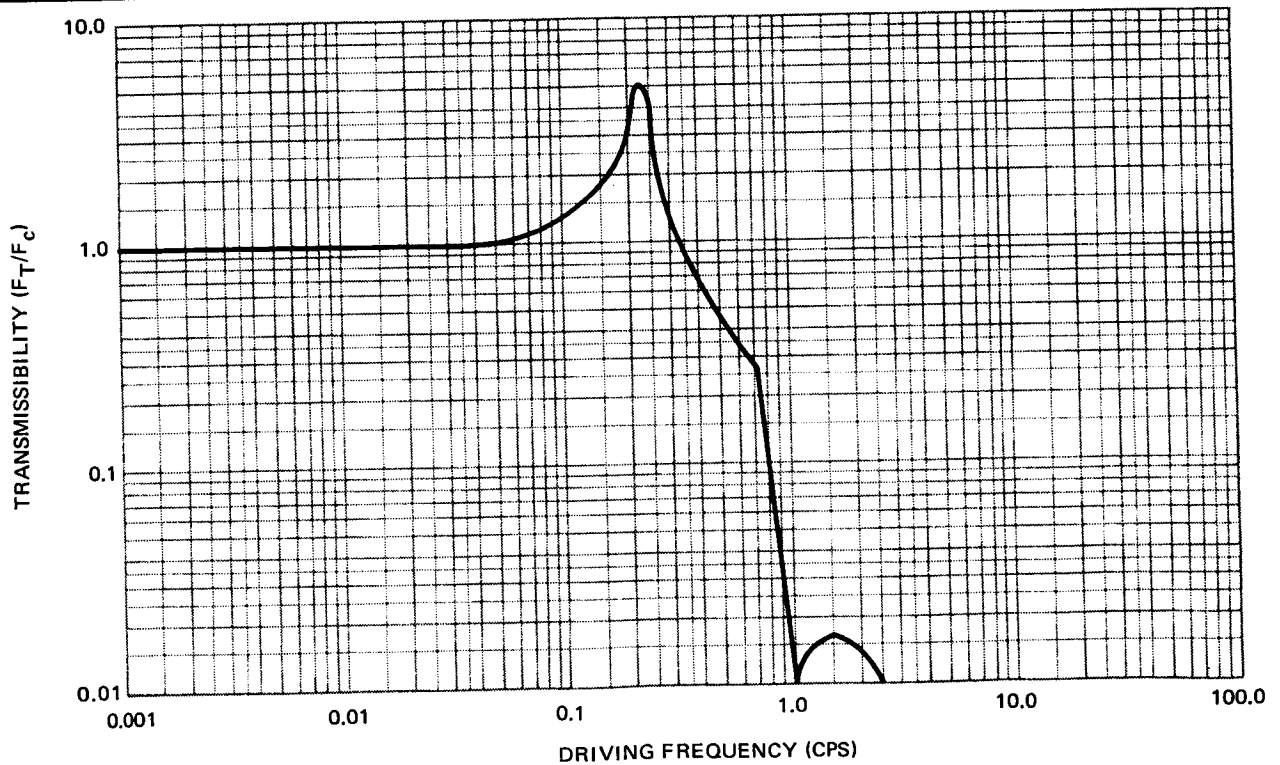


Figure 4-17. Transmissibility vs Driving Frequency

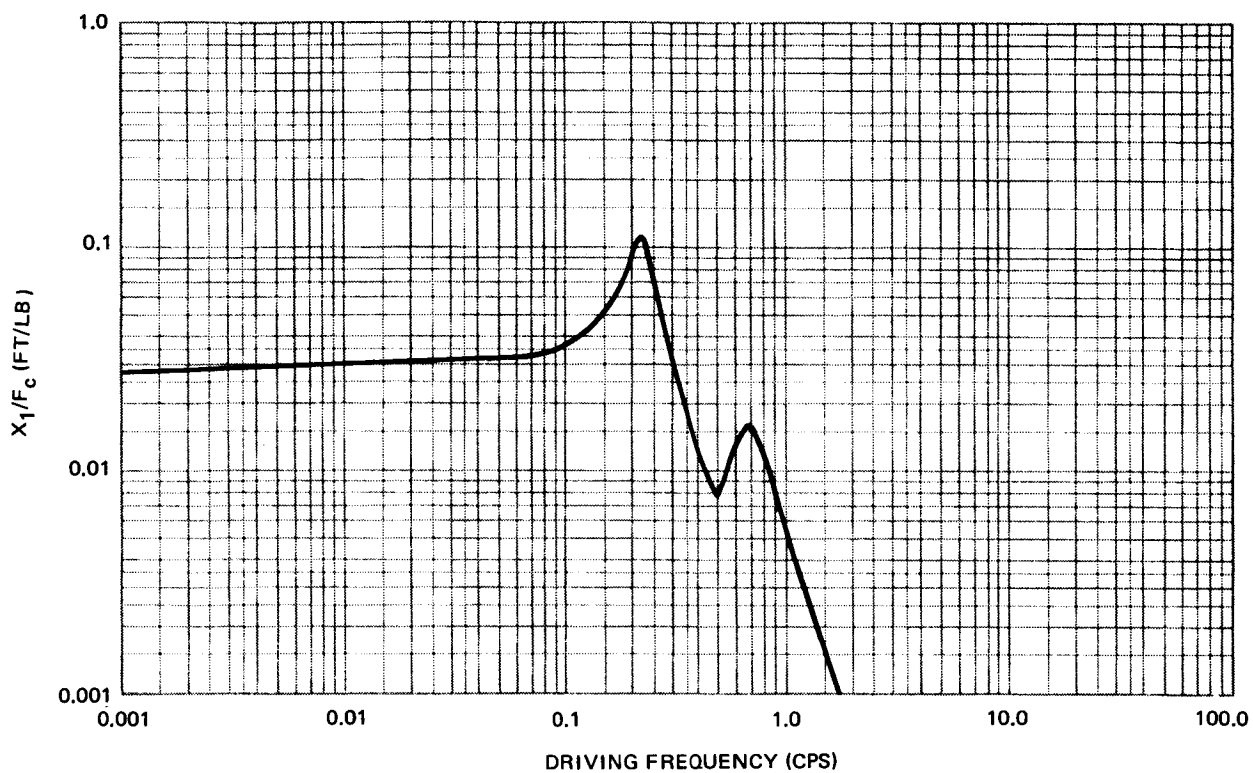


Figure 4-18. Ratio X_1/F_c vs Driving Frequency

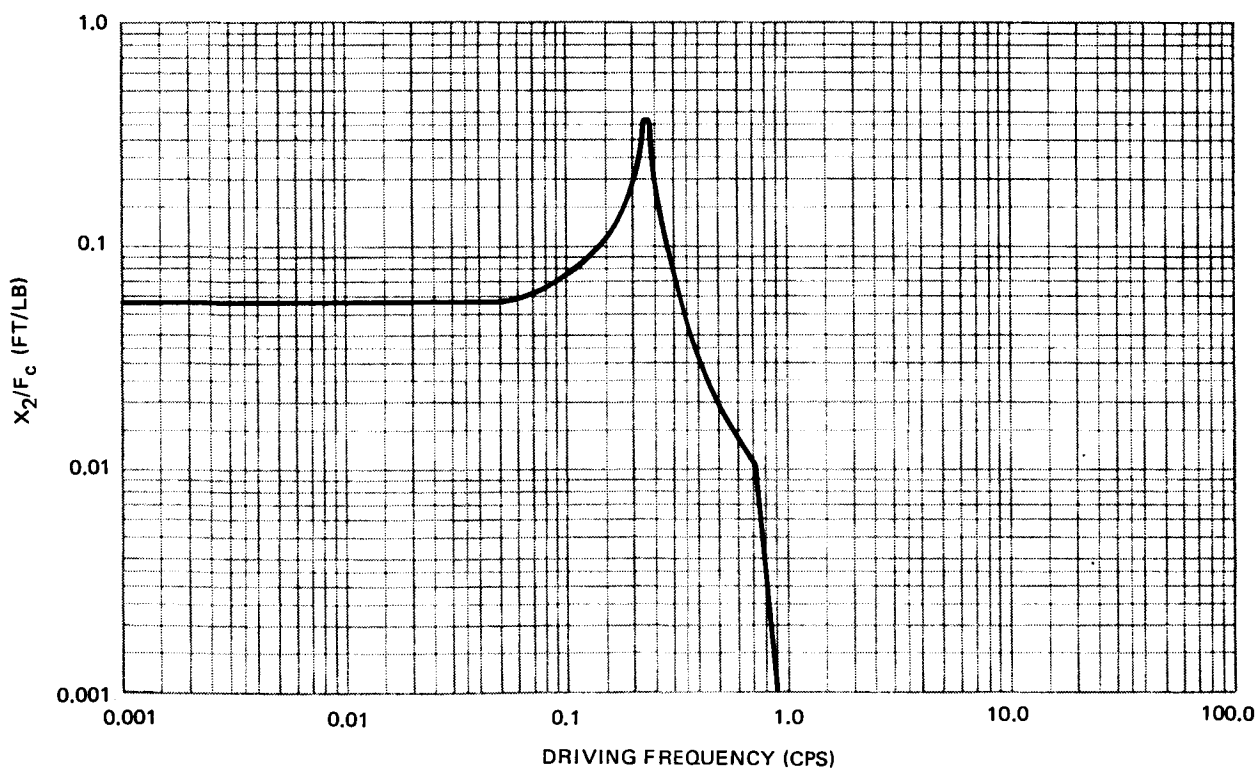


Figure 4-19. Ratio X_2/F_c vs Driving Frequency

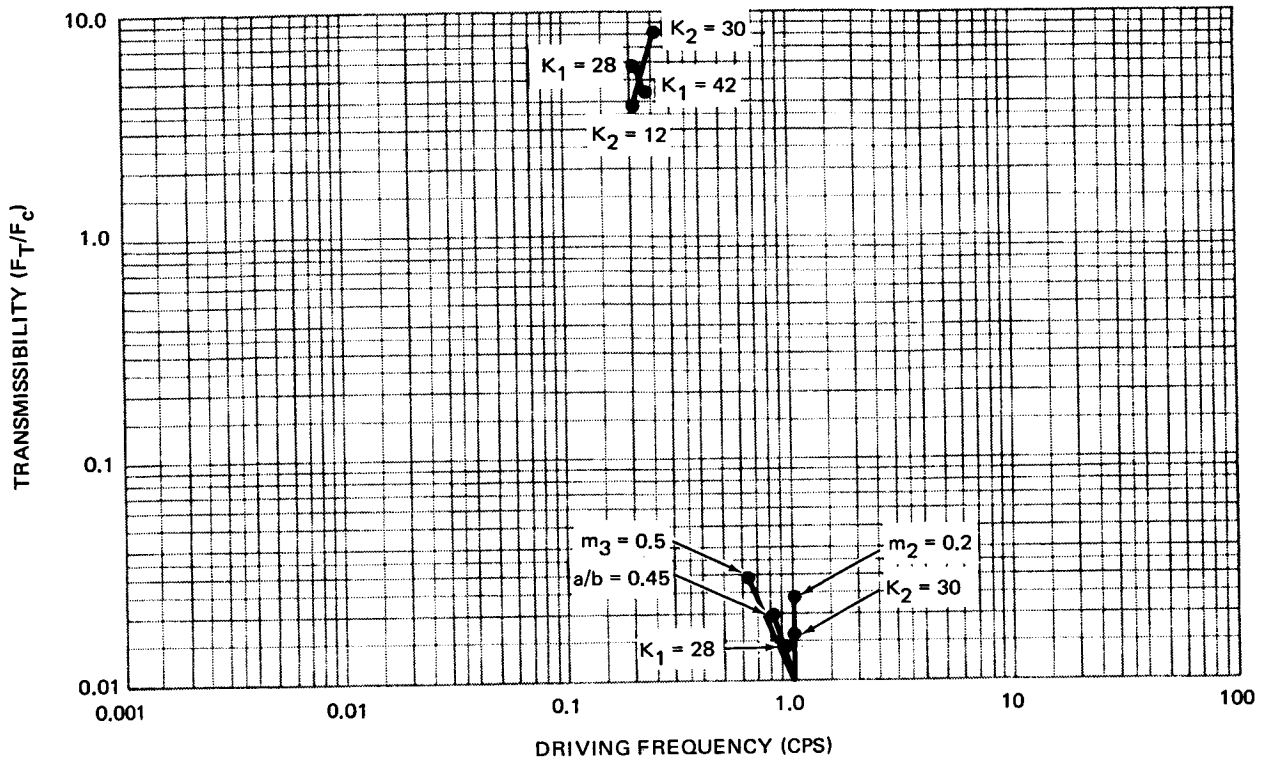


Figure 4-20. Sensitivity of Transmissibility Function

required at the notch, changes in k_1 or k_2 will simultaneously reduce the unwanted peak value. Figure 4-21 shows how the transmissibility function varies with the damping constant c_2 . The transient response characteristics of this system were investigated by an analog simulation; the response to two typical force histories (cough and arm motion) were investigated for the two damping values of Figure 4-21. (It was felt that the lower peak in the frequency domain, corresponding to the dashed curve, might result in a lower peak in the transient, but this was not the case.) The results of this analog study are shown in Figures 4-22 and 4-23. For arm motion, the ratio of peak transmitted force (0.93 lb) to peak input force (10 lb) is 0.093. The same ratio for the cough is $0.645/18 = 0.0358$. The larger reduction ratio for the cough is because of the higher frequencies prevalent in its force history.

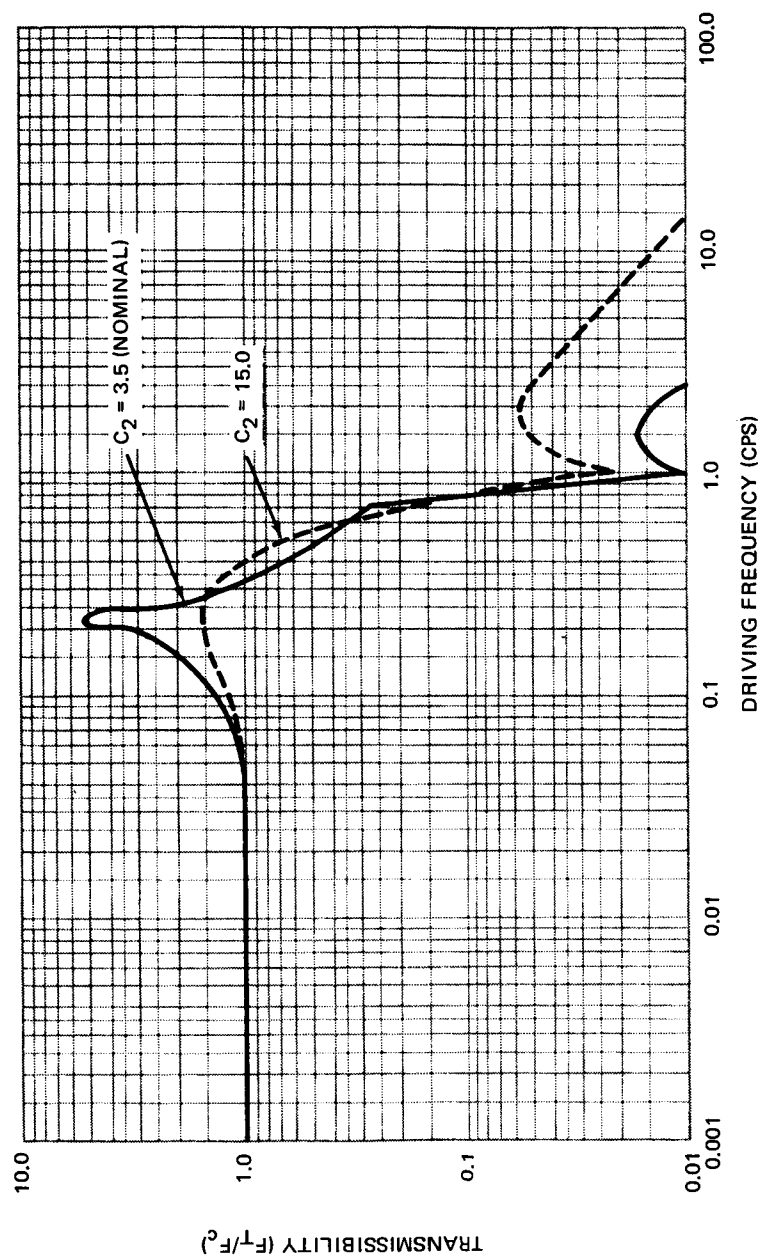


Figure 4-21. Sensitivity of Transmissibility to C_2

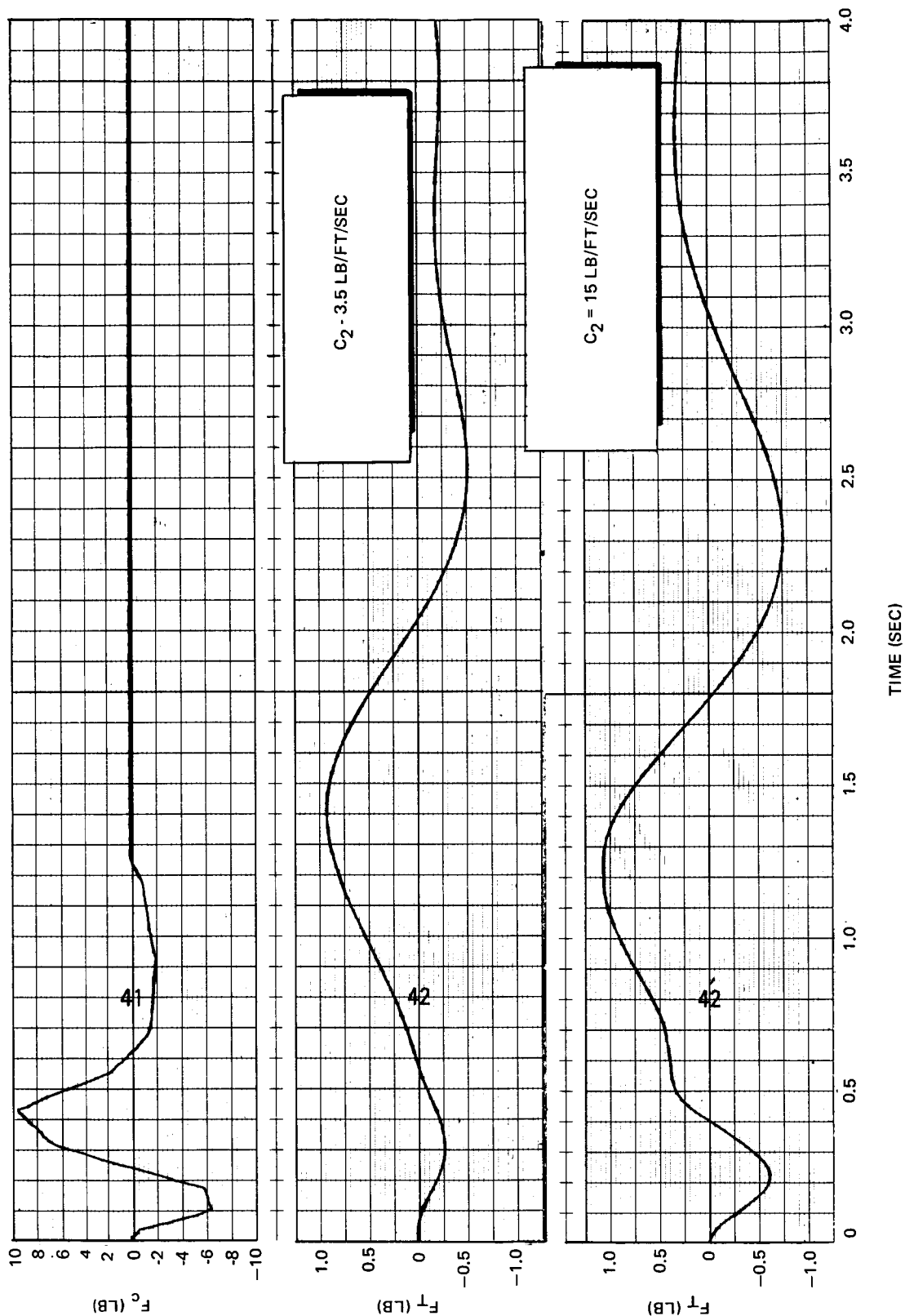


Figure 4-22. Transmitted Force vs Time for Arm Motion

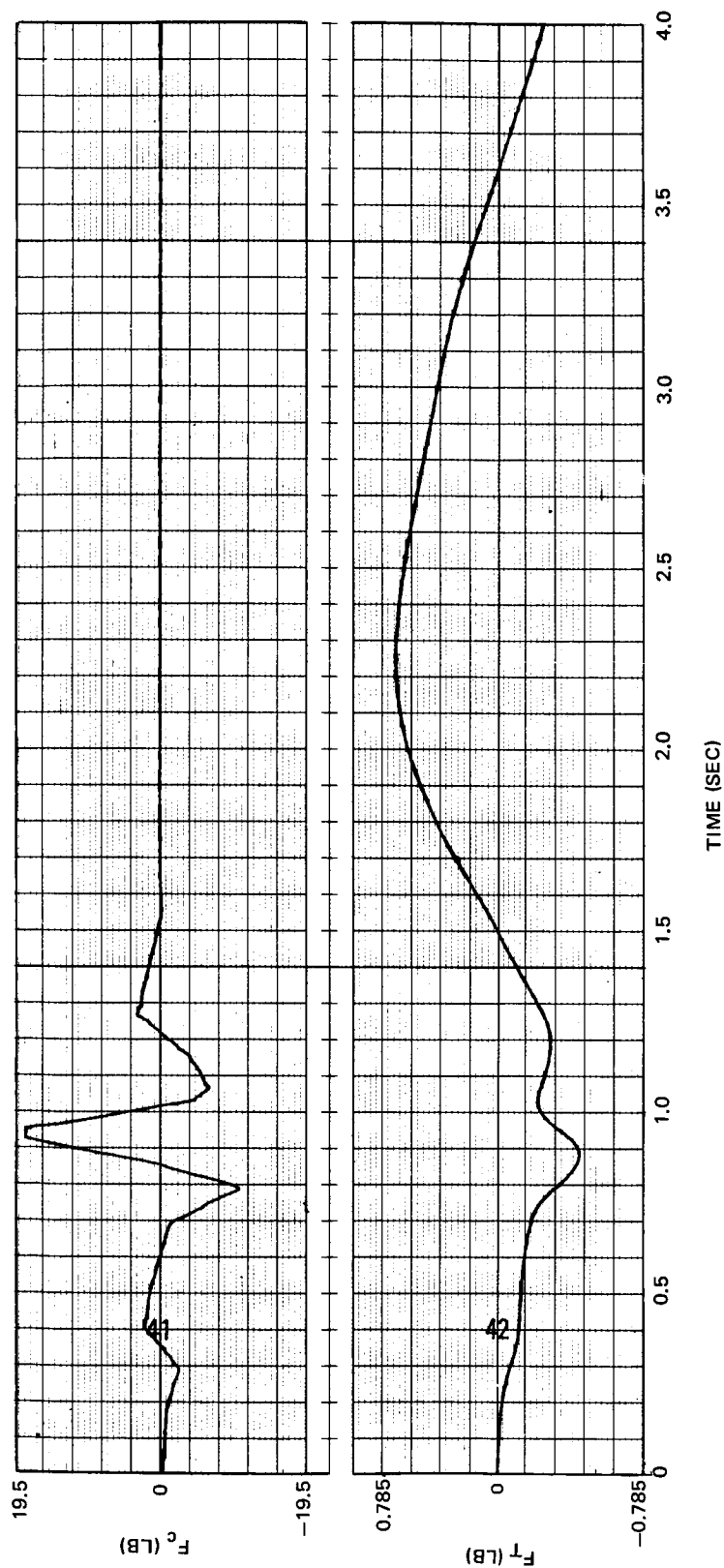


Figure 4-23. Transmitted Force vs Time for Cough

Section 5

CONCLUSIONS AND RECOMMENDATIONS

Crew motion is a major source of disturbance in an orbiting laboratory. Crew-motion forces cause significant disturbance of experiments requiring extremely accurate acceleration profiles, attitude, or attitude rate. Even those crew motions arising from crew-station activities cause accelerations that exceed the requirements of a majority of Project Thermo Experiments. The vehicle attitude errors arising from crew-station activities exceed the requirements of a minority of the ATM experiments and those experiments summarized in Figure 1-1.

The acceleration tolerances quoted for Project Thermo are conservative estimates of the actual requirements. The latter are known to depend on the frequency content of the acceleration histories. This fact reflects the basic lack of understanding of the phenomena involved in the behavior of propellants under low gravity which makes the Project Thermo experiments all the more urgent. In anticipation of that time when these requirements can be specified in a more exact form, the data in this report has been extended beyond showing peak accelerations to include what hopefully will prove to be useful criteria, namely, the peak velocity and RMS velocity (or average kinetic energy) at possible experiment locations.

The conclusions regarding the attitude accuracies of the larger laboratories are in conflict with many of the previously held theories. These results indicate that crew-station operations will have much less affect than previously believed. This difference exists because the previous estimates of crew-motion effect were based on assumed models of crew motion rather than on experimental data.

A number of suggestions are made in Section 2 for ways in which considerations of crew motion could affect design of the crew station. It is pointed out that data relating the effect of crew immobility on crew performance is

unavailable. Also required is data on the frequency of body functions and the effects on crew performance and comfort of lowering these frequencies to extend the periods of crew immobility.

The preliminary analyses presented indicate that two isolation devices have a high probability of providing successful isolation of crew motion. These devices as presented would provide an order of magnitude reduction in transmitted force, and hence would lower the attitude errors to within the requirements of all pointing experiments considered. Acceleration errors would be lowered to include approximately 40% more Project Thermo experiments. Further analysis and design of the isolators and the isolation of the experiment package as well would further increase the number of low-acceleration experiments realizable on the larger laboratories. However, it is felt that prospect of a manned version of Project Thermo using the smaller laboratory configuration (Configuration 3), as well as those experiments requiring a tolerance of 10^{-7} g are unfeasible.

Based on the above conclusions and the experience obtained during this study the following recommendations are made.

1. An effort should be made to establish the frequency dependence of the Project Thermo acceleration tolerances.
2. In light of the favorable pointing accuracy results, the need for additional fine-pointing stabilization systems for experiments should be reviewed, if in fact, crew motion were the primary consideration for their incorporation.
3. Further analysis, design, and testing should be performed on the two isolation devices (Figures 4-9 and 4-16) found to show promise. The analysis should include investigation of base driving characteristics and transient response. The transient characteristics should be investigated by including models of the isolators in the CREWMO Digital Computing Program used in this study and establishing actual reductions in acceleration and pointing errors. If the further analysis shows promise, prototype units should be constructed and tested. The testing procedure should consider the recommendations in Item 5 below. The force histories corresponding to a cough should be verified by further testing.

4. Research should be conducted in the areas of body function frequency and the effects on crew immobility.
5. If any further simulations of crew-station operations are conducted, an effort should be made to more closely approximate the actual crew stations and tasks as well as the crew members themselves. The credibility of the resulting data will be greatly enhanced if a true zero-g environment were used, such as an aircraft flown ballistic trajectory (this approach may not be as expensive as one would at first believe if the simulation work were being done by or for a government agency). More consideration should be given to the eventual use of the data before the experiment is designed. For instance, a power spectrum of individual crew motions as well as a composite power spectrum of all crew-station operations would be useful in the design of the isolators mentioned above in Item 3 and to a control system analysis in which RMS pointing error is the desired result.

Appendix A

SURVEY OF REQUIRED DYNAMIC ENVIRONMENT

In order to provide a yardstick for judging the data of this study, a survey was conducted to determine what tolerances on dynamic environment are required by those experiments being considered for inclusion in the orbiting laboratory program. Three experiment categories were considered: Project Thermo low-g propellant experiments, Apollo Telescope Mount (ATM) experiments, and the Orbiting Research Laboratory (ORL) experiments.

A.1 PROJECT THERMO EXPERIMENTS

Tables A-1 through A-6 identify the six major categories of investigation in Project Thermo. They include the experiment number, the applied longitudinal acceleration levels, and the duration required for these levels.

These tables are summarized in Figure 1-2, which shows the distribution of experiment duration with required lateral acceleration tolerances for Project Thermo. The data shown in Figure 1-2 represents the 343 separate experiments from the six major categories of investigation in Project Thermo. Of these 343 experiments, approximately 85% require an acceleration duration of 1 to 100 min. It should be noted that the trend of these experiments does not favor manned operations since, in general, the more critical experiments require more time. The circles of various sizes are used to show relative concentrations of experiments requiring identical acceleration and duration. The 2 largest circles represent a concentration of 31 experiments for a 3-min acceleration duration at a tolerance of $10^{-5}g$ and a concentration of 23 experiments for a 3.3-min acceleration duration at a tolerance of $5 \times 10^{-5}g$ respectively. These two circles are not exactly proportional to the number of experiments represented.

The magnitude and direction of applied longitudinal acceleration is predetermined for each experiment. The allowable tolerance for lateral acceleration is $\pm 10\%$ of the longitudinally applied acceleration. Discussions with the

Table A-1
PROJECT THERMO--INTERFACE STABILITY (page 1 of 3)

Required Axial Acceleration (Earth g's)	Acceleration Tolerance (Earth g's)	Experiment Number	Required Acceleration Duration (Seconds)
10^{-3}	$\pm 10^{-4}$	14	580
		88	250
		89	250
5×10^{-4}	$\pm 5 \times 10^{-5}$	105	640
		27	636 (Twice)
		104	480
		103	400
		54	324
		36	316
		86	314
		6, 7, 32, 35, 51, 52, 53, 97, 111, 113, 114, 115, 116, 117, 118, 119	300
		71	265
		47, 65, 100	222
		2, 3, 4, 5, 12, 16, 19, 28, 29, 30, 31, 34, 77, 81, 93, 94, 95, 96, 106, 107, 108, 109, 110	200
		83	150
		20	134
		8	120

Table A-1 (page 2 of 3)

Required Axial Acceleration (Earth g's)	Acceleration Tolerance (Earth g's)	Experiment Number	Required Acceleration Duration (Seconds)
5×10^{-4}	$\pm 5 \times 10^{-5}$	12, 17, 18, 78, 80, 82	120
		92	104
		85	100
		79	90
		9	88
		11, 84	80
		21	20
		73	14
10^{-5}	$\pm 10^{-6}$	50	2, 572
		99	2, 312
		33	2, 206
		66	1, 404
		91	1, 340
		15	1, 114
		90	1, 020
		112	952
		48	744
		14	580
		22	520
		73	465

Table A-1 (page 3 of 3)

Required Axial Acceleration (Earth g's)	Acceleration Tolerance (Earth g's)	Experiment Number	Required Acceleration Duration (Seconds)
10^{-5}	$\pm 10^{-6}$	13	360
		46, 64	348
		10	300
		88, 89	250 (Drag)
		38, 40, 42, 43, 44, 45, 56, 58, 60, 61, 62, 63, 74, 76, 101	200
		37, 39, 41, 49, 55, 57, 59, 75	170
		87	150
		98	100
-10^{-5}	$\pm 10^{-6}$	24	780
		26	520
		72	465
		70	312
		68	310
-5×10^{-3}	$\pm 5 \times 10^{-4}$	23	95
		67	87
		72	60
		25, 69	27
		72	7

Table A-2
PROJECT THERMO--PROPELLANT TRANSFER

Required Axial Acceleration (Earth g's)	Acceleration Tolerance (Earth g's)	Experiment Number	Required Acceleration Duration (Minutes)
5×10^{-4}	$\pm 5 \times 10^{-5}$	1	25.8
		8	24.9
		6	20.4
		12	14.1
		4	13.6
		11	13.5
		2	12.9
		9, 17	12.8
		3	12.5
		5, 7, 10, 13, 14, 15, 16, 18	3.7
10^{-4}	$\pm 10^{-5}$	15	10.4
10^{-5}	$+10^{-6}$	13	55.2
		18	41.1
		16	26.2
		7	23.2
		14	19.7
		10	12.9
		5	12.4

Table A-3
PROJECT THERMO--HIGH PERFORMANCE INSULATION

Required Axial Acceleration (Earth g's)	Acceleration Tolerance (Earth g's)	Experiment Number	Required Acceleration Duration (Minutes)
10^{-3}	to	$+10^{-4}$	
		2	12
		2	4
		3*	4
		4**	2

*This level occurs five times during the acceleration profile of Experiment H-3.

**This level occurs six times during the acceleration profile of Experiment H-4.

Table A-4
PROJECT THERMO--STRATIFICATION/DESTRATIFICATION

Required Axial Acceleration (Earth g's)	Acceleration Tolerance (Earth g's)	Experiment Number	Required Acceleration Duration
10^{-3}	$\pm 10^{-4}$	1	2.2 hours
		4	7.93 min
		2, 3, 12	4.0 min
		13	1.98 min
		6, 9, 10, 11	2.0 min
5×10^{-4}	$\pm 5 \times 10^{-5}$	6	15.6 min
10^{-4}	$\pm 10^{-5}$	2	20.934 hours
10^{-5}	$\pm 10^{-6}$	3	34.967 hours
		5a	13.066 hours
		6	36.0 min
10^{-6}	$\pm 10^{-7}$	9	69.867 hours
		4	51.351 hours
		10	32.067 hours
		7	14.410 hours
		12	10.067 hours
		11	9.634 hours
		8	8.010 hours
		13	3.6 sec
		5b	5.734 hours

Table A-5

PROJECT THERMO--BOILING HEAT TRANSFER (page 1 of 4)

Required Axial Acceleration (Earth g's)	Acceleration Tolerance (Earth g's)	Experiment Number	Required Acceleration Duration
10^{-3}	$\pm 10^{-4}$	BV-1	1.33 hours
		BO-115	36.96 min
		BV-2	31.80 min
		BV-3	12.0 min
		BV-4	7.2 min
		BV-5, 10	4.14 min
		BV-6 to 9, 11, 12	3.06 min
10^{-4}	$\pm 10^{-5}$	BV-113, BH-28	3.04 hours
		BV-14, BH-29, BVS-60	1.64 hours
		BV-15, BH-30, BVS-61	1.34 hours
		BS-49	48.0 min
		BO-114	36.96 min
		BV-16, BH-31, BVS-62	30.0 min
		BS-50	15.0 min
		BV-17, 25, BH-32, 40, BVS-63, 69	12.60 min
		BW-43	5.4 min
		BS-51, 57	4.8 min
		BV-26, BH-33, 41, BW-44, BVS-64, 70	3.6 min

Table A-5 (page 2 of 4)

Required Axial Acceleration (Earth g's)	Acceleration Tolerance (Earth g's)	Experiment Number	Required Acceleration Duration
10^{-4}	$\pm 10^{-5}$	BV-18 to 24, 27, BH-34 to 39, 42, BW-45 to 48, BS-52 to 56, 58, 59, BVS-65 to 68, 71	3.0 min
10^{-5}	$\pm 10^{-6}$	BV-72, BH-109	10.05 hours
		BV-73, BVS-85, BH-110	8.05 hours
		BV-74, BVS-86	1.80 hours
		BH-111	1.50 hours
		BV-75, BVS-88, BH-112	1.15 hours
		BO-113	36.96 min
		BVS-89	36.0 min
		BV-76, 82, BVS-90, 92, BH-113, 119	8.4 min
		BV-77, 83, BH-114	6.0 min
		BVS-87	4.8 min
		BV-79, 80, 81, 84, BVS-91, BH-115 to 118, 120	3.6 min
		BV-78	0.36 min
10^{-6}	$\pm 10^{-7}$	BV-134	50.0 hours
		BH-135	20.0 hours
		BV-93	19.95 hours
		BH-102	8.25 hours
		BH-136	8.0 hours

Table A-5 (page 3 of 4)

Required Axial Acceleration (Earth g's)	Acceleration Tolerance (Earth g's)	Experiment Number	Required Acceleration Duration
10^{-6}	$\pm 10^{-7}$	BV-94, BVS-121	7.83 hours
		BS-164	4.75 hours
		BH-139, BHS-153	2.5 hours
		BH-104, 140, BHS-154, BS-167	2.44 hours
		BV-98, 147, BVS-125, 131	2.02 hours
		BH-106, 141, BHS-155, BS-169	1.70 hours
		BV-146	1.60 hours
		BH-103, 137, BHS-151, BS-165	1.45 hours
		BH-105, 138, BHS-152, BS-166	1.44 hours
		BS-170	1.2 hours
		BV-101	1.07 hours
		BV-95, 143, BVS-122	1.03 hours
		BV-96, 144, BVS-123	1.02 hours
		BV-97, 145, 149, BVS-124, 126, 129, 133	1.0 hour
		BW-157	54.0 min
		BH-107, BS-168	53.4 min
		BV-142	46.98 min
		BH-108, BHS-156	44.4 min

Table A-5 (page 4 of 4)

Required Axial Acceleration (Earth g's)	Acceleration Tolerance (Earth g's)	Experiment Number	Required Acceleration Duration
10^{-6}	$\pm 10^{-7}$	BVS-130, BV-150	42.0 min
		BV-99, BVS-127, 132	28.2 min
		BV-100, 148, BVS-128	19.2 min
		BW-158	12.0 min
		BW-159	9.0 min
		BW-160 to 163	6.0 min

Table A-6

PROJECT THERMO--BOILOVER AND ENTRAINMENT

Required Axial Acceleration (Earth g's)	Acceleration Tolerance (Earth g's)	Experiment Number	Required Acceleration Duration (Minutes)
10^{-3}	$\pm 10^{-4}$	9	6
		10, 11, 12	5
		15	3
10^{-4}	$\pm 10^{-5}$	1 to 15	10
		1	6
		2, 3, 4	5
		13	3
10^{-5}	$\pm 10^{-6}$	5, 9	30
		4, 8, 12	22
		13, 14, 15	20
		1, 3, 7, 11	15
		2, 5, 10	10
10^{-5}	$\pm 10^{-6}$	5	6
		6, 7, 8	5
		14	3

responsible parties have indicated that these lateral acceleration tolerances are specified for constant or bias acceleration errors, and that transient acceleration effects could probably exceed these tolerances without adversely affecting the experiment. However, due to the basic lack of understanding concerning the mechanism of these phenomena, it is impossible to put specific quantitative tolerances on the acceleration levels at this time.

A.2 ATM EXPERIMENTS

One objective of the solar Apollo Telescope Mount (ATM) experiments is to investigate specific solar features in detail from above the Earth's atmosphere with a complement of instruments measuring in the white light, ultraviolet, extreme ultraviolet, and X-ray regions of the spectrum. Table A-7 is a brief summary of the pointing requirements and specifications for eight instruments used in the ATM experiments. These data were obtained from References 14 through 22.

The ATM experiments with the eight instruments listed in Table A-7 can be grouped into three general categories according to the maximum length of time required for the completion of an exposure period. These three categories are maximum exposure periods of 1, 1.66 and 15 min.

Figure A-1 is plotted on a semilog scale and represents the ATM experimental requirements for pointing accuracy. Of the 9 experiments represented in this figure, only 3 of them require stringent accuracies of 2.5 arc sec or less. These 3 experiments with the critical pointing accuracies have a corresponding maximum exposure period of 15 min, which further imposes operational sensitivity upon the experiments.

Figure A-2 is plotted on a semilog scale and represents the ATM experimental requirements for spatial resolution. The data available from 8 instruments show that 3 instruments require a spatial resolution of 2 arc sec or less. These 3 instruments have a corresponding maximum exposure period of 15 min, which introduces difficulty in fulfilling the overall operational resolution requirements.

Table A-7 12

ATM EXPERIMENT POINTING REQUIREMENTS

ATM Experiments	Pointing Reference	Pointing Accuracy	Pointing Stability	Pointing Orientation	Offset Requirement	Verification of Offset	Boresight Display	Field of View	Spatial Resolution	Exposure Time	In-Flight Alignment
High-Altitude Observatory White Light Coronagraph	Center of the sun	±20 arc sec	Roll Stability: 7.5 arc min per 15 min. Drift and Jitter Rate: 5 arc sec per sec for $\Delta t = 2$ sec. Roll Rate Limit: 180 arc sec/sec.	No roll position preferred. Know roll attitude to 1° of arc.	None	Not Applicable	Experiment has internal sensors (silicon cell detection) which will provide left-right, up-down indicators with accuracy to ±20 arc sec.	3°	15 arc sec (the experiment can tolerate this disturbance on film).	1 to 5 sec	Internal silicon cell detectors mounted on aperture pitch and yaw error.
Naval Research Laboratory EUV Spectro-Heliograph	Selected active regions on sun	±1 arc min	Pitch and Yaw Limits: ±2.5 arc sec. Roll Control Stability for 15 min: ±9 arc min; Pitch and Yaw Jitter (Rate): 1 arc sec/sec. Roll Rate: 1 arc min/sec.	Accuracy: ±9 arc min for 15 min (2.5 arc sec on limb).	±16 arc min	Yes. Accuracy:	Video display being proposed.	32 arc min (Reference 18) 50 x 50 arc min (Reference 6)	1 arc sec	0.10 sec to 15.0 min, maximum.	
EUV Spectrograph	Selected active regions on sun	±2 arc sec	Pitch and Yaw Limits: ±2.5 arc sec. Roll Control: 20 arc min. Pitch and Yaw Jitter (Rate): 1 arc sec/sec. Roll Rate: 1 arc min/sec.	Accuracy: ±9 arc min for 15 min (2.5 arc sec on limb). Has ±180° capability.	±16 arc min	Yes. Accuracy: (±1.25 arc sec over range of ±24 min).	Video display	80 arc sec x 2 or more arc sec. (Reference 18) 5 x 5 arc min (Reference 6).	Not Available	0.10 sec to 15.0 min, maximum	Can roll to any position during an experiment.
Harvard College Observatory UV Spectro-Heliometer	Selected active regions on sun	±2.5 arc sec	Roll excursion of 7.5 arc min per 15 min. (Length of slit should be held tangent to limb.)	None	Pure pitch or yaw movement: ±16 arc min	Yes. Possible coordinate system voice communication received of astronaut's voice.	Video display	5 arc sec x 5 arc sec.	5 arc sec	15-min scan duration.	Video display
UV Spectrometer	Selected active regions on sun and limb of sun	±2.5 arc sec	Roll excursion of 7.5 arc min per 15 min. (Length of slit should be held tangent to limb.)	None	±16 arc min	Yes.	Video display	1.9 arc sec x 30 arc sec slit.	1.5 arc sec	15-min scan duration.	
Hydrogen-Alpha Telescope/Camera	Entire solar disk	±10 arc sec	Roll excursion of 7.5 arc min per 15 min. (Length of slit should be held tangent to limb.)	None	Not Applicable	Not Applicable	No	~60 arc min (Reference 18) 30 to 40 arc min (Reference 22).	2 arc sec	0.01 to 0.02 sec	No requirement for offset pointing
Goddard Space Flight Center X-ray/EUV Telescope	Selected active regions on sun	±1 arc min	Pitch and Yaw: ±2.5 arc sec per 100 sec; Roll Stability: 15 arc min/100 sec.	None	±16 arc min	Yes. Voice communication offset readout device.	X-ray activity meter (visual indication of realtime solar X-ray activity).	~48 arc min	5 arc sec	1 to 100 sec, maximum	No
American Science and Engineering, Inc. X-ray Spectro-Heliograph	Selected active regions on sun	±2 arc min	Pitch and Yaw Limits: ±2.5 arc sec, Pitch and Yaw Jitter (Rate): 1 arc sec/sec	None	±16 arc min	Yes	Flare detector video display. 50 line/sec scan rate (1 scan per sec).	~40 arc min	2 arc sec	Approximate exposure time: 60 sec	Inflight instrument alignment to be maintained to within ±2 arc min with a max of ±2 arc sec jitter during exposure.

TABLE A-7 14

FOLDOUT FRAME 2

FOLDOUT FRAME 3

Table A-7C

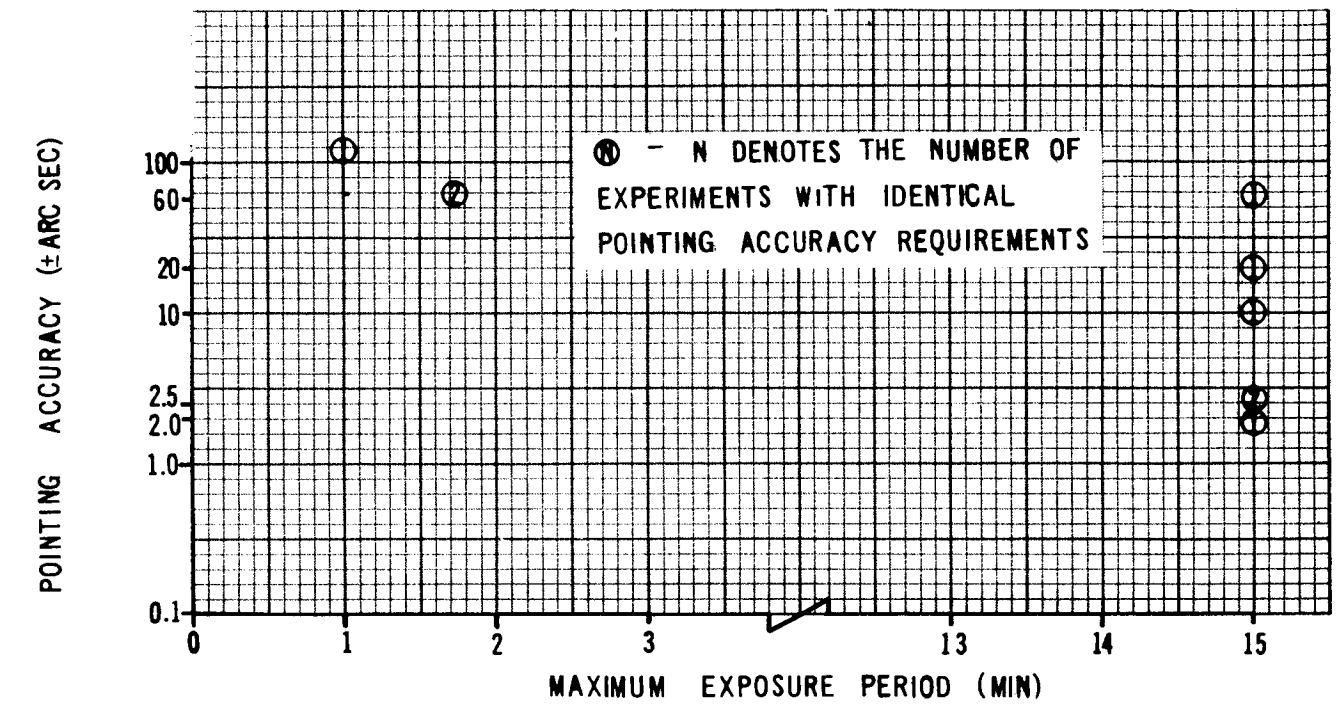


Figure A-1. Atmosphere Experiments Point Accuracy Requirements

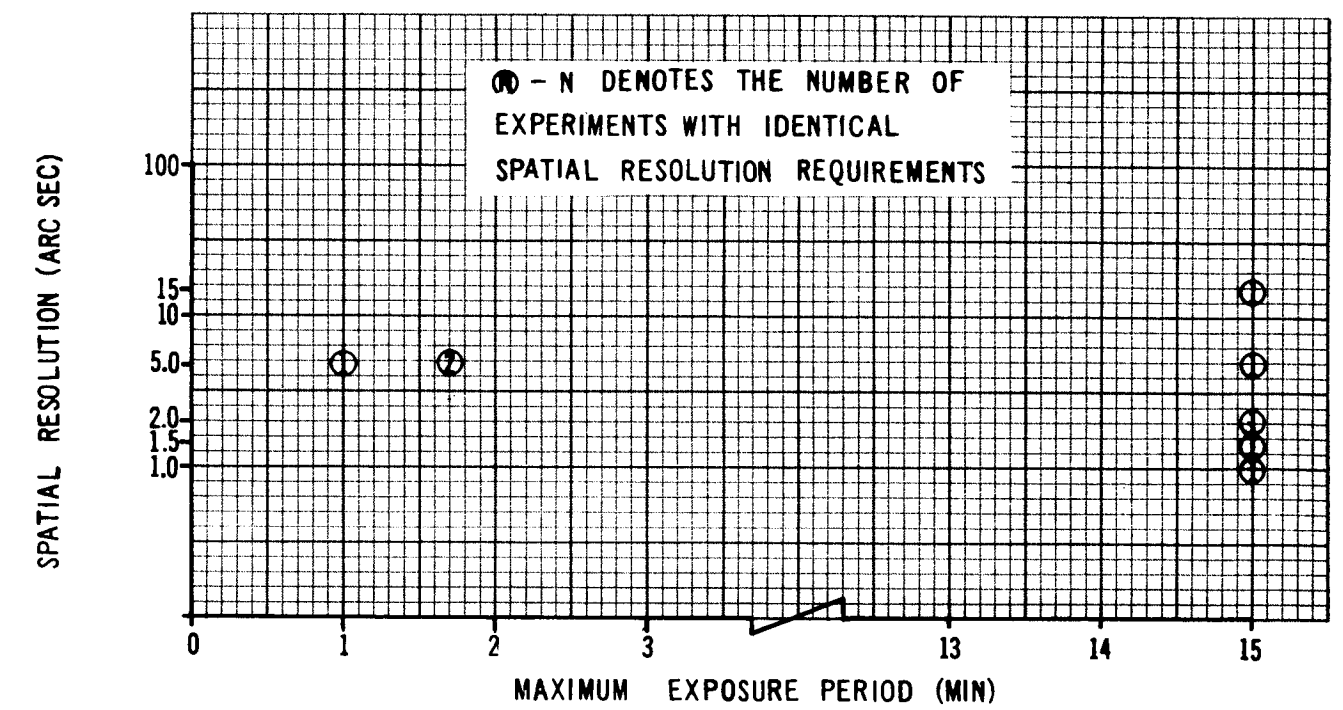


Figure A-2. Atmosphere Experiments Spatial Resolution Requirements

Analysis of the ATM instrument requirements from Table A-7 presents operational pointing stability specifications in various expressions of non-uniform units. One major difference in the unit expressions is the varying range of exposure periods and the dependence of the corresponding pointing stability parameters upon the maximum exposure period. To standardize these pointing stability specifications, the parametric pointing value was divided by the maximum experimental exposure period. The resulting values of pointing stability are plotted in Figure A-3.

The data in Figure A-3 is plotted on a semilog scale and represents the ATM experimental requirements for pointing stability. Several related parameters make up the pointing stability specifications. These include roll stability, control and excursion, roll-rate limit, pitch and yaw jitter rate, and pitch and yaw limits. Pointing orientation accuracy and limb accuracy data for two instruments are included in Figure A-3 for relative comparisons with pointing stability magnitude. Of the 20 pointing stability parameters plotted for the 9 instruments in Table A-1, 14 have values of 2.5 arc sec/sec or lower. Ten of these 14 parameters have a corresponding maximum exposure period of 15 min, which further imposes operational sensitivity upon the experiments.

A. 3 ORL EXPERIMENTS

Figure 1-1 is a summary of 97 experiments in an experiment package to be flown on an early mid-1970, one-year mission of a proposed Earth orbiting space station. The experiment package is contained in the "1971 to 1972 Earth Orbital Preliminary Baseline Experiment Program," Vol. I, II, and III. This package is partial fulfillment of Contract No. NAS 8-21064, dated March 15, 1967--S-IV B Station Module Study.

This summary includes the experiments which require pointing stabilization and gives an approximate distribution of experiments with required pointing accuracy and duration. The relative size of the data points provides a comparison of the number of experiments at each particular point. It should be noted that the trend here is in favor of manned operations since the more critical experiments are in general of shorter duration.

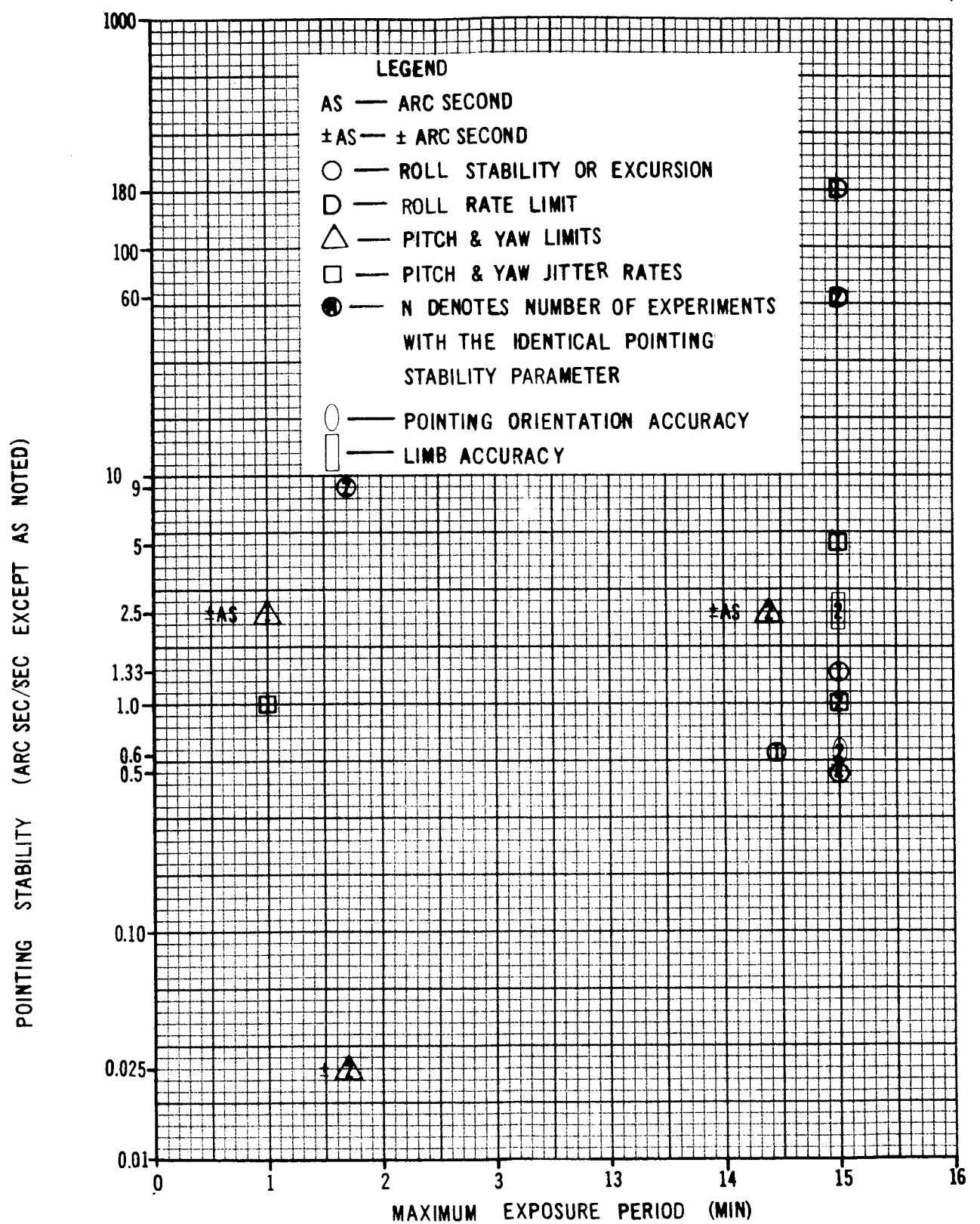


Figure A-3. Atmosphere Experiments Pointing Stability

These experiments are taken from such categories as physical sciences, Earth resources, space medicine, astronomy, atmospheric sciences, space biology, communications, and manned operations. The greatest demand for stabilization accuracy is from the astronomy experiments, 13 of which require a stabilization of 1 ± 1 arc sec with variable durations from 100 to 10,000 sec.

Appendix B

COMPUTING PROGRAMS

Two computing programs were written for this study. The first program, CREWMO, computes the open-loop dynamic effects on the vehicle caused by crew-motion forces and moments. The second program FORCE takes sampled data force and moment inputs and computes the coefficients of Fourier series expansions of the forces and moments for use in program CREWMO. The coefficients of the Fourier expansion are corrected to conform to the dynamical constraints as discussed in Section 3.4. The following is a listing of the input variables to program CREWMO.

$[A]_{3 \times 7}$	The array of cosine coefficients in the force expansion (lb).
$[AK]_{3 \times 7}$	The array of cosine coefficients in the moment expansion (in. -lb).
$[BK]_{3 \times 7}$	The array of sine coefficients in the moment expansion (in. -lb).
$[D]_{3 \times 7}$	The array of sine coefficients in the force expansion (lb).
DELT	The integration time increment (sec).
IB	Index for type of computation 0 for rigid-body effects only; 1 for addition of elastic effects.
N	Number of output stations (may not use more than 10).
NF	Index for location of input: 1 if on main body of vehicle; 0 if on a branch.
ϕ MEG1	Circular frequency of first bending mode (rad/sec).
ϕ MEG2	Circular frequency of second bending mode (rad/sec).

$[\text{PHI1}]_3$	Modal deflection coefficients for input station first mode (in.).
$[\text{PHI2}]_3$	Modal deflection coefficients for input station second mode (in.).
$[\text{PHIS1}]_3$	Modal slope coefficients for input station first mode (rad).
$[\text{PHIS2}]_3$	Modal slope coefficients for input station second mode (rad).
$[\text{PHI}\phi 1]_{3 \times 10}$	Array of modal deflection coefficients for the output stations first bending mode (in.).
$[\text{PHI}\phi 2]_{3 \times 10}$	Array of modal deflection coefficients for the output stations second bending mode (in.).
$[\text{PHIS}\phi 1]_{3 \times 10}$	Array of modal slope coefficients for the output stations first bending mode (rad).
$[\text{PHIS}\phi 2]_{3 \times 10}$	Array of modal slope coefficients for the output stations second bending mode (rad).
PI1	
PI2	Principal moments of inertia (in. -lb/sec ²).
PI3	
PRT	Print interval (sec).
$[\text{R}\phi]_{3 \times 10}$	Array of coordinates of output stations (in.).
$[\text{RCG}]_3$	Coordinates of vehicle center of gravity (in.).
$[\text{RX}]_3$	Coordinates of crew station origin (in.).
$[\text{RZ}]_3$	Coordinates of force input in crew reference frame (in.).
TF	Total integration time (sec).
TS	Time duration of crew motion forces.
$[\text{TFS}]_{3 \times 3}$	Direction cosine matrix of the transformation from crew station to spacecraft geometric axes.